

ALMA MATER STUDIORUM - UNIVERSITA' DI BOLOGNA

Dottorato di Ricerca in Fisica
Ciclo XXXI

Settore concorsuale di afferenza: 02/A2

Settore scientifico disciplinare: FIS/02

Inflation and Dark Matter From String Theory

Presentata da: Victor Alfonso
Diaz

Coordinatrice Dottorato:
Prof.ssa Silvia Arcelli

Supervisore:
Prof. Michele Cicoli

Esame finale anno 2019

“...Not only is the Universe stranger than we think, it is stranger than we can think...”

Werner Heisenberg

Dedicada a mí.

Acknowledgements

I would like to thank all the collaborators who made possible the creation of this remarkable work: Michele Cicoli, David Ciupke, Veronica Guidetti, Francesco Muia, Francisco Pedro, Marcus Rummel, Pramod Shukla. I'm particularly grateful to my supervisor, Michele Cicoli, who trusted me to decide what type of research I would like to do and also for give me the freedom to do it at my own pace. I am also really grateful for the figures who taught basically everything that I know about string theory: Anamaria Font and Fernando Quevedo, two amazing people that will always be in my mind

This thesis was assembled during my stay at the Max-Planck Institute for Physics in Munich, Germany. I am really grateful for the amazing hospitality given by Prof. Ralph Blumenhagen and the Max-Planck Institute in the finishing stage of my PhD.

Declaration

This thesis is based on the results presented in the following papers:

[1] **2017, August.**

M. Cicoli, **V. A. Diaz**, V. Guidetti and M. Rummel,
“The 3.5 keV Line from Stringy Axions,”
JHEP **1710**, 192 (2017), arXiv:1707.02987 [hep-th].

[2] **2017, September.**

M. Cicoli, D. Ciupke, **V. A. Diaz**, V. Guidetti, F. Muia and P. Shukla,
“Chiral Global Embedding of Fibre Inflation Models,”
JHEP **1711**, 207 (2017), arXiv:1709.01518 [hep-th].

[3] **2018, March.**

M. Cicoli, **V. A. Diaz** and F. G. Pedro,
“Primordial Black Holes from String Inflation,”
JCAP **1806**, no. 06, 034 (2018), arXiv:1803.02837 [hep-th].

Abstract

In the present thesis I have described my research work in particle phenomenology and cosmology, arising mainly from a class of string models called *fibre inflation*. The work is presented as a merge of models. It is divided into two parts. In the first part, inflation from string theory, we show the construction of explicit examples of fibre inflation models which are globally embedded in type IIB orientifolds with chiral matter on D7-branes and full closed string moduli stabilisation, which has never been built before. For the second part, dark matter from string theory, we present two independent models describing dark matter. One work shows how a single-field string inflationary model, which allows the generation of primordial black holes in the low mass region, can account for a significant fraction of the dark matter abundance, while in the second one we present how stringy axions can be used to describe the 3.5 keV line observed in galaxy clusters.

Contents

I	Introduction	5
1	Introduction	7
1.1	The standard model of cosmology	7
1.2	Inflation	12
1.3	Dark Matter	15
1.4	String theory	18
1.4.1	String compactification	19
1.4.2	Calabi-Yau manifolds	21
1.4.3	Moduli space	23
1.4.4	Orientifolds	24
1.4.5	$\mathcal{N} = 1$ Type IIB Orientifold	27
1.4.6	Supersymmetry and no-scale structure	34
II	Inflation	
	from String Theory	39
2	Chiral Global Embedding of Fibre Inflation Models	41
2.1	Chiral global inflationary models	45
2.1.1	Fibre inflation in a nutshell	45
2.1.2	Requirements for chiral global embedding	47
2.2	A chiral global example	48
2.2.1	Toric data	49
2.2.2	Orientifold involution	51
2.2.3	Brane setup	52
2.2.4	Gauge fluxes	53
2.2.5	FI-term and chirality	55
2.2.6	Inflationary potential	56
2.3	Inflationary dynamics	58

2.3.1	Single-field evolution	59
2.3.2	Multi-field evolution	70
2.4	Summary	78
 III Dark Matter		
From String Theory		81
 3 Primordial Black Holes from String Inflation		83
3.1	Fibre inflation models	86
3.2	PBH formation	90
3.3	PBHs from Fibre inflation	93
3.4	Summary	99
 4 The 3.5 keV Line from Stringy Axions		101
4.1	Phenomenology and microscopic realisation	106
4.1.1	Observational constraints	107
4.1.2	Phenomenological features	108
4.1.3	Calabi-Yau threefold	114
4.1.4	Brane set-up and fluxes	116
4.1.5	Low-energy 4D theory	119
4.2	Moduli stabilisation	121
4.2.1	Stabilisation at $\mathcal{O}(1/\mathcal{V}^2)$	122
4.2.2	Stabilisation at $\mathcal{O}(1/\mathcal{V}^3)$	123
4.2.3	Stabilisation at $\mathcal{O}(1/\mathcal{V}^{3+p})$	125
4.3	Mass spectrum and couplings	127
4.3.1	Canonical normalisation	127
4.3.2	Mass spectrum	128
4.3.3	DM-ALP coupling	129
4.4	Summary	132
 IV Conclusions		135
 5 Summary and final remarks		137
 A Warped Type IIB SUGRA: equations of motion		141
A.0.1	Equation of motion for the metric g_{MN}	142
A.0.2	Equation of motion for the 5-form \tilde{F}_5	143

B	Another chiral global example	145
B.0.1	Toric data	145
B.0.2	Orientifold involution	147
B.0.3	Brane setup	148
B.0.4	Gauge fluxes	149
B.0.5	FI-term and chirality	150
B.0.6	Inflationary potential	152
C	Computational details	157
C.0.1	Closed string axion decay constants	157
C.0.2	Canonical normalisation	158
C.0.3	Mass matrix	161
	Bibliography	163

Preface

The history of our universe had been described for several decades. The appealing to unveil the unknown or ask questions such as how do we got here? or what are we made from? are natural and they have been wandering for hundreds of years. Just to even find a glimmering look of how they could be solved is really exciting. For that reason, we have focused so much work and resources to have a drop of that ‘glimmering true’. In order to do so, we have developed different tools and methods to try to unravel all the mystery with the minimal amount of ambiguity.

Several years of theoretical research and experimental measurements [4, 5, 6] have established the Λ CDM model as the standard model of cosmology. A few facts are known about our Universe, in particular in the Λ CDM model the Universe is filled with 68% of dark energy (DE), 27% of dark matter (DM), and only 5% of baryonic mass (ordinary atoms) [7]. Despite the lack of knowledge an important fact, which is well understood, is that our Universe is well-described by the Friedmann-Robertson-Walker metric

$$ds^2 = -dt^2 + a^2(t)d\mathbf{x}^2, \quad (1)$$

where $a(t)$ is the scale factor. In the Universe described by the Λ CDM model, causal signal travels a finite distance between the time of the initial singularity and the time of formation of the first neutral atoms. Although, it has been observed that *Cosmic Microwave Background* (CMB) anisotropies have powerful correlations to scale grater than this finite distance. Such correlation remains unexplained by this model. In the beginning of the 1980s inflation was introduced to explain different problems of the Λ CDM model, such as these possible correlations on large scales, also known as the Horizon problem; together with the lack of explanation of the overall homogeneity, isotropy, and flatness of the Universe [8, 9]. Inflation is an early phase of a quasi-de Sitter evolution that drives the primordial Universe towards these conditions. Quantum fluctuations during this period of exponential accelerated expansion are the origin of all structures in the Universe [10, 11]. Many models have been made trying to give a microscopic description of inflation, [12, 13, 14, 15] but until today there has not been a definitive answer. The inflationary models

constructed so far are mainly embedded in a low energy effective theory and are based on the premise that a single field (or multi-field), called the *inflaton*, drives the inflationary evolution. Two methods are generally used to build these models, the ‘top-down’ and the ‘bottom-up’ approaches. In the ‘top-down’ approach one starts with a completed theory in the ultraviolet (UV) and try to derive inflation as a low energy consequence. In the case of the ‘bottom-up’ approach a low energy theory is given and degrees of freedom are added in a controlled way to complete the UV theory. In both cases a potential for the inflaton is generated or given. For a single field inflation this potential has certain features. In particular, a flat region and a global minimum.

The inflaton potential might suffer from fundamental problems such as instabilities of the flat region due to extra quantum corrections. Therefore, the most natural step is to embed inflation in a theory where the potential is protected by the presence of symmetries against possible quantum corrections which can spoil its flatness, a ‘top-down’ approach. An example of these theories is given by string theory. String theory is the best candidate known so far to give a complete UV description of the standard model of particle physics (SM) and general relativity (GR). For physical consistency the theory needs to be formulated in 10 dimensions. In order to make contact with the usual 4-dimensional physics that is testable in the current labs like the Large Hadron Collider (LHC) in Switzerland, 6 out of those 10 dimensions need to be *compactified*. The 6 dimensional space is taken to be a compact with a size usually of order $\sim (10^{-33} \text{ cm})^6$. Regrettably the 4-dimensional physics that is generated will depend on the compact space. However, regardless of the compact space, the presence of these extra-dimensions gives rise to several scalar field uncharged by the SM, called *moduli*, that might play the role of the inflaton.

This thesis was created as a merge of models that try to give an explanation to various puzzles inside the standard model of cosmology, using string theory as the main playground for the solutions. Initially, we gave a basic introduction to the concept needed to understand each one of the models. We explained the basics aspects of the standard model of cosmology, together with a brief introduction of inflation and dark matter. After that we reviewed some basic knowledge of string compactification later used in the development of the models within this thesis.

The main text of this work is organized in two parts. The first part is dedicated to inflation, and is called inflation from string theory. In this chapter, we construct explicit examples of fibre inflation models which are globally embedded in type IIB orientifolds with chiral matter on D7-branes and full closed string moduli stabilisation. One of the interesting features this model is that is the first one to in-

clude full moduli stabilisation with a chiral matter sector. The second part is called dark matter from string theory. This section is divided into two works. The first one is called primordial black holes from string inflation, where we described how a single-field string inflationary model, which allows the generation of primordial black holes in the low mass region, can account for a significant fraction of the dark matter abundance. In the second one we show how axion like particles coming from string compactifications can be used to describe the 3.5 keV line observed in galaxy clusters. The model described in this chapter explains the morphology of the 3.5 keV signal and its non-observation in dwarf spheroidal galaxies, involving a 7 keV dark matter particle decaying into a pair of ultra-light axions that convert into photons in the magnetic field of the clusters.

Finally, we finish with an overall summary and conclusion of the thesis. We include as well few appendices where we further developed some of the topics in each chapter. This work is more than just a merge of models, is the unification of two amazing areas of physics which for long time it was thought to be impossible to put together. These areas are phenomenological cosmology and string theory. I hope it is useful and easy to read.

Part I

Introduction

Chapter 1

Introduction

In this chapter we introduce some aspects needed for the development of the models in this thesis. Initially, we give an brief summary of the standard model of cosmology and its shortcomings, to give rise to the introduction of the period of inflationary expansion of the Universe at early times, also called *Inflation*. We also give a brief description of dark matter and its possible candidates. After we have finished with the cosmological description we moved on to the review of the best candidate to embed all these cosmological models, which is string theory. We give a short review of string compactification and moduli stabilisation.

1.1 The standard model of cosmology

The standard model of cosmology was created by the combination of the standard model of particle physics and general relativity describing gravity at the classical level. In this section we focus in the description of the general relativity building block. In general the dynamics of the space-time is described by a metric tensor $g_{\mu\nu}$. The equation of motion for the metric is derived by taking the variation of the *Einstein-Hilbert* action

$$S_{EH} = \frac{M_p^2}{2} \int d^4x \sqrt{-g} R, \quad (1.1)$$

with $g = \det(g_{\mu\nu})$ and R is the Ricci scalar. The coupling constant M_p is called the reduced Mass Planck and is given by

$$M_p = \frac{1}{\sqrt{8\pi G}} \simeq 2.4 \cdot 10^{18} \text{ GeV}, \quad (1.2)$$

where G is the universal gravitational constant. Taking the variation respect to the metric of (1.1), we find the Einstein equations

$$R_{\mu\nu} - \frac{1}{2} R g_{\mu\nu} = 0, \quad (1.3)$$

with $R_{\mu\nu}$ the Ricci tensor. The above equation is valid in absence of extra sources in the action (1.1), when we have extra terms in the action, the equation (1.3) cease to be homogeneous and can be written in general as

$$R_{\mu\nu} - \frac{1}{2} R g_{\mu\nu} = 8\pi G T_{\mu\nu}, \quad (1.4)$$

where $T_{\mu\nu}$ is the energy-momentum tensor associated to the extra sources.

The standard model of cosmology assume the Universe started hot and dense which adiabatically expands. The first assumption is that the space-time can be described by the metric

$$ds^2 = dt^2 - a(t)^2 \left[\frac{dr^2}{1 - kr^2} + r^2 (d\theta^2 + \sin^2 \theta d\varphi^2) \right]. \quad (1.5)$$

Also called the *Friedmann-Robertson-Walker* metric (FRW). This metric describes a slicing of the space-time where the spatial section is re-scaled by the scale factor $a(t)$. The constant k takes the values $k = \{-1, 0, 1\}$, which represent a hyperbolic, flat, and spherical spaces respectively. Basically, the dynamics of this model is attached to the evolution of the scale factor. The form of the scale factor depends on the source of energy which dominate the Universe at a given time. We can classify the sources of energy mainly in three classes and these are: radiation, matter, and dark energy associated to the *Cosmological Constant* Λ . Due to the form of the metric (1.5) and the symmetries of the space-time we can write the equation (1.4) in a perfect fluid form where

$$T_{\mu\nu} = \begin{pmatrix} \rho & 0 & 0 & 0 \\ 0 & -P & 0 & 0 \\ 0 & 0 & -P & 0 \\ 0 & 0 & 0 & -P \end{pmatrix}, \quad (1.6)$$

with P the pressure and ρ the energy density. Therefore, the general 10 equations

reduce to just two equations

$$H^2 = \left(\frac{\dot{a}}{a}\right)^2 = \frac{8\pi G}{3} \left[\rho - \frac{3k}{8\pi G a^2} \right]; \quad (1.7)$$

$$\dot{H} + H^2 = \frac{\ddot{a}}{a} = -\frac{4\pi G}{3} (\rho + 3P), \quad (1.8)$$

where we have defined the *Hubble parameter* $H = \dot{a}/a$. The above equations are also known as the Friedmann equations. Here the energy density ρ can be written as $\rho = \rho_{\text{radiation}} + \rho_{\text{matter}} + \rho_{\Lambda}$, where each term corresponds to the contribution of each class of energy density mentioned before. Combining the equation (1.7) and (1.8), we find the energy conservation law

$$\frac{d\rho}{dt} + 3H(\rho + P) = 0, \quad (1.9)$$

which can also be found from the Bianchi identity $\nabla^{\mu}T_{\mu\nu} = 0$. Assuming that the equation of state takes the form

$$P = \omega\rho, \quad (1.10)$$

where ω a constant, we can see from the equation (1.9) that

$$\rho \propto a^{-3(1+\omega)} \quad (1.11)$$

and

$$a(t) \propto \begin{cases} t^{\frac{2}{3(1+\omega)}} & , \quad \omega \neq -1 \\ e^{Ht} & , \quad \omega = -1 \end{cases}. \quad (1.12)$$

The value of ω describe which class of energy density we have. For example, for radiation $\omega = 1/3$ which implies $\rho_{\text{radiation}} \propto a^{-4}$ and for matter $\omega = 0$ having $\rho_{\text{matter}} \propto a^{-3}$.

Using (1.11) we can re-write the first Friedmann equation (1.7) in terms of the current fraction of energy density

$$\Omega_i = \frac{\rho_i}{\rho_{cr}} \quad , \quad \Omega_{\text{curv}} = -\frac{k}{a_0^2 H_0^2}, \quad (1.13)$$

where $i = \{\text{matter}, \text{radiation}, \Lambda\}$. Here, we have defined the critical energy density

$\rho_{cr} = \frac{3}{8\pi G} H_0^2 = 5 \cdot 10^{-6} \text{ GeV/cm}^3$, then (1.7) is given by

$$\left(\frac{H}{H_0}\right)^2 = \left[\Omega_{matter} \left(\frac{a_0}{a}\right)^3 + \Omega_{radiation} \left(\frac{a_0}{a}\right)^4 + \Omega_\Lambda + \Omega_{curv} \left(\frac{a_0}{a}\right)^2 \right]. \quad (1.14)$$

At present time we have $\sum_i \Omega_i + \Omega_{curv} = 1$. From the above equation we can actually deduce which energy density was dominating in a given period of time. For example, it is clear that at early time, when $a \ll a_0$, the radiation was dominating the Universe. Subsequently a matter dominated era began around a time $t_{matter} \simeq 10^5$ yrs. Finally, an epoch of dark energy, a period in which the contribution of the cosmological constant Λ dominates, started around a time $t_\Lambda \simeq 7 \cdot 10^9$ yrs. Although, the power corresponding to the curvature fraction is greater than the one of dark energy this one is suppressed by experimental observation where $|\Omega_{curv}| < 0.005$. At the present time this fractions are given by [7]

$$\Omega_{matter} \simeq 0.315 \quad , \quad \Omega_{radiation} \simeq 5 \cdot 10^{-5} \quad , \quad \Omega_\Lambda \simeq 0.685 \quad , \quad \text{and} \quad |\Omega_{curv}| < 0.005. \quad (1.15)$$

The fraction corresponding to the matter can be divided into two classes

$$\Omega_{baryonic} \simeq 0.045 \quad \text{and} \quad \Omega_{DM} \simeq 0.27. \quad (1.16)$$

Here, $\Omega_{baryonic}$ correspond to the fraction of baryonic matter which include atoms of any sort, and Ω_{DM} correspond to the fraction of Dark Matter.

Although, the standard model of cosmology has been well tested, still it has few problems specially related to initial conditions. The evolution of any dynamical system is governed by its initial conditions. The Universe itself is consider a system, where the matter is distributed homogeneously and isotropically on scales larger than several megaparsecs. Therefore, it is natural to ask what were the initial conditions that lead such homogeneity and isotropy.

In order to solve this question, we need to made few assumptions, such as [16]:

- In-homogeneity cannot be dissolved by expansion;
- Non-perturbative quantum gravity does not play any role at sub-Planckian curvatures.

Once we have made these assumptions, we can try to characterize the initial conditions. There are two independent sets that describe matter in our universe:

1. The spatial distribution of matter in the system that can be described by the energy density $\rho(\mathbf{x})$;

2. The initial velocities of the distribution.

Trying to unveil the origin of these two independent sets, we find that they lead to two very well-known problems of the standard model of cosmology. These are:

- *The horizon problem.* Let us assume that the Universe started at some time t_i . Then, the maximum distance travelled by light, also called *particle horizon*, is given by

$$\chi_p(t) = \int_{t_i}^t \frac{dt'}{a(t')} = \int_{a_i}^a \frac{da}{Ha^2} \sim a^{(1+3\omega)/2} - a_i^{(1+3\omega)/2}, \quad (1.17)$$

where we have used the equation (1.12). During the standard Big Bang evolution, $\ddot{a} < 0$ and the comoving Hubble radius $(aH)^{-1} = (\dot{a})^{-1}$ grows with time. For values of $\omega > -1/3$ we notice that the particle horizon grows in time and is dominated by late times. This means that at every instant of time new regions enter in causal contact. Therefore, If the Universe started in a homogeneous state, they should look very different from one to another. However, it has been observed that the Universe seems to be homogeneous on scales that came in causal contact recently.

- *The flatness problem.* The Universe today appears to be extremely flat, with $|\Omega_{curv}| < 0.005$. Given the current content of matter it seems that in the early times it was even closer to zero of the order $\frac{\rho(t_i)}{\rho_{cr}} \sim 10^{-61}$. We can connect this high fine-tuning of the initial density energy with the total energy of the system (and clearly its velocity). We can see that for a given energy density distribution the initial Hubble velocities must be adjusted so that the huge negative gravitational energy, associated to gravitational self-interaction, is compensated by a huge positive kinetic energy to an order of $10^{-59}\%$. Therefore, an error exceeding this percentage implies: either the Universe re-collapses or become empty too early.

Together with these fundamentals problems there exists other issues within the standard model of cosmology. For example, the monopole problem which states that topological defects such as monopoles would have been created in the early universe. Since they are stable objects, they should be still present to date in such a quantity that they would dominate the energy density of the universe, but still they have not been observed. As well as the unexplained CMB anisotropies which are small temperature fluctuations in the black body radiation left over from the Big Bang. Therefore, we need to extend or propose a new model where all these

problems might be solved. Here is where the introduction of a transient phase of accelerated expansion arrive. This phase of the early Universe is known as *Inflation*.

1.2 Inflation

Nowadays Inflation has become a standard topic in cosmology books. We give a brief review on this subject. Mainly we described single-field inflation, but this can be easily be generalize in a multi-field case. For further reading we refer to [16, 17, 18].

As we mentioned in the previous section for values of $\omega > -1/3$ the particle horizon is dominated by contributions from late times. So, if we postulate that the comoving Hubble radius was decreasing on time, the particle horizon would be dominated by early times, it would give us an additional span of conformal time between the initial singularity of the Big Bang and the creation of neutral atoms. This imply that all points in the CMB originate from a causally connected region, solving in principle the Horizon problem. The assumption of shrinking comoving Hubble radius implies

$$\frac{d}{dt}(aH)^{-1} = -\frac{1}{a} \left[\frac{\dot{H}}{H^2} + 1 \right] < 0 \quad \Rightarrow \quad \epsilon \equiv -\frac{\dot{H}}{H^2} < 1. \quad (1.18)$$

The definition of inflation can be stated as the period where the Hubble parameter evolves slowly, $\epsilon < 1$. Therefore, in the case where we have a de Sitter space ($\epsilon \rightarrow 0$), the space grows exponentially $a(t) \propto e^{Ht}$. So, from the equation (1.12), we see that this correspond to a period dominated by an equation of state with $\omega = -1$. The simplest example to generate such equation of state is given by the addition of a single scalar field, ϕ called *inflaton*, on top a rather flat potential. This is realized by the adding to the action (1.1), the following terms

$$S_\phi = \int d^4x \sqrt{-g} \left[\frac{1}{2} g^{\mu\nu} \partial_\mu \phi \partial_\nu \phi - V(\phi) \right], \quad (1.19)$$

where $V(\phi)$ is the scalar potential. For simplification, we will work in the units where $M_p = 1$, and M_p will be appropriately restored when we discuss cosmological applications. Assuming the scalar field is homogeneous $\phi(t, \mathbf{x}) = \phi(t)$, the equation of motion can be written as

$$\frac{\delta S_\phi}{\delta \phi} = \frac{1}{\sqrt{-g}} \partial_\mu (\sqrt{-g} g^{\mu\nu} \partial_\nu \phi) + \frac{\partial V(\phi)}{\partial \phi} = 0 \quad \Rightarrow \quad \ddot{\phi} + 3H\dot{\phi} + \frac{\partial V(\phi)}{\partial \phi} = 0, \quad (1.20)$$

and the Friedmann equations can be written as

$$H^2 = \frac{1}{3} \left(\frac{1}{2} \dot{\phi}^2 + V(\phi) \right), \quad (1.21)$$

$$\frac{\ddot{a}}{a} = H^2 \left(1 - \frac{\dot{\phi}^2}{H^2} \right). \quad (1.22)$$

If we assume a perfect fluid form, we can easily identify the energy density and the pressure as

$$\rho_\phi = \frac{1}{2} \dot{\phi}^2 + V(\phi), \quad (1.23)$$

$$P_\phi = \frac{1}{2} \dot{\phi}^2 - V(\phi). \quad (1.24)$$

Then, we can see that the ω parameter can be written as

$$\omega_\phi = \frac{P_\phi}{\rho_\phi} = \frac{\frac{1}{2} \dot{\phi}^2 - V(\phi)}{\frac{1}{2} \dot{\phi}^2 + V(\phi)}. \quad (1.25)$$

An equation of state with $\omega_\phi \simeq -1$, would require $\dot{\phi}^2 \ll V(\phi)$, *i.e.* the potential energy dominates the evolution of the scalar field, and the field ‘rolls slowly’. This condition can be also written as

$$\epsilon = -\frac{\dot{H}}{H^2} \sim \frac{\dot{\phi}}{V(\phi)} \ll 1. \quad (1.26)$$

If the friction term in equation (1.20) is large enough then $\dot{\phi} \sim \frac{1}{3H} \frac{\partial V}{\partial \phi}$ is an attractor solution. To be in this trajectory we would need to satisfy

$$\eta = -\frac{\ddot{\phi}}{H\dot{\phi}} \ll 1. \quad (1.27)$$

Both conditions (1.26) and (1.27) are called *slow-roll conditions*, and characterize the well-known ‘slow-roll inflation’. Once we adapt the slow-roll solution, we can express all parameter in terms of the scalar potential as

$$\epsilon \simeq \frac{1}{2} \left(\frac{\partial_\phi V}{V} \right)^2 \ll 1 \quad , \quad \eta \simeq \frac{(\partial_{\phi\phi} V)}{V} \ll 1. \quad (1.28)$$

As well we have that

$$H^2 \simeq \frac{V}{3} \simeq \text{const.} \quad , \quad a \sim e^{Ht}. \quad (1.29)$$

This period of accelerated expansion ends when ω cease to be -1, *i.e.* when $\epsilon \sim \eta \sim 1$.

We have seen how we can solve the horizon problem creating this new period before the Big Bang. However, how can we address the flatness problem? In order to see this, we need to look at the energy density fraction of the curvature Ω_{curv} , which is given by

$$\Omega_{curv} = -\frac{k}{a^2 H^2} \rightarrow 0 \text{ during inflation.} \quad (1.30)$$

Therefore, if we start with a given value at the beginning of inflation, lets say $\Omega_{curv}(a_{in}) = 1$, at the end of inflation is given by

$$\Omega_{curv}(a_{end}) = \Omega_{curv}(a_{in}) \frac{a_{in}^2}{a_{end}^2} \sim \frac{a_{in}^2}{a_{end}^2} = e^{-2N}, \quad (1.31)$$

where N is the number of e-folding defined as $N = \log\left(\frac{a_{end}}{a}\right)$ and it's used as a clock to measure the duration of inflation. So, if we observe that at the epoch of the Big Bang Nucleosynthesis (BBN), period where the first nuclei were form, the fraction is given by $\Omega_{curv}(a_{BBN}) \sim 10^{-18}$ and this epoch just started after inflation. The duration of the accelerated expansion should last around 20 e-folds but this value could change depending on the initial temperature of the Universe. In general if the temperature is around the GUT scale (10^{16} GeV), inflation should last around 60 e-folds.

All the previous discussion was purely at the classical level and described a uniform Universe, which is not what we observe. We still need to explain the temperature anisotropies found in the CMB as well as try to explain the formation of large scales structures. All these phenomena can be explained as consequences of quantum fluctuations of the inflaton field $\delta\phi$ and the metric $\delta g_{\mu\nu}$ around the homogeneous background. These fluctuations have substantial amplitudes only on scales close to the Planck length, but during the inflationary expansion they get stretched to galactic scales with almost unchanged amplitudes. Therefore, inflation links the large-scales structure with the microscopical aspects of the theory. Also we can give a clean explanation and prediction for the CMB anisotropies tracing them through the spectrum of these inhomogeneities. The most important measures of these fluctuations are the power spectrum P_k and P_h , associated to the scalar and tensor fluctuations respectively,

$$P_k = \Delta_{\mathcal{R}}^2(k) \quad , \quad \langle \mathcal{R}_k \mathcal{R}_{k'} \rangle = (2\pi)^3 \delta(\mathbf{k} + \mathbf{k}') \frac{2\pi^2}{k^3} \Delta_{\mathcal{R}}^2(k); \quad (1.32)$$

$$P_h = \Delta_h^2(k) \quad , \quad \langle h_k h_{k'} \rangle = (2\pi)^3 \delta(\mathbf{k} + \mathbf{k}') \frac{\pi^2}{k^3} \Delta_h^2(k), \quad (1.33)$$

where \mathcal{R} is the comoving curvature perturbation and h represent the degrees of freedom of the metric. Here, the subscript \mathbf{k} denotes the Fourier mode expansion of \mathcal{R} and h . The explicit form of the dimensionless power spectrum in the slow-roll approximation is given by

$$\Delta_{\mathcal{R}}^2(k) = \frac{1}{8\pi^2} \frac{H_*^4}{\dot{\phi}_*^2}, \quad \Delta_h^2(k) = 2 \left(\frac{H_*}{\pi} \right)^2. \quad (1.34)$$

Here the $*$ denotes the quantities are evaluated at horizon exit, *i.e.* when $k = aH$. Fluctuations that are scale invariant would require $\Delta_{\mathcal{R}}^2(k) = \text{constant}$. Therefore, deviation of this can be measure by the *spectral tilt*

$$n_s - 1 \equiv \frac{d \ln \Delta_{\mathcal{R}}^2}{d \ln k}. \quad (1.35)$$

For vanishing slow-roll parameter we would have never ending inflationary epoch and $n_s \approx 1$. Then, we expect a deviation of unity. In fact, the observed comological data is given by [7]

	Obs. constraints at $k_* = 0.05 \text{ Mpc}^{-1}$ with 68% CL
n_s	0.9650 ± 0.0050
$\frac{dn_s}{d \ln k}$	-0.009 ± 0.008

These observational constraints are important in order to construct a successful model of inflation. Still inflation is a hypothesis but until now there has not been a better explanation for the observed anisotropies of the Universe. In the section 1.4, we will introduce one of the possible playgrounds in which inflation could be realized. Inflation give us a possible explanation of some of the problems within the standard model of cosmology, however there is another unexplained puzzle in the Λ CDM which is the origin of Dark Matter (DM).

1.3 Dark Matter

DM is one of the largest and gravitationally dominant components of the Universe. Its origin, as we mentioned, is unknown. All the evidence for the existence of DM and constraints on its nature come from astronomy. We can infer from the CMB and large-scale structures that DM comprise around 27% of the density energy of the Universe. The electromagnetic properties of DM are severely constrained, because if dark matter had small electric charge, and either a small electric or magnetic dipole moment, it would couple to the photon-baryon fluid before recombination,

thus altering the sub-degree-scale features of the CMB as well as the matter power spectrum.

DM is part of a new sector of physics. We expect that is self-interacting or just interact with other new particles beyond the standard model (BSM). Even though these new BSM particles just interact within the ‘hidden sector’ and have no coupling with the SM, they might affect some astrophysical phenomena such as the structure of DM halos observe in galaxy clusters [19].

There has been a lot of proposal for the origin of this new particle, we enumerate few of the possible candidates as follows:

1. **Weakly-interacting massive particles (WIMPs).** This class of model was originally introduced by Steigman & Turner [23]. The model assumes the DM as a BSM particle, which is stable, initially in thermal equilibrium in the early Universe, and decoupling as a non-relativistic species. An interesting feature of the model is that it might make up for all DM in the Universe. If WIMPs are in thermal bath in the early Universe with other particles, having been born out of decays of the inflaton, then we can solve Boltzmann equations to find that WIMPs ‘freeze out’ at a comoving density that is inversely proportional to the WIMP annihilation cross section σ_a . Unless decays are important, this comoving number density is fixed for all future time. Using dimensional analysis, the annihilation cross section should be $\sigma \propto \alpha^2/m^2$, with $\alpha \sim 0.01$ and m the mass. Replacing this cross section into the early-Universe Boltzmann equations, the comoving number density of WIMPs matches the number density inferred from cosmological observations. This matching is known as ‘the WIMP miracle’.

Due to the fact that WIMPs only interact gravitationally and weakly, they are really difficult to detect. Basically, there exist two ways for their detection:

- *Direct detection:* This type of detection refers to observations of effects of a WIMP-nucleus collision as the DM passes through a detector in an Earth laboratory. There exist several techniques for this type of detections, such as *Cryogenic Crystal Detectors* used in the Cryogenic Dark Matter Search (CDMS), as well as *Noble Gas Scintillators* used by XENON and LUX-ZEPLIN experiments [20, 21].
- *Indirect detection.* Unlike direct detection that focused in detection in a laboratory, indirect detection focusses on locations where WIMP DM is thought to be more present such as: in centres of galaxies and galaxy clusters. Experiments essentially search for gamma rays excess, which are

predicted by Compton scattering. Problems with this type of detection is that the bounds will be model dependent. Experiments that have manage to put some bounds on WIMP annihilation is the Fermi-LAT gamma ray telescope [22].

2. **QCD axion.** Another candidate as DM particles is the QCD axion. The QCD axion was introduced by Pecci and Quinn (PQ) [24] as a possible solution of the CP problem of the strong interactions. The solution essentially come from the Chern-Simons term

$$\mathcal{L}_{\theta QCD} = \frac{\theta_{QCD}}{32 \pi^2} \text{Tr} G_{\mu\nu} \tilde{G}^{\mu\nu} , \quad (1.36)$$

where $G_{\mu\nu}$ is the gluon field and $\tilde{G}^{\mu\nu} = \epsilon^{\mu\nu\sigma\rho} G_{\sigma\rho}$ is the Hodge-dual. Here the trace is over the color indices of the SU(3) color group, and θ in this case is a constant. The extra contribution (1.36) does not affect the equation of motion of the G field, hence its name topological. The important feature of (1.36) is that it violates CP invariance explicitly, explaining the CP violation of the strong interaction. In order to restore the CP symmetry, we just need to set $\theta_{QCD} = 0$. The way in which PQ solve the CP problem was introducing two essential ingredients which are: the Goldstone theorem and non-perturbative effects. A global chiral $U(1)_{PQ}$ symmetry is introduced, which is broken spontaneously. Then, the Goldstone boson ϕ , the axion, with a vacuum expectation value (VEV) $\langle \phi \rangle = f_a/\sqrt{2}$, with f_a the axion ‘decay constant’. In the quantum theory the $U(1)_{PQ}$ symmetry is anomalous. Via the anomaly, the axion is couple to the QCD Chern-Simons term (1.36), where $\theta_{QCD} \propto \phi/f_a$. Since the only other term in the axion action is the kinetic term, we are free to shift the axion field by an arbitrary constant and absorb the value of θ_{QCD} into ϕ by a field redefinition, making ϕ/f_a dynamical. The non-perturbative effects come into play for the generation of the axion mass, through instantons contributions, which are classical solutions of the field equations. By dilution of these instantons a potential energy for the vacuum energy is generated

$$V_{vac} \propto \left[1 - \cos(\mathcal{C} \frac{\phi}{f_a}) \right] , \quad (1.37)$$

where \mathcal{C} is the color anomalous coefficient. The potential is easily minimize for $\mathcal{C} \frac{\langle \phi \rangle}{f_a} = 0 \text{ mod } 2\pi$, explaining why θ_{QCD} has such a small value. In the early universe, there is no reason for the QCD axion to sit exactly at the CP conserving minimum, and it is usually assumed that the initial position, ϕ_*/f_a ,

is of order of unity. Then, the QCD axion starts to oscillate about the CP conserving minimum around the QCD phase transition, and the coherently oscillating axion becomes DM.

3. **String axions.** In general, we can define axions as pseudoscalar fields enjoying the $U(1)_{PQ}$ PQ symmetry. Not necessarily they have to be the QCD axion explained above. For example, axions a_i arise in string compactifications from the integration of p -form gauge potentials A_p over p -cycles $C_{p,i}$ of the compact space

$$a_i = \int_{C_{p,i}} A_p. \quad (1.38)$$

In type IIB string theory, there are axions associated with the NS-NS two form B_2 , and the R-R forms C_2, C_4 . The generation of these fields will be discussed in section 1.4. These important fields can be used as building blocks for the construction of DM models, as we will present in the chapter 4.

4. **Primordial black holes (PBHs).** The only major non-particle candidate for DM are primordial black holes. PBHs are Black Holes (BHs) formed when local over density collapsed due to gravitational instabilities. The formation of these PBHs relies on the amplification of the density perturbations during inflation of order $\delta\rho \sim 0.1\rho$ collapsing to form a BH at horizon re-entry[25]. Recent detection of gravitational waves (GWs) emitted by a BH binary observed by the LIGO/VIRGO collaboration re-opened the consideration of DM as PBHs[26, 27].

As we can see we have a plethora of candidates for DM. In this work, we focus mainly on axions, as well as PBHs. All the models presented come from string compactifications. Therefore, it is natural to give some basic introduction to string theory.

1.4 String theory

As we just saw in section 1.2, the dynamics of the inflationary models are fully dependent of the scalar potential V of the inflaton field ϕ . The inflaton potential might suffer from fundamental problems such as instabilities of the flat region due to extra quantum corrections. Then, we need to build models where this flat region is protected by symmetries. A ‘top-down’ approach is one of the best ways to achieve such task. An example of these theories is given by string theory. String theory

can be defined as a theory in which the elementary objects are not point-like as in particle physics, but rather they are one-dimensional objects with a given length. In this section we want to give a brief review of string compactification. For further reading we recommend the following references [28, 29, 30, 31].

1.4.1 String compactification

The critical dimension of supersymmetric string theories is $D = 10$, which arise from the conservation of Lorentz invariance as a global symmetry. The dimension in string theory presents a big problem for the construction of possible realistic models. However, there exist some mechanisms, for instance, Kaluza-Klein (KK) compactification [32], in which the 10-dimensional space \mathcal{M}_{10} can be written as the product of a 4-dimensional space \mathcal{M}_4 times a compact space X_6 , that is, $\mathcal{M}_{10} = \mathcal{M}_4 \times X_6$. By making this assumption, we are saying that the metric of the full 10-dimensional space can be split as

$$ds_{10}^2 = g_{\mu\nu}(x) dx^\mu dx^\nu + \tilde{g}_{mn}(y) dy^m dy^n, \quad (1.39)$$

where x^μ and y^m are local coordinates on \mathcal{M}_4 and X_6 respectively. A possible generalization of this ansatz is considering the warped metric

$$ds_{10}^2 = e^{2A(y)} g_{\mu\nu}(x) dx^\mu dx^\nu + e^{-2A(y)} \tilde{g}_{mn}(y) dy^m dy^n, \quad (1.40)$$

where $A(y)$ is called the warp factor.

Under the branching of \mathcal{M}_{10} , the Lorentz group $SO(1, 9)$ breaks into

$$SO(1, 3) \times SO(6), \quad (1.41)$$

inducing a change in the transformation laws of different fields. For example, a vector A_M , $M = 0, \dots, 9$, transforming in the fundamental representation $\mathbf{10}$ of $SO(10)$ will be split in $\mathbf{10} = (\mathbf{4}, \mathbf{1}) \oplus (\mathbf{1}, \mathbf{6})$, where the first entry of the brackets represent the dimension of a $SO(1, 3)$ representation and the second a representation of dimension of $SO(6)$. In terms of fields, this branching means the presence of a vector A_μ , where $\mu = 0, \dots, 3$, of \mathcal{M}_4 transforming in the $(\mathbf{4}, \mathbf{1})$ of $SO(1, 3) \times SO(6)$ and six scalars A_m , where $m = 4, \dots, 9$, of \mathcal{M}_4 transforming in the $(\mathbf{1}, \mathbf{6})$.

The procedure applied above for a vector can be performed on spinors of $SO(1, 9)$ with the peculiar difference that spinors on \mathcal{M}_{10} will transform only as a spinors on \mathcal{M}_4 . For example, a Weyl spinor ψ in $D = 10$ transform in the $\mathbf{16}$ of $SO(1, 9)$

under the branching given in (1.41). More precisely,

$$\mathbf{16} = (\mathbf{2}_L, \mathbf{4}) \oplus (\mathbf{2}_R, \bar{\mathbf{4}}), \quad (1.42)$$

where $\mathbf{2}_L$ and $\mathbf{2}_R$ denote the left- and right-handedness under $SO(1, 3)$. Hence, we can see that KK compactification of spinors leads only to spinors on \mathcal{M}_4 .

Our main interest is to review compactifications which preserve supersymmetry. The condition of supersymmetry invariance under the compactification is non-trivial and quite restrictive and can be described as follows. In type II theories, we have 32 supercharges transforming locally on \mathcal{M}_{10} in the spinor representation of $SO(1, 9)$. If we want to have supersymmetry on \mathcal{M}_4 after the compactification, a subset of these supercharges have to be well defined on X_6 , that is, only the subset of supercharges that remain invariant under a parallel transport through a closed path C will lead to supersymmetry on \mathcal{M}_4 . Hence, the condition of supersymmetry invariance after the compactification is translated to the existence of 6-dimensional Killing spinors $\xi(y^m)$ on X_6 , which satisfies

$$\nabla_{X_6} \xi(y^m) = 0, \quad (1.43)$$

where $\nabla_{X_6} = \partial_m + \omega_m^{AB} \frac{1}{4} \Gamma_{AB}$, where $A, B, m = 1, \dots, 6$, Γ_{AB} is the generator of the spinor representation of $SO(6)$, and ω_m^{AB} is the spin connection.

The existence of the Killing spinors to preserve supersymmetry on the compactification can be seen in terms of the *holonomy group* H of X_6 . The set of rotations suffered by the spinors for all possible closed paths C on X_6 , in general given by $SO(6)$, is called *holonomy group* H of X_6 . The case in which $H = SO(6)$, any of the spinors get unrotated, as we can see in (1.42) (none of the spinors are singlets of $SO(6)$). In order to preserve supersymmetry on \mathcal{M}_4 , X_6 have to be a manifold with *special holonomy group* H' . A simple example is the case when we take $H' = SU(3)$ ($SO(6) \supset SU(3)$), then after the compactification we have

$$\begin{aligned} SO(1, 9), & \longrightarrow SO(1, 3) \times SO(6), & \longrightarrow & SO(1, 3) \times SU(3), \\ \mathbf{16}, & (\mathbf{2}_L, \mathbf{4}) \oplus (\mathbf{2}_R, \bar{\mathbf{4}}), & (\mathbf{2}_L, \mathbf{3}) \oplus (\mathbf{2}_R, \bar{\mathbf{3}}) \oplus (\mathbf{2}_L, \mathbf{1}) \oplus (\mathbf{2}_R, \mathbf{1}). \end{aligned} \quad (1.44)$$

Choosing $H' = SU(3)$, we manage to find 2 spinors Q_α and $\bar{Q}_{\dot{\alpha}}$ transforming into $\mathbf{2}_L, \mathbf{2}_R$ of $SO(1, 3)$, respectively, hence leading to $\mathcal{N} = 2$ supersymmetry on \mathcal{M}_4 .

1.4.2 Calabi-Yau manifolds

A set of manifolds with $SU(N)$ holonomy groups have been classified and are called Calabi-Yau manifolds or Calabi-Yau N -folds (CY_N). A Calabi-Yau manifold is a $2N$ -dimensional Ricci-flat Kähler manifold. There are several examples of these spaces. A very simple and often used example is the torus T^2 with $SU(1)$ holonomy. Another famous example is the Z -manifold which can be found by solving the singularities of the T^6/\mathbb{Z}_3 orbifold. The last example is the $K3$ complex surface which has $SU(2)$ holonomy.

In the following discussion, we will focus only on compact Calabi-Yau 3-folds but this can be easily generalized to Calabi-Yau N -folds. Every compact CY_3 manifold is equipped with a mixed tensor I_m^n , where $m, n = 1, \dots, 6$, satisfying $I_m^n I_\ell^n = -\delta_\ell^m$ which is called the complex structure, and a $(3, 0)$ holomorphic harmonic form Ω_3 called the complex volume form. On a real basis (y^j, \tilde{y}^j) , where $j = 1, 2, 3$, I_m^n can be written as

$$I = \begin{pmatrix} 0 & \mathbb{I}_3 \\ -\mathbb{I}_3 & 0 \end{pmatrix}. \quad (1.45)$$

Making use of I_m^n and (y^j, \tilde{y}^j) , we can construct a set of local complex coordinates (z^j, \bar{z}^j) with $j = 1, 2, 3$, as

$$dz^j = dy^j + iI_i^j \tilde{y}^i, \quad d\bar{z}^j = dy^j - iI_i^j \tilde{y}^i. \quad (1.46)$$

In this basis, the only non zero components of the metric \tilde{g}_{mn} are the ones with mixed indices $g_{i\bar{j}}$, where the index i (\bar{j}) means the components contracted with dz^i ($d\bar{z}^j$). Therefore, using the metric to lower down one index of I_i^j , we find a $(1, 1)$ form. Then, we can write

$$J = ig_{i\bar{j}} dz^i \wedge \bar{z}^{\bar{j}}, \quad (1.47)$$

where the factor i is just convention. If J is a closed form ($dJ = 0$), then it is called the Kähler form. On this basis the volume forms Ω_3 can be written as

$$\Omega_3 = (dy^1 + iI_1^i \tilde{y}^i) \wedge (dy^2 + iI_2^i \tilde{y}^i) \wedge (dy^3 + iI_3^i \tilde{y}^i). \quad (1.48)$$

For example, on a torus $T^6 = T^2 \times T^2 \times T^2$ is

$$\Omega_3 = (dy^1 + iU_1 \tilde{y}^1) \wedge (dy^2 + iU_2 \tilde{y}^2) \wedge (dy^3 + iU_3 \tilde{y}^3), \quad (1.49)$$

satisfy the correct geometrical properties.

1.4.3 Moduli space

As mentioned in Section 1.4.1, the splitting of the 10-dimensional space-time \mathcal{M}_{10} implies the branching of the metric as shown in (1.39). We can see this branching as the dimensional reduction of the metric, that is, we can look for the zero modes of the 10-dimensional metric. These zero modes are exactly the 4-dimensional metric $g_{\mu\nu}$, and a set of scalars \tilde{g}_{mn} (from the 4-dimensional point of view), which give origin to the internal metric.

Since, we are interested in supersymmetric invariant compactifications, which implies compactifications on Calabi-Yau manifolds having a special holonomy metric. Studying fluctuations of this metric, we can find a number of ways in which the background metric can be deformed preserving supersymmetry and its Calabi-Yau topology. The vev's of these deformations are called *moduli fields*.

In order to study the metric fluctuations, we just have to analyze small variations of the metric

$$\tilde{g}_{mn} \longrightarrow \tilde{g}_{mn} + \delta\tilde{g}_{mn}, \quad (1.53)$$

and demand that the new background still satisfies the Calabi-Yau conditions. In particular,

$$R(\tilde{g} + \delta\tilde{g}) = 0. \quad (1.54)$$

Imposing this condition leads to differential equations of δg . The number of solutions of these equations give the number of independent ways in which the metric can be deformed preserving supersymmetry and the topology. Using the basis (z^j, \bar{z}^j) introduced in (1.46), it can be proved that the equations for the mixed components $\delta g_{i\bar{j}}$ and the pure components δg_{ij} decouple. Each of these solutions have different geometric meaning, which is explained below.

- $\delta g_{i\bar{j}}$

The deformations $\delta g_{i\bar{j}}$ are closely related to fluctuations of the Kähler form J , because $J_{i\bar{j}} = ig_{i\bar{j}}$. To discuss these fluctuations is equivalent to discuss about Kähler form deformations. To ensure positiveness of the metric, we need to impose

$$\int_C J > 0 \quad , \quad \int_S J \wedge J > 0 \quad , \quad \int_{X_6} J \wedge J \wedge J > 0, \quad (1.55)$$

for any path C and surface S on X_6 . The Kähler form can not be an exact form, ($J \neq df$) because $\int J \wedge J \wedge J \propto$ volume of X_6 . Precisely,

$$\mathcal{V} = \frac{1}{6} \int_{X_6} J \wedge J \wedge J, \quad (1.56)$$

where \mathcal{V} is the volume of X_6 . Since J is not an exact form, this implies that it is cohomologically non-trivial. Then, J can be written in a basis ω_a of $H^{1,1}(X_6)$ as

$$J = \sum_{a=1}^{h^{1,1}} t^a \omega_a, \quad (1.57)$$

where the coefficients t^a are called the Kähler moduli. The geometric interpretations of these moduli is that they control the size of the 2-cycles of X_6 .

On string theory, in particular on type IIB compactifications, the Kähler form receives a contribution from the compactification of the Ramond/Ramond 4-form \hat{C}_4 .

- δg_{ij}

In this case, the fluctuations δg_{ij} are related to symmetric deformations of the holomorphic or anti-holomorphic form Ω_3 . We can not expand δg_{ij} on a basis of $H^{2,0}(X_6)$ because $h^{2,0} = 0$. Making use of Ω_3 we can put $H^{2,0}(X_6)$ in one to one correspondence with $H^{1,2}(X_6)$ in the following way

$$\delta g_{ij} = \frac{i}{\|\Omega_3\|^2} \bar{U}^\alpha (\bar{\chi}_\alpha)_{i\bar{k}\bar{\ell}} \Omega_j^{\bar{k}\bar{\ell}}, \quad (1.58)$$

where $\|\Omega_3\|^2 = \Omega_{ijk} \bar{\Omega}^{ijk}/3!$ and χ_α is a basis for $H^{1,2}(X_6)$ with $\alpha = 1, \dots, h^{1,2}$. The coefficients U^α are called the complex structure moduli.

In the end, at tree level, the full moduli space can be separated as

$$\mathcal{M}_{moduli} = \mathcal{M}_{h^{1,1}}^K \times \mathcal{M}_{h^{1,2}}^{cs}, \quad (1.59)$$

where \mathcal{M}^K and \mathcal{M}^{cs} are spaces parametrized by t^a and U^α , respectively.

1.4.4 Orientifolds

The idea of orientifolds came from the construction of orbifold compactifications in which the worldsheet parity Ω is gauged away. The worldsheet parity Ω interchanges

the left movers with the right movers. Gauging away this symmetry leads to a collection of non-oriented surfaces spanned by string propagation. These ideas have been carried out on Calabi-Yau compactifications. In these cases, together with the parity Ω an internal symmetry σ , which acts solely on X_6 and leave \mathcal{M}_4 untouched, is modded out. One can show that for 3-folds, σ leaves the Kähler form J invariant but acts non-trivially on Ω_3 . Depending on the transformation properties of Ω_3 two different symmetry operations \mathcal{O} can be modded out, that is,

$$\mathcal{O}_\epsilon = (-1)^{\epsilon F_L} \Omega \sigma^* \quad , \quad \sigma^* \Omega_3 = (-1)^\epsilon \Omega_3 \quad , \quad \epsilon = 0, 1. \quad (1.60)$$

Here, F_L is the space-time fermion number in the left moving sector and σ^* denotes the action of σ on forms. Modding out by \mathcal{O}_0 , leads to the possibility of having O5- and O9-planes while \mathcal{O}_1 allows O3- and O7-planes.

We are interested in studying the orientifold compactifications of type IIB string theory. Before going through the orientifold compactification, let us review the simplest compactification of type IIB string theory on a Calabi-Yau 3-fold. The massless spectrum of type IIB string theory in $D = 10$ consists in:

- NSNS sector: the dilaton φ , a 2-form \hat{B}_2 , and the graviton (metric) \hat{g} ;
- RR sector: the axion C_0 , a 2-form \hat{C}_2 , and a 4-form \hat{C}_4 with field strength self-dual.

Under the compactification on a Calabi-Yau 3-fold, these 10-dimensional field will change. For instance, the dilaton and the axion will remain massless scalar fields under the compactification but the metric g is split as (1.39). On the other hand, the forms on the spectrum have the following decomposition:

- NSNS sector.

In the NSNS sector, we only have the form \hat{B}_2 .

	Decomposition	Degeneracy
\hat{B}_2 :	$B_{\mu\nu}$	1
	$B_{\mu m}$	$h^{1,0} + h^{0,1} = 0$
	B_{mn}	$h^{2,0} + h^{1,1} + h^{0,2} = h^{1,1}$

(1.61)

where $\mu, \nu = 0, \dots, 3$ and $m, n = 1, \dots, 6$. Using the basis ω_a of $H^{1,1}(X_6)$, we can write

$$\hat{B}_2 = B_2(x) + b^a(x)\omega_a \quad , \quad a = 1, \dots, h^{1,1}. \quad (1.62)$$

Here, B_2 is a 4-dimensional two form and b^a 's are a set of 4-dimensional scalar fields.

- RR sector.

In this case, we have two forms \hat{C}_2 and \hat{C}_4 . The decomposition of \hat{C}_2 is exactly same as \hat{B}_2 . Therefore, we show only the decomposition of \hat{C}_4 .

	Descomposition	Degeneracy
\hat{C}_4 :	$C_{\mu\nu\sigma\rho}$	1
	$C_{\mu\nu\sigma m}$	$h^{1,0} + h^{0,1} = 0$
	$C_{\mu\nu mn}$	$h^{2,0} + h^{1,1} + h^{0,2} = h^{1,1}$
	$C_{\mu mn l}$	$h^{3,0} + h^{1,2} + h^{2,1} + h^{0,3} = 2h^{1,2} + 2$
	$C_{mnl p}$	$h^{2,2} = h^{1,1}$

(1.63)

As before, we can write \hat{C}_2 and \hat{C}_4 as

$$\hat{C}_2 = C_2(x) + c^a(x)\omega_a, \quad a = 1, \dots, h^{1,1} \quad (1.64)$$

$$\hat{C}_4 = D_2^a(x) \wedge \omega_a + V^K(x) \wedge \alpha_K - Q_K(x) \wedge \beta^K + \rho_a(x)\tilde{\omega}^a, \quad K = 0, \dots, h^{1,2}. \quad (1.65)$$

Here, we are using a basis $\tilde{\omega}^a$ of $H^{2,2}(X_6)$, which is dual to ω_a , and a real symplectic basis (α_K, β^K) of $H^3(X_6)$, which satisfies

$$\int \alpha_K \wedge \beta^L = \delta_K^L, \quad \int \alpha_K \wedge \alpha_L = \int \beta^K \wedge \beta^L = 0. \quad (1.66)$$

The 4-dimensional fields appearing in (1.64) and (1.65) are the scalar fields $c^a(x)$, $\rho_a(x)$, the 1-forms $V^K(x)$, $Q_K(x)$, and the 2-forms $C_2(x)$, $D_2^a(x)$. The 4-form $C_{\mu\nu\sigma\rho}$ has no dynamics because is proportional to the 4-dimensional volume form $\epsilon_{\mu\nu\sigma\rho}$. The self-duality of the field stretch of \hat{C}_4 removes half of the degrees of freedom. In favour of V^K and ρ_a , we choose to eliminate D_2^a and Q_K . The other choice is possible, which leads to a different spectrum but we are not considering this case. We need to keep in mind that we still have the geometric moduli t^a and U^α coming from the metric deformations.

Altogether, the $\mathcal{N}=2$ massless 4-dimensional spectrum of type IIB on a Calabi-Yau 3-fold consists in:

- one gravity multiplet $(g_{\mu\nu}, V^0)$;

- $h^{1,2}$ vector multiplets (V^α, U^α) ;
- $h^{1,1}$ hypermultiplets (t^a, b^a, c^a, ρ_a) ;
- one double tensor multiplet (B_2, C_2, φ, C_0) ;
- one 4-form C_4 .

Every multiplet has its fermionic components, which are not shown here. To get the orientifold compactification we need to mod out the non-invariant states under the action of $(-1)^{\epsilon F_L} \Omega \sigma^*$. The projection of the states is explained in the following section.

1.4.5 $\mathcal{N} = 1$ Type IIB Orientifold

The models present in the next chapters are based on one type of orientifold compactification, we will focus only on $\epsilon = 1$ having possible O3/O7-planes. To project out the states in the spectrum, we need to know how $(-1)^{F_L} \Omega \sigma^*$ acts on the fields. The field transformations under Ω and F_L are well known. Under the worldsheet parity, Ω the fields φ , \hat{g} , and \hat{C}_2 are even while \hat{B}_2 , C_0 and \hat{C}_4 are odd. The operator $(-1)^{F_L}$ leaves NSNS fields invariant but changes the sign in the RR sector. The new ingredient is the addition of the internal symmetry σ , which acts on the Calabi-Yau but leaves \mathcal{M}_4 invariant. Other requirements of σ are: to be an involution ($\sigma^2 = 1$) and to act holomorphically on the Calabi-Yau coordinates. With all these information, we can easily check that φ , C_0 , \hat{g} , and \hat{C}_4 are even under $(-1)^{F_L} \Omega$ while \hat{B}_2 and \hat{C}_2 are odd. Therefore, we can deduce the action of σ^* on the 10-dimensional forms as

$$\begin{aligned}
\sigma^* \varphi &= \varphi & , & & \sigma^* C_0 &= C_0, \\
\sigma^* \hat{g} &= \hat{g} & , & & \sigma^* \hat{C}_2 &= -\hat{C}_2, \\
\sigma^* \hat{B}_2 &= -\hat{B}_2 & , & & \sigma^* \hat{C}_4 &= \hat{C}_4.
\end{aligned} \tag{1.67}$$

keeping in mind that σ has to satisfy $\sigma^* J = J$ and $\sigma^* \Omega_3 = -\Omega_3$.

Since σ is a holomorphic involution, the cohomology groups $H^{p,q}(X_6)$ split into two eigenspaces under σ^* , that is

$$H^{p,q}(X_6) = H_+^{p,q}(X_6) \oplus H_-^{p,q}(X_6), \tag{1.68}$$

where the $+$ ($-$) shows whether the elements of the group are even (odd) under the action of σ^* . The dimension of $H^{p,q}(X_6)$ became $h^{p,q} = h_+^{p,q} + h_-^{p,q}$, where $h_+^{p,q} = \dim H_+^{p,q}(X_6)$ and $h_-^{p,q} = \dim H_-^{p,q}(X_6)$. All of these hodge numbers are not

independent. The action of σ^* fix them. For instance, in a Calabi-Yau 3-fold we have:

- $h_{\pm}^{1,1} = h_{\pm}^{2,2}$ because the Hodge $*$ -operator commutes with σ^* ;
- $h_{\pm}^{2,1} = h_{\pm}^{1,2}$ due to the holomorphicity of σ ;
- $h_{+}^{3,0} = h_{-}^{0,3} = 0$ and $h_{-}^{3,0} = h_{-}^{0,3} = 1$ because we need to satisfy $\sigma^* \Omega_3 = -\Omega_3$;
- $h_{+}^{0,0} = h_{+}^{3,3} = 1$ and $h_{-}^{0,0} = h_{-}^{3,3} = 0$ because the volume form, which is proportional to $\Omega_3 \wedge \bar{\Omega}_3$, is σ^* invariant.

Collecting all the transformation laws under the action of $(-1)^{FL} \Omega \sigma^*$, we can write the invariant in each sector as:

- NSNS sector.

In this sector the invariant states are the dilaton φ and the metric g splits as described in (1.39), where deformations of \tilde{g}_{mn} give rise to the geometric moduli t^a and U^α . Under the projection σ^* , the Kähler form is even while the (3,0)-form is odd. Then, we can write

$$J = t^{a+}(x)w_{a+} \quad , \quad a_+ = 1, \dots, h_+^{1,1}. \quad (1.69)$$

For deformations of the metric δg_{ij} , we find that

$$\delta g_{ij} = \frac{i}{\|\Omega_3\|^2} \bar{U}^{\alpha-} (\bar{\chi}_{\alpha-})_{i\bar{k}\bar{l}} \Omega_j^{\bar{k}\bar{l}} \quad , \quad \alpha_- = 1, \dots, h_-^{1,2}. \quad (1.70)$$

Here we are using bases ω_{a+} and $\bar{\chi}_{\alpha-}$ of $H_+^{1,1}(X_6)$ and $H_-^{1,2}(X_6)$, respectively. Using (1.67), we can mod out all the even components of \hat{B}_2 on (1.62) which gives

$$\hat{B}_2 = b^{a-}(x)\omega_{a-} \quad , \quad a_- = 1, \dots, h_-^{1,1}, \quad (1.71)$$

where ω_{a-} is a basis for $H_-^{1,1}(X_6)$.

- RR sector.

In this case, we have to perform the projection (1.67) on the forms C_0 , \hat{C}_2 , and \hat{C}_4 . We find that C_0 is invariant, and only the odd part of \hat{C}_2 and the

even part \hat{C}_4 survive. Therefore, we can write

$$\hat{C}_2 = c^{a-}(x)\omega_{a-} \quad , \quad a_- = 1, \dots, h_-^{1,1} \quad (1.72)$$

$$\hat{C}_4 = D_2^{a+}(x) \wedge \omega_{a+} + V^\kappa(x) \wedge \alpha_\kappa - Q_\kappa(x) \wedge \beta^\kappa + \rho_{a+}(x)\tilde{\omega}^{a+}, \quad \kappa = 1, \dots, h_+^{1,2}. \quad (1.73)$$

Here we are using the bases ω_{a-} and $\tilde{\omega}_{a+}$ of $H_-^{1,1}(X_6)$ and $H_+^{2,2}(X_6)$, respectively. Also we introduced a symplectic basis $(\alpha_\kappa, \beta^\kappa)$ of $H^3(X_6)$, which satisfies (1.66) with $K, L \rightarrow \kappa, \lambda$.

The 4-dimensional fields on (1.71), (1.72), and (1.73) are three scalar fields $b^{a-}(x)$, $c^{a-}(x)$, and $\rho_{a+}(x)$, two 1-forms $V^\kappa(x)$, $Q_\kappa(x)$, and one 2-form $D_2^{a+}(x)$. Again the self duality of the field strength of \hat{C}_4 removes half of the degrees of freedom and keep only (V^κ, ρ_{a+}) . Altogether the $\mathcal{N}=1$ massless 4-dimensional spectrum consist in:

- One gravitational multiplet $g_{\mu\nu}$;
- $h_+^{1,2}$ vector multiplets V_κ ;
- $h_-^{1,1} + h_-^{1,2} + 1$ chiral multiplets $(b^{a-}, c^{a-}, \rho_{a+}, t^{a+}, U^{\alpha-}, \varphi, C_0)$.

After the compactification, we will work with the 4-dimensional low energy effective theory. It is established that the $\mathcal{N}=1$ 4-dimensional supergravity action is expressed in terms of the Kähler potential K , a holomorphic superpotential W , and a holomorphic gauge-kinetic coupling functions f , which is given by [33]

$$S_{(4)} = -\frac{1}{2} \int R * 1 + K_{I\bar{J}} D\Phi^I \wedge * D\bar{\Phi}^{\bar{J}} + \text{Re} f_{ab} F^a \wedge * F^b + \text{Im} f_{ab} F^a \wedge F^b + 2V * 1 \quad (1.74)$$

where

$$V = e^K \left(K^{I\bar{J}} D_I W D_{\bar{J}} \bar{W} - 3|W|^2 \right) + \frac{1}{2} (\text{Re} f)^{-1\kappa\lambda} D_\kappa D_\lambda. \quad (1.75)$$

Here, R is the Ricci scalar, Φ^I is the set of scalars fields $(b^{a-}, c^{a-}, \rho_{a+}, t^{a+}, U^{\alpha-}, \varphi, C_0)$, and $K_{I\bar{J}}$ is a Kähler metric satisfying $K_{I\bar{J}} = \partial_I \partial_{\bar{J}} K(\Phi, \bar{\Phi})$. It is important to say that the powers of M_p will be restored when cosmological applications are discussed. The potential V is given in terms of the covariant derivative $D_I W = \partial_I W + (\partial_I K) W$ and the D-terms given as

$$D_\kappa = \left[K_I + \frac{W_I}{W} \right] (T_\kappa)_{IJ} \Phi_J, \quad (1.76)$$

where T_κ are the generators of the gauge group.

The fields Φ_I in the action (1.74) are not necessarily $(b^{a-}, c^{a-}, \rho_{a+}, t^{a+}, U^{\alpha-}, \varphi, C_0)$. For $O3/O7$ -planes, one finds [34]

- The axion/dilaton $S = e^{-\varphi} - iC_0^1$;
- Two-form moduli $G^{a-} = c^{a-} - iSb^{a-}$, $a_- = 1, \dots, h_-^{1,1}$;
- Complex structure moduli $U^{\alpha-}$, $\alpha_- = 1, \dots, h_-^{1,2}$;
- Kähler moduli

$$T_{a_+} = \tau_{a_+} - \frac{1}{2(S + \bar{S})} k_{a_+b_-c_-} G^{b_-} (G - \bar{G})^{c_-} + i\rho_{a_+}. \quad (1.77)$$

The variable τ_{a_+} must be understood as a function of the t^{a_+} and is given by

$$\tau_{a_+} = \frac{\partial \mathcal{V}}{\partial t^{a_+}}, \quad (1.78)$$

where \mathcal{V} is the volume of X_6 given by (1.56). The coefficients $k_{a_+b_-c_-}$ are called the intersection numbers and are defined as

$$k_{a_+b_-c_-} = \int_{X_6} \omega_{a_+} \wedge \omega_{b_-} \wedge \omega_{c_-}. \quad (1.79)$$

In terms of the intersection numbers \mathcal{V} can be written as $\mathcal{V} = \frac{1}{6} k_{abc} t^a t^b t^c$. Then,

$$\tau_{a_+} = \frac{1}{2} k_{a_+b_-c_-} t^{b_-} t^{c_-}. \quad (1.80)$$

With these new variables, the Kähler potential can be written as

$$\begin{aligned} K_{tree} &= K_k(S, T, G) + K_S(S, \bar{S}) + K_{cs}(U, \bar{U}) \\ &= -2 \ln[\mathcal{V}] - \ln[S + \bar{S}] - \ln \left[-i \int \Omega_3(U) \wedge \bar{\Omega}_3(\bar{U}) \right], \end{aligned} \quad (1.81)$$

where the volume $\mathcal{V} = \mathcal{V}(T + \bar{T})$.

From now on, we will only consider compactifications with $h_-^{1,1} = 0$, which implies $h_+^{1,1} = h_+^{1,1}$. Therefore, the Kähler form can be written as (1.57) and the Kähler moduli became

$$T_a = \tau_a + i\rho_a. \quad (1.82)$$

¹Also there exist the definition $\tau = iS = C_0 + ie^{-\varphi}$.

For the case in which $h_+^{1,1} = 1$ its easy to find the form of the Kähler potential $K_k(S, T, G)$, which becomes

$$K_k = -3 \ln [T + \bar{T}]. \quad (1.83)$$

With all this information, the resulting moduli space to work (at tree level) is

$$\mathcal{M}_{moduli} = \mathcal{M}_{h_-^{1,2}}^{cs} \times \mathcal{M}_{h^{1,1}+1}^K, \quad (1.84)$$

where the 1 in \mathcal{M}^K is the axion/dilaton.

Let us consider the low energy approximation of the type IIB string theory compactified on a Calabi-Yau in presence of a non-trivial background composed by NSNS and RR 3-forms H_3 and F_3 , respectively. The interaction of these forms is purely gravitational which shows that the 10-dimensional space \mathcal{M}_{10} does not split in the product $\mathcal{M}_4 \times X_6$. The full solution is described as follows.

The 10-dimensional action of type IIB supergravity in Einstein frame is given by [31]

$$\begin{aligned} S_{\text{IIB}} = & \frac{1}{2\kappa_{10}^2} \int d^{10}x \sqrt{-g} \left(R - \frac{\partial_M \tau \partial^M \bar{\tau}}{2(\text{Im}\tau)^2} - \frac{1}{2}|F_1|^2 - \frac{|G_3|^2}{2\text{Im}\tau} - \frac{1}{4}|\tilde{F}_5|^2 \right) \\ & + \frac{1}{2\kappa_{10}^2} \int C_4 \wedge \frac{G_3 \wedge \bar{G}_3}{4i \text{Im}\tau} + S_{\text{local}}. \end{aligned} \quad (1.85)$$

Here $2\kappa_{10}^2 = (2\pi)^7 \alpha'^4$, with $\alpha' = \frac{1}{2\pi T}$ where T is the string tension. The fields in the action (1.85) are

$$\tau = C_0 + ie^{-\varphi} \quad , \quad G_3 = F_3 - \tau H_3, \quad (1.86)$$

with $H_3 = dB_2$ and $F_3 = dC_2$, and

$$\tilde{F}_5 = F_5 - \frac{1}{2}C_2 \wedge H_3 + \frac{1}{2}B_2 \wedge F_3, \quad (1.87)$$

with $F_5 = dC_4$. The self-duality condition $*_{10}\tilde{F}_5 = \tilde{F}_5$ is imposed at the level of the equations of motion. The term S_{local} is the action of localized objects of the 10-dimensional supergravity fields, for instance, D3-branes or O3-planes.

We are considering compactifications with warped metric (1.40) and components

of G_3 only along the compact directions. Precisely,

$$ds_{10}^2 = e^{2A(y)} \eta_{\mu\nu} dx^\mu dx^\nu + e^{-2A(y)} \tilde{g}_{mn}(y) dy^m dy^n, \quad (1.88)$$

$$\mathcal{L}_G = -\frac{1}{4\kappa_{10}^2} \int d^{10}x \sqrt{-g} \frac{|G_3|^2}{\text{Im}\tau} = -\frac{1}{8\kappa_{10}^2} \int_{X_6} d^6y \frac{G_3 \wedge *_6 \bar{G}_3}{\text{Im}\tau}. \quad (1.89)$$

In addition, we set $F_1 = 0$ and $\tau = \text{constant}$. Furthermore, we require H_3 and F_3 to be source-less ($dH_3 = 0$, $dF_3 = 0$) and to satisfy the Dirac quantization condition

$$\frac{1}{2\pi\alpha'} \int_\gamma F_3 \in 2\pi\mathbb{Z}_\gamma, \quad \frac{1}{2\pi\alpha'} \int_\gamma H_3 \in 2\pi\mathbb{Z}_\gamma, \quad (1.90)$$

where γ 's are 3-cycles in X_6 . Assuming 4-dimensional Poincaré invariance, we propose

$$\tilde{F}_5 = (1 + *_{10}) [d\alpha \wedge dx^0 \wedge dx^1 \wedge dx^2 \wedge dx^3], \quad (1.91)$$

where the function α only depends on the compact directions y^m with $m = 1, \dots, 6$.

We want to find restrictions for the ansatz (1.88), (1.89), and (1.91), that is, restrictions for the form G_3 , the function $\alpha(y)$, and the warp factor $A(y)$. It is known that under these assumptions G_3 is an imaginary self-dual (ISD) form and $\alpha = e^{4A}$ [35]. In order to prove this statement we use of the equations of motion.

The equation of motion for the non-compact components of the metric is²

$$R_{\mu\nu} = -\eta_{\mu\nu} e^{2A} \left(\frac{G_{mnp} \bar{G}^{mnp}}{48 \text{Im}\tau} + \frac{e^{-8A}}{4} \partial_m \alpha \partial^m \alpha \right) + \kappa_{10}^2 \left(T_{\mu\nu}^{\text{loc}} - \frac{1}{8} \eta_{\mu\nu} e^{2A} T^{\text{loc}} \right) \quad (1.92)$$

For the contractions of the indices m , n , and p , we use the Calabi-Yau metric \tilde{g}_{mn} . Using the ansatz for the metric (1.88), we can compute the non-compact components of the Ricci tensor $R_{\mu\nu}$, given by

$$R_{\mu\nu} = -\eta_{\mu\nu} e^{4A} \left(\partial_n \partial^n A + \tilde{\Gamma}_{mn}^m \partial^n A \right) \equiv -\eta_{\mu\nu} e^{4A} \tilde{\nabla}^2 A, \quad (1.93)$$

where $\tilde{\Gamma}_{mn}^p$ are the Christoffel symbols using the metric \tilde{g}_{mn} . We can rewrite the equation (1.93) as

$$-\eta_{\mu\nu} e^{4A} \tilde{\nabla}^2 A = -\frac{1}{4} \left(\tilde{\nabla}^2 e^{4A} - e^{-4A} \partial_m e^{4A} \partial^m e^{4A} \right). \quad (1.94)$$

²The computation of the equations of motion for the action (1.85) are in the Appendix A.

Replacing this equation in (1.92) and then tracing, we find

$$\tilde{\nabla}^2 e^{4A} = e^{2A} \frac{G_{mnp} \tilde{G}^{mnp}}{12 \text{Im}\tau} + e^{-6A} [\partial_m \alpha \partial^m \alpha + \partial_m e^{4A} \partial^m e^{4A}] + \frac{\kappa_{10}^2}{2} e^{2A} (T_m^m - T_\mu^\mu)^{\text{loc}} \quad (1.95)$$

In addition, we have the equation of motion/Bianchi identity for the RR 5-form

$$d\tilde{F}_5 = d *_{10} \tilde{F}_5 = H_3 \wedge F_3 + 2\kappa_{10}^2 \mu_3 \rho_3^{\text{loc}}, \quad (1.96)$$

where $\mu_3 \rho_3^{\text{loc}}$ is the localized source contribution coming from the D3-branes and O3-planes. In terms of the function, α , (1.96) can be written as

$$\tilde{\nabla}^2 \alpha = i e^{2A} \frac{G_{mnp} (*_6 \tilde{G}^{mnp})}{12 \text{Im}\tau} + 2e^{-6A} \partial_m \alpha \partial^m e^{4A} + 2\kappa_{10}^2 e^{2A} \mu_3 \rho_3^{\text{loc}}. \quad (1.97)$$

Now, subtracting equations (1.95) with (1.97), we obtain

$$\tilde{\nabla}^2 (e^{4A} - \alpha) = \frac{e^{2A}}{12 \text{Im}\tau} |iG_3 - *_6 G_3|^2 + e^{-6A} |\partial(e^{4A} - \alpha)|^2 + 2\kappa_{10}^2 e^{2A} \left[\frac{1}{4} (T_m^m - T_\mu^\mu)^{\text{loc}} - \mu_3 \rho_3^{\text{loc}} \right]. \quad (1.98)$$

By integrating the above expression over X_6 , we find that the left-hand side becomes zero and all the terms in the right-hand side are positive, assuming $\frac{1}{4} (T_m^m - T_\mu^\mu)^{\text{loc}} = \mu_3 \rho_3^{\text{loc}}$. Therefore, we obtain conditions for G_3 and α , which are:

- Imaginary self-duality (ISD): $*_6 G_3 = iG_3$;
- $\alpha = e^{4A}$.

As we will see in the section 2.2, the ISD condition is important for having supersymmetric invariant 4-dimensional space.

From the Bianchi equation (1.96), we find another important condition, which has to be satisfied. This condition constraints the values of the number of D3-branes and O3-planes in the theory. We can find it as follows. Integrating the equation (1.96) over the compact space X_6 gives

$$\frac{1}{2\kappa_{10}^2 \mu_3} \int_{X_6} H_3 \wedge F_3 + Q_3^{\text{loc}} = 0, \quad (1.99)$$

where Q_3^{loc} is the total charge of the localized objects, for examples, D3-branes and O3-planes. Recalling the definitions of $2\kappa_{10}^2 = (2\pi)^7 \alpha'^4$, $\mu_3 = (2\pi)^{-3} \alpha'^{-2}$, and the

charge of O3-planes $-\frac{1}{4}\mu_3$, we can write [31]

$$\frac{1}{2}N_{\text{flux}} + N_{\text{D3}} - \frac{1}{4}N_{\text{O3}} = 0. \quad (1.100)$$

Here, N_{D3} and N_{O3} are the number of D3-branes and O3-planes, respectively. The quantity N_{flux} is defined as

$$N_{\text{flux}} = \frac{1}{((2\pi)^2\alpha')^2} \int_{X_6} H_3 \wedge F_3. \quad (1.101)$$

The equation (1.100) is known as the RR tadpole cancellation condition and restrict the number of D3-branes and O3-planes in the theory.

From imaginary self-duality of G_3 one can prove that the contribution of the fluxes N_{flux} to the RR tadpole condition has to be positive. Precisely, we can write the ISD condition of G_3 as

$$e^{-\varphi} *_6 H_3 = -(F_3 - C_0 H_3). \quad (1.102)$$

Then, replacing this equation into (1.101), we obtain

$$N_{\text{flux}} = \frac{e^{-\varphi}}{((2\pi)^2\alpha')^2} \int_{X_6} H_3 \wedge *_6 H_3 = \frac{e^{-\varphi}}{((2\pi)^2\alpha')^2} \int_{X_6} |H_3|^2 > 0. \quad (1.103)$$

Hence, the RR tadpole cancellation condition require the presence of negative D3-branes charges, making this ansatz a suitable scenario for string theory because these objects are present in this theory, for example, O3-planes.

1.4.6 Supersymmetry and no-scale structure

We want to study the 4-dimensional effective supersymmetric theory of the construction explained in the section 2.1, in particular, we want to discuss the structure of the scalar potential and the conditions to preserve supersymmetry. As we mentioned in section 1.2.1, the 4-dimensional effective theory is expressed in terms of the Kähler potential K , a holomorphic superpotential W , and a holomorphic gauge-kinetic coupling functions f 's. The form of the superpotential is given by [35]

$$W_{\text{tree}}(S, U) = \int_{X_6} G_3 \wedge \Omega_3. \quad (1.104)$$

This superpotential is known as the Gukov-Vafa-Witten (GVW) superpotential.

In the following discussion, we will consider only the case of one Kähler moduli

T and $\kappa_4^2 = 1$. In this case, we know that the Kähler potential is of the form

$$K = -3 \ln [T + \bar{T}] - \ln [S + \bar{S}] - \ln \left[-i \int \Omega_3(U) \wedge \bar{\Omega}_3(\bar{U}) \right], \quad (1.105)$$

and the scalar potential is

$$V = e^K \left[K^{S\bar{S}} D_S W D_{\bar{S}} \bar{W} + K^{U_\alpha \bar{U}_\beta} D_{U_\alpha} W D_{\bar{U}_\beta} \bar{W} + K^{T\bar{T}} D_T W D_{\bar{T}} \bar{W} - 3|W|^2 \right] \quad (1.106)$$

where K is the Kähler potential (1.105). The dependence of W and the form of the Kähler potential K implies the existence of a no-scale structure of the potential V , that is, a potential of the form

$$V = e^K \left[K^{S\bar{S}} D_S W D_{\bar{S}} \bar{W} + K^{U_\alpha \bar{U}_\beta} D_{U_\alpha} W D_{\bar{U}_\beta} \bar{W} \right]. \quad (1.107)$$

We can see in the above equation that $V \geq 0$. Therefore, in order to have a supersymmetric preserving minimum, we need to satisfy the equation

$$D_I W = 0, \quad (1.108)$$

where $I = \{S, U_i, T_j\}$.

The supersymmetric conditions in our case take the following form:

The condition for the axion/dilaton is

$$D_S W = -\frac{1}{S + \bar{S}} \int_{X_6} \bar{G}_3 \wedge \Omega_3 = 0. \quad (1.109)$$

For the complex structure moduli, we use the relation

$$\partial_{U_\alpha} \Omega_3 = K_{U_\alpha} \Omega_3 + \chi_\alpha, \quad (1.110)$$

where $K_{U_\alpha} = \partial_\alpha K$ and χ_α is a basis for (2,1)-forms. Therefore,

$$D_{U_\alpha} W = \int_{X_6} G_3 \wedge \chi_\alpha = 0. \quad (1.111)$$

We also have the condition for the Kähler moduli

$$D_T W = -\frac{3}{T + \bar{T}} \int_{X_6} G_3 \wedge \Omega_3 = 0. \quad (1.112)$$

All these equations implies the following conditions over G_3

$$G_3|_{(3,0)} = 0 \quad , \quad G_3|_{(1,2)} = 0 \quad , \quad G_3|_{(0,3)} = 0, \quad (1.113)$$

where (p, q) indicates the (holomorphic, anti-holomorphic) components of G_3 . Therefore, we conclude that in order to have supersymmetric invariant minimum, we need a $G_3 \in H^{2,1}(X_6)$, where G_3 is ISD and $G_3 \wedge J = 0$. The last condition comes from the fact that in a Calabi-Yau 3-fold there is not 5-form.

The presence of fluxes allows the stabilisation of the complex structure moduli U_α and the axion dilaton S at the SUSY global minimum. However, the Kähler moduli remained as flat directions. Intuitively speaking the presence of fluxes force the ISD condition of G_3 but this condition is invariant under rescaling of the internal metric in $*_6$, the Hodge-dual map in 6-dimension. Therefore, rescaling the size of internal cycles is allowed. However, we could add corrections, perturbative and non-perturbative, that break this freedom of rescaling and then give a non-vanishing potential to the Kähler moduli. These corrections can be encoded in the superpotential W and in the Kähler potential K , schematically we can write

$$W = W_0 + W_{np} \quad \text{and} \quad K = K_0 + K_p + K_{np}. \quad (1.114)$$

Here, the subscript p and np correspond to perturbative and non-perturbative contributions respectively. The superpotential can only receive non-perturbative corrections due the non-renormalization theorem.

As we just said the introduction of this extra corrections break SUSY and the non-scale structure of the theory, generating a non-vanishing scalar potential for the Kähler moduli. From the 10-dimensional perspective, the corrections produce non-vanishing components for $G_3^{(3,0)}$, $G_3^{(1,2)}$, and $G_3^{(0,3)}$. An interesting feature is that they are produced at sub-leading order in the effective field theory, because the Kähler scalar potential is generated at order $\mathcal{O}(\mathcal{V}^{-3})$ while the SUSY fluxes at order $\mathcal{O}(\mathcal{V}^{-2})$. For the large volume regime, $\mathcal{V} \gg 1$, they are considered a perturbation around the SUSY minima.

We can enumerate few of these corrections as:

1. **α' -corrections.** These contributions come from higher order derivative corrections of the effective action in 10 dimensions. In particular, one of the possible contributions come from the tensorial structure of the Ricci scalar R^4 in 10 dimensions. This tensorial structure is completely understood and give

rise to a correction to the tree level Kähler potential of the form [36]

$$K \supset -2 \log \left(\mathcal{V} + \frac{\hat{\xi}}{2} \right), \quad (1.115)$$

where $\hat{\xi} = -\frac{(\alpha')^3 \zeta(3) \chi(X_6)}{2^{5/2} (2\pi)^3} (S + \bar{S})^{3/2}$ with $\chi(X_6)$ the Euler characteristic of the CY 3-fold X_6 , and $\zeta(3) \simeq 1.202$. Extra contributions coming from orientifold planes might affect the equation (1.115) by shifting the Euler characteristic to [37]

$$\chi(X_6) \rightarrow \chi(X_6) + 2 \int_{X_6} D_{O_7} \wedge D_{O_7} \wedge D_{O_7}, \quad (1.116)$$

where D_{O_7} is the divisor wrapped by the $O7$ -plane.

2. String loop corrections. The 10 dimensional effective action for type IIB strings also receive string loop contributions. These contributions are unknown in a generic CY compactification. Despite of the lack of information, we can classify them into two classes [38, 39, 40, 41, 42]:

- *KK-correction.* These contributions come from the exchange between D3-branes (or O3-planes) and D7-branes (or O7-planes) of closed strings which carry KK momentum. Schematically we can write their contribution in the Kähler potential as

$$\delta K_{(g_s)}^{KK} \propto \sum_{i=1}^{h^{1,1}} \frac{\mathcal{C}_i^{KK}(U, \bar{U})}{\text{Re}(S) \mathcal{V}} t_i^\perp, \quad (1.117)$$

where $\mathcal{C}_i^{KK}(U, \bar{U})$ are unknown coefficients depending on the complex structure moduli U_α , and t_i^\perp are the cycles controlling the distance between the D3-branes/O3-planes and D7-branes/ O7-planes.

- *Winding corrections.* In this case, the contributions are generated from the exchange of winding strings between intersecting stacks of D7-branes (or between intersecting D7-branes and O7-planes). Their contribution to the scalar potential can be written as

$$\delta V_{(g_s)}^W \propto -\frac{g_s W_0^2}{\mathcal{V}^2} \sum_i \frac{\mathcal{C}_i^W(U, \bar{U})}{t_i^\cap}, \quad (1.118)$$

where g_s is the sting loop coupling constant, W_0 is the tree level superpotential, $\mathcal{C}_i^W(U, \bar{U})$ are unknown coefficients depending on U_α , and t_i^\cap is

the volume of the cycle intersected by the D7-branes and the O7-planes.

3. **Non-perturbative corrections.** Mainly the non-perturbative contributions come from instantons. Instantons are classical solutions of the classical field equations in Euclidean space with finite action. For example, for D3-brane instantons the superpotential takes the form

$$W = W_0 + \sum_j A_j(U, \phi, S) e^{-a_j T_j}. \quad (1.119)$$

This form of the superpotential can be also obtained by gaugino condensation of stacks of D7-branes. Here, $A_j(U, \phi, S)$ is a coefficient that depends on the complex structure moduli U_α , the axion/dilaton S , and possible fields ϕ parametrizing the positions of stack of D7-branes wrapping the cycle t_j . The values of a_j will depend on the generation of the correction. For example for D3-branes instantons $a_j = 2\pi$ and for gaugino condensation $a_j \sim \frac{2\pi}{N}$ with N the number of D7-branes in the stack.

The first example which used these corrections to stabilise the Kähler moduli in the large volume regime is given in the references [43, 44], and it is also called the *LARGE Volume Scenario* (LVS). The LVS has become a standard topic in the branch of moduli stabilisation, we recommend the reader to check the reference [43, 44], for full review in the topic. The models constructed in this thesis are based on the LARGE volume together with the addition of the string loop corrections. We adapt the CY manifold accordingly in each model in order to build the cosmological models. Each chapter is self-contained and easy to read. We hope you enjoy them.

Part II

Inflation
from String Theory

Chapter 2

Chiral Global Embedding of Fibre Inflation Models

Cosmic inflation is an early period of accelerated expansion of our universe which can provide a solution to the flatness and horizon problems of standard Big Bang cosmology. Moreover, quantum fluctuations during inflation can source primordial perturbations that caused the formation of large scale structures and the temperatures anisotropies observed in the cosmic microwave background.

From a microscopic point of view, inflation is expected to be driven by the dynamics of a scalar field undergoing a slow-roll motion along a very shallow potential that mimics a positive cosmological constant. An important feature of inflationary models is the distance travelled by the inflaton in field space during inflation since it is proportional to the amount of primordial gravitational waves which get produced [45]. From an effective field theory point of view, in small field models with a sub-Planckian inflaton excursion, dimension six operators can easily spoil the flatness of the inflationary potential. On the other hand, quantum corrections to large field models with a trans-Planckian field range lead to an infinite series of unsuppressed higher-dimensional operators which seem to bring the effective field theory approach out of control.

These dangerous operators can be argued to be absent or very suppressed only in the presence of a symmetry whose origin can only be postulated from an effective field theory perspective but can instead be derived from an underlying UV complete theory. For this reason inflationary model building in string theory has received a lot of attention [46, 47, 13, 48]. Besides the presence of additional symmetries, string compactifications naturally provide many 4D scalars which can play the rôle of the inflaton. Promising inflaton candidates are type IIB Kähler moduli which parametrise the size of the extra dimensions and enjoy non-compact rescaling

symmetries inherited from the underlying no-scale structure [49].

Identifying a natural inflaton candidate with an appropriate symmetry that protects the flatness of its potential against quantum corrections is however not sufficient to trust inflationary model building in string compactifications. In fact, three additional requirements to have a successful string inflationary model are *(i)* full moduli stabilisation, *(ii)* a global embedding into consistent Calabi-Yau orientifolds with D-branes and fluxes and *(iii)* the realisation of a chiral visible sector.

The first condition is crucial to determine all the energy scales in the model and to check the stability of the inflationary dynamics by controlling the behaviour of the scalar directions orthogonal to the inflaton one. The second condition is instead fundamental to guarantee the consistency of the inflation model from the microscopic point of view by checking the cancellation of all D-brane tadpoles and Freed-Witten anomalies and the actual generation of all the effects needed to stabilise the moduli and to develop the inflationary potential. Finally the requirement of having a model which can give rise to inflation and reproduce at the same time a chiral visible sector is crucial for two main reasons: to ensure the absence of any dangerous interplay between chirality and moduli stabilisation which can forbid the generation of D-terms or non-perturbative effects needed to fix the moduli [50], and to determine the post-inflationary evolution of our universe starting from the reheating process where the inflaton energy density gets converted into the production of visible sector degrees of freedom [51, 52, 53, 54]. Other important post-inflationary issues which can affect the predictions of important inflationary observables like the number of efoldings N_e , the scalar spectral index n_s and the tensor-to-scalar ratio r are periods of matter domination due to light moduli [55, 56, 57], the production of axionic dark radiation from moduli decays [58, 59, 60, 61], non-thermal dark matter [62, 63, 63, 64, 221], moduli-induced baryogenesis [65, 66] and the interplay between the inflationary and the supersymmetry breaking scale [67, 68, 69, 70].

A comprehensive global chiral model which satisfies all these conditions for models where the inflaton is a local blow-up mode [71] has been recently constructed in [72]. The chiral visible sector lives on D3-branes at an orientifolded singularity and full closed string moduli stabilisation in a dS vacuum is achieved by following the LVS procedure [43, 42]. The main limitation of this model is the emergence of an η -problem associated with the presence of large g_s corrections to the effective action which tend to spoil the flatness of the inflationary potential if their flux-dependent coefficients are not tuned small.

In this regard, fibre inflation models [14] look more promising. In these constructions, the inflaton is a fibration modulus which remains exactly massless when only

the leading order no-scale breaking effects are included. The inflationary potential is then generated only at subleading order by a combination of string loop corrections [39, 40, 73, 74] and higher derivative terms [75, 76]. This hierarchy of scales is guaranteed by the extended no-scale cancellation and provides a natural solution to the η -problem [41]. This solution can also be understood from the point of view of an effective non-compact rescaling symmetry for the Kähler moduli [49].

Different versions of fibre inflation models have been constructed so far depending on the microscopic nature of the effects which drive the inflationary dynamics: Kaluza-Klein and winding string loops [14], Kaluza-Klein loops and $\mathcal{O}(\alpha'^3) F^4$ terms [77], and winding g_s loops combined with higher derivative terms [78]. In all cases the inflationary potential is plateau-like and takes a simple form with a constant term and negative exponentials. Additional positive exponentials show up with coefficients which are naturally very small and give rise to a rising behaviour at large field values. Ref. [79] provided a generalised description of fibre inflation models showing how they can reproduce the correct spectral index observed by Planck [80, 7] while the predicted value of the tensor-to-scalar ratio is in the range $0.001 \lesssim r \lesssim 0.01$. Such a large value of r is compatible with the fact that these are large field models where the inflaton range is around 5 Planck units. An effective supergravity description of fibre inflation models as α -attractors has also been recently given in [81].

Despite all these successes, fibre inflation models are still lacking a complete global embedding into chiral string compactifications. However a first step forward has already been made in [82] where these inflationary models have been successfully embedded in consistent type IIB orientifolds with moduli stabilisation but without a chiral visible sector. In order to have a viable inflationary and moduli stabilisation mechanism, the internal Calabi-Yau manifold has to have at least $h^{1,1} = 3$ Kähler moduli and its volume form has to feature a K3 or T^4 fibration over a \mathbb{P}^1 base and a rigid shrinkable blow-up mode [42, 83]. Starting from concrete Calabi-Yau threefolds with these topological properties, ref. [82] provided several different examples with an explicit choice of orientifold involution and D3/D7 brane setups which are globally consistent and can generate corrections to the 4D effective action that can fix all closed string moduli inside the Kähler cone and reproduce the form of the inflationary potential of fibre inflation models. However the case with $h^{1,1} = 3$ is too simple to allow for non-trivial D7 worldvolume fluxes which give rise to chiral matter. In fact, non-zero gauge fluxes induce moduli dependent Fayet-Iliopoulos terms which, in combination with soft term contributions for $U(1)$ -charged matter fields, would lift the leading order flat direction, making the inflaton too heavy to

drive inflation.

In this chapter we shall extend the results of [82] by considering more complicated Calabi-Yau threefolds with $h^{1,1} = 4$ in order to build global fibre inflation models with a chiral visible sector. After analysing the topological conditions on the underlying compactification manifold to allow a successful chiral global embedding of fibre inflation models, we find that the simplest examples involve Calabi-Yau threefolds with 3 K3 divisors and a toroidal-like volume with a diagonal del Pezzo divisor suitable to support non-perturbative effects to freeze the moduli. The internal volume is therefore controlled by 3 Kähler moduli and can equivalently be seen as different K3 fibrations over 3 different \mathbb{P}^1 bases. After searching through the Kreuzer-Skarke list of Calabi-Yau manifolds embedded in toric varieties [84], we find several concrete examples which admit these topological features.

We then focus on one of them and describe several possible choices of orientifold involution, D-brane setup and gauge fluxes which satisfy global consistency conditions and generate perturbative g_s and α' corrections to the 4D Kähler potential and non-perturbative effects in the superpotential that are suitable to both stabilise the moduli and reproduce the typical potential of fibre inflation models. In particular, non-zero gauge fluxes induce chiral matter on D7-branes wrapped around smooth combinations of the four-cycles which control the overall volume.¹ Moreover, a moduli-dependent Fayet-Iliopoulos term lifts one of the Kähler moduli, so that after D-term stabilisation the effective number of Kähler moduli is reduced to 3 and the internal volume simplifies to the standard expression of fibre inflation models used in the examples of [82].

After computing all relevant loop and higher derivative effects in full detail, we analyse the resulting inflationary dynamics finding an interesting result: the Kähler cone bounds set severe constraints on the allowed inflaton field range when they are combined with other phenomenological requirements, like the generation of the correct amplitude of the power spectrum by the inflaton quantum fluctuations, and consistency conditions like the stability of the inflaton evolution against possible orthogonal runaway directions, the fact that the gravitino mass remains always smaller than any Kaluza-Klein scale in the model and finally that dangerous higher derivative effects do not spoil the flatness of the inflationary potential before achieving enough efoldings of inflation.² Because of this tension, we also perform a full multi-field numerical analysis of the inflationary evolution showing how an early period of

¹We do not consider K3 fibred cases where the visible sector lives on D3 branes at singularities since they would lead to dark radiation overproduction [85].

²These last two consistency conditions are qualitatively similar since the superspace derivative expansion is under control if $m_{3/2} \ll M_{\text{KK}}$ [86].

accelerated expansion occurs generically. On the other hand, the inflaton quantum fluctuations can generate the right amplitude of the density perturbations only if the microscopic parameters take appropriate values.

We believe that our results make fibre inflation models more robust since they represent the first concrete models which are globally consistent and chiral. Nonetheless several issues still need to be investigated further. The most important ones are the inclusion of an explicit uplifting mechanism to realise a dS vacuum, a thorough derivation of the perturbative corrections to the 4D effective action and a better determination of the Calabi-Yau Kähler cone, going beyond its approximated expression inherited from the toric ambient space. We leave the study of these issues for the future.

This chapter is organised as follows. In Sec. 2.1, after presenting a basic review of fibre inflation models, we summarise the minimal requirements that are needed for the construction of a fully consistent global embedding with a chiral visible sector. In Sec. 2.2 we provide a concrete Calabi-Yau example, describing the orientifold involution, the D-brane setup, the choice of gauge fluxes and the resulting chiral spectrum, Fayet-Iliopoulos term and inflationary potential generated by g_s and α' effects. The inflationary evolution is analysed in full detail in Sec. 2.3 by focusing first on the single-field approximation and by studying then the multi-field dynamics. In Sec. 2.4 we draw our conclusions and we discuss a few open issues. App. B contains additional explicit chiral global examples.

2.1 Chiral global inflationary models

Let us begin by briefly reviewing the setup of fibre inflation and proceed afterward by displaying the minimal requirements for a successful chiral global embedding of fibre inflation models.

2.1.1 Fibre inflation in a nutshell

Fibre inflation models are based on a class of type IIB orientifold flux compactifications with D3/D7-branes and O3/O7-planes where the Calabi-Yau (CY) threefold takes a so-called ‘weak Swiss-cheese’ form:

$$\mathcal{V} = f_{3/2}(\tau_j) - \sum_{i=1}^{N_{\text{small}}} \lambda_i \tau_i^{3/2} \quad \text{with} \quad j = 1, \dots, N_{\text{large}}, \quad (2.1)$$

where $h^{1,1} = N_{\text{large}} + N_{\text{small}}$ and $f_{3/2}$ is a homogeneous function of degree $3/2$. In these models, the stabilisation of the Kähler moduli is performed in two steps. Firstly, the total volume \mathcal{V} as well as the volumes of the N_{small} rigid blow-up divisors τ_i are fixed following the LVS procedure [43, 42] where the leading order α'^3 corrections to the Kähler potential [36, 37, 87] are balanced against non-perturbative contributions to the superpotential [88]. This leaves $N_{\text{flat}} = N_{\text{large}} - 1 = h^{1,1} - N_{\text{small}} - 1$ flat directions which are natural inflaton candidates. These directions can receive a potential at subleading order by g_s corrections due to the exchange of Kaluza-Klein (KK) and winding modes [39, 40, 73, 74, 41] as well as by $(\alpha')^3 F^4$ -terms [75, 76]. In the simplest fibre inflation models $h^{1,1} = 3$ and $N_{\text{small}} = 1$, so that $N_{\text{flat}} = 1$. This leading order flat direction corresponds to a Kähler modulus τ_f which parametrises the volume of a K3 surface and the total scalar potential schematically looks like [14, 77, 78, 79]:

$$V = V_{LVS}(\mathcal{V}, \tau_s) + V_{\text{dS}}(\mathcal{V}) + V_{\text{inf}}(\mathcal{V}, \tau_s, \tau_f), \quad (2.2)$$

where $V_{\text{inf}}(\mathcal{V}, \tau_s, \tau_f) = V_{g_s}^{\text{KK}} + V_{g_s}^{\text{W}} + V_{F^4} \ll V_{LVS}(\mathcal{V}, \tau_i)$ is the inflationary potential. V_{LVS} is the leading order LVS potential which fixes \mathcal{V} and τ_s , V_{dS} is an uplifting contribution to get a dS vacuum which can originate from anti D3-branes [88, 89, 90, 91, ?], hidden sector T-branes [92] or non-perturbative effects at singularities [93], while $V_{g_s}^{\text{KK}}$, $V_{g_s}^{\text{W}}$ and V_{F^4} are respectively KK and winding string loops and F^4 terms.

In fibre inflation models, the underlying CY threefold is a K3 fibration over a \mathbb{P}^1 base which has two decompactification limits, corresponding to either the K3 fibre or the base growing large. Thus, kinematically it is expected that the fibre volume can traverse several Planck units. These LVS inflationary models present a variety of distinct features that make them very promising candidates to realise large field inflation and to discuss explicit global embeddings:

1. The de Sitter uplift is independent of the inflaton. This is contrary to a hypothetical KKLT embedding [88], where the uplift would be inflaton-dependent and, thus, large field inflation would typically destroy the KKLT minimum.
2. The back-reaction of heavy moduli is incorporated and under control, in particular, due to the fact that moduli stabilisation is done in two steps and the leading order potential is independent of the inflaton because of the extended no-scale cancellation [41]. This is in contrast with the majority of large field models of inflation [94].
3. The possibility to achieve tensor-to-scalar ratios between $r \sim 0.01$ and $r \sim$

0.001 which can be tested by future CMB observations [95, 96].

An explicit realisation of fibre inflation not only places several constraints on the underlying CY geometry, but also on the setup of D-branes and O-planes. In the following section we list the sufficient requirements to build a viable global model which also allows for a chiral visible sector.

2.1.2 Requirements for chiral global embedding

The simplest global embedding of fibre inflation models requires at least three Kähler moduli [82]. However, in order to incorporate also a chiral visible sector we need at least $h^{1,1} = 4$ Kähler moduli. Here we will focus on obtaining chiral matter on D7-branes wrapped around a suitable divisor with world-volume gauge fluxes turned on. In this case D7 gauge fluxes induce a D-term potential for the Kähler moduli that fixes a particular combination thereof. Thus, D-term fixing and the leading order LVS stabilisation mechanism leave just a single flat direction, in our case a K3 fibre, which will play the rôle of the inflaton. In order to obtain a viable chiral global model we require the following ingredients and consistency conditions:

1. A Calabi-Yau with $h^{1,1} = 4$ featuring three large cycles and a shrinkable rigid divisor, so that the internal volume takes the form (2.1) with $N_{\text{small}} = 1$. In the explicit example described in Sec. 2.2 the volume simplifies further to:

$$\mathcal{V} = c_a \sqrt{\tau_1 \tau_2 \tau_3} - c_b \tau_s^{3/2}, \quad (2.3)$$

with $c_a > 0$ and $c_b > 0$. Each of the 3 moduli τ_1 , τ_2 and τ_3 controls the volume of a K3 surface while τ_s parametrises the size of a ‘diagonal’ del Pezzo divisor [83]. D-term stabilisation will fix $\tau_3 \propto \tau_2$ while the standard LVS procedure will freeze the overall volume $\mathcal{V} \simeq c_a \sqrt{\tau_1 \tau_2 \tau_3}$ and the blow-up mode τ_s . The leading order flat direction can be parametrised by τ_1 which will drive inflation.

2. An orientifold involution and a D3/D7-brane setup with gauge fluxes on the visible D7-brane stacks such that tadpole cancellation is satisfied with enough room for bulk three-form fluxes to be turned on for complex structure and dilaton stabilisation. The D-brane and O-plane setup must also allow for the generation of KK- and/or winding string loop corrections which have the correct form to generate a suitable inflationary potential.
3. A choice of world-volume fluxes which cancels all Freed-Witten anomalies [97, 98] but leads, at the same time, to just a single moduli-dependent Fayet-Iliopoulos (FI) term [99, 100] in order to leave a leading order inflationary

flat direction by lifting just one of the two flat directions leftover by the LVS stabilisation mechanism.

4. There should be no chiral intersection between the visible sector and the del Pezzo divisor supporting non-perturbative effects required for LVS moduli fixing as otherwise the prefactor of the non-perturbative superpotential would be vanishing [50]. The absence of these dangerous chiral intersections should be guaranteed by an appropriate choice of gauge fluxes.
5. Moduli stabilisation and inflation have to take place inside the CY Kähler cone and the effective field theory should be well under control with $\langle \mathcal{V} \rangle \gg 1$ and $g_s \ll 1$.
6. In order to trust inflationary model building within an effective field theory, the following hierarchy of scales should be satisfied from horizon exit to the end of inflation:

$$m_{\text{inf}} < H < m_{3/2} < M_{\text{KK}}^{(i)} < M_s < M_p, \quad (2.4)$$

where m_{inf} is the inflaton mass, H is the Hubble constant, $m_{3/2}$ is the gravitino mass which sets the mass scale of all the heavy moduli during inflation, $M_{\text{KK}}^{(i)}$ denote various KK scales associated with bulk modes and open string excitations on D7-branes wrapped around four-cycles, M_s is the string scale and M_p is the reduced Planck mass $M_p = 2.4 \cdot 10^{18}$ GeV. Notice that, apart from M_p , all these energy scales are moduli dependent and so evolve during inflation. After stabilising \mathcal{V} and τ_s à la LVS and fixing one large modulus in terms of another large direction via setting the FI-term to zero, we find that the ‘reduced’ moduli space of the inflationary direction is in fact a compact interval. Therefore the field space available for inflation is kinematically finite (albeit in general trans-Planckian), a feature of the model which has so far been overlooked. We will state the precise phenomenological and consistency conditions for successful inflation in Sec. 2.3.

2.2 A chiral global example

In this section, we shall present all the topological and model-building details of the global embedding of fibre inflation models into explicit chiral CY orientifolds with $h^{1,1} = 4$.

2.2.1 Toric data

Let us consider the following toric data for a CY threefold whose volume takes the form $\mathcal{V} = c_a \sqrt{\tau_1 \tau_2 \tau_3} - c_b \tau_s^{3/2}$ discussed above:

	x_1	x_2	x_3	x_4	x_5	x_6	x_7	x_8
4	0	0	0	1	1	0	0	2
4	0	0	1	0	0	1	0	2
4	0	1	0	0	0	0	1	2
8	1	0	0	1	0	1	1	4
	dP ₇	NdP ₁₁	NdP ₁₁	K3	NdP ₁₁	K3	K3	SD

The Hodge numbers are $(h^{2,1}, h^{1,1}) = (98, 4)$, the Euler number is $\chi = -188$, while the Stanley-Reisner ideal is:

$$\text{SR1} = \{x_1 x_4, x_1 x_6, x_1 x_7, x_2 x_7, x_3 x_6, x_4 x_5 x_8, x_2 x_3 x_5 x_8\}.$$

This corresponds to the polytope ID #1206 in the CY database of Ref. [101]. A detailed divisor analysis using `cohomCalc` [102, 103] shows that the divisor D_1 is a del Pezzo dP₇ while each of the divisors $\{D_4, D_6, D_7\}$ is a K3 surface. Moreover, each of the divisors $\{D_2, D_3, D_5\}$ is a ‘rigid but not del Pezzo’ surface with $h^{1,1} = 12$ which we denote as NdP₁₁ while D_8 is a ‘special deformation’ divisors with Hodge diamond:

$$\text{SD} \equiv \begin{array}{ccc} & & 1 \\ & 0 & 0 \\ 23 & 160 & 23 \\ & 0 & 0 \\ & & 1 \end{array}$$

The intersection form in the basis of smooth divisors $\{D_1, D_4, D_6, D_7\}$ can be written as:

$$I_3 = 2 D_4 D_6 D_7 + 2 D_1^3. \quad (2.5)$$

Writing the Kähler form in the above basis of divisors as $J = t_1 D_1 + t_4 D_4 + t_6 D_6 + t_7 D_7$ and using the intersection polynomial (2.5), the CY overall volume becomes:

$$\mathcal{V} = 2 t_4 t_6 t_7 + \frac{t_1^3}{3}. \quad (2.6)$$

The Kähler cone conditions can be derived from the following generators of the

Kähler cone:

$$K_1 = -D_1 + D_4 + D_6 + D_7, \quad K_2 = D_7, \quad K_3 = D_4, \quad K_4 = D_6. \quad (2.7)$$

Expanding the Kähler form as $J = \sum_{i=1}^4 r_i K_i$, the Kähler cone is defined via the following conditions on the two-cycle moduli:

$$r_1 = -t_1 > 0, \quad r_2 = t_1 + t_7 > 0, \quad r_3 = t_1 + t_4 > 0, \quad r_4 = t_1 + t_6 > 0. \quad (2.8)$$

Notice that this expression of the CY Kähler cone is only approximate since it is inherited from the Kähler cone of the ambient toric variety.³ However this procedure can either overcount some curves of the CY threefold, for example if they do not intersect with the CY hypersurface, or miss some of them, if they cannot be obtained as the intersection between two divisors of the ambient space and the CY hypersurface. Hence the actual CY Kähler cone can turn out to be either larger or smaller. This analysis would require a deeper investigation which is however beyond the scope of this chapter.⁴ Here we just mention that this analysis has been performed in detail in [104] where the CY Kähler cone turned out to be larger than the approximated version.

The four-cycle moduli, which can be computed as $\tau_i = \partial_{t_i} \mathcal{V}$, look like:

$$\tau_1 = t_1^2, \quad \tau_4 = 2 t_6 t_7, \quad \tau_6 = 2 t_4 t_7, \quad \tau_7 = 2 t_4 t_6, \quad (2.9)$$

and so, using the Kähler cone conditions (2.8), the overall volume reduces to:

$$\mathcal{V} = t_4 \tau_4 - \frac{1}{3} \tau_1^{3/2} = t_6 \tau_6 - \frac{1}{3} \tau_1^{3/2} = t_7 \tau_7 - \frac{1}{3} \tau_1^{3/2} = \frac{1}{\sqrt{2}} \sqrt{\tau_4 \tau_6 \tau_7} - \frac{1}{3} \tau_1^{3/2}, \quad (2.10)$$

which shows clearly that the CY threefold X features three K3 fibrations over different \mathbb{P}^1 bases. The second Chern class of X is given by:

$$c_2(X) = D_4 D_5 + 4 D_5^2 + 12 D_5 D_6 + 12 D_5 D_7 + 12 D_6 D_7, \quad (2.11)$$

³If the same CY threefold can be realised as a hypersurface embedded in different ambient spaces, the CY Kähler cone is approximated as the intersection of the Kähler cones of the different toric varieties [101].

⁴We however expect that the CY Kähler cone cannot get smaller. In fact, if this were the case, there should exist an extra constraint from requiring the positivity of a curve of the CY which is trivial in the ambient space. But this does not seem to be possible since each CY divisor is inherited from a single toric divisor (i.e. we do not have a toric divisor which splits into two CY divisors, and so where $h^{1,1}$ of the CY is larger than $h^{1,1}$ of the ambient space). In fact, if this trivial curve existed, it should have a dual divisors, and so $h^{1,1}$ of the CY should be larger than $h^{1,1}$ of the ambient case, which is however not the case.

which results in the following values of the topological quantities $\Pi_i = \int_X c_2 \wedge \hat{D}_i$:

$$\Pi_1 = 8, \quad \Pi_2 = \Pi_3 = 16, \quad \Pi_4 = 24, \quad \Pi_5 = 16, \quad \Pi_6 = \Pi_7 = 24, \quad \Pi_8 = 128. \quad (2.12)$$

The intersection curves between two coordinate divisors are given in Tab. 2.1 while their volumes are listed in Tab. 2.2.

	D_1	D_2	D_3	D_4	D_5	D_6	D_7	D_8
D_1	\mathcal{C}_3	\mathbb{T}^2	\mathbb{T}^2	\emptyset	\mathbb{T}^2	\emptyset	\emptyset	\mathcal{C}_3
D_2	\mathbb{T}^2	$\mathbb{P}^1 \sqcup \mathbb{P}^1$	$\mathbb{P}^1 \sqcup \mathbb{P}^1$	\mathbb{T}^2	$\mathbb{P}^1 \sqcup \mathbb{P}^1$	\mathbb{T}^2	\emptyset	\mathcal{C}_3
D_3	\mathbb{T}^2	$\mathbb{P}^1 \sqcup \mathbb{P}^1$	$\mathbb{P}^1 \sqcup \mathbb{P}^1$	\mathbb{T}^2	$\mathbb{P}^1 \sqcup \mathbb{P}^1$	\emptyset	\mathbb{T}^2	\mathcal{C}_3
D_4	\emptyset	\mathbb{T}^2	\mathbb{T}^2	\emptyset	\emptyset	\mathbb{T}^2	\mathbb{T}^2	\mathcal{C}_9
D_5	\mathbb{T}^2	$\mathbb{P}^1 \sqcup \mathbb{P}^1$	$\mathbb{P}^1 \sqcup \mathbb{P}^1$	\emptyset	$\mathbb{P}^1 \sqcup \mathbb{P}^1$	\mathbb{T}^2	\mathbb{T}^2	\mathcal{C}_3
D_6	\emptyset	\mathbb{T}^2	\emptyset	\mathbb{T}^2	\mathbb{T}^2	\emptyset	\mathbb{T}^2	\mathcal{C}_9
D_7	\emptyset	\emptyset	\mathbb{T}^2	\mathbb{T}^2	\mathbb{T}^2	\mathbb{T}^2	\emptyset	\mathcal{C}_9
D_8	\mathcal{C}_3	\mathcal{C}_3	\mathcal{C}_3	\mathcal{C}_9	\mathcal{C}_3	\mathcal{C}_9	\mathcal{C}_9	\mathcal{C}_{81}

Table 2.1: Intersection curves of two coordinate divisors. Here \mathcal{C}_g denotes a curve with Hodge numbers $h^{0,0} = 1$ and $h^{1,0} = g$.

	D_1	D_2	D_3	D_4	D_5	D_6	D_7	D_8
D_1	$2t_1$	$-2t_1$	$-2t_1$	0	$-2t_1$	0	0	$-4t_1$
D_2	$-2t_1$	$2t_1$	$2(t_1 + t_4)$	$2t_6$	$2(t_1 + t_6)$	$2t_4$	0	$4(t_1 + t_4 + t_6)$
D_3	$-2t_1$	$2(t_1 + t_4)$	$2t_1$	$2t_7$	$2(t_1 + t_7)$	0	$2t_4$	$4(t_1 + t_4 + t_7)$
D_4	0	$2t_6$	$2t_7$	0	0	$2t_7$	$2t_6$	$4(t_6 + t_7)$
D_5	$-2t_1$	$2(t_1 + t_6)$	$4(t_1 + t_7)$	0	$2t_1$	$2t_7$	$2t_6$	$4(t_1 + t_6 + t_7)$
D_6	0	$2t_4$	0	$2t_7$	$2t_7$	0	$2t_4$	$4(t_4 + t_7)$
D_7	0	0	$2t_4$	$2t_6$	$2t_6$	$2t_4$	0	$4(t_4 + t_6)$
D_8	$-4t_1$	$4(t_1 + t_4 + t_6)$	$4(t_1 + t_4 + t_7)$	$4(t_6 + t_7)$	$4(t_1 + t_6 + t_7)$	$4(t_4 + t_7)$	$4(t_4 + t_6)$	$8(t_1 + 2(t_4 + t_6 + t_7))$

Table 2.2: Volumes of intersection curves between two coordinate divisors.

2.2.2 Orientifold involution

We focus on orientifold involutions of the form $\sigma : x_i \rightarrow -x_i$ with $i = 1, \dots, 8$ which feature an O7-plane on D_i and O3-planes at the fixed points listed in Tab. 2.3. The effective non-trivial fixed point set in Tab. 2.3 has been obtained after taking care of the SR ideal symmetry. Moreover, the total number of O3-planes N_{O3} is obtained from the triple intersections restricted to the CY hypersurface, while the effective

Euler number χ_{eff} has been computed as:⁵

$$\chi_{\text{eff}} = \chi(X) + 2 \int_X [\text{O7}] \wedge [\text{O7}] \wedge [\text{O7}]. \quad (2.13)$$

In what follows we shall focus on the orientifold involution $\sigma : x_8 \rightarrow -x_8$ which features just a single O7-plane located in D_8 and no O3-plane.

σ	O7	O3	N_{O3}	$\chi(\text{O7})$	χ_{eff}
$x_1 \rightarrow -x_1$	D_1	$\{D_2D_3D_4, D_2D_4D_6, D_2D_5D_6, D_3D_4D_7, D_3D_5D_7, D_4D_6D_7, D_5D_6D_7\}$	14	10	-184
$x_2 \rightarrow -x_2$	$D_2 \sqcup D_7$	$D_1D_3D_5$	2	38	-192
$x_2 \rightarrow -x_3$	$D_3 \sqcup D_6$	$D_1D_2D_5$	2	38	-192
$x_4 \rightarrow -x_4$	$D_4 \sqcup D_5$	$D_1D_2D_3$	2	38	-192
$x_5 \rightarrow -x_5$	$D_4 \sqcup D_5$	$D_1D_2D_3$	2	38	-192
$x_6 \rightarrow -x_6$	$D_3 \sqcup D_6$	$D_1D_2D_5$	2	38	-192
$x_7 \rightarrow -x_7$	$D_2 \sqcup D_7$	$D_1D_3D_5$	2	38	-192
$x_8 \rightarrow -x_8$	D_8	\emptyset	0	208	-28

Table 2.3: Fixed point set for the involutions which are reflections of the eight coordinates x_i with $i = 1, \dots, 8$.

2.2.3 Brane setup

If the D7-tadpole cancellation condition is satisfied by placing four D7-branes on top of the O7-plane, the string loop corrections to the scalar potential can involve only KK effects between this D7-stack and O3-planes or D3-branes since winding contributions are absent due to the absence of any intersection between D7-branes and/or O7-planes. Thus loop effects are too simple to generate a viable inflationary plateau. They might even be completely absent in our case since there are no O3-planes and the D3-tadpole cancellation condition could be satisfied without the need to include D3-branes (i.e. just switching on appropriate background three-form fluxes). We shall therefore focus on a slightly more complicate D7-brane setup which gives rise to winding loop effects. This can be achieved by placing D7-branes not

⁵The effective Euler number controls the strength of $N = 1$ $\mathcal{O}(\alpha'^3)$ corrections due to O7-planes [37].

entirely on top of the O7-plane as follows:

$$8[\text{O7}] \equiv 8([D_8]) = 16([D_2] + [D_4] + [D_6]) . \quad (2.14)$$

This brane setup involves three stacks of D7-branes wrapped around the divisors D_2 , D_4 and D_6 . Moreover, the condition for D3-tadpole cancellation becomes:

$$N_{\text{D3}} + \frac{N_{\text{flux}}}{2} + N_{\text{gauge}} = \frac{N_{\text{O3}}}{4} + \frac{\chi(\text{O7})}{12} + \sum_a \frac{N_a (\chi(D_a) + \chi(D'_a))}{48} = 38 ,$$

showing that there is space for turning on both gauge and background three-form fluxes for complex structure and dilaton stabilisation.⁶ As shown in [105], three-form fluxes stabilise also D7 position moduli and open string moduli living at the intersection between two different stacks of D7-branes since they generate soft supersymmetry breaking mass terms for each of these scalars. On the other hand, there are no Wilson line moduli in our model since $h^{1,0}(D_2) = h^{1,0}(D_4) = h^{1,0}(D_6) = 0$.

Let us point out that other orientifold involutions which could allow for D7-branes not entirely on top of the O7-plane are $x_4 \rightarrow -x_4$, $x_6 \rightarrow -x_6$ or $x_7 \rightarrow -x_7$. In each of these cases, the O7-plane is located on a K3 surface. However, given that $D_4 = D_1 + D_5$, $D_6 = D_1 + D_3$ and $D_7 = D_1 + D_2$, from Tab. 2.1 and 2.2 we see that the resulting D7-brane stacks are either non-intersecting (and so no winding corrections are generated) or the volumes of the intersection curves depend just on the ‘small’ dP_7 divisor (and so winding loops are inflaton-independent). This is the reason why we chose the involution $x_8 \rightarrow -x_8$ where the O7-plane is located on the ‘special deformation’ divisor D_8 which gives more freedom for D7-brane model building.

2.2.4 Gauge fluxes

In order to obtain a chiral visible sector on the D7-brane stacks wrapping D_2 , D_4 and D_6 we need to turn on worldvolume gauge fluxes of the form:

$$\mathcal{F}_i = \sum_{j=1}^{h^{1,1}} f_{ij} \hat{D}_j - \frac{1}{2} c_1(D_i) - \iota_{D_i}^* B \quad \text{with} \quad f_{ij} \in \mathbb{Z} \quad \text{and} \quad i = 2, 4, 6 , \quad (2.15)$$

where the half-integer contribution is due to Freed-Witten anomaly cancellation [97, 98].

⁶We focus on flux vacua where the dilaton is fixed in a regime where our perturbative type IIB analysis is under control.

However we want to generate just one moduli-dependent Fayet-Iliopoulos term in order to fix only one Kähler modulus via D-term stabilisation. In fact, if the number of FI-terms is larger than one, there is no light Kähler modulus which can play the rôle of the inflaton. Moreover we wrap a D3-brane instanton on the rigid divisor D_1 in order to generate a non-perturbative contribution to the superpotential which is crucial for LVS moduli stabilisation. In order to cancel the Freed-Witten anomaly, the D3-instanton has to support a half-integer flux, and so the general expression of the total gauge flux on D_1 becomes (with $c_1(D_1) = -\hat{D}_1$):

$$\mathcal{F}_1 = \sum_{j=1}^{h^{1,1}} f_{1j} \hat{D}_j + \frac{1}{2} \hat{D}_1 - \iota_{D_1}^* B \quad \text{with} \quad f_{1j} \in \mathbb{Z}. \quad (2.16)$$

However a non-vanishing \mathcal{F}_1 would not be gauge invariant, and so would prevent a non-perturbative contribution to the superpotential. We need therefore to check if it is possible to perform an appropriate choice of B -field which can simultaneously set $\mathcal{F}_4 = \mathcal{F}_6 = 0$ (we choose to have a non-vanishing gauge flux only on D_2 to have just one moduli-dependent FI-term) and $\mathcal{F}_1 = 0$. Recalling that both D_4 and D_6 are K3 surfaces which are spin divisors with $c_1(D_4) = c_1(D_6) = 0$ (since the K3 is a CY two-fold), if we set:

$$B = \frac{1}{2} \hat{D}_1, \quad (2.17)$$

the condition $\mathcal{F}_1 = \mathcal{F}_4 = \mathcal{F}_6 = 0$ reduces to the requirement that the following forms are integer:

$$\iota_{D_4}^* \left(\frac{1}{2} \hat{D}_1 \right) \quad \text{and} \quad \iota_{D_6}^* \left(\frac{1}{2} \hat{D}_1 \right), \quad (2.18)$$

since in this case the integer flux quanta f_{ij} can always be adjusted to yield vanishing gauge fluxes. Taking an arbitrary integer form $A \in H^2(\mathbb{Z}, X)$ which can be expanded as $A = a_j \hat{D}_j$ with $a_j \in \mathbb{Z}$, the pullbacks in (2.18) give rise to integer forms if:

$$\begin{aligned} b_4 &\equiv \int_X \left(\frac{1}{2} \hat{D}_1 \right) \wedge \hat{D}_4 \wedge A \in \mathbb{Z} \\ b_6 &\equiv \int_X \left(\frac{1}{2} \hat{D}_1 \right) \wedge \hat{D}_6 \wedge A \in \mathbb{Z} \end{aligned}$$

Using the intersection polynomial (2.5) we find $b_4 = b_6 = 0$, showing how the choice of B -field in (2.17) can indeed allow for $\mathcal{F}_1 = \mathcal{F}_4 = \mathcal{F}_6 = 0$. The only non-zero gauge flux is \mathcal{F}_2 whose half-integer contribution can be cancelled by adding an additional term to the B -field of the form $\frac{1}{2} \hat{D}_2$. Given that all the intersection numbers are even, this new term in B does not modify our previous results on the pullbacks of

the B -field on D_1 , D_4 and D_6 . Moreover the pullback of the B -field on D_2 will also generate an integer flux contribution. We shall therefore consider a non-vanishing gauge flux on the worldvolume of D_2 of the form:

$$\mathcal{F}_2 = \sum_{j=1}^{h^{1,1}} f_{2j} \hat{D}_j \quad \text{with} \quad f_{2j} \in \mathbb{Z}. \quad (2.19)$$

2.2.5 FI-term and chirality

Given that the divisor D_2 is transversely invariant under the orientifold involution and it is wrapped by eight D7-branes, it supports an $Sp(16)$ gauge group which is broken down to $U(8) = SU(8) \times U(1)$ by a non-zero flux \mathcal{F}_2 along the diagonal $U(1)$. This non-trivial gauge flux \mathcal{F}_2 induces also a $U(1)$ -charge q_{i2} for the i -th Kähler modulus of the form:

$$q_{i2} = \int_X \hat{D}_i \wedge \hat{D}_2 \wedge \mathcal{F}_2. \quad (2.20)$$

Thus $\mathcal{F}_2 \neq 0$ yields (using $D_2 = D_7 - D_1$):

$$q_{12} = -2f_{21} \quad q_{42} = 2f_{26} \quad q_{62} = 2f_{24} \quad q_{72} = 0, \quad (2.21)$$

together with a flux-dependent correction to the gauge kinetic function which looks like:

$$\text{Re}(f_2) = \alpha_2^{-1} = \frac{4\pi}{g_2^2} = \tau_2 - h(\mathcal{F}_2) \text{Re}(S), \quad (2.22)$$

where:

$$h(\mathcal{F}_2) = \frac{1}{2} \int_X \hat{D}_2 \wedge \mathcal{F}_2 \wedge \mathcal{F}_2 = \frac{1}{2} (f_{21} q_{12} + f_{24} q_{42} + f_{26} q_{62}). \quad (2.23)$$

Moreover a non-vanishing gauge flux \mathcal{F}_2 induces a moduli-dependent FI-term of the form:

$$\xi = \frac{1}{4\pi\mathcal{V}} \int_X \hat{D}_2 \wedge J \wedge \mathcal{F}_2 = \frac{1}{4\pi\mathcal{V}} \sum_{j=1}^{h^{1,1}} q_{j2} t_j = \frac{1}{4\pi\mathcal{V}} (q_{12} t_1 + q_{42} t_4 + q_{62} t_6). \quad (2.24)$$

For vanishing open string VEVs (induced for example by non-tachyonic scalar masses), a leading-order supersymmetric stabilisation requires $\xi = 0$ which implies:

$$t_4 = -\frac{q_{12}}{q_{42}} t_1 - \frac{q_{62}}{q_{42}} t_6. \quad (2.25)$$

This $U(1)$ factor becomes massive via the Stückelberg mechanism and develops an $\mathcal{O}(M_s)$ mass by eating up a linear combination of an open and a closed string axion which is mostly given by the open string mode.

Besides breaking the worldvolume gauge group and inducing moduli-dependent FI-terms, non-trivial gauge fluxes on D7-branes generate also 4D chiral modes. In fact, open strings stretching between the D7-branes on D_2 and the O7-planes or the image branes give rise to the following zero-modes in the symmetric and antisymmetric representations of $U(8)$:

$$I_2^{(S)} = -\frac{1}{2} \int_X \hat{D}_2 \wedge [\text{O7}] \wedge \mathcal{F}_2 - \int_X \hat{D}_2 \wedge \hat{D}_2 \wedge \mathcal{F}_2 = 2q_{12} - q_{42} - q_{62}, \quad (2.26)$$

$$I_2^{(A)} = \frac{1}{2} \int_X \hat{D}_2 \wedge [\text{O7}] \wedge \mathcal{F}_2 - \int_X \hat{D}_2 \wedge \hat{D}_2 \wedge \mathcal{F}_2 = q_{42} + q_{62}. \quad (2.27)$$

Due to the absence of worldvolume fluxes on the D7-branes wrapped around D_4 and D_6 , both of these two D7-stacks support an $Sp(16)$ gauge group (since both D_4 and D_6 are transversely invariant) which are both unbroken. Thus open strings stretched between the D7-branes on D_2 and D_4 or D_6 (or their image branes) give rise to 4D chiral zero-modes in the bi-fundamental representation $(8,16)$ of $U(8)$ and $Sp(16)$ whose number is:

$$I_{24} = \int_X \hat{D}_2 \wedge \hat{D}_4 \wedge \mathcal{F}_2 = q_{42}, \quad I_{26} = \int_X \hat{D}_2 \wedge \hat{D}_6 \wedge \mathcal{F}_2 = q_{62}. \quad (2.28)$$

We need finally to check that there are no chiral intersections between the D7s on D_2 and the instanton on D_1 to make sure that the prefactor of the non-perturbative contribution to the superpotential is indeed non-zero. This is ensured if:

$$I_{21} = \int_X \hat{D}_2 \wedge \hat{D}_1 \wedge \mathcal{F}_2 = q_{12} = -2f_{21} = 0. \quad (2.29)$$

This condition can be easily satisfied by choosing $f_{21} = 0$. In turn, this choice simplifies the D-term constraint (2.25) to:

$$t_4 = -\frac{q_{62}}{q_{42}} t_6 \equiv \alpha t_6. \quad (2.30)$$

2.2.6 Inflationary potential

Using the D-term fixing relation (2.30), the Kähler cone conditions (2.8) simplify to $t_7 > -t_1 > 0$ together with $t_6 > -t_1 > 0$ if $\alpha \geq 1$ or $\alpha t_6 > -t_1 > 0$ if $\alpha \leq 1$.

Moreover the CY volume (2.6) reduces to:

$$\mathcal{V} = 2\alpha t_7 t_6^2 + \frac{t_1^3}{3} = t_7 \tau_7 - \frac{1}{3} \tau_1^{3/2} = \frac{1}{\sqrt{2\alpha}} \sqrt{\tau_7} \tau_6 - \frac{1}{3} \tau_1^{3/2}. \quad (2.31)$$

Given that this form is linear in t_7 , the effective CY volume after D-term stabilisation looks like a single K3 fibre τ_7 over a \mathbb{P}^1 base t_7 and reduces to the typical form used in fibre inflation models. The blow-up mode τ_1 and the overall volume \mathcal{V} are stabilised in the LVS fashion by means of a non-perturbative correction to W generated by an Euclidean D3-brane instanton wrapping D_1 . This leaves the fibre modulus τ_7 as a flat direction which receives a potential at subleading order.

Let us now focus on the inflationary potential. The winding loop corrections can be written as (with $\kappa = g_s/(8\pi)$ for $e^{K_{cs}} = 1$):

$$V_{g_s}^w = -2\kappa \frac{W_0^2}{\mathcal{V}^3} \sum_i \frac{C_i^w}{t_i^\Omega}, \quad (2.32)$$

where t_i^Ω are the volumes of the two-cycles where D7-branes/O7-planes intersect. Notice that if two coordinate divisors D_i and D_j are wrapped by D7-branes and/or O7-planes, the scalar potential receives t^Ω -dependent winding loop corrections only if their intersection curve contains non-contractible 1-cycles, i.e. if $h^{1,0}(D_i \cap D_j) \neq 0$. In our case, we have an O7-plane located on D_8 and three stacks of D7-branes wrapping D_2 , D_4 and D_6 . Using Tab. 2.1 and 2.2, we see all D7s intersect with each other and with the O7 and that winding corrections can arise from any of these intersections. Thus we end up with:

$$V_{g_s}^w = -\kappa \frac{W_0^2}{\mathcal{V}^3} \left[\frac{1}{\sqrt{\tau_7}} \left(C_w - \tilde{C}_w(\tau_7) \right) - \frac{\tau_7}{\mathcal{V}} \left(|C_3^w| - \hat{C}_w(\tau_7) \right) \right], \quad (2.33)$$

where (setting $t_4 = \alpha t_6$, $C_3^w = -|C_3^w| < 0$ and $C_4^w = -|C_4^w| < 0$):

$$C_w = \sqrt{2\alpha} \left(C_1^w + \frac{C_2^w}{\alpha} \right) \quad \tilde{C}_w(\tau_7) = \frac{|C_4^w|}{(\alpha + 1)} \sqrt{\frac{\alpha}{2}} \left(1 - \frac{\sqrt{2\alpha}}{(\alpha + 1)} \sqrt{\frac{\langle \tau_1 \rangle}{\tau_7}} \right)^{-1}, \quad (2.34)$$

and:

$$\hat{C}_w(\tau_7) = \frac{C_5^w}{2} \left(1 + \frac{1}{\sqrt{2\alpha}} \frac{\tau_7^{3/2}}{\mathcal{V}} \right)^{-1} + \frac{C_6^w}{2} \left(1 + \sqrt{\frac{\alpha}{2}} \frac{\tau_7^{3/2}}{\mathcal{V}} \right)^{-1}. \quad (2.35)$$

Due to the absence of O3-planes (we also assume that the D3-tadpoles are cancelled

without including any spacetime-filling D3-branes) and the fact that all D7s intersect with each other and with the O7-plane, there are no 1-loop corrections due to the exchange of closed strings carrying KK momentum.⁷

On the other hand, higher derivative $\alpha'^3 F^4$ corrections to the scalar potential can be written as [75]:⁸

$$V_{F^4} = -\kappa^2 \frac{\lambda W_0^4}{g_s^{3/2} \mathcal{V}^4} \sum_{i=1}^{h^{1,1}} \Pi_i t_i, \quad (2.36)$$

where λ is an unknown combinatorial factor which is expected to be of order 10^{-3} [75, 76] and the topological quantities Π_i are given in (2.12). After imposing the D-term condition (2.30), the F^4 contributions can be rewritten as (ignoring the t_1 -dependent term):

$$V_{F^4} = -24\kappa^2 \frac{\lambda W_0^4}{g_s^{3/2} \mathcal{V}^3} \left[\frac{(\alpha + 1)}{\sqrt{2\alpha}} \frac{\sqrt{\tau_7}}{\mathcal{V}} + \frac{1}{\tau_7} \right]. \quad (2.37)$$

Therefore the total inflationary potential becomes:

$$V = V_{g_s^w} + V_{F^4} = \kappa \frac{W_0^2}{\mathcal{V}^3} \left(\frac{A_1}{\tau_7} - \frac{A_2}{\sqrt{\tau_7}} + \frac{B_1 \sqrt{\tau_7}}{\mathcal{V}} + \frac{B_2 \tau_7}{\mathcal{V}} \right), \quad (2.38)$$

where (with $\lambda = -|\lambda| < 0$):

$$A_1 = \frac{3}{\pi} \frac{|\lambda| W_0^2}{\sqrt{g_s}} \quad A_2 = C_w - \tilde{C}_w(\tau_7) \quad B_1 = \frac{(\alpha + 1)}{\sqrt{2\alpha}} A_1 \quad B_2 = |C_3^w| - \hat{C}_w(\tau_7).$$

2.3 Inflationary dynamics

In this section we shall analyse the inflationary dynamics by studying first the single-field approximation and then by focusing on the full multi-field evolution.

⁷Strictly speaking, there might be 1-loop corrections associated with the exchange of KK modes between the Euclidean D3-instanton on D_1 and the D7-branes which do not intersect D_1 . However, we expect such corrections to be exponentially suppressed and, thus, not relevant for the analysis.

⁸This expression displays merely the leading order $\mathcal{O}(\mathcal{V}^{-4})$ terms which are corrected at subleading order in inverse volume by additional corrections as discussed in [78]. Furthermore, additional higher-derivative corrections mediated by the auxiliary fields sitting in the supergravity multiplet might emerge at order $\mathcal{O}(\mathcal{V}^{-5})$ [78, 106].

2.3.1 Single-field evolution

In order to realise single-field slow-roll inflation where the potential for the inflaton τ_7 features a plateau-type region [14, 78], the overall volume has to be approximately constant during the whole inflationary dynamics. Therefore, in order to get enough efoldings before reaching the dangerous limit where the base of the fibration t_7 becomes smaller than the string scale, we need to focus on the region in field space where the inflaton minimum is of order $\langle \tau_7 \rangle \ll \mathcal{V}^{2/3}$. For $g_s \lesssim \mathcal{O}(0.1)$, $|\lambda| \sim \mathcal{O}(10^{-3})$ and natural $\mathcal{O}(1)$ values of the coefficients of the string loop effects, in the vicinity of the minimum the terms in (2.38) proportional to B_1 and B_2 are therefore both negligible with respect to the terms proportional to A_1 and A_2 . Numerical estimates show that we need values of order $\langle \tau_7 \rangle \sim \mathcal{O}(1)$ and $\mathcal{V} \sim \mathcal{O}(10^4)$ which, in turn, imply $W_0 \sim \mathcal{O}(100)$ in order to match the observed amplitude of the density perturbations.

The scalar potential (2.38) written in terms of the canonically normalised inflaton shifted from its minimum $\phi = \langle \phi \rangle + \hat{\phi}$, where $\tau_7 = \langle \tau_7 \rangle e^{k\hat{\phi}}$ with $k = 2/\sqrt{3}$, becomes:

$$V = \kappa \frac{A_2 W_0^2}{\mathcal{V}^3 \sqrt{\langle \tau_7 \rangle}} \left(C_{\text{ds}} + c e^{-k\hat{\phi}} - e^{-\frac{k\hat{\phi}}{2}} + \mathcal{R}_1 e^{\frac{k\hat{\phi}}{2}} + \mathcal{R}_2 e^{k\hat{\phi}} \right), \quad (2.39)$$

where:

$$c = \frac{3}{\pi \left(C_{\text{w}} - \tilde{C}_{\text{w}}(\tau_7) \right)} \frac{|\lambda| W_0^2}{\sqrt{g_s \langle \tau_7 \rangle}} \sim \mathcal{O}(1),$$

while for $\langle \tau_7 \rangle \sim \mathcal{O}(1) \ll \mathcal{V}^{2/3}$:

$$\mathcal{R}_1 = \frac{(\alpha + 1)c \langle \tau_7 \rangle^{3/2}}{\sqrt{2\alpha} \mathcal{V}} \ll 1 \quad \text{and} \quad \mathcal{R}_2 = \frac{\left(|C_3^{\text{w}}| - \hat{C}_{\text{w}}(\tau_7) \right) \langle \tau_7 \rangle^{3/2}}{\left(C_{\text{w}} - \tilde{C}_{\text{w}}(\tau_7) \right) \mathcal{V}} \ll 1.$$

Notice that in (2.39) we added a constant $C_{\text{ds}} = 1 - c - \mathcal{R}_1 - \mathcal{R}_2$ to obtain a Minkowski (or slightly dS) vacuum. It is important to say that at this stage we are working in units where $M_p = 1$, for the later cosmological discussion we will restore the power of M_p .

Given that no O3-planes are present in our model, the usual uplift mechanism where an anti D3-brane is located in a resolved conifold region of the extra dimensions would require additional effort to implement. We leave the explicit embedding of the source of uplift to future research.

The two negative exponentials in (2.39) compete to give a minimum at $\langle \tau_7 \rangle \sim \mathcal{O}(1)$ while the two positive exponentials cause a steepening behaviour at large $\hat{\phi}$. Thus we need to make sure that both $\mathcal{R}_1 \ll 1$ and $\mathcal{R}_2 \ll 1$ to prevent the two positive exponentials from destroying the inflationary plateau before achieving

enough efoldings of inflation.⁹ The condition $\mathcal{R}_1 \ll 1$ could be satisfied for $c \ll 1$, for example for $W_0 \sim \mathcal{O}(1)$ and $\langle \tau_7 \rangle \gg 1$, in which case the minimum could be obtained by balancing the two terms in the coefficient A_2 . However, as we shall see below, if $\langle \tau_7 \rangle \gg 1$, the Kähler cone bounds restrict the allowed field space so much that it becomes impossible to realise enough efoldings of inflation. Hence we shall focus the region where $\mathcal{R}_1 \ll 1$ and $\mathcal{R}_2 \ll 1$ are satisfied by $\langle \tau_7 \rangle \sim \mathcal{O}(1) \ll \mathcal{V}^{2/3}$ (and possibly by allowing some tuning of the complex structure moduli-dependent coefficients of the loop corrections or by considering $|\lambda| \ll 1$).

Turning now to the explicit numerical examples, let us formulate the necessary conditions that have to be satisfied in order to have a viable model:

1. Stringy effects can be neglected if each four-cycle in string frame has a volume larger than the string scale: $\text{Vol}_s^{1/4} \gg \sqrt{\alpha'}$. Given that string and Einstein frame volumes are related as $\text{Vol}_s = g_s \text{Vol}_E = g_s \tau_E \ell_s$ with $\ell_s = 2\pi\sqrt{\alpha'}$, we end up with the condition:

$$\epsilon_{\tau_i} \equiv \frac{1}{g_s (2\pi)^4 \tau_i} \ll 1 \quad \forall i. \quad (2.40)$$

2. The whole inflationary dynamics should take place inside the Kähler cone. This implies in particular that:

$$\begin{aligned} 2\alpha \langle \tau_1 \rangle < \tau_7 < \frac{\mathcal{V}}{\sqrt{\langle \tau_1 \rangle}} & \quad \text{if} \quad \alpha \geq 1, \\ \frac{2}{\alpha} \langle \tau_1 \rangle < \tau_7 < \frac{\mathcal{V}}{\sqrt{\langle \tau_1 \rangle}} & \quad \text{if} \quad \alpha \leq 1. \end{aligned} \quad (2.41)$$

Notice that these conditions guarantee the absence of any singularity in the inflationary potential (2.39) which could originate from the shrinking of a two-cycle to zero size. Rewriting these conditions in terms of the canonically normalised inflaton field, we end up with:

$$\begin{aligned} \frac{\sqrt{3}}{2} \ln \left(\frac{2\alpha \langle \tau_1 \rangle}{\langle \tau_7 \rangle} \right) < \hat{\phi} < \frac{\sqrt{3}}{2} \ln \left(\frac{\mathcal{V}}{\langle \tau_7 \rangle \sqrt{\langle \tau_1 \rangle}} \right) & \quad \text{if} \quad \alpha \geq 1, \\ \frac{\sqrt{3}}{2} \ln \left(\frac{2 \langle \tau_1 \rangle}{\alpha \langle \tau_7 \rangle} \right) < \hat{\phi} < \frac{\sqrt{3}}{2} \ln \left(\frac{\mathcal{V}}{\langle \tau_7 \rangle \sqrt{\langle \tau_1 \rangle}} \right) & \quad \text{if} \quad \alpha \leq 1. \end{aligned} \quad (2.42)$$

In order to be able to describe within a consistent EFT, not just inflation but

⁹If this is the case, these steepening terms could then be responsible for an interesting power loss at large angular scales [107].

also the post-inflationary evolution of our model, $\hat{\phi}$ should reach its minimum before hitting the lower bounds in (2.42). Moreover the inflaton should drive enough efoldings of inflation before hitting the upper bounds in (2.42).

3. Horizon exit at $\hat{\phi} = \hat{\phi}_*$ should yield the required number of efoldings:

$$N_e \simeq 57 + \frac{1}{4} \ln(r_* V_*) - \frac{1}{3} \ln\left(\frac{V_{\text{end}}}{T_{\text{rh}}}\right), \quad (2.43)$$

where the reheating temperature T_{rh} can be estimated in terms of the inflaton mass at the minimum $m_{\hat{\phi}}$ as:

$$T_{\text{rh}} \simeq \left(\frac{90}{\pi^2 g_*(T_{\text{rh}})}\right)^{1/4} \sqrt{\Gamma_{\hat{\phi}} M_p} \simeq 0.1 m_{\hat{\phi}} \sqrt{\frac{m_{\hat{\phi}}}{M_p}}. \quad (2.44)$$

4. Horizon exit at $\hat{\phi} = \hat{\phi}_*$ should reproduce the observed amplitude of the density perturbations:

$$\frac{V_*^3}{V_*'^2} \simeq 2.6 \cdot 10^{-7}. \quad (2.45)$$

5. The α' expansion of the potential can be trusted only if:

$$\epsilon_\xi = \frac{\xi}{2g_s^{3/2}\mathcal{V}} \ll 1. \quad (2.46)$$

6. The effective field theory is under control if throughout all the inflationary dynamics:

$$m_{\text{inf}} < H < m_{3/2} < M_{\text{KK}}^{(i)} < M_s < M_p \quad \forall i = \text{bulk}, 2, 4, 6, \quad (2.47)$$

where m_{inf} is the inflaton mass, $H \simeq \frac{V}{3M_p^2}$ is the Hubble scale, $m_{3/2} = e^{K/2} W_0 = \sqrt{\kappa} \frac{W_0}{\mathcal{V}} M_p$ is the gravitino mass which sets the mass scale of all complex structure moduli, the dilaton and the Kähler modulus $T_1 = \tau_1 + i \int_{D_1} C_4$ and $M_{\text{KK}}^{(i)} = \frac{\sqrt{\pi}}{\sqrt{\mathcal{V}} \tau_i^{1/4}} M_p$ are the different KK scales in the model associated with bulk KK modes for $\tau_{\text{bulk}}^{3/2} = \mathcal{V}$ and KK replicas of open string modes living on D7-branes wrapped around D_2 , D_4 and D_6 . The bulk KK scale should be below the string scale $M_s = \frac{g_s^{1/4} \sqrt{\pi}}{\sqrt{\mathcal{V}}} M_p$ while we do not need to impose $V^{1/4} < M_{\text{KK}}^{(i)}$ since no energy can be extracted from the vacuum during an adiabatic inflationary expansion where $H \ll M_{\text{KK}}^{(i)}$.

7. Besides the two ultra-light axions associated with the base and the fibre which

develop just negligible isocurvature fluctuations during inflation if they do not contribute significantly to dark matter, only the volume mode has a mass below $m_{3/2}$. In order to trust our single field approximation, we need therefore to check that the mass of the volume mode $m_{\mathcal{V}}$ does not become smaller than the Hubble scale H . This condition boils down to:

$$\delta = \frac{H}{m_{\mathcal{V}}} \simeq \sqrt{\frac{V_*}{3V_{\alpha'}}} \lesssim 1, \quad (2.48)$$

where $V_{\alpha'}$ is the leading $\mathcal{O}(\alpha'^3)$ contribution to the scalar potential and reads [36]:

$$V_{\alpha'} = \kappa \frac{3\xi W_0^2}{4g_s^{3/2}\mathcal{V}^3} \quad \text{with} \quad \xi = -\frac{\zeta(3)\chi(X)}{2(2\pi)^3}. \quad (2.49)$$

If $\delta \simeq 1$, the inflationary energy density can either destabilise the volume direction or cause a significant shift of the volume minimum. Hence the inflationary dynamics can effectively become a multi-field evolution. However, as analysed in [14], the motion might still remain mainly along the τ_7 direction, and so the predictions for the inflationary observables could be basically unaltered apart from the fact that the number of allowed efoldings slightly increases. Notice also that in LVS models the CY Euler number together with the string coupling fixes the minimum of the blow-up mode τ_1 as: $\langle \tau_1 \rangle = (3\xi/2)^{2/3} g_s^{-1}$. This value is important to evaluate the Kähler cone conditions in (2.42).

We shall now focus on single-field slow-roll inflation where:

$$\epsilon(\hat{\phi}) = \frac{1}{2} \left(\frac{V'}{V} \right)^2 \ll 1 \quad \text{and} \quad \eta(\hat{\phi}) = \frac{V''}{V} \ll 1.$$

Notice that the condition $\eta \ll 1$ guarantees that the inflaton is lighter than H during inflation. In order to illustrate the main features of our inflationary model, we shall now consider two different choices of the underlying parameters characterised by different values of the coefficients ξ and λ which control the strength of the $\mathcal{O}(\alpha'^3)$ corrections to the effective action at $\mathcal{O}(F^2)$ and $\mathcal{O}(F^4)$. According to [37], $N = 1$ $\mathcal{O}(\alpha'^3)$ corrections due to O7-planes cause a shift of the CY Euler number $\chi(X)$ to $\chi_{\text{eff}}(X)$ defined in (2.13) and given in Tab. 2.3. From (2.49) this modification would give $\xi = 0.067$. Moreover the coefficient λ of higher derivative $\mathcal{O}(\alpha'^3)$ effects has been estimated to be negative and of order 10^{-3} [75, 76]. Hence the first set of parameters will be characterised by $\xi = 0.067$ and $\lambda = -0.001$. However both of these corrections still lack a full supersymmetric analysis, and so in the second case we shall focus on a situation where the CY Euler number is not modified, and so

$\xi = 0.456$, and the size of the coefficient λ is much smaller: $|\lambda| \lesssim 10^{-6}$.

Case 1: $\xi = 0.067$ and $|\lambda| = 0.001$

Let us now provide an explicit numerical example set to demonstrate the features of our inflationary model:

$$\begin{aligned} \alpha &= 1, & C_1^w &= C_2^w = 15, & |C_3^w| &= 0.013, & |C_4^w| &= 18, & C_5^w &= C_6^w = -5, \\ g_s &= 0.114, & \mathcal{V} &= 10^4, & \langle \tau_1 \rangle &= 1.91, & W_0 &= 80, & |\lambda| &= 0.001, \end{aligned} \quad (2.50)$$

with $\chi(X) = \chi_{\text{eff}}(X) = -28$ in (2.49) which gives $\xi = 0.067$. Notice that the tuning of the steepening term here is mild since the difference between the largest and the smallest winding coefficient is between one and two orders of magnitude. The form of the inflationary potential is plotted in Fig. 2.1 and it is characterised by:

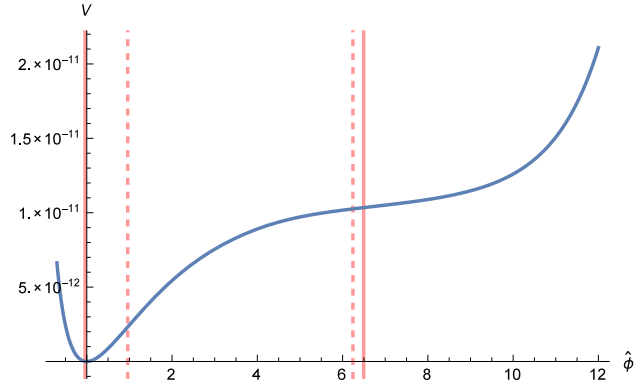


Figure 2.1: Plot of the inflationary potential for the example set (2.50). The red vertical lines correspond to the walls of the Kähler cone while the dashed vertical lines denote horizon exit and the end of inflation where $\epsilon = 1$. We work in units of $M_p = 1$.

- $\langle \tau_7 \rangle = 4.002$ leading to $\epsilon_{\langle \tau_7 \rangle} = 0.0014$. Moreover $2\langle \tau_1 \rangle \simeq 3.8$, and so the distance of the minimum from the lower bound of the Kähler cone is $\Delta\tau_7 \simeq 0.178$ which is still larger than the string scale since, using (2.40), we have that:

$$\epsilon_{\Delta\tau_7} = \frac{1}{g_s(2\pi)^4 \Delta\tau_7} \simeq 0.03. \quad (2.51)$$

- The Kähler cone bounds (2.42) in terms of the canonically normalised inflaton become $\hat{\phi}_{\min} \simeq -0.04 < \hat{\phi} < \hat{\phi}_{\max} \simeq 6.49$. Inflation ends at $\hat{\phi} = \hat{\phi}_{\text{end}} \simeq 0.96$ where $\epsilon(\hat{\phi}_{\text{end}}) = 1$ and $V_{\text{end}} \simeq (7 \cdot 10^{15} \text{ GeV})^4$. Horizon exit takes place at

$\hat{\phi} = \hat{\phi}_* \simeq 6.24$ where $r = 16\epsilon = 0.009$, $n_s = 1 + 2\eta_* - 6\epsilon_* = 0.983$, $V_* \simeq (1 \cdot 10^{16} \text{ GeV})^4$ and the amplitude normalisation (2.45) is satisfied. Notice that such a largish value of the scalar spectral index is in perfect agreement with Planck data in the presence of dark radiation since, using $\Delta N_{\text{eff}} = 0.39$ as a prior, [7] gives as best fit $n_s = 0.983 \pm 0.006$. This prior is fully justified in string models like ours where reheating is driven by the decay of the lightest modulus which naturally tends to produce extra axionic contributions to dark radiation [58, 59, 60, 61].

- Horizon exit occurs well inside the Kähler cone since from (2.41) we have:

$$\tau_7^* = e^{\kappa(\langle\phi\rangle + \hat{\phi}_*)} \simeq 5404.82 < \tau_7^{\text{max}} = \frac{\mathcal{V}}{\sqrt{\langle\tau_1\rangle}} \simeq 7231.87 \quad \Rightarrow \quad \tau_7^{\text{max}} - \tau_7^* \simeq 1827.06.$$

- The mass of the inflaton around the minimum is $m_{\hat{\phi}} \simeq 4.25 \cdot 10^{13} \text{ GeV}$ which from (2.44) implies a reheating temperature $T_{\text{rh}} \simeq 1.8 \cdot 10^{10} \text{ GeV}$.
- The number of efoldings computed as:

$$N_e = \int_{\hat{\phi}_{\text{end}}}^{\hat{\phi}_*} \frac{V}{V'} d\hat{\phi}, \quad (2.52)$$

gives $N_e = 52$ as required by the estimate (2.43). The maximum number of efoldings between $\hat{\phi}_{\text{end}}$ and $\hat{\phi}_{\text{max}}$ is $N_e^{\text{max}} \simeq 60$.

- The α' expansion is under control even if in our inflationary model the inflaton travels over a trans-Planckian distance of order $\Delta\hat{\phi} = \hat{\phi}_* - \hat{\phi}_{\text{end}} = 5.28$ since we have $\epsilon_\xi \sim 10^{-4}$.
- The mass of the volume mode is of order the Hubble scale during inflation since $\delta \simeq 1.6$. Hence the inflationary energy density could either cause a significant shift of the original LVS minimum or destabilise the volume direction. A definite answer to this question would require a more careful multi-field analysis. As mentioned above, a similar situation has been studied in [14], where the authors found that for $\delta \sim 1$ the minimum for the volume mode gets a large shift but the inflationary evolution still remains mostly single-field since $m_{\text{inf}} \ll m_\nu \sim H$. However if $\delta \sim 1$, the inflationary potential generated by string loops and $\alpha'^3 F^4$ terms is of the same order as the $\alpha'^3 F^2$ contribution, and so one also should carefully check if additional higher derivative corrections can be safely neglected.

- The effective field theory approximation is valid during the whole inflationary evolution since $H \simeq 2 \cdot 10^{13} \text{ GeV} < m_{3/2} \simeq 1 \cdot 10^{15} \text{ GeV} < M_{\text{KK}}^{\text{bulk}} \simeq 9 \cdot 10^{15} \text{ GeV} < M_s \simeq 2.5 \cdot 10^{16} \text{ GeV}$.

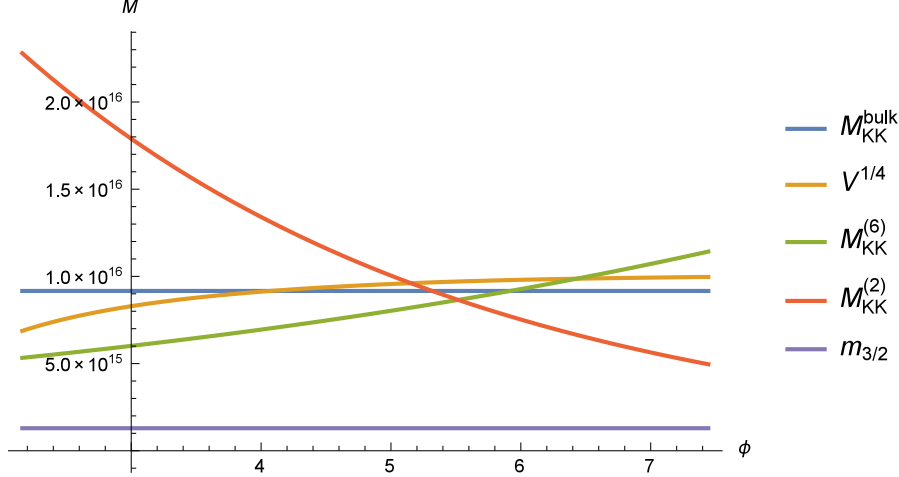


Figure 2.2: Comparison between the different KK masses, $m_{3/2}$ and the inflationary energy density $V^{1/4}$ from horizon exit to the end of inflation. Note that $M_{\text{KK}}^{(4)} = M_{\text{KK}}^{(6)}$ which is why only one of them is displayed here.

We display the evolution of the different KK masses as compared to the gravitino mass and the inflationary scale $M_{\text{inf}} = V^{1/4}$ in Fig. 2.2. Notice, in particular, that at the end of inflation the inflationary scale is of order $M_{\text{KK}}^{\text{bulk}}$ and, above all, mildly exceeds the KK scale $M_{\text{KK}}^{(4)}$ by a factor of roughly 1.3. As we stressed above, during an adiabatic expansion no energy can be extracted from the vacuum, and so our EFT is still valid even if some KK scales become smaller than $V^{1/4}$ since they are all always larger than $m_{3/2}$ which is, in turn, larger than H . However, since all the inflationary energy density could instead be converted into particle production at reheating, one should make sure that there is enough Hubble friction between the end of inflation and reheating to bring the inflaton energy density below the relevant KK scale. This effect can be estimated by noticing that from:

$$\rho(\phi) = \frac{1}{2}\dot{\phi}^2 + V(\phi) = 3H^2 M_p^2 \quad \Leftrightarrow \quad \partial_t \rho(\phi) = -3H\dot{\phi}^2, \quad (2.53)$$

we can obtain the following relation between the energy density at the end of inflation and at reheating:

$$\rho_{\text{rh}} = \rho_{\text{end}} - 3\langle \dot{\phi}^2 \rangle \int_{\text{end}}^{\text{rh}} \frac{da}{a} = \rho_{\text{end}} - 3N_{\text{rh}} \langle \dot{\phi}^2 \rangle, \quad (2.54)$$

where $\langle \dot{\phi}^2 \rangle$ is the time average between the end of inflation and reheating and $N_{\text{rh}} = \ln(a_{\text{rh}}/a_{\text{end}})$ is the number of efoldings of the reheating epoch. At the end of inflation when $\epsilon = 1$ we have:

$$\frac{1}{2}\dot{\phi}^2 = H^2 M_p^2 \quad \Leftrightarrow \quad \rho_{\text{end}} = \frac{3}{2}V_{\text{end}} \simeq 10 \left(M_{\text{KK}}^{(4)}\right)^4. \quad (2.55)$$

On the other hand at reheating $V(\phi_{\text{rh}}) \simeq 0$, and so $\rho_{\text{rh}} \simeq \dot{\phi}_{\text{rh}}^2/2$. If we then write the time-average kinetic energy as $\langle \dot{\phi}^2 \rangle = \dot{\phi}_{\text{rh}}^2/x \simeq 2\rho_{\text{rh}}/x$ with $x > 0$, we end up with the following bound:

$$\rho_{\text{rh}} \simeq \frac{10}{1 + \frac{6}{x}N_{\text{rh}}} \left(M_{\text{KK}}^{(4)}\right)^4 < \left(M_{\text{KK}}^{(4)}\right)^4. \quad (2.56)$$

Using the fact that:

$$N_{\text{rh}} \simeq \frac{1}{3} \ln \left(\frac{H_{\text{end}}^2 M_p^2}{T_{\text{rh}}^4} \right) - \frac{1}{3} \ln \left(\frac{\pi^2 g_*}{90} \right) \simeq 16, \quad (2.57)$$

the bound (2.56) becomes $x < \frac{2}{3}N_{\text{rh}} \simeq 10$. Our model should satisfy this bound since we expect $\dot{\phi}_{\text{end}}$ to approach $\dot{\phi}_{\text{rh}}$ relatively quickly due to the steepness of the potential near the end of inflation. However a definite answer would require a detailed study of the post-inflationary epoch which is beyond the scope of this chapter.¹⁰

Let us also mention that, due to the absence of KK corrections, this scenario represents a chiral global embedding of the α' -inflation models discussed in [78]. Moreover, no KK scale becomes smaller than the gravitino mass even if $r \simeq 0.01$ and $\Delta\hat{\phi} \simeq 5$ in Planck units. In fact, if we focus for example on the KK scale $M_{\text{KK}}^{(2)}$ associated with the K3 fibre (similar considerations apply to the KK scale $M_{\text{KK}}^{(6)}$ associated with the base), we have:

$$\frac{m_{3/2}}{M_{\text{KK}}^{(2)}} = \alpha_1 e^{\alpha_2 \phi} \simeq 0.03 e^{\alpha_2 \phi}, \quad (2.58)$$

with:

$$\alpha_1 = \sqrt{\frac{W_0}{2\pi}} \left(\frac{g_s}{2\pi}\right)^{1/4} \sqrt{\frac{m_{3/2}}{M_p}} \simeq 0.03 \quad \text{and} \quad \alpha_2 = \frac{1}{2\sqrt{3}}. \quad (2.59)$$

¹⁰Let us also point out that, even if $\rho_{\text{rh}} \gtrsim \left(M_{\text{KK}}^{(4)}\right)^4$, our model is not necessarily ruled out but we would just need to describe reheating within a 6D EFT where the base of the fibration is much larger than the characteristic size of the fibre. It would also be interesting to find brane setups where this problem is automatically absent since there is no D7-brane wrapped around the base.

If we set $\phi = \phi_0 + \hat{\phi}_{\text{he}} \simeq 7.44$, the ratio in (2.58) becomes $m_{3/2}/M_{\text{KK}}^{(2)} \simeq 0.26$, and so the KK scale $M_{\text{KK}}^{(2)}$ is always larger than the gravitino mass throughout all the inflationary dynamics. Notice that this result seems to be in slight disagreement with the swampland conjecture of [108, 109] where the underlying parameters α_1 and α_2 were generically assumed to be of order unity.

As explained above, given that in this case $\delta \simeq 1.6$, the inflationary dynamics can be fully trusted only after determining the proper multi-field evolution. Due to the difficulty to perform a full numerical analysis, in the next section we shall instead still focus on a single-field case where $\delta \sim 0.05$ since ξ is larger, and so the volume mode mass is larger, while $|\lambda|$ is smaller, and so F^4 steepening terms can be easily neglected throughout the whole inflationary dynamics. The full three-field evolution for both of these cases will then be presented in Sec. 2.3.2.

Case 2: $\xi = 0.456$ and $|\lambda| = 10^{-7}$

According to the discussion above, we shall now focus on the following different choice of the underlying parameters:

$$\begin{aligned} \alpha &= 1, & C_1^{\text{w}} = C_2^{\text{w}} = 0.034, & |C_3^{\text{w}}| = 10^{-5}, & |C_4^{\text{w}}| = 0.068, & C_5^{\text{w}} = C_6^{\text{w}} = -0.024, \\ g_s &= 0.25, & \mathcal{V} = 4500, & \langle \tau_1 \rangle = 3.10, & W_0 = 150, & |\lambda| = 10^{-7}, \end{aligned} \quad (2.60)$$

with $\chi(X) = \chi_{\text{eff}}(X) = -188$ in (2.49) which gives $\xi = 0.456$. A larger value of the coefficient ξ is helpful to increase the control on the single-field approximation since, as can be seen from (2.49), the leading $\mathcal{O}(\alpha^3)$ contribution to the scalar potential is proportional to ξ . The form of the inflationary potential is plotted in Fig. 2.3 and it is characterised by:

- $\langle \tau_7 \rangle \simeq 6.41$ leading to $\epsilon_{\langle \tau_7 \rangle} \simeq 0.0004$ and $\langle \phi \rangle \simeq 1.61$. Moreover $2\langle \tau_1 \rangle \simeq 6.2$, and so the minimum is located close to the walls of the Kähler cone but at a distance $\Delta\tau_7 \simeq 0.21$ which is still larger than the string scale since, using (2.40), we have that:

$$\epsilon_{\Delta\tau_7} = \frac{1}{g_s(2\pi)^4 \Delta\tau_7} \simeq 0.01. \quad (2.61)$$

- The Kähler cone bounds (2.42) in terms of the canonically normalised inflaton become $\hat{\phi}_{\text{min}} \simeq -0.028 < \hat{\phi} < \hat{\phi}_{\text{max}} \simeq 5.19$. Inflation ends at $\hat{\phi} = \hat{\phi}_{\text{end}} \simeq 0.93$ where $\epsilon(\hat{\phi}_{\text{end}}) = 1$ and $V_{\text{end}} = (4.4 \cdot 10^{15} \text{ GeV})^4$. Horizon exit takes place at $\hat{\phi} = \hat{\phi}_* \simeq 5.10$ where $r = 16\epsilon = 0.0014$, $n_s = 1 + 2\eta_* - 6\epsilon_* = 0.963$,

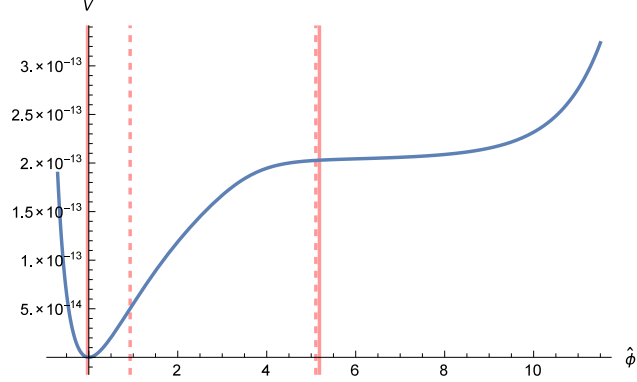


Figure 2.3: Plot of the inflationary potential for the example set (2.60). The red vertical lines correspond to the walls of the Kähler cone while the dashed vertical lines denote horizon exit and the end of inflation where $\epsilon = 1$. We work in units of $M_p = 1$.

$V_* = (6.2 \cdot 10^{15} \text{ GeV})^4$ and the amplitude normalisation (2.45) is satisfied. Notice that horizon exit occurs far away from the upper bound of the Kähler cone since from (2.41) we have:

$$\tau_7^* = e^{\kappa(\langle\phi\rangle + \hat{\phi}_*)} \simeq 2325.79 < \tau_7^{\max} = \frac{\mathcal{V}}{\sqrt{\langle\tau_1\rangle}} \simeq 2554.55 \quad \Rightarrow \quad \tau_7^{\max} - \tau_7^* \simeq 228.76.$$

- The mass of the inflaton around the minimum is $m_{\hat{\phi}} \simeq 1.85 \cdot 10^{13} \text{ GeV}$ which from (2.44) implies a reheating temperature $T_{\text{rh}} \simeq 5.16 \cdot 10^9 \text{ GeV}$.
- The number of efoldings computed as:

$$N_e = \int_{\hat{\phi}_{\text{end}}}^{\hat{\phi}_*} \frac{V}{V'} d\hat{\phi}, \quad (2.62)$$

gives $N_e = 51$ as required by the estimate (2.43). The maximum number of efoldings between $\hat{\phi}_{\text{end}}$ and $\hat{\phi}_{\text{max}}$ is $N_e^{\max} \simeq 57.5$.

- The α' expansion is under control even if in our inflationary model the inflaton travels over a trans-Planckian distance of order $\Delta\hat{\phi} = \hat{\phi}_* - \hat{\phi}_{\text{end}} = 4.17$ since we have $\epsilon_\xi \simeq 0.0004$.
- The single-field approximation is under control since $\delta \simeq 0.05$.
- The effective field theory approximation is valid during the whole inflationary evolution since $H \simeq 7 \cdot 10^{12} \text{ GeV} < m_{3/2} \simeq 8 \cdot 10^{15} \text{ GeV} < M_{\text{KK}}^{\text{bulk}} \simeq 1.6 \cdot 10^{16} \text{ GeV} < M_s \simeq 4.5 \cdot 10^{16} \text{ GeV}$.

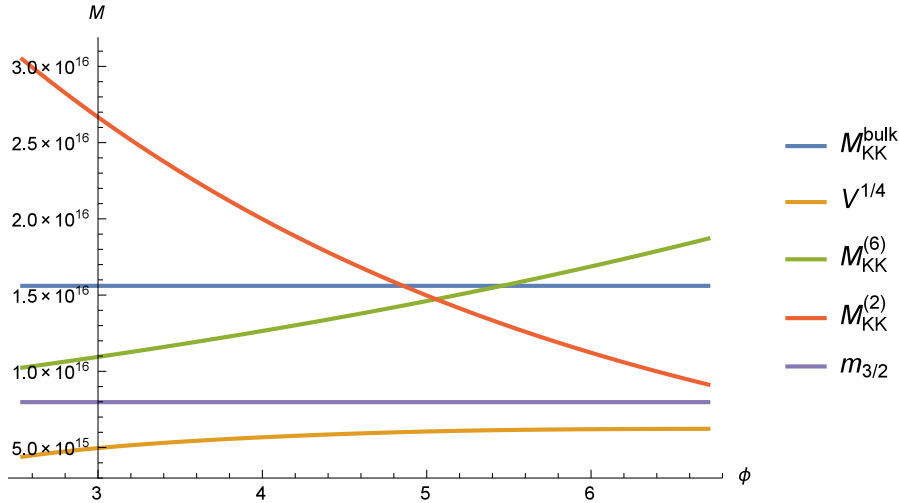


Figure 2.4: Comparison between the different KK masses, the gravitino mass $m_{3/2}$ and the inflationary energy $V^{1/4}$ from horizon exit to the end of inflation. Note that $M_{\text{KK}}^{(4)} = M_{\text{KK}}^{(6)}$ which is why only one of them is displayed here.

We display the evolution of the different KK masses as compared to the gravitino mass and the inflationary energy density $M_{\text{inf}} = V^{1/4}$ in Fig. 2.4. Notice that, contrary to case 1 where $r = 0.01$, all KK scales remain above M_{inf} throughout all the inflationary dynamics. The reason is that in this scale the tensor-to-scalar ratio, and so also the inflationary scale, is smaller since $r = 0.001$. Moreover, as stressed above, no energy can be extracted from the vacuum during an adiabatic expansion, and so the consistency condition to be imposed during inflation is $H \ll M_{\text{KK}}^{(i)}$ which is clearly satisfied since $H = \frac{M_{\text{inf}}}{\sqrt{3}} \left(\frac{M_{\text{inf}}}{M_p} \right) < M_{\text{inf}}$. Moreover, no KK scale becomes smaller than the gravitino mass $m_{3/2} \simeq 8 \cdot 10^{15}$ GeV. If we focus for example on the KK scale $M_{\text{KK}}^{(2)}$ associated with the K3 fibre (similar considerations apply to the KK scale $M_{\text{KK}}^{(6)}$ associated with the base of the fibration), we have:

$$\frac{m_{3/2}}{M_{\text{KK}}^{(2)}} = \alpha_1 e^{\alpha_2 \phi} \simeq 0.126 e^{\alpha_2 \phi}, \quad (2.63)$$

with:

$$\alpha_1 = \sqrt{\frac{W_0}{2\pi}} \left(\frac{g_s}{2\pi} \right)^{1/4} \sqrt{\frac{m_{3/2}}{M_p}} \simeq 0.126 \quad \text{and} \quad \alpha_2 = \frac{1}{2\sqrt{3}}. \quad (2.64)$$

If we set $\phi = \phi_0 + \hat{\phi}_{\text{he}} \simeq 6.71$, the ratio in (2.63) becomes $m_{3/2}/M_{\text{KK}}^{(2)} \simeq 0.87$, and so the KK scale $M_{\text{KK}}^{(2)}$ is always larger than the gravitino mass throughout all the inflationary dynamics. This result seems to be more in agreement with the swampland conjecture of [108, 109] than the one of case 1 since r is smaller,

$r \simeq 0.001$, and the field range is slightly reduced, $\Delta\hat{\phi} \simeq 4$. Moreover larger values of ϕ would bring the effective field theory approach out of control.

Even if this example satisfies all consistency and phenomenological constraints and the single-field inflationary analysis is under control, in Sec. 2.3.2 we shall perform a more precise multifield analysis where the motion along the orthogonal directions enlarges the field space as well as the allowed number of efoldings.

2.3.2 Multi-field evolution

The following five consistency conditions require generically a multi-field study of the inflationary evolution (which might however still be mainly along a single direction in field space):

1. The whole inflationary dynamics takes place well inside the Kähler cone described by the conditions in (2.41);
2. The quantum fluctuations of the inflaton produce a correct amplitude of the density perturbations at horizon exit;
3. The directions orthogonal to the inflaton are not destabilised by the inflationary dynamics. This is guaranteed if inflation occurs in field space along a through which can however bend;
4. Throughout all the inflationary dynamics, no Kaluza-Klein scale becomes smaller than the gravitino mass;
5. The steepening of the inflationary potential due to F^4 corrections is negligible, so that enough efoldings can be obtained before destroying slow roll inflation.

If $\mathcal{V} \sim 10^3$ and $W_0 \sim \mathcal{O}(1)$, the last four conditions can be easily satisfied but the Kähler cone conditions (2.41) for such a small value of the volume would give an upper bound on the inflaton direction which would not allow to generate enough efoldings. In order to enlarge the inflaton field space, the value of the volume has therefore to be larger, of order $\mathcal{V} \sim 10^4$. In the large volume regime where we can trust the 4D EFT, the inflationary potential then becomes more suppressed, and so the COBE normalisation condition (2) above can be satisfied only if $W_0 \sim \mathcal{O}(100)$. However, given that the gravitino mass is proportional to W_0 , for such a large value of the flux-generated superpotential, it is hard to satisfy the fourth condition above keeping $m_{3/2}$ below all KK scales during the whole inflationary evolution. Moreover, it becomes harder to suppress higher derivative corrections (condition (5) above)

unless their numerical coefficient λ turns out to be extremely small: $|\lambda| \lesssim 10^{-6}$. This is the example of case 2 above of Sec. 2.3.1.

Another option for $\mathcal{V} \sim 10^4$ could be to keep $W_0 \sim \mathcal{O}(1)$, so that the gravitino mass can remain small and the F^4 terms are still negligible, and to tune the background fluxes to increase the complex structure-dependent coefficients of the winding loop corrections. This would however make the inflaton-dependent potential of the same order of magnitude of the leading order α' correction. Hence the mass of the volume mode becomes of order the Hubble scale during inflation. This is the example of case 1 of Sec. 2.3.1 where $\delta \simeq 1.6$. This situation could either cause a considerable shift of the original LVS minimum or even a destabilisation, and so in this case one should perform a careful multi-field analysis to check that the condition (3) above is indeed satisfied.¹¹

In what follows we shall therefore focus on the multifield case with $\mathcal{V} \sim 10^4$, $W_0 \sim \mathcal{O}(100)$ and $|\lambda| \lesssim 10^{-6}$. We shall also present an example with $W_0 \sim \mathcal{O}(1)$ and $|\lambda| \sim 10^{-3}$ which satisfies all conditions above except for condition (2) since the amplitude of the density perturbations turns out to be too small. The correct value could be generated by the quantum fluctuations of the two light bulk axions which could play the rôle of curvaton fields [111]. This study is however beyond the scope of this work, and so we leave it for future work.

We analyse now the full three-field cosmological evolution involving the Kähler moduli τ_7 , \mathcal{V} and τ_1 . Their dynamics is governed by the following evolution equations for non-canonically normalised fields:

$$\begin{cases} \ddot{\phi}^i + 3H\dot{\phi}^i + \Gamma_{jk}^i \dot{\phi}^j \dot{\phi}^k + g^{ij} \frac{\partial V}{\partial \phi^j} = 0, \\ H^2 = \left(\frac{\dot{a}}{a}\right)^2 = \frac{1}{3} \left(\frac{1}{2} g_{ij} \dot{\phi}^i \dot{\phi}^j + V \right), \end{cases} \quad (2.65)$$

where the ϕ_i 's represent the scalar fields τ_7 , \mathcal{V} and τ_1 , a is the scale factor and Γ_{jk}^i are the target space Christoffel symbols using the metric g_{ij} for the set of real scalars ϕ^i such that $\frac{\partial^2 K}{\partial \Phi^I \partial \Phi^{*J}} \partial^\mu \Phi^I \partial_\mu \Phi^{*J} = \frac{1}{2} g_{ij} \partial_\mu \phi^i \partial^\mu \phi^j$.

For numerical purposes it is more convenient to express the cosmological evolution of the fields as a function of the number of efoldings N rather than time. In fact, by using $a(t) = e^N$ and $\frac{d}{dt} = H \frac{d}{dN}$, we can directly obtain $\tau_7(N)$, $\mathcal{V}(N)$ and $\tau_1(N)$ without having to solve for the scale factor. The equations of motion turn

¹¹A similar situation arises in Kähler moduli inflation where however a detailed multifield analysis shows that the minimum of the volume mode is shifted during inflation without developing a runaway direction [72, 110].

out to be (with ' denoting a derivative with respect to N):

$$\begin{aligned}
\tau_7'' &= -(\mathcal{L}_{\text{kin}} + 3) \left(\tau_7' + \tau_7 \mathcal{V} \frac{V_{,\mathcal{V}}}{V} + 2\tau_7^2 \frac{V_{,\tau_7}}{V} + 2\tau_7 \tau_1 \frac{V_{,\tau_1}}{V} \right) + \frac{\tau_7'^2}{\tau_7} + \frac{\tau_7 \tau_1'}{\mathcal{V}} \left(\frac{\tau_1'}{\sqrt{\tau_1}} - \frac{\tau_7'}{2\sqrt{\tau_7}} \right), \\
\mathcal{V}'' &= -(\mathcal{L}_{\text{kin}} + 3) \left(\mathcal{V}' + \frac{3\mathcal{V}^2}{2} \frac{V_{,\mathcal{V}}}{V} + \tau_7 \mathcal{V} \frac{V_{,\tau_7}}{V} + \tau_1 \mathcal{V} \frac{V_{,\tau_1}}{V} \right) + \frac{\mathcal{V}'^2}{\mathcal{V}}, \\
\tau_1'' &= -(\mathcal{L}_{\text{kin}} + 3) \left(\tau_1' + \tau_1 \mathcal{V} \frac{V_{,\mathcal{V}}}{V} + 2\tau_7 \tau_1 \frac{V_{,\tau_7}}{V} + 4\mathcal{V} \sqrt{\tau_1} \frac{V_{,\tau_1}}{V} \right) \\
&\quad + \frac{\tau_1'^2}{4\tau_1} + \frac{\tau_1 \mathcal{V}'}{\mathcal{V}} \left(\frac{\tau_1'}{\tau_1} - \frac{\tau_7'}{\tau_7} \right) + \frac{\tau_1 \tau_7'}{2\tau_7} \left(\frac{3\tau_7'}{2\tau_7} - \frac{\sqrt{\tau_1}}{\mathcal{V}} \tau_1' \right),
\end{aligned} \tag{2.66}$$

where the kinetic Lagrangian reads:

$$\mathcal{L}_{\text{kin}} = \frac{1}{2} \left(-\frac{\mathcal{V}'^2}{\mathcal{V}^2} + \frac{\mathcal{V}' \tau_7'}{\mathcal{V} \tau_7} - \frac{3\tau_7'^2}{4\tau_7^2} + \frac{\sqrt{\tau_1} \tau_7' \tau_1'}{2\mathcal{V} \tau_7} - \frac{\tau_1'^2}{4\mathcal{V} \sqrt{\tau_1}} \right), \tag{2.67}$$

and the full inflationary potential V is given by the sum of the standard LVS potential, the g_s loops and F^4 terms given in (2.38) and an uplifting contribution proportional to δ_{up} which could come from an anti D3-brane at the tip of a warped throat:

$$\begin{aligned}
V &= \kappa \left[32A_s^2 \pi^2 \frac{\sqrt{\tau_1}}{\mathcal{V}} e^{-4\pi\tau_1} - 8\pi A_s \frac{W_0 \tau_1}{\mathcal{V}^2} e^{-2\pi\tau_1} + \frac{3\zeta}{4g_s^{3/2}} \frac{W_0^2}{\mathcal{V}^3} \right. \\
&\quad \left. + \frac{W_0^2}{\mathcal{V}^3} \left(\frac{A_1}{\tau_7} - \frac{A_2}{\sqrt{\tau_7}} + \frac{B_1 \sqrt{\tau_7}}{\mathcal{V}} + \frac{B_2 \tau_7}{\mathcal{V}} \right) + \frac{\delta_{\text{up}}}{\mathcal{V}^{4/3}} \right].
\end{aligned} \tag{2.68}$$

$|\lambda| = 10^{-6}$ and correct amplitude of the density perturbations

Setting $\alpha = 1$ and performing the following choice of the underlying parameters:

$$\begin{aligned}
A_s &= 6 \cdot 10^5 & \chi &= -188 & \Rightarrow & \zeta = -\frac{\zeta(3)\chi(X)}{2(2\pi)^3} = 0.456 & W_0 &= 50 & g_s &= 0.25 \\
C_1^{\text{w}} &= C_2^{\text{w}} = 0.05 & |C_3^{\text{w}}| &= 10^{-4} & |C_4^{\text{w}}| &= 0.1 & C_5^{\text{w}} &= C_6^{\text{w}} = -0.05 & \lambda &= -10^{-6},
\end{aligned}$$

the total potential (2.68) admits a Minkowski global minimum at:

$$\langle \mathcal{V} \rangle = 2690.625, \quad \langle \tau_7 \rangle = 6.503 \quad \langle \tau_1 \rangle = 3.179 \quad \text{for} \quad \delta_{\text{up}} = 5.9598 \cdot 10^{-4}.$$

Notice that this minimum is inside the Kähler cone since $\langle \tau_7 \rangle > 2\langle \tau_1 \rangle = 6.358$, which respects the lower bound in (2.41). At this level of approximation, the closed string axions associated to \mathcal{V} and τ_7 are flat directions. They receive a tiny potential from highly suppressed non-perturbative effects, and so they remain very light. Being so

light, they do not affect the inflationary dynamics but would acquire isocurvature fluctuations of order H during inflation. If they do not play the rôle of dark matter, their final contribution to the amplitude of the isocurvature perturbations is negligible. On the other hand, if they are heavy enough to decay, their isocurvature fluctuations get converted into standard density perturbations, and so these bulk axions could behave as curvaton fields [111].

Let us now shift τ_7 away from its minimum at the initial condition $\tau_7(N=0) = \langle \tau_7 \rangle + 2030$ and recompute the new minimum for the other two directions $\langle \mathcal{V} \rangle(\tau_7)$ and $\langle \tau_1 \rangle(\tau_7)$. These values would set the initial conditions for these fields, ensuring that the inflationary dynamics takes place along a stable trough in field space:

$$\mathcal{V}(0) = \langle \mathcal{V} \rangle(\tau_7(0)) = 3671.432, \quad \tau_7(0) = 2036.503, \quad \tau_1(0) = \langle \tau_1 \rangle(\tau_7(0)) = 3.227.$$

Notice that these initial conditions are again inside the Kähler cone since $\tau_7(0) < \frac{\mathcal{V}(0)}{\sqrt{\tau_1(0)}} = 2043.7$, which satisfies the upper bound in (2.41). We shall also focus on vanishing initial velocities for all scalar fields: $\mathcal{V}'(0) = \tau_7'(0) = \tau_1'(0) = 0$.

Considering this set of initial conditions, we solved the system of equations of motion (2.66) finding the cosmological evolution of each scalar field as a function of the number of efoldings N . Inflation occurs in the region in field space where the generalised ϵ -parameter:

$$\epsilon(N) = -\frac{1}{4\mathcal{L}_{\text{kin}}V^2} (V_{,\mathcal{V}}\mathcal{V}' + V_{,\tau_7}\tau_7' + V_{,\tau_1}\tau_1')^2, \quad (2.69)$$

is much smaller than unity. As can be seen from Fig. 2.5, $\epsilon \ll 1$ during the first 57 efoldings and then quickly increases and reaches $\epsilon = 1$ at $N = 57.93$ where inflation ends.

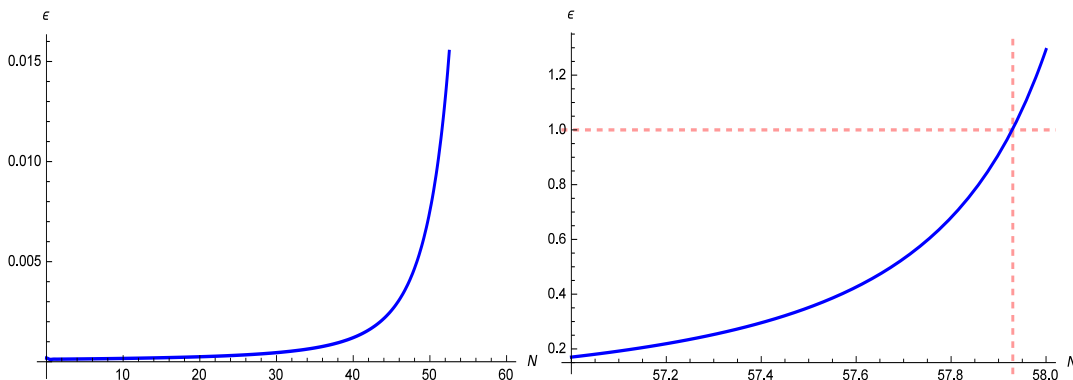


Figure 2.5: Evolution of the ϵ -parameter as a function of the number of efoldings N for (left) the entire inflationary dynamics and (right) for the last efoldings.

Using the variable N to parametrise the cosmological evolution of the scalar fields and denoting by N_e the physical number of efoldings of inflation, $N_e = 52$, as estimated in Sec. 2.3.1, at $N_* = 5.93$. This is the point of horizon exit in field space where $\epsilon(N_*) = 1.456 \cdot 10^{-4}$ which yields a tensor-to-scalar ratio $r = 16\epsilon(N_*) = 0.0023$. The amplitude of the scalar power spectrum is:

$$\sqrt{P(N_*)} = \frac{1}{10\pi} \sqrt{\frac{2V(N_*)}{3\epsilon(N_*)}} = 1.035 \cdot 10^{-5}, \quad (2.70)$$

reproducing the reference COBE value $\sqrt{P_{\text{COBE}}} \simeq 2 \cdot 10^{-5}$ with a good accuracy. Moreover the scalar spectral index is given by:

$$n_s(N_*) = 1 + \left. \frac{d}{dN} \ln P(N) \right|_{N=N_*} = 0.9701, \quad (2.71)$$

in good agreement with Planck data [80, 7].

Fig. 2.6, 2.7 and 2.8 show the cosmological evolution of the three scalar fields τ_7 , \mathcal{V} and τ_1 during the whole inflationary dynamics and their final settling into the global minimum after a few oscillations. Fig. 2.9 shows instead the path of the inflationary trajectory in the (τ_7, \mathcal{V}) -plane (on the left) and in the (τ_7, τ_1) -plane (on the right). Clearly, as expected from the single-field analysis of Sec. 2.3.1, the inflaton travels mainly along the τ_7 -direction.

Finally Fig. 2.10 presents a plot with the cosmological evolution of all KK mass scales, the inflationary scale $M_{\text{inf}} = V^{1/4}$ and the gravitino mass $m_{3/2}$ from horizon exit to the final settling into the global minimum. The fact that M_{inf} remains always below all the KK scales, ensures that the Hubble scale during inflation $H = \frac{M_{\text{inf}}}{\sqrt{3}} \left(\frac{M_{\text{inf}}}{M_p} \right) < M_{\text{inf}}$ is also always below each KK scale. The gravitino mass also remains always smaller than $M_{\text{KK}}^{(i)} \forall i$. This guarantees that the 4D effective field theory is under control. In particular, $M_{\text{KK}}^{(2)}$, $M_{\text{KK}}^{(6)}$ and the inflationary scale evolve from $M_{\text{KK}}^{(2)}(N_*) \simeq 1.1 \cdot 10^{16}$ GeV, $M_{\text{KK}}^{(6)}(N_*) \simeq 2.1 \cdot 10^{16}$ GeV and $M_{\text{inf}}(N_*) \simeq 5.3 \cdot 10^{15}$ GeV at horizon exit to $M_{\text{KK}}^{(2)}(N = 60) \simeq 6.2 \cdot 10^{16}$ GeV, $M_{\text{KK}}^{(6)}(N = 60) \simeq 1.3 \cdot 10^{16}$ GeV and $M_{\text{inf}}(N = 60) \simeq 9.3 \cdot 10^{14}$ GeV around the final minimum. On the other hand the other scales remain approximately constant during the whole inflationary evolution around: $H \simeq 5 \cdot 10^{12}$ GeV $< m_{3/2} \simeq 4 \cdot 10^{15}$ GeV $< M_{\text{KK}}^{\text{bulk}} \simeq 2 \cdot 10^{16}$ GeV.

$|\lambda| = 10^{-3}$ and negligible amplitude of the density perturbations

We shall now relax the condition of generating the correct amplitude of the density perturbations from the inflaton quantum fluctuations. As explained above, the right

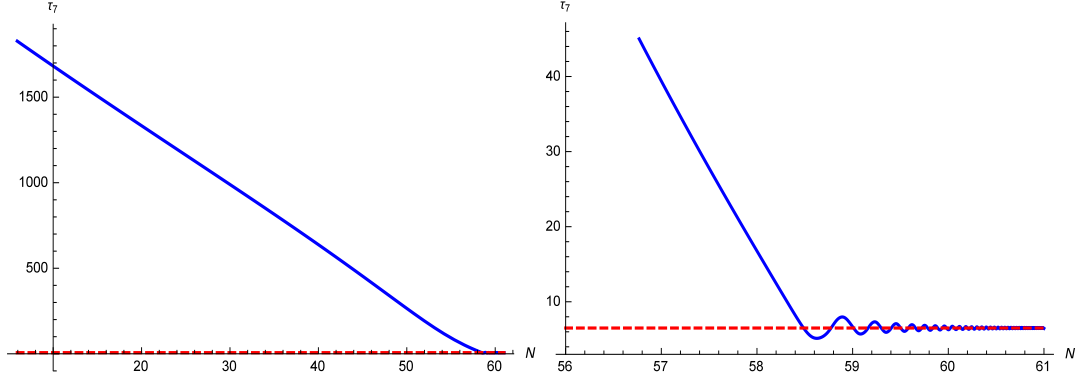


Figure 2.6: Evolution of τ_7 as a function of the number of efoldings N for (left) the entire inflationary dynamics and (right) for the last 2 efoldings. The dashed red line represents the position of the final global minimum. We work in units of $M_p = 1$.

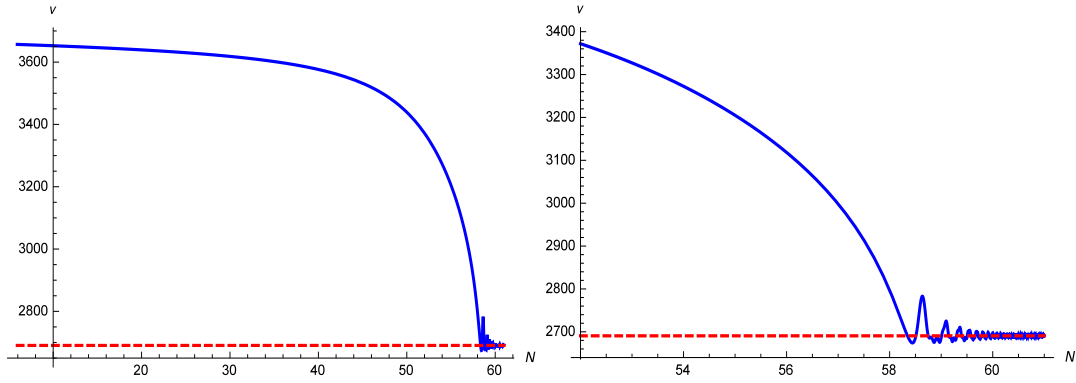


Figure 2.7: Evolution of \mathcal{V} as a function of the number of efoldings N for (left) the entire inflationary dynamics and (right) for the last 6 efoldings. The dashed red line represents the position of the final global minimum. We work in units of $M_p = 1$.

COBE value of the amplitude of the power spectrum could instead be reproduced in a non-standard way by a curvaton-like mechanism involving the quantum fluctuations of the two light bulk axions [111]. In this case we can focus on $\mathcal{V} \sim 5 \cdot 10^3$, $W_0 \sim \mathcal{O}(1)$, $\lambda \sim 10^{-3}$ and relatively small values of the coefficients of the winding loop corrections which generate the plateau, so that all the remaining four conditions listed at the beginning of Sec. 2.3.2 are fully satisfied.

We shall set $\alpha = 1$ and perform the following choice of the underlying parameters:

$$\begin{aligned}
 A_s &= 1 \cdot 10^4 & \chi &= -188 & \Rightarrow & \zeta = -\frac{\zeta(3)\chi(X)}{2(2\pi)^3} = 0.455 & W_0 &= 1 & g_s &= 0.25 \\
 C_1^w &= C_2^w = 0.05 & C_3^w &= -10^{-4} & C_4^w &= -0.1 & C_5^w &= C_6^w = -0.05 & \lambda &= -0.001,
 \end{aligned}$$

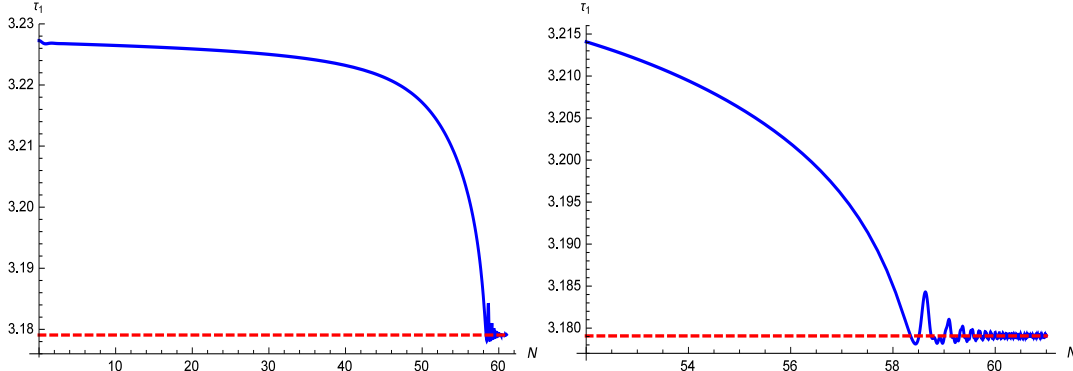


Figure 2.8: Evolution of τ_1 as a function of the number of efoldings N for (left) the entire inflationary dynamics and (right) for the last 6 efoldings. The dashed red line represents the position of the final global minimum.

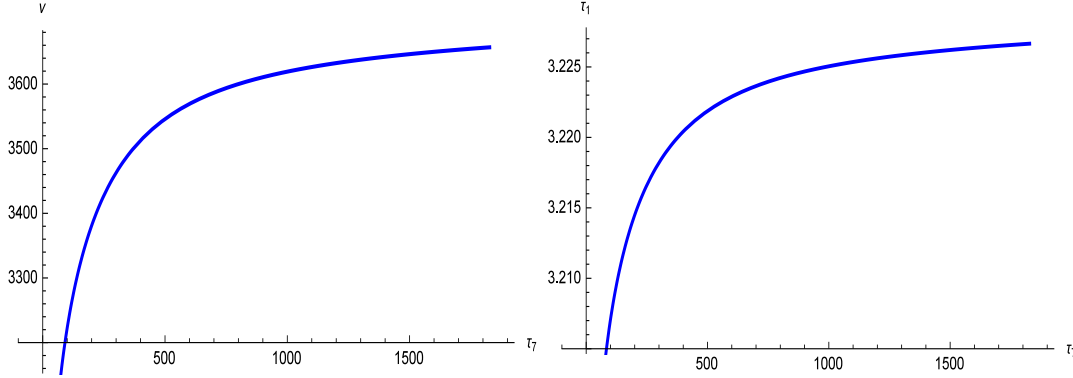


Figure 2.9: Plot of the whole inflationary evolution in the (τ_7, \mathcal{V}) -plane (on the left) and in the (τ_7, τ_1) -plane (on the right). Notice that the scales are different on the two axes since the inflaton travels mainly along the τ_7 -direction.

which yield a global Minkowski minimum inside the Kähler cone at:

$$\langle \mathcal{V} \rangle = 3220.899, \quad \langle \tau_7 \rangle = 6.403 \quad \langle \tau_1 \rangle = 3.179 \quad \text{for} \quad \delta_{\text{up}} = 1.76588 \cdot 10^{-7}.$$

The initial conditions for the inflationary evolution are again derived in the same way: the fibre modulus τ_7 is shifted away from its minimum at $\tau_7(N=0) = \langle \tau_7 \rangle + 2450$ and the other two directions $\langle \mathcal{V} \rangle(\tau_7)$ and $\langle \tau_1 \rangle(\tau_7)$ are set at the new minimum:

$$\mathcal{V}(0) = \langle \mathcal{V} \rangle(\tau_7(0)) = 4436.094, \quad \tau_7(0) = 2456.403, \quad \tau_1(0) = \langle \tau_1 \rangle(\tau_7(0)) = 3.228.$$

Notice that these initial conditions are inside the Kähler cone since $\tau_7(0) < \frac{\mathcal{V}(0)}{\sqrt{\tau_1(0)}} =$

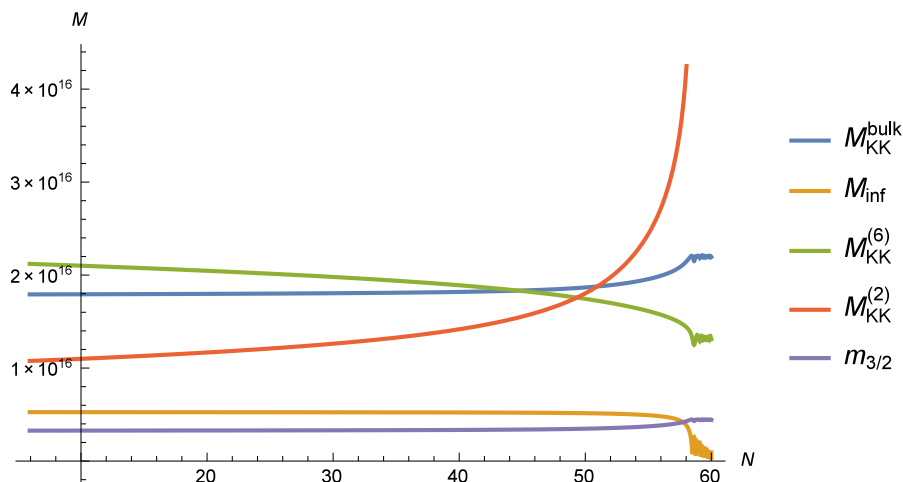


Figure 2.10: Evolution of all KK masses (with $M_{\text{KK}}^{(4)} = M_{\text{KK}}^{(2)}$), the inflationary scale $M_{\text{inf}} = V^{1/4}$ and the gravitino mass $m_{3/2}$ in GeV units from horizon exit to the final settling into the global minimum.

2468.95, which satisfies the upper bound in (2.41). Focusing again on vanishing initial velocities for all scalar fields, i.e. $\mathcal{V}'(0) = \tau_7'(0) = \tau_1'(0) = 0$, we worked out the cosmological evolution of each scalar field as a function of N by solving the system of equations of motion (2.66). Looking for a slow-roll region in field space where the generalised ϵ -parameter (2.69) is much smaller than unity, we found that $\epsilon \ll 1$ during the first 69 efoldings and then quickly increases and reaches $\epsilon = 1$ at $N = 69.15$ where inflation ends. The point of horizon exit corresponding to a physical number of efoldings of inflation $N_e = 52$ is localised at $N_* = 17.15$ where $\epsilon(N_*) = 1.36 \cdot 10^{-4}$. The main cosmological observables at horizon exit take the following values:

$$n_s(N_*) = 1 + \left. \frac{d}{dN} \ln P(N) \right|_{N=N_*} = 0.9676, \quad r = 16\epsilon(N_*) = 0.0022,$$

$$\sqrt{P(N_*)} = \frac{1}{10\pi} \sqrt{\frac{2V(N_*)}{3\epsilon(N_*)}} = 1.64 \cdot 10^{-7}.$$

The scalar spectral index n_s and the tensor-to-scalar ratio r are in good agreement with Planck data [80, 7] while the amplitude of the scalar power spectrum, as expected, is much smaller than the reference COBE value $\sqrt{P_{\text{COBE}}} \simeq 2 \cdot 10^{-5}$. As can be seen from Fig. 2.11, in this case the low-energy 4D effective field theory is fully under control since throughout all the inflationary evolution all KK scales are much higher than both the gravitino mass and the inflationary scale (and so also

the Hubble scale).

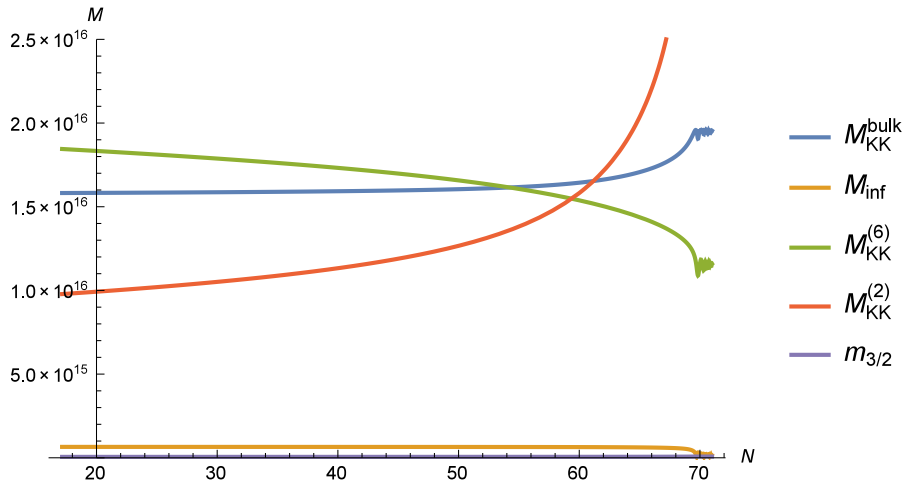


Figure 2.11: Evolution of all KK masses (with $M_{\text{KK}}^{(4)} = M_{\text{KK}}^{(2)}$), the inflationary scale $M_{\text{inf}} = V^{1/4}$ and the gravitino mass $m_{3/2}$ in GeV units from horizon exit to the final settling into the global minimum.

In particular, $M_{\text{KK}}^{(2)}$, $M_{\text{KK}}^{(6)}$ and the inflationary scale evolve from $M_{\text{KK}}^{(2)}(N_*) \simeq 9.8 \cdot 10^{15}$ GeV, $M_{\text{KK}}^{(6)}(N_*) \simeq 1.8 \cdot 10^{16}$ GeV and $M_{\text{inf}}(N_*) \simeq 6.5 \cdot 10^{14}$ GeV at horizon exit to $M_{\text{KK}}^{(2)}(N = 70) \simeq 5.5 \cdot 10^{16}$ GeV, $M_{\text{KK}}^{(6)}(N = 70) \simeq 1.2 \cdot 10^{16}$ GeV and $M_{\text{inf}}(N = 70) \simeq 1.4 \cdot 10^{14}$ GeV around the final minimum. On the other hand the other scales remain approximately constant during the whole inflationary evolution around: $H \simeq 8 \cdot 10^{11}$ GeV $< m_{3/2} \simeq 6 \cdot 10^{13}$ GeV $< M_{\text{KK}}^{\text{bulk}} \simeq 2 \cdot 10^{16}$ GeV.

2.4 Summary

The study of large field inflationary models is particularly interesting from both a phenomenological and a theoretical point of view. In fact, from one side the next generation of CMB observations will be able to test values of the tensor-to-scalar ratio in the window $0.001 \lesssim r \lesssim 0.01$, while on the other hand trans-Planckian inflaton excursions need a symmetry mechanism to trust the effective field theory approach.

Natural inflaton candidates from type IIB string compactifications are Kähler moduli which enjoy non-compact shift-symmetries [49]. In particular, fibre inflation models provide promising plateau-like potentials which seem to fit Planck data rather well and lead to the prediction of observable tensor modes [14, 77, 78, 79]. These inflationary models are built within LVS moduli stabilisation scenarios and can be globally embedded in K3-fibred Calabi-Yau manifolds [82].

In this chapter we found that the inflationary dynamics is strongly constrained by the Kähler cone conditions which never allow for enough efoldings of inflation if the internal volume is of order $\mathcal{V} \sim 10^3$. For larger values of the Calabi-Yau volume of order $\mathcal{V} \sim 10^4$, the Kähler cone becomes large enough for the inflaton to drive $N_e \simeq 52$ efoldings, as required by an estimate of the post-inflationary evolution. However such a large value of \mathcal{V} tends to suppress the amplitude of the density perturbations below the reference COBE value. This can be avoided by considering large values of either the coefficients of the winding loops which generate the plateau, or the flux superpotential W_0 . Let us stress that in the string landscape this choice is guaranteed to be possible by the fact that both of these microscopic parameters are flux-dependent.

However, as shown in Sec. 2.3.1, large values of the coefficients of the winding g_s corrections make the Hubble scale during inflation of the same order of magnitude of the mass of the volume mode. This could either cause a large shift of the original LVS minimum or even a problem for the stability of the inflationary direction against orthogonal runaway directions. A definite answer to this issue hence requires a proper multi-field analysis even if the two-field study of [14] revealed that the inflationary motion is still mostly single-field.

On the other hand, if the flux superpotential is of order $W_0 \sim 100$, the gravitino mass can become too close to some KK scale in the model, destroying the 4D effective field theory. Moreover, F^4 terms are proportional to $|\lambda|W_0^4$. Thus if W_0 is large, these higher derivative effects can spoil the flatness of the inflationary potential before achieving enough efoldings of inflation if $|\lambda|$ is not small enough. Hence in Sec. 2.3.1 we presented a model with $W_0 \sim 100$ and a very small value of $|\lambda|$ of order $|\lambda| = 10^{-7}$ which makes the F^4 terms harmless. The gravitino mass also turns out to be slightly smaller than any KK scale throughout the whole inflationary dynamics.

Part III

Dark Matter

From String Theory

Chapter 3

Primordial Black Holes from String Inflation

The origin of dark matter remains one of the biggest mysteries in fundamental physics. One of the simplest explanations, which would rely neither on the presence of new particles nor on modifications of the gravitational interaction, is black holes. An interesting region in parameter space where the contribution of black holes to the total dark matter abundance could be between 10% and 100% depending on astrophysical uncertainties is $10^{-17}M_{\odot} \lesssim M_{\text{BH}} \lesssim 10^{-13}M_{\odot}$ [124, 25, 116], where the lower bound comes from extra-galactic γ rays produced due to Hawking evaporation [117]. This region, even if it is far from the one probed by LIGO, is very interesting since there is no known astrophysical explanation for black hole formation in this small mass window.¹ On the other hand, these tiny black holes could be seeded by the dynamics of the early universe [121, 122]. A tantalizing idea for the formation of these primordial black holes (PBHs) relies on an amplification of the density perturbations during inflation of order $\delta\rho \sim 0.1\rho$ which then collapse to form PBHs at horizon re-entry.

This enhancement of the scalar power spectrum has to take place at momentum scales which are much larger than the ones associated with CMB observations where $\delta\rho \sim 10^{-5}\rho$. From the theoretical point of view, it is therefore important to identify mechanisms to generate the necessary enhancement at the right scales. Guided again by simplicity, we focus on single-field inflationary models which also reproduce the

¹Depending on the interpretation of astrophysical and cosmological data, X-ray and CMB observations seem to rule out the case where black holes in the LIGO mass region can constitute a fraction of the dark matter abundance above 10% [118, 119, 120]. Moreover the single-field inflationary dynamics seems to be very unlikely to generate black holes with masses as large as a few solar masses when the scalar spectral index is required to be compatible with CMB data [25].

Planck data rather well [80].² It has already been pointed out that the required inflationary potentials feature a slow-roll behaviour followed by a near inflection point region where the power spectrum is amplified since the system enters an ultra slow-roll regime [126, 127, 128, 129, 25].

Despite the fact that dark matter as PBHs formed during single-field inflation might seem a very appealing idea, its explicit realisation in concrete models has turned out to be rather complicated since the inflationary potential has to possess enough tuning freedom to allow for such dynamics [130]. Examples based on a radiative plateau have been recently studied in [128, 129, 25]. This is a bottom up perspective which tries to single out the simplest potential which allows for PBH formation via an inflationary plateau followed by a near inflection point. However this approach ignores the fundamental issue of deriving the model from a UV consistent theory.

In this chapter we shall instead take a more top down approach and search for concrete examples of inflationary models in string theory whose structure is rich enough to allow for PBH formation. One of the main advantages of embedding inflation in string theory is the possibility to motivate the presence of a symmetry which can protect the inflaton potential against quantum corrections which can spoil its flatness [47, 48]. Particularly interesting cases include inflaton candidates which are pseudo Nambu-Goldstone bosons associated with slightly broken shift symmetries. Abelian symmetries involves both axions [131], which are associated to compact $U(1)$ factors, and Kähler moduli [13], which are associated with non-compact rescaling symmetries [49].³

This global rescaling symmetry is explicitly realised at tree-level in type IIB no-scale models since the Kähler moduli τ remain exact flat directions but needs to be slightly broken to generate the inflationary potential. This can be done either by non-perturbative effects or by perturbative power-law corrections which become exponential in terms of the canonically normalised inflaton: $V_0/\tau^n \sim V_0 e^{-n\phi/f}$. Notice that the shape of the inflationary potential is determined by both the effective ‘decay constant’ f , i.e. the geometry of the moduli space (determined by the topology of the divisor whose volume is parameterised by the inflaton) and n , i.e. the exact moduli-dependence of the symmetry-breaking effects which develop the inflationary potential [79]. Once a proper uplifting to dS has been achieved via the addition of a constant contribution (which can have several dynamical origins [88, 89, 90, 91, 132, 192, 92, 93]), these models tend to give rise to an inflationary

²For PBH formation in multi-field inflationary models see [123, 124, 125].

³The non-Abelian case leads to a multi-field inflationary scenario which tends to be disfavoured by non-Gaussianity observations [80].

potential of the schematic form [79]:

$$V_{\text{inf}} = V_0 (1 - e^{-n\phi/f}) . \quad (3.1)$$

These models go under the name of *Fibre Inflation* since the underlying Calabi-Yau compactification manifold has a typical fibration structure [14, 77, 78]. They are interesting since they drive inflation successfully via a plateau-like region at large ϕ and also allow for a detailed analysis of the post-inflationary evolution [54, 113, 114]. Moreover they provide string theory embeddings of Starobinsky inflation [133] and supergravity α -attractors [134, 135, 136] (where in our notation $\alpha \simeq (f/n)^2$). Nevertheless the potential (3.1) is too simple to generate PHBs via a period of ultra slow-roll dynamics towards the end of inflation. However recent global constructions of fibre inflation models in concrete Calabi-Yau orientifolds with explicit brane setup and closed string moduli stabilisation have revealed the existence of new string loop corrections which look schematically like [82, 2]:

$$\delta V_{\text{inf}} = -\epsilon_1 V_0 \frac{e^{2n\phi/f}}{1 + \epsilon_2 e^{3n\phi/f}} , \quad (3.2)$$

where $\epsilon_1 \ll 1$ and $\epsilon_2 \ll 1$ are two parameters which are tunable since they depend on background fluxes and the Calabi-Yau intersection numbers, and turn out to be naturally small since they are suppressed by inverse powers of the compactification volume, an exponentially large quantity [43, 42]. Thanks to the additional perturbative contribution (3.2), we will show that fibre inflation models are rich enough to produce a near inflection point region before the end of inflation which is perfectly suitable to generate PBHs in the mass window $10^{-17} M_\odot \lesssim M_{\text{PBH}} \lesssim 10^{-13} M_\odot$ where they could constitute a significant fraction of the total dark matter abundance.

As pointed out in [137, 129, 25, 138], the slow-roll approximation ceases to be valid in the near inflection point region. The primordial power spectrum has to be computed by solving the Mukhanov-Sasaki equations for the curvature perturbations [139, 140]. By following this procedure, we shall show that the primordial power spectrum can feature the required enhancement for appropriate values of the underlying parameters. Let us stress that even if the choice of microscopic parameters needed for successful PBH formation looks very non-generic from the string landscape point of view, the values of these parameters are technically natural since they are protected against large quantum corrections by the effective rescaling shift symmetry typical of these models [49].

This chapter is organised as follows. In Sec. 3.1 we provide a very brief review of fibre inflation models while in Sec. 3.2 we describe the mechanism of PBH generation

in some detail. In Sec. 3.3 we then perform a careful analysis of the process of PBH formation in fibre inflation by implementing the Mukhanov-Sasaki formalism to derive the primordial power spectrum. We finally discuss our results and present our conclusions in Sec. 4.4.

3.1 Fibre inflation models

Fibre inflation is a class of string inflationary models built within the framework of type IIB flux compactifications [14, 77, 78, 79]. The inflaton τ_{K3} is a Kähler modulus controlling the size of a K3 divisor fibred over a \mathbb{P}^1 base with volume $t_{\mathbb{P}^1}$. The simplest fibre inflation models feature a Calabi-Yau (CY) volume which looks like:

$$\mathcal{V} = t_{\mathbb{P}^1} \tau_{\text{K3}} - \tau_{\text{dP}}^{3/2}, \quad (3.3)$$

where τ_{dP} is the volume of a diagonal del Pezzo divisor which supports non-perturbative effects. Several effects come into play to stabilise the Kähler moduli in a typical large volume scenario (LVS) vacuum [43, 42]. At leading order in a $1/\mathcal{V} \ll 1$ expansion only two directions, \mathcal{V} and τ_{dP} , are lifted by non-perturbative contributions to the superpotential W [88] and perturbative α' corrections to the Kähler potential K [36, 37, 87].⁴ Hence the remaining flat direction, which can be parametrised by τ_{K3} , represents a very promising inflaton candidate since it enjoys an effective non-compact rescaling symmetry which can be used to protect the flatness of the inflationary potential against quantum corrections [49].⁵

In order to generate the inflationary potential, this effective shift symmetry has to be slightly broken. This is realised by open string 1-loops which depend on all Kähler moduli [39, 40, 73, 74] but are subdominant with respect to the leading α' effects thanks to the extended no-scale structure typical of these models [41]. Higher loops are expected to be suppressed by positive powers of the string coupling $g_s \ll 1$ and negative powers of the exponentially large volume $\mathcal{V} \gg 1$ [14, 79]. Other contributions to the inflationary potential arise from higher derivative α' effects

⁴At this level of approximation, also the axionic partner of τ_{dP} is fixed by non-perturbative effects.

⁵There are actually other two flat directions corresponding to the axions associated with the base and the fibre which turn out to be much lighter than τ_{K3} since they acquire tiny masses only at non-perturbative level (suppressed with respect to the mass of τ_{K3} by $e^{-\pi\tau_{\text{K3}}} \sim e^{-\pi\mathcal{V}^{2/3}} \sim 10^{-137} \ll 1$ for $\mathcal{V} \sim 10^3$ from Tab. 3.1). Hence these fields are in practice massless and acquire isocurvature fluctuations during inflation. However present strong bounds on isocurvature fluctuations do not apply to our case since these axions tend to be too light to behave as dark matter (see eq. (B.16) of [187]). On the other hand, these ultra-light axions could behave as extra relativistic degrees of freedom produced from the inflaton decay [60].

[75, 76] but these are also \mathcal{V} -suppressed if the superspace derivative expansion is under control [86]. Moreover, all these corrections give rise to an AdS vacuum which needs to be uplifted to dS by the inclusion of anti-branes [88, 89, 90, 91], hidden sector T-branes [132, 192, 92] or non-perturbative effects at singularities [93]. It is important to stress that all these uplifting effects are inflaton-independent since they depend just on the overall volume \mathcal{V} . Thus they give rise to a constant contribution to the inflationary potential which is crucial to develop a plateau-like behaviour at large inflaton values.

After canonical normalisation of the inflaton field, the resulting potential is qualitatively very similar to the one of Starobinsky inflation [133] and α -attractor supergravity models [134, 135, 136]. In fact, fibre inflation models require a trans-Planckian field range to obtain enough e-foldings of inflationary expansion, and so they can predict a tensor-to-scalar ratio as large as $r \sim 0.005 - 0.01$. These models are particularly interesting also because they can be embedded into globally consistent CY orientifold compactifications with an explicit brane setup and chiral matter [82, 2]. In the study of concrete CY realisations of string models where the inflaton is a Kähler modulus, it has been recently realised that the underlying Kähler cone conditions set strong geometrical constraints on the allowed inflaton range [112]. Interestingly, it has been found that the distance travelled by inflaton in field space can generically be trans-Planckian only for K3-fibred CY threefolds which are exactly the necessary ingredients to construct fibre inflation models.

The two moduli which are stabilised at leading order in $1/\mathcal{V}$ are heavier than the Hubble constant whose size is set by the uplifting contribution. Hence \mathcal{V} and τ_{dP} do not play a significant rôle during inflation which is instead driven mainly by the light field τ_{K3} . Fibre inflation models are therefore, to a very good level of approximation, single-field inflationary models whose potential looks like [14, 77, 78]:

$$V_{\text{inf}} = \left(\frac{C_{\text{up}}}{\mathcal{V}^{4/3}} + g_s^2 \frac{C_{\text{KK}}}{\tau_{\text{K3}}^2} + \frac{W_0^2}{\sqrt{g_s}} \frac{\epsilon_{\mathcal{F}4}}{\mathcal{V} \tau_{\text{K3}}} - \frac{C_{\text{W}}}{\mathcal{V} \sqrt{\tau_{\text{K3}}}} + g_s^2 D_{\text{KK}} \frac{\tau_{\text{K3}}}{\mathcal{V}^2} + \delta_{\mathcal{F}4} \frac{W_0^2}{\sqrt{g_s}} \frac{\sqrt{\tau_{\text{K3}}}}{\mathcal{V}^2} \right) \frac{W_0^2}{\mathcal{V}^2}, \quad (3.4)$$

where $g_s \ll 1$ is the string coupling and $W_0 \sim \mathcal{O}(1 - 10)$ is the superpotential generated by background fluxes which is constant after the dilaton and the complex structure moduli are stabilised at tree-level. C_{up} controls the uplifting contribution and, depending on the particular mechanism employed it can have a different dependence on the internal volume \mathcal{V} , background or gauge fluxes. $C_{\text{KK}} > 0$, $D_{\text{KK}} > 0$ and C_{W} are the coefficients of 1-loop open string corrections which have been conjectured to come respectively from the tree-level exchange of closed Kaluza-Klein strings between non-intersecting stacks of branes, and winding closed strings be-

tween intersecting branes [39, 40, 73, 74]. These constants are also functions of the vacuum expectation values of the complex structure moduli and are expected to be of order unity: $C_{\text{KK}} \sim D_{\text{KK}} \sim C_{\text{W}} \sim \mathcal{O}(1)$. On the other hand, $\epsilon_{\mathcal{F}4}$ and $\delta_{\mathcal{F}4}$ are the coefficients of higher derivative α' F^4 effects which depend just on the topological properties of the underlying geometry and are expected to be positive but relatively small: $\epsilon_{\mathcal{F}4} \sim \delta_{\mathcal{F}4} \sim \mathcal{O}(10^{-3})$ [75, 76].

The potential (3.4) is rich enough to generate a minimum for small $\tau_{\text{K}3}$, an inflationary plateau-like behaviour at large $\tau_{\text{K}3}$ and finally a steepening region at very large $\tau_{\text{K}3}$ where the system is in a fast-roll regime.⁶ In order to perform a proper study of the inflationary dynamics, the field $\tau_{\text{K}3}$ has to be written in terms of its canonically normalised counterpart ϕ as [14]:

$$\tau_{\text{K}3} = e^{\frac{2}{\sqrt{3}}\phi} = \langle \tau_{\text{K}3} \rangle e^{\frac{2}{\sqrt{3}}\hat{\phi}}, \quad (3.5)$$

where we have expanded ϕ around its minimum as $\phi = \frac{\sqrt{3}}{2} \ln \langle \tau_{\text{K}3} \rangle + \hat{\phi}$. Substituting (3.5) in (3.4), we end up with:

$$V_{\text{inf}} = V_0 \left(C_1 + C_2 e^{-\frac{4}{\sqrt{3}}\hat{\phi}} + C_3 e^{-\frac{2}{\sqrt{3}}\hat{\phi}} - e^{-\frac{1}{\sqrt{3}}\hat{\phi}} + C_4 e^{\frac{2}{\sqrt{3}}\hat{\phi}} + C_5 e^{\frac{1}{\sqrt{3}}\hat{\phi}} \right), \quad (3.6)$$

where, parameterising the inflaton minimum as $\langle \tau_{\text{K}3} \rangle^{3/2} \equiv \gamma \mathcal{V}$, we have:

$$\begin{aligned} V_0 &= \frac{C_{\text{W}} W_0^2}{\gamma^{1/3} \mathcal{V}^{10/3}}, & C_1 &= \gamma^{1/3} \frac{C_{\text{up}}}{C_{\text{W}}}, & C_2 &= g_s^2 \frac{C_{\text{KK}}}{\gamma C_{\text{W}}}, \\ C_3 &= \frac{W_0^2}{\gamma^{1/3} C_{\text{W}} \sqrt{g_s} \mathcal{V}^{1/3}}, & C_4 &= \gamma g_s^2 \frac{D_{\text{KK}}}{C_{\text{W}}}, & C_5 &= \gamma C_3 \frac{\delta_{\mathcal{F}4}}{\epsilon_{\mathcal{F}4}}. \end{aligned} \quad (3.7)$$

Notice that we work in units of $M_p = 1$. The potential (3.6) can have a plateau-like region which can support enough efoldings of inflation only if the coefficients of the positive exponentials are suppressed, i.e. $C_4 \ll 1$ and $C_5 \ll 1$, which, in turn, requires $\gamma \ll 1$. This is naturally achieved if the three negative exponentials compete to give a minimum since this can happen when $\gamma \sim g_s^2 \ll 1$. The inflationary plateau is then generated mainly by the fourth term in (3.6). Notice that the Hubble constant during inflation is set by V_0 and scales as $H^2 \sim M_p^2 / \mathcal{V}^{10/3}$.⁷ The mass of the inflaton around the minimum is of order H but then quickly becomes exponentially smaller than H for $\hat{\phi} > 0$.

Even if (3.6) is a very promising potential to drive inflation, it is not rich enough

⁶Pre-inflationary fast to slow-roll transitions in fibre inflation models can give rise to a power loss at large angular scales [107, 141].

⁷ M_p denotes the reduced Planck mass $M_p = 1/\sqrt{8\pi G} \simeq 2.4 \cdot 10^{18}$ GeV.

to generate primordial black holes due to the requirement of a significant enhancement of the power spectrum at large momentum scales. However recent explicit constructions of fibre inflation models in concrete type IIB CY compactifications with D3/D7-branes and O3/O7-planes have reproduced the potential (3.4) in a slightly generalised form since [82, 2]:

- In general the coefficient C_w is not a constant but a function of the fibre modulus τ_{K3} of the form:

$$C_w \rightarrow C_w(\tau_{K3}) = C_w - \frac{A_w \sqrt{\tau_{K3}}}{\sqrt{\tau_{K3}} - B_w}, \quad (3.8)$$

where the parameters $C_w \sim \mathcal{O}(1)$ and $A_w \sim \mathcal{O}(1)$ depend on the vacuum expectation values of the complex structure moduli, while $B_w \sim \mathcal{O}(1)$ depends on topological properties of the underlying CY threefold like the intersection numbers and the Euler number.

- The effective action features additional winding 1-loop corrections to the inflationary potential which will turn out to be crucial for the formation of primordial black holes and look like:

$$\delta V_w = W_0^2 \frac{\tau_{K3}}{\mathcal{V}^4} \left(D_w - \frac{G_w}{1 + R_w \frac{\tau_{K3}^{3/2}}{\mathcal{V}}} \right), \quad (3.9)$$

where again $D_w \sim \mathcal{O}(1)$ and $G_w \sim \mathcal{O}(1)$ become constants only after complex structure moduli stabilisation, while $R_w \sim \mathcal{O}(1)$ depends on the topological features of the extra dimensions.

Depending on the details of a given brane setup (in particular the presence of intersections between D-branes and O-planes and the topological properties of two-cycles where different stacks can intersect), several contributions to the generic scalar potential (3.4), supplemented with (3.8) and (3.9), can be absent by construction. In what follows, we shall therefore focus just on winding 1-loop corrections that represent the simplest situation which can lead to a successful generation of primordial black holes. This is justified for example by the fact that the global chiral embedding of fibre inflation presented in [2] does not feature any Kaluza-Klein loop correction, i.e. $C_{KK} = D_{KK} = 0$.⁸ Moreover higher derivative F^4 terms tend also to be negligible

⁸Even if both C_{KK} and D_{KK} are non-zero, in a vast region of the parameter space, Kaluza-Klein loops would still be subdominant with respect to winding loops due to the extra factors of $g_s^2 \ll 1$ in (3.7). This is due to the fact that Kaluza-Klein loops feature an extended no-scale cancellation, and so they contribute to the scalar potential effectively only at 2-loop order [41].

since, as can be seen from (3.7), they should be suppressed by both inverse volume powers and by $\epsilon_{\mathcal{F}4} \ll 1$ and $\delta_{\mathcal{F}4} \ll 1$. Hence in Sec. 3.3 we shall study primordial black hole formation for the following simplified inflationary potential:

$$V_{\text{inf}} = \frac{W_0^2}{\mathcal{V}^3} \left[\frac{C_{\text{up}}}{\mathcal{V}^{1/3}} - \frac{C_{\text{w}}}{\sqrt{\tau_{\text{K}3}}} + \frac{A_{\text{w}}}{\sqrt{\tau_{\text{K}3}} - B_{\text{w}}} + \frac{\tau_{\text{K}3}}{\mathcal{V}} \left(D_{\text{w}} - \frac{G_{\text{w}}}{1 + R_{\text{w}} \frac{\tau_{\text{K}3}^{3/2}}{\mathcal{V}}} \right) \right], \quad (3.10)$$

which, when expressed in terms of the canonically normalised inflaton shifted from its minimum, takes the form:

$$V_{\text{inf}} = V_0 \left[C_1 - e^{-\frac{1}{\sqrt{3}}\hat{\phi}} \left(1 - \frac{C_6}{1 - C_7 e^{-\frac{1}{\sqrt{3}}\hat{\phi}}} \right) + C_8 e^{\frac{2}{\sqrt{3}}\hat{\phi}} \left(1 - \frac{C_9}{1 + C_{10} e^{\sqrt{3}\hat{\phi}}} \right) \right], \quad (3.11)$$

with:

$$\begin{aligned} C_1 &= \gamma^{1/3} \frac{C_{\text{up}}}{C_{\text{w}}} \sim \mathcal{O}(1), & C_6 &= \frac{A_{\text{w}}}{C_{\text{w}}} \sim \mathcal{O}(1), & C_7 &= \frac{B_{\text{w}}}{\gamma^{1/3} \mathcal{V}^{1/3}} \sim \mathcal{O}(1), \\ C_8 &= \gamma \frac{D_{\text{w}}}{C_{\text{w}}} \ll 1, & C_9 &= \frac{G_{\text{w}}}{D_{\text{w}}} \sim \mathcal{O}(1), & C_{10} &= \gamma R_{\text{w}} \ll 1. \end{aligned} \quad (3.12)$$

Notice that the potential (3.11) scales as $V_0 \sim H^2 M_p^2 \sim M_p^4 / \mathcal{V}^{10/3}$ while the leading order potential which gives mass to \mathcal{V} and τ_{dP} scales as $V_{\text{lead}} \sim M_p^4 / (g_s^{3/2} \mathcal{V}^3)$ [43, 42]. Hence for $g_s \ll 1$ and $\mathcal{V} \gg 1$, the dynamics which generates PBHs is effectively single-field.

3.2 PBH formation

Primordial black holes form when large and relatively rare density perturbations re-enter the Hubble horizon and undergo gravitational collapse. The fraction of the total energy density in PBHs with mass M at PBH formation is given by:

$$\beta_{\text{f}}(M) = \frac{\rho_{\text{PBH}}(M)}{\rho_{\text{tot}}} \Big|_{\text{f}}. \quad (3.13)$$

The curvature perturbations are assumed to follow a Gaussian distribution with width $\sigma_{\text{M}} \equiv \sigma(M)$.⁹ The probability of large fluctuations leading to the formation

⁹See [142] for the case when non-Gaussianity effects cannot be neglected.

of PBHs with mass M is then given by:

$$\beta_f(M) = \int_{\zeta_c}^{\infty} \frac{1}{\sqrt{2\pi} \sigma_M} e^{-\frac{\zeta^2}{2\sigma_M^2}} d\zeta, \quad (3.14)$$

where ζ_c denotes the critical value for the collapse into a PBH to take place and plays a fundamental rôle in this discussion. It is usually taken to be close to unity, see e.g. [25, 138, 129].¹⁰ For such a Gaussian distribution $\sigma_M^2 \sim \langle \zeta \zeta \rangle$ which on CMB scales is $\mathcal{O}(10^{-9})$. As we will show below, $\sigma_M \ll \zeta_c$ and so we can approximate (3.14) as:

$$\beta_f(M) \sim \frac{\sigma_M}{\sqrt{2\pi} \zeta_c} e^{-\frac{\zeta_c^2}{2\sigma_M^2}}. \quad (3.15)$$

If PBHs are to be a significant fraction of dark matter, the fluctuations that give rise to them must not be too rare, meaning that σ_M cannot be arbitrarily smaller than ζ_c . This implies that on smaller distance scales the scalar power spectrum must be orders of magnitude larger than on CMB scales. Let us quantify this statement and discuss how it may be achieved in single field models of inflation.

The mass of a PBH forming when a large density perturbation re-enters the horizon is assumed to be proportional to the horizon mass:

$$M = \gamma_G \frac{4\pi}{3} \frac{\rho_{\text{tot}}}{H^3} \Big|_f = 4\pi\gamma_G \frac{M_p^2}{H_f}, \quad (3.16)$$

where γ_G is a correction factor which depends on the details of the gravitational collapse and H_f denotes the Hubble parameter at the moment the perturbation re-enters the horizon. Noting that PBHs behave as matter, the fraction of the total energy density in PBHs at formation time (3.13) can be related to the present PBH energy density as:

$$\beta_f(M) = \left(\frac{H_0}{H_f}\right)^2 \frac{\Omega_{\text{DM}}}{a_f^3} f_{\text{PBH}}(M), \quad (3.17)$$

where a_f denotes the scale factor at PBH formation time, H_0 is the Hubble scale today, $\Omega_{\text{DM}} = 0.26$ is the present fraction of the total energy density in dark matter and $f_{\text{PBH}}(M)$ is the fraction of the total dark matter energy density in PBHs with mass M today. PBHs in the low mass region, which can be interesting dark matter candidates, get formed before matter-radiation equality in an epoch of radiation

¹⁰We note that some authors [127, 128] take it to be of the order 10^{-1} or 10^{-2} . Given the exponential dependence of β on ζ_c this significantly decreases the level of tuning required of the inflationary potential in models where PBHs are created within single field inflation.

dominance. Hence the Hubble scale at PBH formation redshifts as:

$$H_{\text{f}}^2 = \Omega_{\text{r}} \frac{H_0^2}{a_{\text{f}}^4} \left(\frac{g_{*\text{f}}}{g_{*0}} \right)^{-1/3}, \quad (3.18)$$

where $\Omega_{\text{r}} = 8 \times 10^{-5}$ is the present fraction of the total energy density in radiation, while g_{*0} and $g_{*\text{f}}$ are respectively the number of relativistic degrees of freedom today and at PBH formation time. Combining (3.16) with (3.18), (3.17) can be rewritten in terms of present day observables and in units of the solar mass M_{\odot} as [143, 144]:

$$\beta_{\text{f}}(M) \simeq \frac{4}{\sqrt{\gamma_{\text{G}}}} \times 10^{-9} \left(\frac{g_{*\text{f}}}{g_{*0}} \right)^{1/4} \sqrt{\frac{M}{M_{\odot}}} f_{\text{PBH}}(M). \quad (3.19)$$

We can now get an estimate of the level of enhancement of the power spectrum required to have PBHs which constitute a significant fraction of dark matter. Setting $\gamma_{\text{G}} = 1$ to be conservative and assuming that only SM degrees of freedom are present so that $g_{*0} = 3.36$ and $g_* = 106.75$, if PBHs with mass M constitute all of dark matter, i.e. $f_{\text{PBH}}(M) = 1$, (3.19) reduces to:

$$\beta_{\text{f}}(M) \simeq 10^{-8} \sqrt{\frac{M}{M_{\odot}}}. \quad (3.20)$$

If we now focus on a mass distribution sharply peaked at $M = 10^{-15} M_{\odot}$, we find $\beta_{\text{f}}(M) \simeq 3 \times 10^{-16}$. Comparing (3.20) with (3.15) for $\zeta_c = 1$, we finally obtain $\sigma_{\text{M}} = 0.12$. This implies that the scalar power spectrum must be enhanced to $\mathcal{O}(10^{-2})$, a value 7 orders of magnitude larger than its value on CMB scales.¹¹ This large enhancement can in principle be achieved within single field inflationary models by inducing an extremely flat and sufficiently long region in the scalar potential. Therefore the problem of PBHs in single field inflation is one of having a sufficiently rich structure in the scalar potential and the freedom to tune in a flat plateau in the later part of inflation.

Let us finally make two important observations:

- In the estimate above of the enhancement of the power spectrum, we considered PBHs with a given mass M . However, more generically, the PBH mass function is broadly peaked, and so the fraction of the total dark matter density

¹¹Had we assumed $\zeta_c = 0.1$, we would have found $\sigma = 0.012$, in agreement with the estimates of [127, 128]. This corresponds to an enhancement of the power spectrum by 5 orders of magnitude between PBH and CMB scales and requires less tuning of the inflationary potential.

in PBHs looks like [145, 116]:

$$f_{\text{PBH}} = \int df_{\text{PBH}}(M) = \int \frac{df_{\text{PBH}}(M)}{d \ln M} d \ln M, \quad (3.21)$$

where $df_{\text{PBH}}(M)$ is the fraction of PBHs with mass between M and $M + d \ln M$, and the integration domain is bounded below by Hawking evaporation of very light PBHs and above by the mass corresponding to PBHs which re-enter the horizon after matter-radiation equality, see e.g. [138].

- Assuming that the Hubble scale during inflation H_{inf} is approximately constant, (3.16) and (3.18) can be used to write the number of efoldings between CMB and PBH horizon exit as [138]:

$$\begin{aligned} \Delta N_{\text{CMB}}^{\text{PBH}} &= \ln \left(\frac{a_{\text{PBH}} H_{\text{inf}}}{a_{\text{CMB}} H_{\text{inf}}} \right) = \ln \left(\frac{a_{\text{f}} H_{\text{f}}}{0.05 \text{ Mpc}^{-1}} \right) \\ &= 18.4 - \frac{1}{12} \ln \left(\frac{g_*}{g_{*0}} \right) + \frac{1}{2} \ln \gamma_{\text{G}} - \frac{1}{2} \ln \left(\frac{M}{M_{\odot}} \right). \end{aligned} \quad (3.22)$$

Setting again $\gamma_{\text{G}} = 1$, $g_{*0} = 3.36$ and $g_* = 106.75$ as in the SM case, the formation of PBHs with masses in the $[10^{-16}, 10^{-14}] M_{\odot}$ range implies that PBH scales leave the horizon approximately 34.2 to 36.5 efoldings after the CMB scales.

3.3 PBHs from Fibre inflation

In order to produce a significant fraction of PBHs from inflationary density perturbations, we shall use the rich structure of the fibre inflation potential (3.10) to induce a near inflection point close to the minimum as depicted in Fig. 3.1 .

Based on the scaling of each term in eq. (3.10) with the fibre modulus τ_{K3} one can see that the second and third terms dominate at small field values and induce a minimum for the modulus around:

$$\langle \tau_{\text{K3}} \rangle \sim \frac{C_{\text{W}} B_{\text{W}}^2}{(\sqrt{C_{\text{W}}} - \sqrt{A_{\text{W}}})^2}. \quad (3.23)$$

The fourth term, being proportional to τ_{K3} , dominates V at large field values, while the fifth term has a maximum at $\frac{2^{2/3}}{(R_{\text{W}}/\mathcal{V})^{2/3}}$ and scales as $-\tau_{\text{K3}}$ at small and as $-\tau_{\text{K3}}^{-1/2}$ at large field values respectively. It is this last term that will be instrumental in generating the enhancement in the scalar power spectrum that will ultimately lead to the formation of primordial black holes in this setup. This can be achieved for

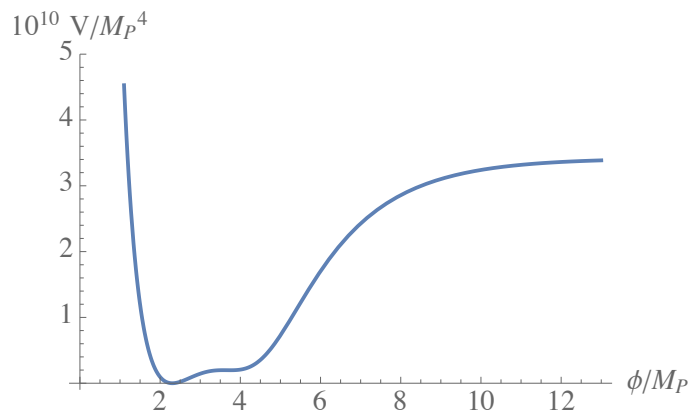


Figure 3.1: Scalar potential for the parameter set \mathcal{P}_2 of Tab. 3.1.

certain values of G_w and R_w such that the potential has a very flat region close to the post-inflationary minimum as illustrated in Fig. 3.1.

Since in slow-roll $P_k \propto H^2/\epsilon_V$, an enhancement of the scalar power spectrum is in principle possible in the limit $\epsilon_V \equiv \frac{V_\phi^2}{2V^2} \rightarrow 0$. Actually the situation is a little more involved since in the plateau the dynamics of the Universe deviates significantly from slow-roll, a fact that has been pointed out in [129] (see also [138]), and that calls for a more careful analysis of the observational signatures of such models, see e.g. [25]. Observables must therefore be computed from solutions to the Mukhanov-Sasaki equation for the rescaled curvature perturbations:

$$u_k''(\eta) + (k^2 - z''/z) u_k(\eta) = 0 , \quad (3.24)$$

where η denotes conformal time, $z \equiv \sqrt{2\epsilon} a$ from which we find that the effective mass of the curvature perturbations is:

$$\frac{z''}{z} = (aH)^2 \left[2 - \epsilon + \frac{3}{2}\eta - \frac{1}{2}\epsilon\eta + \frac{1}{4}\eta^2 + \frac{1}{2}\eta\kappa \right] , \quad (3.25)$$

where:

$$\epsilon = -\frac{\dot{H}}{H^2} , \quad \eta = \frac{\dot{\epsilon}}{\epsilon H} , \quad \kappa = \frac{\dot{\eta}}{\eta H} , \quad (3.26)$$

are the Hubble slow-roll parameters.

One assumes that deep inside the horizon, the perturbations behave as if in flat space, which fixes the initial conditions to be of the Bunch-Davies type [146]:

$$\lim_{k\eta \rightarrow -\infty} u_k(\eta) = \frac{e^{-ik\eta}}{\sqrt{2k}} . \quad (3.27)$$

This determines the solution to be given by a Hankel function of the first kind:

$$u_k(\eta) = \frac{\sqrt{-\pi\eta}}{2} H_\nu^{(1)}(-k\eta) , \quad (3.28)$$

with index ν determined from eq. (3.25) once a given background is chosen.

For comparison with observations one is interested in the dimensionless power spectrum, defined as:

$$P_k = \frac{k^3}{2\pi^2} \left| \frac{u_k}{z} \right|^2 , \quad (3.29)$$

which in the superhorizon limit $k\eta \rightarrow 0$ can be written as:

$$P_k = \frac{H^2}{8\pi^2\epsilon} \frac{2^{2\nu-1} |\Gamma(\nu)|^2}{\pi} \left(\frac{k}{aH} \right)^{3-2\nu} . \quad (3.30)$$

On CMB scales this is bound to be $P_k|_{\text{CMB}} = 2 \times 10^{-9}$ and as shown in Sec. 3.2 it must be significantly enhanced on smaller scales if PBHs are to be significant fraction of all dark matter.

Up to this point the discussion of the behaviour of the perturbations assumed nothing about the type of background in which they evolve. In order to produce a significant amount of PBH from a inflection point in single field inflation, we will see that the universe has to evolve from a slow-roll inflation phase into a transient constant-roll background, where the scalar field acceleration plays an important role. These backgrounds are characterised by the parameter α defined as [147, 148]:

$$\ddot{\phi} \equiv -(3 + \alpha)H\dot{\phi} . \quad (3.31)$$

Solutions with $\alpha = 0$ are called ultra slow-roll [149, 150, 151], whereas vanilla slow-roll inflation corresponds to $\alpha = -3$. The transient constant-roll period arises due the presence of an extremely flat region in the potential that causes the scalar field to brake upon reaching it, leading to a non negligible acceleration in the Klein-Gordon equation and consequently a departure from the slow-roll background. This behaviour is illustrated in Fig. 3.2 where we plot the evolution of the slow-roll parameters for evolution in the potential of Fig. 3.1, corresponding to the parameter set \mathcal{P}_2 of Tab. 3.1. It is evident that the system undergoes a transition from slow-roll ($N_e > 19$) to constant-roll ($15 < N_e < 19$) and finally to a large η slow-roll phase ($N_e < 15$).

In slow-roll $\epsilon, \eta, \kappa \ll 1$, and consequently the effective mass takes the form $z''/z \approx \frac{2}{\eta^2} (2 + 3\epsilon + 3\eta)$, or equivalently $\nu = 3/2 + \epsilon + \eta/2$. One can then see that the curvature perturbations $\zeta = u/z$ remain constant on super-horizon scales

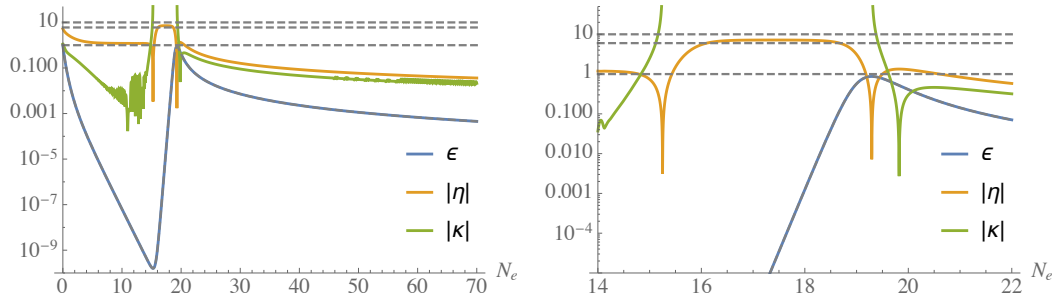


Figure 3.2: Slow-roll parameters as functions of the number of efoldings N_e from the end of inflation for parameter set \mathcal{P}_2 . It is clear that the background evolves from slow-roll ($N_e > 19$) to constant-roll ($15 < N_e < 19$) and back to slow-roll again ($N_e < 15$). Dashed lines represent 10, 6 and 1.

and the two point function can therefore be evaluated at horizon crossing, yielding the familiar slow-roll result:

$$P_k = \frac{H^2}{8\pi^2\epsilon} \Big|_{k=aH} . \quad (3.32)$$

Eq. (3.30) also captures the momentum dependence of the two point function, which can be written in terms of the spectral index n_s and its running α , given by:

$$n_s \equiv \frac{d \ln P_k}{d \ln k} = 1 - 2\epsilon - \eta , \quad (3.33)$$

and:

$$\frac{dn_s}{d \ln k} = -2\epsilon\eta - \eta\kappa . \quad (3.34)$$

Both these quantities are subject of tight observational constraints [80]. For this work we take:

$$n_s = 0.9650 \pm 0.0050 \quad \text{and} \quad \frac{dn_s}{d \ln k} = -0.009 \pm 0.008 \quad (3.35)$$

at 68%CL and at a scale $k_* = 0.05 \text{ Mpc}^{-1}$.

In the transient constant-roll regime one has $\eta \approx -2(3 + \alpha - \epsilon)$ which implies $\epsilon \propto a^{-2(3+\alpha)}$. In the cases we consider $\alpha \in [0, 1]$. In such a background the super-horizon behaviour of the power spectrum is determined by:

$$P_k \propto H^{|2\alpha+3|-1} a^{3+2\alpha+|3+2\alpha|} . \quad (3.36)$$

Note that since ϵ is small and decreasing rapidly with the expansion (for $\alpha > -3$), one can take H to be constant. We therefore see that for $-3 \leq \alpha < -3/2$ the

curvature perturbations are frozen beyond the horizon (this includes the previously discussed case of slow-roll inflation, $\alpha = -3$), whereas for $\alpha > -3/2$, $P_k \propto a^{2(3+2\alpha)}$, signaling the presence of a growing solution to the MS equation, and the breakdown of the approximation of (3.32). In order to determine the two-point function in such backgrounds one must therefore solve the MS equation and evaluate P_k at the end of inflation.

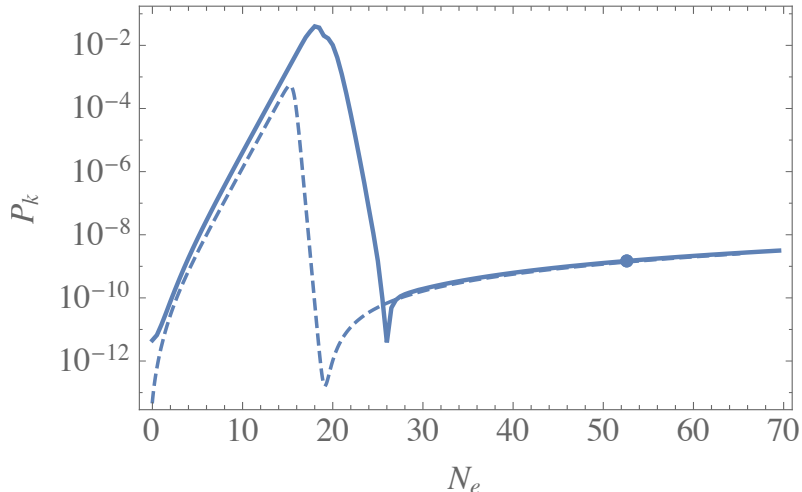


Figure 3.3: Power spectrum (3.29) for the potential of Fig. 3.1 with parameter set \mathcal{P}_2 . The dashed line represents the slow-roll estimate of (3.32) while the continuous line is obtained from the solutions to the MS equation. The circle correspond to the CMB scales if the peak is to be associated with PBH of mass $M = 10^{-14}M_\odot$.

In Fig. 3.3 we plot the power spectrum for scalar perturbations for the potential of Fig. 3.1 (parameter set \mathcal{P}_2) calculated from the solutions of (3.24) (continuous line) and the slow-roll estimate of (3.32) (dashed line). As expected the slow-roll approximation breaks down for modes that cross the horizon close to the onset of the constant-roll phase. Crucially for the production of PBH, the slow-roll result underestimates the power spectrum by several orders of magnitude in this range of momentum modes. This is to be expected given the existence of a growing mode solution in constant-roll backgrounds with $\alpha \in [0, 1]$. The presence of the growing mode also implies that the actual position of the peak in the power spectrum is shifted towards larger scales/PBH masses with respect to the slow-roll estimate.¹² In Fig. 3.4 we plot the evolution of the power spectrum for modes leaving the horizon 53 and 22 efoldings before the end of inflation, corresponding to CMB and PBH scales respectively. While both scales are affected by the growing mode during

¹²These results are qualitatively similar to the findings of [25] since both models feature the same dynamics.

the constant roll phase, their superhorizon growth is determined by $\frac{k}{aH}$ at the onset of the constant roll period. This quantity is minute for modes on CMB scales but not for those on the PBH region. As a result the CMB mode essentially follow the slow-roll estimate of (3.32) after crossing the horizon, while on small scales we see that there is a large amplification of P_k leading to a breakdown of the slow-roll approximation. Finally let us note that the $\mathcal{O}(1)$ deviation from the slow-roll estimate for modes on the smallest scales ($N_e \lesssim 15$) can be attributed to the fact that in the final phase of expansion before the end of inflation, $\eta = \mathcal{O}(1)$.

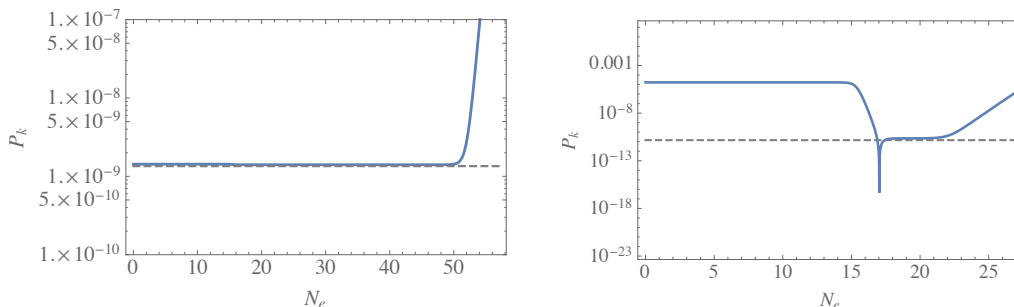


Figure 3.4: Evolution of the curvature perturbations on different scales for example \mathcal{P}_2 . On the left panel a mode that corresponds to CMB scales, leaving the horizon 53 e-foldings before the end of inflation, and keeping a constant value thereafter. On the right panel a mode that corresponds to PBH scales, leaving the horizon 22 e-foldings before the end of inflation and undergoing super-horizon growth during the constant-roll phase (the same evolution was found in Fig. 2 of [152]). In both plots the dashed line corresponds to the slow-roll estimate of (3.32).

In Tables 3.1 and 3.2 we present three numerical examples corresponding to cases where all DM is composed of $10^{-14}M_\odot$ PBHs, assuming $\zeta_c = 1$. We stress that the choices of the underlying parameters are in line with their microscopic origin as explained in Sec. 3.1 and that the desire to have PBH DM does not constrain the compactification volume, which varies by several orders of magnitude in between the three examples. All the digits presented in Tab. 3.1 are required in order to fully reproduce our results. In particular, G_w and R_w control the position of the near inflection point and the velocity with which the field goes through that region. Changing any of these two quantities will change the amplitude and position of the peak of Fig. 3.3, and therefore the mass and abundance of PBHs.

All examples lead to a spectral index that is slightly more than 3 sigma redder than the current best fit, while giving rise to a spectral index running and a tensor fraction that are in line with current bounds. Notice that, for sake of simplicity, we did not analyse the full potential (3.4) but we just considered the simplest form

which gives rise to PBH formation. However, if we had included terms which behave as $1/\tau_{K3}$, we would have obtained larger values of n_s which would alleviate the tension with present observational constraints.

	C_w	A_w	B_w	G_w	R_w	$\langle\tau_{K3}\rangle$	$\langle\mathcal{V}\rangle$
\mathcal{P}_1	1/10	2/100	1	0.1398533	0.706811	3.89	107.3
\mathcal{P}_2	4/100	2/100	1	3.080548×10^{-2}	0.7071067	14.30	1000
\mathcal{P}_3	1.978/100	1.65/100	1.01	4.628858×10^{-3}	0.7070	168.03	5×10^4

Table 3.1: Examples of parameters leading to the production of PBHs with a mass peaked at $10^{-14}M_\odot$, together with geometrical compactification data. All examples exhibit $D_w = 0$ which can be guaranteed by construction via a proper choice of intersections between stacks of D7-branes [82, 2]. Otherwise D_w has been tuned to values of $\mathcal{O}(10^{-6})$ via an appropriate choice of background fluxes.

	n_s	r	$\frac{dn_s}{d \ln k}$	$\Delta N_{\text{CMB}}^{\text{PBH}}$	$P_k _{\text{peak}}$
\mathcal{P}_1	0.9457	0.015	-0.0017	34.5	0.01365
\mathcal{P}_2	0.9437	0.015	-0.0017	34.5	0.03998
\mathcal{P}_3	0.9457	0.015	-0.0019	34.5	0.013341

Table 3.2: Inflationary observables on CMB and PBH scales for the examples of Tab. 3.1. CMB scales correspond to 53 efoldings before the end of inflation.

3.4 Summary

In this chapter we have presented the first explicit example of a string inflationary model which can potentially be consistent with cosmological observations at CMB scales and, at the same time, can generate PBHs at small distance scales via an efficient enhancement of the power spectrum due to a period of ultra slow-roll. Our model leads to PBHs in the low-mass region where they constitute a significant fraction of the total dark matter abundance.

Three interesting features of fibre inflation models relevant for PBH formation are the following: (i) the coefficients of the different contributions to the inflationary potential depend on microscopic parameters like background fluxes and Calabi-Yau intersection numbers which take different values in the string landscape, and so give a very large tuning freedom that can be used to generate a near inflection point; (ii) the potential enjoys an approximate Abelian rescaling symmetry inherited from the underlying extended no-scale structure which suppresses quantum corrections

to the inflationary dynamics; *(iii)* the contribution to the inflationary potential responsible for the emergence of a near inflection point at large momentum scales has been derived in global embeddings of fibre inflation models in explicit Calabi-Yau compactifications with chiral brane setup compatible with moduli stabilisation.

Moreover our model is characterised by a trans-Planckian field range during inflation, and so it predicts a large tensor-to-scalar ratio of order $r \sim 0.01$ which might be detected by the next generation of cosmological measurements. Similarly to previous works on PBH formation in single-field inflation [128, 25], the scalar spectral index turns out to be a bit too red since it is more than 3σ away from the Planck reference value. This tension might be resolved by the inclusion of non-zero neutrino masses which might make our result compatible with CMB data within just 2σ [25, 153]. The tension in the values of n_s can also decrease in compactifications where the approach to the inflationary plateau occurs faster than the $1/\sqrt{\tau_{K3}}$ considered here, a possibility in potentials of the form (3.4). Another interesting cosmological observable in our model is the running of the spectral index which turns out to be sizable.

Notice that the tension with the observed value of the scalar spectral index is the main reason why our mechanism cannot produce PBHs in the large mass region probed by LIGO since they would correspond to scales which are too close to CMB scales. Hence the large enhancement required for PBHs to be a significant fraction of DM, would make n_s in strong conflict with present data. Given that the results of previous works focused on PHB formation in similar setups are qualitatively equivalent [25], the generation of PBHs in the small mass window seems to be a generic property of single-field models with an inflationary plateau followed by a near inflection point.

Chapter 4

The 3.5 keV Line from Stringy Axions

Recently several studies have shown the appearance of a photon line at $E \sim 3.5$ keV, based on stacked X-ray data from galaxy clusters and the Andromeda galaxy [161, 162]. The line has been detected in galaxy clusters by the X-ray observatories XMM-Newton, Chandra and Suzaku [163, 164] and in Andromeda with XMM-Newton [162]. The Hitomi satellite would have been able to study the 3.5 keV line with unprecedented energy resolution. However, unfortunately Hitomi was lost after only a few weeks in operation and the limited exposure time on the Perseus cluster only allows to put upper bounds on the 3.5 keV line which are consistent with the detection of the other satellites [165]. The findings of [161, 162] have inspired further searches in other astrophysical objects such as the galactic center [166, 167, 168, 169], galaxies [170], dwarfs [171, 172, 173] and other galaxy clusters [174, 175].¹ Currently, a compelling standard astrophysical explanation, e.g. in terms of atomic lines of the (cluster) gas is lacking.² This gives rise to the possibility that the 3.5 keV line is a signal related to dark matter (DM) physics.

A much explored model is that of dark matter decay, e.g. a sterile neutrino with mass $m_{\text{DM}} \sim 7$ keV decaying into an active neutrino and a photon [178, 179]. In this case, the photon flux from an astrophysical object is solely determined by the lifetime of the dark matter particle and the dark matter column density. The width of the line is due to Doppler broadening. There are several observational tensions, if one wants to explain the (non-)observation of the 3.5 keV line in currently analysed astrophysical objects. Most prominently, these are:

- Non-observation of the 3.5 keV line from dwarf spheroidal galaxies [171, 172,

¹For a summary of observations and models on the 3.5 keV line see [176].

²See however [167, 177].

173]. The dark matter density of these objects is rather well known and the X-ray background is low, making dwarf spheroidals a prime target for detecting decaying dark matter.

- Non-observation of the 3.5 keV line from spiral galaxies [170], where again the X-ray background is low. According to the dark matter estimates of [170], the non-observation of a 3.5 keV signal from spiral galaxies excludes a dark matter decay origin of the 3.5 keV line very strongly at 11σ .
- The radial profile of the 3.5 keV line in the Perseus cluster peaks on shorter scales than the dark matter profile, rather following the gas profile than the dark matter profile [161, 169]. However, the observed profile with Suzaku is only in mild tension with the dark matter profile [164].

These tensions, even though they could be potentially explained by uncertainties in the dark matter distributions in these objects [176], motivate different dark matter models than direct dark matter decay into a pair of 3.5 keV photons.

A dark matter model that is consistent with all the present (non-)observations was given in [180]. A dark matter particle with mass $m_{\text{DM}} \sim 7$ keV decays into an almost massless ($m_{\text{ALP}} \lesssim 10^{-12}$ eV) axion-like particle (ALP) with energy 3.5 keV which successively converts into 3.5 keV photons that are finally observed. Compared to direct dark matter decay into photons, the observed photon flux does not depend just on the dark matter column density, but also on the probability for ALPs to convert into photons. This is determined by the size and coherence scale of the magnetic field and the electron density in e.g. a galaxy cluster.

The 3.5 keV emission is stronger in astrophysical regions with relatively large and coherent magnetic field. This is verified by the experimental fact that cool core clusters like the Perseus cluster have stronger magnetic fields than non-cool core clusters and also a higher 3.5 keV flux is observed from such an object. Furthermore, the fact that central regions of a cool core cluster host particularly strong magnetic fields explains the radial morphology of the 3.5 keV flux from Perseus as the signal comes disproportionately from the central region of the cluster. The model has made the prediction that galaxies can only generate a non-negligible 3.5 keV photon flux if they are spiral and edge-on as for instance the Andromeda galaxy [180]. In this case, the full length of the regions with regular magnetic field can be used efficiently for ALP to photon conversion. These predictions agree with the experimental results of non-observation of the 3.5 keV signal from generic (edge-on and face-on) spiral galaxies and dwarf galaxies [181].³

³Despite the successful interpretation of all these observations, this model would not be able

Given that the 4D low-energy limit of string compactifications generically leads to several light ALPs [183, 184, 185, 186, 187], it is natural to try to embed the model of [180] in string theory. This is the main goal of this chapter where we focus in particular on type IIB flux compactifications where moduli stabilisation has already been studied in depth.

In 4D string models, ALPs can emerge either as closed string modes arising from the dimensional reduction of 10D anti-symmetric forms or as phases of open string modes charged under anomalous $U(1)$ symmetries on stacks of D-branes [183, 184, 185, 186, 187]. Some of these modes can be removed from the low-energy spectrum by the orientifold projection which breaks $N = 2$ supersymmetry down to $N = 1$, others can be eaten up by anomalous $U(1)$'s via the Green-Schwarz mechanism for anomaly cancellation or can become as heavy as the gravitino if the corresponding saxions are stabilised by the same non-perturbative effects which give mass to the axions. However the axions enjoy a shift symmetry which is broken only at non-perturbative level. Therefore when the corresponding saxions are frozen by perturbative corrections to the effective action, the axions remain exactly massless at this level of approximation. They then develop a mass via non-perturbative effects which are however exponentially suppressed with respect to perturbative corrections. Hence whenever perturbative contributions to the effective scalar potential play a crucial rôle for moduli stabilisation, the axions are exponentially lighter than the associated saxions [63]. Notice that this case is rather generic in string compactifications for two main reasons: (i) if the background fluxes are not tuned, non-perturbative effects are naturally subleading with respect to perturbative ones; (ii) it is technically difficult to generate non-perturbative contributions to the superpotential which depend on all moduli (because of possible extra fermionic zero modes [188], chiral intersections with the visible sector [50] or non-vanishing gauge fluxes due to Freed-Witten anomaly cancellation [98]).

String compactifications where some moduli are fixed by perturbative effects are therefore perfect frameworks to derive models for the 3.5 keV line with light ALPs which can behave as either the 7 keV decaying DM particle or as the ultra-light ALP which converts into photons. The main moduli stabilisation mechanism which exploits perturbative corrections to the Kähler potential is the LARGE Volume Scenario (LVS) [43, 44, 42]. We shall therefore present an LVS model with the following main features (see Fig. 4.1 for a pictorial view of our microscopic setup):

- The underlying Calabi-Yau (CY) manifold is characterised by $h^{1,1} = 5$ Kähler

to explain the dip around 3.5 keV in the Perseus AGN spectrum which might arise from Chandra data [182].

moduli $T_i = \tau_i + ic_i$ where the c_i 's are closed string axions while the τ_i 's control the volume of 5 different divisors: a large four-cycle D_b , a rigid del Pezzo four-cycle D_s which intersects with a 'Wilson divisor' D_p ($h^{0,1}(D_p) = 1$ and $h^{0,2}(D_p) = 0$) and two non-intersecting blow-up modes D_{q_1} and D_{q_2} .

- The two blow-up modes D_{q_1} and D_{q_2} shrink down to zero size due to D-term stabilisation and support D3-branes at the resulting singularities. These constructions are rather promising to build a semi-realistic visible sector with SM-like gauge group, chiral spectrum and Yukawa couplings [189, 190]. If D_{q_1} and D_{q_2} are exchanged by the orientifold involution, the visible sector features two anomalous $U(1)$ symmetries (this is always the case for any del Pezzo singularity) [104, 191, 192], while if the two blow-up modes are separately invariant, one of them supports the visible sector and the other a hidden sector [193, 72]. Each of the two sectors is characterised by a single anomalous $U(1)$ factor.
- A smooth combination of D_s and D_p is wrapped by a stack of D7-branes which give rise to string loop corrections to the Kähler potential K [39, 40, 41]. Moreover, non-vanishing world-volume fluxes generate moduli-dependent Fayet-Iliopoulos (FI) terms [99, 100]. An ED3-instanton wraps the rigid divisor D_s and generates standard T_s -dependent non-perturbative corrections to the superpotential W . A second ED3-instanton wraps the Wilson divisor D_p . Due to the presence of Wilson line modulini, this ED3-instanton contributes to the superpotential only via T_p -dependent poly-instanton effects [194, 195].
- At leading order in an inverse volume expansion, the moduli are fixed supersymmetrically by requiring vanishing D- and F-terms. These conditions fix the dilaton and the complex structure moduli in terms of three-form flux quanta together with the blow-up modes τ_{q_1} and τ_{q_2} in terms of charged open string fields, and hidden matter fields on the D7-stack in terms of τ_p .
- Quantum corrections beyond tree-level break supersymmetry and stabilise most of the remaining flat directions: α' corrections to K [36] and single non-perturbative corrections to W [88] fix τ_b , τ_s and c_s , while soft supersymmetry breaking mass terms and g_s loop corrections to K fix τ_p .
- Subdominant T_p -dependent poly-instanton corrections to W stabilise the local closed string axion c_p while a highly suppressed T_b -dependent non-perturbative superpotential fixes the bulk closed string axion c_b . Sequestered soft term

contributions stabilise instead the radial component of $U(1)$ -charged matter fields $C = |C| e^{i\theta}$ living on the D3-brane stacks.

- Both c_b and c_p are exponentially lighter than the gravitino, and so could play the rôle of the decaying DM particle with $m_{\text{DM}} \sim 7$ keV. On the other hand the ultra-light ALP with $m_{\text{ALP}} \lesssim 10^{-12}$ eV which converts into photons is given by the open string phase θ . Notice that if D_{q_1} and D_{q_2} are identified by the orientifold involution, there are two open string phases in the visible sector: one behaves as the standard QCD axion, which is however heavier than 10^{-12} eV, and the other is the ultra-light ALP θ . If instead D_{q_1} and D_{q_2} are separately invariant under the involution, θ is an open string axion belonging to a hidden sector.
- The coupling of the closed string axions c_b and c_p to the open string ALP θ is induced by kinetic mixing due to non-perturbative corrections to the Kähler potential. However we shall show that the scale of the induced DM-ALP coupling can be compatible with observations only if the DM candidate is the local closed string axion c_p .
- If the ultra-light ALP θ belongs to the hidden sector, its coupling to ordinary photons can be induced by $U(1)$ kinetic mixing which gets naturally generated by one-loop effects [196]. Interestingly, the strength of the resulting interaction can easily satisfy the observational constraints if the open string sector on the D3-brane stack is both unsequestered and fully sequestered from the sources of supersymmetry breaking in the bulk.
- The branching ratio for the direct axion DM decay into ordinary photons is negligible by construction since it is induced by kinetic mixing between Abelian gauge boson on the D7-stack and ordinary photons on the D3-stack which gives rise to an interaction controlled by a scale which is naturally trans-Planckian.

This chapter is organised as follows. In Sec. 4.1 we first discuss the phenomenology of the dark matter to ALP to photon model for the 3.5 keV line and its observational constraints, and then we describe how these phenomenological conditions turn into precise requirements on the Calabi-Yau geometry, the brane setup and gauge fluxes, the 4D fields which can successfully play the rôle of either the DM particle or the ultra-light ALP, the form of the various interactions and the resulting low-energy 4D supergravity. Sec. 4.2 provides a thorough discuss of moduli stabilisation showing how different sources of corrections to the effective action can fix all closed string moduli and the $U(1)$ -charged open string modes. In Sec. 4.3

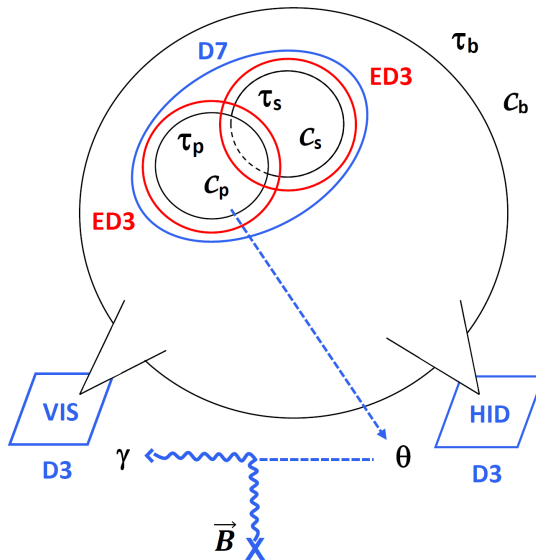


Figure 4.1: Pictorial view of our setup: a stack of D7-branes wraps the combination $\tau_s + \tau_p$, two ED3-instantons wrap respectively the rigid cycle τ_s and the Wilson divisor τ_p while two stacks of D3-branes at singularities support the visible and a hidden sector. The DM particle is the closed string axion c_p which acquires a 7 keV mass due to tiny poly-instanton effects and decays to the ultra-light open string ALP θ that gives the 3.5 keV line by converting into photons in the magnetic field of galaxy clusters.

we first derive the expressions for the canonically normalised fields and their masses and then we use these results to work out the strength of the DM-ALP coupling before presenting our conclusions in Sec. 4.4. Several technical details are relegated to App. C.

4.1 Phenomenology and microscopic realisation

In this section we first discuss the observational constraints of the model of [180] for the 3.5 keV line, and we outline the main phenomenological features of our embedding in LVS type IIB flux compactifications. We then provide the technical details of the microscopic realisation of the DM to ALP to photon model for the 3.5 keV line. We start by illustrating the geometry of the underlying Calabi-Yau compactification manifold. We then present the brane setup and gauge fluxes, and we finally describe the main features of the resulting low-energy 4D effective field theory.

4.1.1 Observational constraints

The effective Lagrangian of the dark matter to ALP to photon model for the 3.5 keV line can be described as follows:

$$\begin{aligned} \mathcal{L} = & -\frac{1}{4}F^{\mu\nu}F_{\mu\nu} - \frac{a_{ALP}}{4M}F^{\mu\nu}\tilde{F}_{\mu\nu} + \frac{1}{2}\partial_\mu a_{ALP}\partial^\mu a_{ALP} - \frac{1}{2}m_{ALP}^2 a_{ALP}^2 \\ & + \frac{a_{DM}}{\Lambda}\partial_\mu a_{ALP}\partial^\mu a_{ALP} + \frac{1}{2}\partial_\mu a_{DM}\partial^\mu a_{DM} - \frac{1}{2}m_{DM}^2 a_{DM}^2, \end{aligned} \quad (4.1)$$

where a_{ALP} is an ALP with mass m_{ALP} that converts into photons in astrophysical magnetic fields via the coupling suppressed by M . a_{DM} is a pseudoscalar which is the dark matter particle with mass $m_{DM} \sim 7$ keV. It decays via the kinetic mixing term in (4.1) with characteristic scale Λ . In order for ALP-photon conversion to be efficient in galaxy cluster magnetic field environments, we require $m_{ALP} \lesssim 10^{-12}$ eV which is the characteristic energy scale of the electron-photon plasma [180]. Otherwise, the ALP to photon conversion is suppressed by $\sim (10^{-12} \text{ eV}/m_{ALP})^4$. Therefore a_{ALP} is too light to be the standard QCD axion but it has instead to be a stringy axion-like particle.

The observed photon flux at an X-ray detector is given by:

$$F_{DM \rightarrow a_{ALP} \rightarrow \gamma} \propto \Gamma_{a_{DM} \rightarrow a_{ALP} a_{ALP}} P_{a_{ALP} \rightarrow \gamma} \rho_{DM}, \quad (4.2)$$

where ρ_{DM} is the dark matter column density and:

$$\Gamma_{a_{DM} \rightarrow a_{ALP} a_{ALP}} = \frac{1}{32\pi} \frac{m_{DM}^3}{\Lambda^2}, \quad (4.3)$$

is the dark matter decay rate and $P_{a_{ALP} \rightarrow \gamma}$ is the ALP to photon conversion probability. It is given as $P_{a_{ALP} \rightarrow \gamma} \propto M^{-2}$ and furthermore depends on the electron density in the plasma, the energy of the ALP/photon, the coherence length and the strength of the magnetic field. Hence, $F_{DM \rightarrow a_{ALP} \rightarrow \gamma} \propto \Lambda^{-2} M^{-2}$. For the ALP to photon conversion conditions in the Perseus cluster magnetic field, the observed 3.5 keV flux then implies [180]:

$$\Lambda \cdot M \sim 7 \cdot 10^{28} \text{ GeV}^2. \quad (4.4)$$

The scales M and Λ are subject to certain constraints. There is a lower bound $M \gtrsim 10^{11}$ GeV from observations of SN1987A [197, 198, 199], the thermal spectrum of galaxy clusters [200] and active galactic nuclei [201, 202, 203]. This lower bound implies an upper bound on Λ via (4.4). To get sufficiently stable dark matter, we assume that the dark matter particle has a lifetime larger than the age of the

universe, i.e. $\Lambda \gtrsim 5 \cdot 10^{12}$ GeV. This implies an upper bound on M via (4.4). To summarise, the parameters M and Λ have to satisfy (4.4) together with the following phenomenological constraints:

$$10^{11} \text{ GeV} \lesssim M \lesssim 10^{16} \text{ GeV}, \quad 5 \cdot 10^{12} \text{ GeV} \lesssim \Lambda \lesssim 7 \cdot 10^{17} \text{ GeV}. \quad (4.5)$$

Notice that ultra-light ALPs with intermediate scale couplings to photons will be within the detection reach of helioscope experiments like IAXO [204] and potentially light-shining-through-a-wall experiments like ALPS [205].

4.1.2 Phenomenological features

The phenomenological requirements for a viable explanation of the 3.5 keV line from dark matter decay to ALPs which then convert into photons, can be translated into precise conditions on the topology and the brane setup of the microscopic realisation. We shall focus on type IIB flux compactifications where moduli stabilisation has already been studied in depth. According to (4.4) and (4.5), we shall focus on the parameter space region where the DM to ALP coupling is around the GUT/Planck scale, $\Lambda \sim 10^{16}$ - 10^{18} GeV, whereas the ALP to photon coupling is intermediate: $M \sim 10^{11}$ - 10^{13} GeV. This region is particularly interesting since an ALP with this decay constant could also explain the diffuse soft X-ray excess from galaxy cluster via axion-photon conversion in the cluster magnetic field [206]. This phenomenological requirement, together with the observation that $m_{\text{DM}} \sim 10$ keV while $m_{\text{ALP}} \lesssim 10^{-12}$ eV, sets the following model building constraints:

- **ALP as an open string axion at a singularity:** From the microscopic point of view, a_{ALP} can be either a closed or an open string axion. In the case of closed string axions, a_{ALP} could be given by the reduction of C_4 on orientifold-even four-cycles or by the reduction of C_2 on two-cycles duals to orientifold-odd four-cycles. As explained in [184, 187] and reviewed in App. C.0.1, since axions are the imaginary parts of moduli, $T_i = \tau_i + i c_i$ (c_i is a canonically unnormalised axion), whose interaction with matter is gravitational, they tend to be coupled to photons with Planckian strength. However this is true only for bulk axions which have $M \simeq M_p$, while the coupling to photons of local axions, associated to blow-up modes of point-like singularities, is controlled by the string scale: $M \simeq M_s$. $M_s \sim M_p/\sqrt{\mathcal{V}}$ can be significantly lower than M_p if the volume of the extra dimensions in string units \mathcal{V} is very large, and so local closed string axions could realise $M \sim M_s \sim 10^{11}$ - 10^{13} GeV.

A moduli stabilisation scheme which leads to an exponentially large \mathcal{V} is the

LARGE Volume Scenario [43, 44, 42] whose simplest realisation requires a Calabi-Yau volume of the form:

$$\mathcal{V} = \tau_b^{3/2} - \tau_s^{3/2} . \quad (4.6)$$

The moduli are fixed by the interplay of the leading order α' correction to the Kähler potential and non-perturbative effects supported on the rigid cycle τ_s . The decay constant of the axionic partner of τ_s , which we denote as c_s , is set by the string scale, $M \sim M_s$, but this mode develops a mass of order the gravitino mass $m_{c_s} \sim m_{3/2} \sim M_p/\mathcal{V}$. The large divisor τ_b is lighter than the gravitino due to the underlying no-scale structure of the 4D effective field theory, $m_{\tau_b} \sim m_{3/2}/\sqrt{\mathcal{V}}$, but it has to be heavier than about 50 TeV in order to avoid any cosmological moduli problem. Hence the local axion c_s is much heavier than 10^{-12} eV, and so cannot play the rôle of a_{ALP} . Moreover, the bulk axion c_b cannot be the desired ALP as well since, even if it is almost massless, its coupling scale to photons would be too high: $M \sim M_p$.

We are therefore forced to consider an open string axion realisation for a_{ALP} . Anomalous $U(1)$ factors appear ubiquitously in both D7-branes wrapped around four-cycles in the geometric regime and in D3-branes at singularities. In the process of anomaly cancellation, the $U(1)$ gauge boson becomes massive by eating up an axion [207]. As explained in [63], the combination of axions which gets eaten up is mostly given by an open string axion for D7-branes and by a closed string axion for D3-branes. The resulting low-energy theory below the gauge boson mass, features a global $U(1)$ which is an ideal candidate for a Peccei-Quinn like symmetry. In the case of D3-branes at singularities, the resulting D-term potential looks schematically like:

$$V_D = g^2 \left(q|\hat{C}|^2 - \xi \right)^2 , \quad (4.7)$$

where we focused just on one canonically normalised charged matter field $\hat{C} = |\hat{C}| e^{i\theta}$ whose phase θ can play the rôle of an axion with decay constant set by the VEV of the radial part $|\hat{C}|$. The FI term $\xi \sim \tau_q/\mathcal{V}$ is controlled by the four-cycle τ_q which gets charged under the anomalous $U(1)$ and whose volume resolves the singularity. A leading order supersymmetric solution fixes $|\hat{C}|^2 = \xi/q$, leaving a flat direction in the $(|\hat{C}|, \tau_q)$ -plane. This remaining flat direction is fixed by subdominant supersymmetry breaking contributions from

background fluxes which take the form [192]:

$$V_F(|\hat{C}|) = c_2 m_0^2 |\hat{C}|^2 + c_3 A |\hat{C}|^3 + O(|\hat{C}|^4), \quad (4.8)$$

where c_2 and c_3 are $\mathcal{O}(1)$ coefficients. If we parametrise the volume dependence of the soft scalar masses as $m_0 \sim M_p/\mathcal{V}^{\alpha_2}$ and the trilinear A-term as $A \sim M_p/\mathcal{V}^{\alpha_3}$, and we use the vanishing D-term condition to write τ_q in terms of $|\hat{C}|$ as $\tau_q \sim |\hat{C}|^2 \mathcal{V}$, the matter field VEV scales as:

$$\begin{aligned} (i) \text{ If } c_2 > 0 \quad |\hat{C}| = 0 &\Leftrightarrow \tau_q = 0, \\ (ii) \text{ If } c_2 < 0 \quad |\hat{C}| \simeq \frac{M_p}{\mathcal{V}^{2\alpha_2 - \alpha_3}} &\Leftrightarrow \tau_q \simeq \frac{1}{\mathcal{V}^{4\alpha_2 - 2\alpha_3 - 1}}. \end{aligned}$$

Only in case (ii) the matter field $|\hat{C}|$ becomes tachyonic and breaks the Peccei-Quinn symmetry, leading to a viable axion realisation. In the presence of flavour D7-branes intersecting the D3-brane stack at the singularity, the soft terms are unsequestered and $\alpha_2 = \alpha_3 = 1$ [208], giving $|\hat{C}| \sim M_p/\mathcal{V} \sim m_{3/2}$ and $\tau_q \simeq \mathcal{V}^{-1} \ll 1$ which ensures that τ_q is still in the singular regime. If the internal volume is of order $\mathcal{V} \sim 10^8$, the large modulus τ_b is heavy enough to avoid the cosmological moduli problem: $m_{\tau_b} \sim 100$ TeV. In turn the gravitino mass, all soft terms and the axion decay constant $f_{a_{ALP}} = |\hat{C}|$ are around 10^9 GeV. Setting $\theta = a_{ALP}/f_{a_{ALP}}$, the axion to photon coupling then takes the form:

$$\frac{g^2}{32\pi^2} \frac{a_{ALP}}{f_{a_{ALP}}} F_{\mu\nu} \tilde{F}^{\mu\nu} \Leftrightarrow M = \frac{32\pi^2 f_{a_{ALP}}}{g^2} = \frac{32\pi^2 f_{a_{ALP}}}{g_s} \sim 10^{12} \text{ GeV}, \quad (4.9)$$

since for D3-branes the coupling $g^{-2} = \text{Re}(S) = g_s^{-1}$ is set by the dilaton S which controls also the size of the string coupling that we assume to be in the perturbative regime: $g_s \simeq 0.1$.

On the other hand, in the absence of flavour D7-branes the soft terms are sequestered with $\alpha_3 = 2$ and $\alpha_2 = 3/2$ or $\alpha_2 = 2$ depending on the form of the quantum corrections to the Kähler metric for matter fields and the effects responsible for achieving a dS vacuum [209, 210]. Notice that possible non-perturbative desequestering effects from couplings in the superpotential of the form $W_{\text{np}} \supset \mathcal{O}_{\text{matter}} e^{-a_s T_s}$ with $\mathcal{O}_{\text{matter}}$ a gauge-invariant operator composed of matter fields, cannot actually change the volume dependence of either the soft scalar masses or the A-terms [211]. Thus if $\alpha_2 = 3/2$ we have $f_{a_{ALP}} = |\hat{C}| \simeq M_p/\mathcal{V}$ and $\tau_q \sim \mathcal{V}^{-1} \ll 1$, while if $\alpha_2 = 2$ the open axion decay constant scales

as $f_{a_{ALP}} = |\hat{C}| \simeq M_p/\mathcal{V}^2$ and $\tau_q \sim \mathcal{V}^{-3} \ll 1$. In both cases without flavour D7-branes the gaugino masses scale as $M_{1/2} \sim 0.1 M_p/\mathcal{V}^2$ and lie around the TeV scale for $\mathcal{V} \sim 10^7$. Considering this value of the volume, the axion-photon coupling therefore becomes:

$$(a) \text{ If } \alpha_2 = \frac{3}{2} \quad M = \frac{32\pi^2 f_{a_{ALP}}}{g_s} \sim 10^3 m_{3/2} \sim 10^{13} \text{ GeV}, \quad (4.10)$$

$$(b) \text{ If } \alpha_2 = 2 \quad M = \frac{32\pi^2 f_{a_{ALP}}}{g_s} \sim 10^3 \frac{m_{3/2}}{\mathcal{V}} \sim 10^6 \text{ GeV}. \quad (4.11)$$

- **ALP-photon coupling induced by $U(1)$ kinetic mixing:** We have shown above that, if the matter field $|\hat{C}|$ charged under the anomalous $U(1)$ develops a non-zero VEV due to a tachyonic soft scalar mass contribution, the open string axion θ can have an intermediate scale coupling to photons. However θ in general plays the rôle of the standard QCD axion which becomes much heavier than $m_{ALP} \lesssim 10^{-12}$ eV due to QCD instanton effects. Hence the simplest realisation of an ultralight ALP with the desired phenomenological features to reproduce the 3.5 keV line requires the existence of at least two open string axions. The Calabi-Yau volume (4.6) has then to be generalised to:

$$\mathcal{V} = \tau_b^{3/2} - \tau_s^{3/2} - \tau_{q_1}^{3/2} - \tau_{q_2}^{3/2}, \quad (4.12)$$

where τ_{q_1} and τ_{q_2} are both collapsed to a singularity via D-term fixing and support a stack of D3-branes. There are two possibilities to realise a viable a_{ALP} :

1. The two blow-up modes τ_{q_1} and τ_{q_2} are exchanged by the orientifold involution [104, 191, 192]. The resulting quiver gauge theory on the visible sector stack of D3-branes generically features two anomalous $U(1)$ symmetries. This is for example always the case for del Pezzo singularities. Hence the visible sector is characterised by the presence of two open string axions: one behaves as the QCD axion while the other can be an almost massless a_{ALP} with $M \sim 10^{11}$ - 10^{12} GeV as in (4.9) or (4.10). In this case the matter field $|\hat{C}|$ which develops a VEV of order the gravitino mass has to be a Standard Model gauge singlet in order not to break any visible sector gauge symmetry at a high scale.
2. The two blow-up divisors τ_{q_1} and τ_{q_2} are invariant under the orientifold involution [193, 72]. Therefore one D3-stack has to reproduce the visible sector while the other represents a hidden sector. Each of the two sectors

features an anomalous $U(1)$ which gives rise to an open string axion with a coupling to the respective photons controlled by the scale M . The visible sector axion plays the rôle of the QCD axion while the hidden sector open string axion can behave as a_{ALP} . Its coupling to ordinary photons can be induced by a $U(1)$ kinetic mixing of the form [196, 212, 213]:

$$\mathcal{L} \supset -\frac{1}{4}F_{\mu\nu}F^{\mu\nu} - \frac{1}{4}G_{\mu\nu}G^{\mu\nu} + \frac{\chi}{2}F_{\mu\nu}G^{\mu\nu} - \frac{a_{QCD}}{4M_{\text{vis}}}F_{\mu\nu}\tilde{F}^{\mu\nu} - \frac{a_{ALP}}{4M_{\text{hid}}}G_{\mu\nu}\tilde{G}^{\mu\nu}, \quad (4.13)$$

where we denoted the QCD axion as a_{QCD} , the kinetic mixing parameter as χ and the visible sector Maxwell tensor as $F_{\mu\nu}$ while the hidden one as $G_{\mu\nu}$. The kinetic mixing parameter is induced at one-loop level and scales as:

$$\chi \sim \frac{g_{\text{vis}}g_{\text{hid}}}{16\pi^2} = \frac{g_s}{16\pi^2} \simeq 10^{-3}. \quad (4.14)$$

After diagonalising the gauge kinetic terms in (4.13) via $G_{\mu\nu} = G'_{\mu\nu} + \chi F_{\mu\nu}$, a_{ALP} acquires a coupling to ordinary photons of the form:

$$\mathcal{L} \supset -\frac{\chi^2 a_{ALP}}{4M_{\text{hid}}}F_{\mu\nu}\tilde{F}^{\mu\nu} \quad \Leftrightarrow \quad M \simeq \frac{M_{\text{hid}}}{\chi^2} \gg M_{\text{hid}}. \quad (4.15)$$

Given that $M \gg M_{\text{hid}}$, a_{ALP} can be a hidden sector open string axion only in case (4.11) where the scale of the coupling to hidden photons of order $M_{\text{hid}} \sim 10^6$ GeV is enhanced via $U(1)$ kinetic mixing to $M \sim 10^{12}$ GeV for the coupling to ordinary photons.

- **DM as a local closed string axion fixed by poly-instanton effects:** In order to produce a monochromatic 3.5 keV line, the DM mass has to be around $m_{\text{DM}} \sim 7$ keV. Such a light DM particle can be a sterile neutrino realised as an open string mode belonging to either the visible or the hidden sector. However we shall focus on a more model-independent realisation of the decaying DM particle as a closed string axion. A generic feature of any 4D string model where the moduli are stabilised by perturbative effects, is the presence of very light axions whose mass is exponentially suppressed with respect to the gravitino mass [63]. Thus closed string axions are perfect candidates for ultra-light DM particles. In LVS models, there are two kinds of axions which remain light:

1. Bulk closed string axion c_b since the corresponding supersymmetric partner τ_b is fixed by α' corrections to the Kähler potential K . This axionic mode develops a tiny mass only via T_b -dependent non-perturbative con-

tributions to the superpotential W : $m_{c_b} \sim m_{\tau_b} e^{-\pi\tau_b} \ll m_{\tau_b} \sim m_{3/2}/\sqrt{\mathcal{V}}$.

2. Local closed string axion c_p whose associated modulus τ_p is stabilised by g_s loop corrections to K . This can happen for so-called ‘Wilson divisors’ D_p which are rigid, i.e. $h^{2,0}(D_p) = 0$, with a Wilson line, i.e. $h^{1,0}(D_p) = 1$ [195]. Under these topological conditions, an ED3-instanton wrapping such a divisor does not lead to a standard non-perturbative contribution to W but it generates a non-perturbative correction to another ED3-instanton wrapping a different rigid divisor τ_s . This gives rise to poly-instanton corrections to W of the form [194]:

$$W_{\text{np}} = A_s e^{-2\pi(T_s + A_p e^{-2\pi T_p})} \simeq A_s e^{-2\pi T_s} - 2\pi A_s A_p e^{-2\pi T_s} e^{-2\pi T_p}. \quad (4.16)$$

In LVS models, the blow-up mode τ_s is fixed by the dominant non-perturbative correction in (4.16) since the leading loop contribution to the scalar potential is vanishing due to the ‘extended no-scale’ structure [41]. Thus the corresponding axion c_s becomes too heavy to play the rôle of a_{DM} since it acquires a mass of the same order of magnitude: $m_{\tau_s} \sim m_{c_s} \sim m_{3/2}$. On the other hand, the T_p -dependent non-perturbative correction in (4.16) has a double exponential suppression, and so τ_p gets frozen by perturbative g_s effects [39, 40]. Given that c_p enjoys a shift symmetry which is broken only at non-perturbative level, this axion receives a potential only due to tiny poly-instanton contributions to W which make it much lighter than τ_p . Hence c_p is a natural candidate for a_{DM} since $m_{c_p} \sim m_{\tau_p} e^{-\pi\tau_p/2} \ll m_{\tau_p} \sim m_{3/2}$. Notice that the presence of a ‘Wilson divisors’ τ_p would modify the volume form (4.12) to [195]:

$$\mathcal{V} = \tau_b^{3/2} - \tau_s^{3/2} - (\tau_s + \tau_p)^{3/2} - \tau_{q_1}^{3/2} - \tau_{q_2}^{3/2}. \quad (4.17)$$

- **DM to ALP decay induced by non-perturbative effects in K :** A DM to ALP coupling controlled by the scale Λ of the form shown in (4.1) can arise from the kinetic mixing between a closed string DM axion and an open string ALP. Given that the kinetic terms are determined by the Kähler potential, a kinetic mixing effect can be induced by non-perturbative corrections to the

Kähler metric for matter fields which we assume to take the form:⁴

$$K_{\text{np}} \supset B_i e^{-b_i \tau_i} \cos(b_i c_i) C \bar{C}, \quad (4.18)$$

where $i = b$ if a_{DM} is a bulk closed string axion or $i = p$ if a_{DM} is a local closed string axion fixed by poly-instanton effects. As we shall show in Sec. 4.3.3 after performing a proper canonical normalisation of both axion fields, the resulting scale which controls the DM-ALP coupling is given by:

$$\Lambda \sim \begin{cases} \frac{e^{b_b \tau_b}}{B_b \mathcal{V}^{4/3}} M_p \sim \frac{e^{b_b \mathcal{V}^{2/3}}}{B_b \mathcal{V}^{4/3}} M_p \gg M_p & \text{for } a_{\text{DM}} = c_b \\ \frac{e^{b_p \tau_p}}{B_p \mathcal{V}^{7/6}} M_p \sim \frac{M_p}{B_p \mathcal{V}^{7/6 - \kappa/N}} & \text{for } a_{\text{DM}} = c_p \end{cases} \quad (4.19)$$

where $b_p = 2\pi/N$, $\kappa = \tau_p/\tau_s$ and we have approximated $\mathcal{V} \sim \tau_b^{3/2} \sim e^{2\pi\tau_s}$. From (4.19) it is clear that Λ can be around the GUT/Planck scale only if the DM particle is a local closed string axion stabilised by tiny poly-instanton corrections to W which can give it a small mass of order $m_{\text{DM}} \sim 7$ keV.

4.1.3 Calabi-Yau threefold

As explained in Sec. 4.1.2, the minimal setup which can yield a viable microscopic realisation of the $a_{\text{DM}} \rightarrow a_{\text{ALP}} \rightarrow \gamma$ model for the 3.5 keV line of [180], is characterised by a Calabi-Yau with $h^{1,1} = 5$ Kähler moduli and a volume of the form (4.17). A concrete Calabi-Yau threefold built via toric geometry which reproduces the volume form (4.17) for $h^{1,1} = 4$ (setting either $\tau_{q_1} = 0$ or $\tau_{q_2} = 0$) is given by example C of [195]. We therefore assume the existence of a Calabi-Yau threefold X with one large divisor controlling the overall volume D_b , three del Pezzo surfaces, D_s , D_{q_1} and D_{q_2} and a ‘Wilson divisor’ D_p .

We expand the Kähler form J in a basis of Poincaré dual two-forms as $J = t_b \hat{D}_b - t_s \hat{D}_s - t_{q_1} \hat{D}_{q_1} - t_{q_2} \hat{D}_{q_2} - t_p \hat{D}_p$, where the t_i ’s are two-cycle volumes and we took a minus sign for the rigid divisors so that the corresponding t_i ’s are positive.

⁴Similar non-perturbative corrections to K induced by ED1-instantons wrapped around two-cycles have been computed for type I vacua in [214] and for type IIB vacua in [215], while similar non-perturbative effects in K from an ED3-instanton wrapped around the K3 divisor in type I’ string theory, i.e. type IIB compactified on $K3 \times T^2/\mathbb{Z}_2$, have been derived in [216].

The Calabi-Yau volume then looks like:

$$\mathcal{V} = \frac{1}{6} \int_X J \wedge J \wedge J = \frac{1}{6} [k_{bbb} t_b^3 - k_{sss} (t_s + \lambda t_p)^3 - \mu t_p^3 - k_{q_1 q_1 q_1} t_{q_1}^3 - k_{q_2 q_2 q_2} t_{q_2}^3], \quad (4.20)$$

where the coefficients λ and μ are determined by the triple intersection numbers $k_{ijk} = \int_X \hat{D}_i \wedge \hat{D}_j \wedge \hat{D}_k$ as:

$$\lambda = \frac{k_{ssp}}{k_{sss}} = \frac{k_{spp}}{k_{ssp}} \quad \text{and} \quad \mu = k_{ppp} - \frac{k_{ssp}^3}{k_{sss}^2}.$$

The volume of the curve resulting from the intersection of the del Pezzo divisor D_s with the Wilson surface D_p is given by:

$$\text{Vol}(D_s \cap D_p) = \int_X J \wedge \hat{D}_s \wedge \hat{D}_p = -(k_{ssp} t_s + k_{spp} t_p) = -k_{ssp} (t_s + \lambda t_p). \quad (4.21)$$

The volume of this curve is positive and the signature of the matrix $\frac{\partial^2 \mathcal{V}}{\partial t_i \partial t_j}$ is guaranteed to be $(1, h^{1,1} - 1)$ (so with 1 positive and 4 negative eigenvalues) [217] if $k_{ssp} < 0$ while all the other intersection numbers are positive and $t_s + \lambda t_p > 0$.⁵ The four-cycle moduli can be computed as:

$$\tau_i = \frac{1}{2} \int_X J \wedge J \wedge \hat{D}_i, \quad (4.22)$$

and so they become:

$$\begin{aligned} \tau_b &= \frac{1}{2} k_{bbb} t_b^2, & \tau_{q_1} &= \frac{1}{2} k_{q_1 q_1 q_1} t_{q_1}^2, & \tau_{q_2} &= \frac{1}{2} k_{q_2 q_2 q_2} t_{q_2}^2, \\ \tau_s &= \frac{1}{2} (k_{sss} t_s^2 + k_{spp} t_p^2 + 2k_{ssp} t_s t_p) = \frac{1}{2} k_{sss} (t_s + \lambda t_p)^2, \\ \tau_p &= \frac{1}{2} (k_{ppp} t_p^2 + k_{ssp} t_s^2 + 2k_{spp} t_s t_p) = \frac{1}{2} k_{ssp} (t_s + \lambda t_p)^2 + \frac{1}{2} \mu t_p^2. \end{aligned} \quad (4.23)$$

The overall volume (4.20) can therefore be rewritten in terms of the four-cycle moduli as:

$$\mathcal{V} = \lambda_b \tau_b^{3/2} - \lambda_s \tau_s^{3/2} - \lambda_p (\tau_p + x \tau_s)^{3/2} - \lambda_{q_1} \tau_{q_1}^{3/2} - \lambda_{q_2} \tau_{q_2}^{3/2}, \quad (4.24)$$

where:

$$\lambda_i = \frac{1}{3} \sqrt{\frac{2}{k_{iii}}}, \quad \forall i = b, s, q_1, q_2, \quad \lambda_p = \frac{1}{3} \sqrt{\frac{2}{\mu}} \quad \text{and} \quad x = -\frac{k_{ssp}}{k_{sss}} > 0.$$

⁵This analysis includes example C of [195] where $k_{sss} = k_{spp} = -k_{ssp} = 9$ and $k_{ppp} = 0$.

Notice that (4.24) reproduces exactly the volume form (4.17).

4.1.4 Brane set-up and fluxes

As explained in Sec. 4.1.2, a_{ALP} can be realised as an open string axion belonging either to the visible sector or to a hidden sector. In the first case the two rigid divisors D_{q_1} and D_{q_2} are exchanged by a proper orientifold involution whereas in the second case they are invariant. As we shall see more in detail in Sec. 4.2.1, these two blow-up modes shrink down to zero size due to D-term stabilisation and support a stack of D3-branes at the resulting singularity.

Full moduli stabilisation requires the presence of non-perturbative corrections to the superpotential. We shall therefore consider an ED3-instanton wrapped around the ‘small’ rigid divisor D_s which generates a standard non-perturbative contribution to W , together with another ED3-instanton wrapped around the Wilson surface D_p which gives rise to poly-instanton effects. In order to make τ_p heavier than the DM axion c_p , we need also to include a D7-stack that generates τ_p -dependent string loop corrections to the Kähler potential. This can be achieved if a stack of D7-branes wraps the divisor D_{D7} (which we assume to be smooth and connected) given by:

$$D_{D7} = m_s D_s + m_p D_p, \quad \text{with } m_s, m_p \in \mathbb{Z}. \quad (4.25)$$

In what follows we shall assume the existence of a suitable orientifold involution and O7-planes which allow the presence of such a D7-stack in a way compatible with D7-tadpole cancellation. The cancellation of Freed-Witten anomalies requires to turn on half-integer world-volume fluxes on the instantons and the D7-stack of the form [98]:

$$F_{D7} = f_s \hat{D}_s + f_p \hat{D}_p + \frac{1}{2} \hat{D}_{D7}, \quad F_s = \frac{1}{2} \hat{D}_s, \quad F_p = \frac{1}{2} \hat{D}_p, \quad (4.26)$$

with $f_s, f_p \in \mathbb{Z}$. In order to guarantee a non-vanishing contribution to W , the total flux $\mathcal{F}_j = F_j - \iota_j^* B$ (with $\iota_j^* B$ the pull-back of the NSNS B -field on D_j) on both instantons has to be zero: $\mathcal{F}_s = \mathcal{F}_p = 0$. This can be achieved if the B -field is chosen such that:

$$B = \frac{1}{2} \hat{D}_s + \frac{1}{2} \hat{D}_p, \quad (4.27)$$

and the pull-back of $\hat{D}_s/2$ on D_p and of $\hat{D}_p/2$ on D_s are both integer forms since in this case we can always turn on integer flux quanta to cancel their contribution to the total gauge flux. This is indeed the case if, for an arbitrary integer form

$\omega = \omega_i \hat{D}_i \in H^2(\mathbb{Z}, X)$ with $\omega_i \in \mathbb{Z}$, we have that:

$$\frac{1}{2} \int_X \hat{D}_s \wedge \hat{D}_p \wedge \omega = \frac{1}{2} (k_{ssp} \omega_s + k_{spp} \omega_p) \in \mathbb{Z}. \quad (4.28)$$

This condition can be easily satisfied if both k_{ssp} and k_{spp} are even.

The total gauge flux on the D7-stack instead becomes:

$$\mathcal{F}_{D7} = f_s \hat{D}_s + f_p \hat{D}_p + \frac{1}{2} (m_s - 1) \hat{D}_s + \frac{1}{2} (m_p - 1) \hat{D}_p = f_s \hat{D}_s + f_p \hat{D}_p,$$

where without loss of generality, we have chosen $m_s = m_p = 1$ so that \mathcal{F}_{D7} is an integer flux. The presence of this flux has several implications:

- The blow-up moduli T_s and T_p get charged under the diagonal $U(1)$ of the D7-stack with charges:

$$q_i = \int_X \mathcal{F}_{D7} \wedge \hat{D}_{D7} \wedge \hat{D}_i = f_s (k_{ssi} + k_{spi}) + f_p (k_{spi} + k_{ppi}), \quad i = s, p, \quad (4.29)$$

which implies $q_p = \mu f_p - x q_s$.

- The coupling constant of the gauge theory living on D_{D7} acquires a flux-dependent shift of the form:

$$g_{D7}^{-2} = \tau_s + \tau_p - h(\mathcal{F}_{D7}) \text{Re}(S), \quad (4.30)$$

where $\text{Re}(S) = e^{-\varphi} = g_s^{-1}$ is the real part of the axio-dilaton while the flux-dependent shift reads:

$$h(\mathcal{F}_{D7}) = \frac{1}{2} \int_X \mathcal{F}_{D7} \wedge \mathcal{F}_{D7} \wedge \hat{D}_{D7} = \frac{f_s}{2} q_s + \frac{f_p}{2} q_p. \quad (4.31)$$

- \mathcal{F}_{D7} generates a moduli-dependent FI-term which looks like:

$$\xi_{D7} = \frac{1}{4\pi \mathcal{V}} \int_X J \wedge \mathcal{F}_{D7} \wedge \hat{D}_{D7} = \frac{1}{4\pi \mathcal{V}} (q_s t_s + q_p t_p). \quad (4.32)$$

- A non-vanishing gauge flux on D_{D7} might induce chiral intersections between the D7 stack and the instantons on D_s and D_p . Their net number is counted by the moduli $U(1)$ -charges as:

$$I_{D7-E3} = \int_X \mathcal{F}_{D7} \wedge \hat{D}_{D7} \wedge \hat{D}_s = q_s, \quad I_{D7\text{-poly}} = \int_X \mathcal{F}_{D7} \wedge \hat{D}_{D7} \wedge \hat{D}_p = q_p. \quad (4.33)$$

The relations (4.33) imply that, whenever an instanton has a non-vanishing chiral intersection with a stack of D-branes, the four-cycle modulus T_{inst} wrapped by the instanton gets charged under the diagonal $U(1)$ on the D-brane stack. Therefore a non-perturbative contribution to the superpotential of the form $W_{\text{np}} \supset e^{-T_{\text{inst}}}$ would not be gauge invariant. Thus a proper combination of $U(1)$ -charged matter fields ϕ_i has to appear in the prefactor in order to make the whole contribution gauge invariant: $W_{\text{np}} \supset \prod_i \phi_i e^{-T_{\text{inst}}}$. If however the ϕ_i are visible sector matter fields, they have to develop a vanishing VEV in order not to break any Standard Model gauge group at high energies [50]. In our case the absence of chiral intersections between the instantons on D_s and D_p and the visible sector is guaranteed by the structure of the intersection numbers since $k_{sq_i j} = 0$ and $k_{pq_i j} = 0 \forall j$ for either $i = 1$ or $i = 2$.

On the other hand, as can be seen from (4.33), there are chiral intersections between the hidden D7-stack on D_{D7} and the two instantons on D_s and D_p . We could kill both of these intersections by setting $\mathcal{F}_{D7} = 0$. However this choice of the gauge flux on D_{D7} would also set to zero the FI-term in (4.32) which is instead crucial to make τ_p heavier than the DM axion c_p . We shall therefore perform a choice of the gauge flux \mathcal{F}_{D7} which sets $I_{D7-E3} = q_s = 0$ but leaves $I_{D7\text{-poly}} = q_p \neq 0$ so that ξ_{D7} can develop a non-trivial dependence on τ_p . This can take place if the flux quanta f_p and f_s are chosen such that:

$$f_p = -\frac{k_{sss} + k_{ssp}}{k_{ssp} + k_{spp}} f_s \quad \Leftrightarrow \quad q_s = 0 \quad \text{and} \quad q_p = \mu f_p. \quad (4.34)$$

The FI-term in (4.32) then becomes:

$$\xi_{D7} = \frac{q_p}{4\pi} \frac{t_p}{\mathcal{V}} = \frac{f_p \sqrt{2\mu}}{4\pi} \frac{\sqrt{\tau_p + x\tau_s}}{\mathcal{V}}, \quad (4.35)$$

while the shift of the gauge coupling in (4.31) simplifies to $h(\mathcal{F}_{D7}) = \frac{\mu}{2} f_p^2$. Due to non-zero chiral intersections between the D7-stack and the divisor D_p , the poly-instanton contribution to the superpotential comes with a prefactor that depends on a $U(1)$ -charged matter field ϕ . In Sec. 4.2.1 we will show that the interplay between D-terms and string loop effects can fix ϕ at a non-zero VEV, so that the poly-instanton correction is non-vanishing. Notice that ϕ belongs to a hidden sector, and so it can safely develop a non-zero VEV at high energies without violating any phenomenological requirement.

4.1.5 Low-energy 4D theory

Type IIB string theory compactified on an orientifold of the Calabi-Yau threefold described in Sec. 4.1.3 with the brane setup and gauge fluxes of Sec. 4.1.4 gives rise to an $N = 1$ 4D supergravity effective field theory characterised by a Kähler potential K and a superpotential W of the form:

$$K = K_{\text{mod}} + K_{\text{matter}} \quad \text{and} \quad W = W_{\text{tree}} + W_{\text{np}}, \quad (4.36)$$

where:

- The moduli Kähler potential receives perturbative α' and g_s corrections beyond the tree-level approximation:

$$K_{\text{mod}} = K_{\text{tree}} + K_{\alpha'} + K_{g_s}, \quad (4.37)$$

with:

$$K_{\text{tree}} = -2 \ln \mathcal{V} + \frac{\tau_{q_1}^2}{\mathcal{V}} + \frac{\tau_{q_2}^2}{\mathcal{V}}, \quad K_{\alpha'} = -\frac{\zeta}{g_s^{3/2} \mathcal{V}}, \quad K_{g_s} = g_s \sum_i \frac{C_i^{\text{KK}} t_i^\perp}{\mathcal{V}}. \quad (4.38)$$

In (4.38) we neglected the tree-level Kähler potential for the dilaton $S = e^{-\varphi} - i C_0$ and the complex structure moduli U_{a_-} , $a_- = 1, \dots, h_-^{1,2}$ and we expanded the effective theory around the singularities obtained by collapsing the two blow-up modes τ_{q_1} and τ_{q_2} (hence the volume \mathcal{V} in (4.38) should be thought of as (4.24) with $\tau_{q_1} = \tau_{q_2} = 0$). Moreover, we included only the leading order α' correction which depends on $\zeta = -\frac{\zeta(3)\chi(X)}{2(2\pi)^3}$ [36] since in the large volume limit higher derivative α' effects yield just subdominant contributions [75]. Finally in K_{g_s} we considered only string loop corrections arising from the exchange of Kaluza-Klein modes between non-intersecting stacks of D-branes and O-planes (C_i^{KK} are complex structure dependent coefficients and t_i^\perp is the two-cycle controlling the distance between two parallel stacks of D-branes/O-planes) while we did not introduce any g_s effects coming from the exchange of winding modes since these arise only in the presence of intersections between D-branes which are however absent in our setup [41, 39, 40].

- In the matter Kähler potential we focus just on the dependence on the matter fields which will develop a non-zero VEV. These are two $U(1)$ -charged matter fields: $\phi = |\phi| e^{i\psi}$ which belongs to the hidden D7-stack on D_{D7} and $C = |C| e^{i\theta}$ which can be either a visible sector gauge singlet (if D_{q_1} and D_{q_2} are exchanged by the orientifold involution) or a hidden sector field (if both D_{q_1} and D_{q_2} are

invariant under the orientifold involution) living on a D3-brane stack [218, 219]:

$$K_{\text{matter}} = \frac{\phi\bar{\phi}}{\text{Re}(S)} + \tilde{K}(T_i, \bar{T}_i) C\bar{C}. \quad (4.39)$$

In (4.39) we wrote down just the tree-level Kähler metric for ϕ while we shall consider both perturbative and non-perturbative corrections to the Kähler metric for C which we assume to take the form:

$$\tilde{K}(T_i, \bar{T}_i) = \frac{f(S, U)}{\mathcal{V}^{2/3}} + \tilde{K}_{\text{pert}} + B_i e^{-b_i\tau_i} \cos(b_i c_i) \quad \text{with } i = b, p, \quad (4.40)$$

where $f(S, U)$ is an undetermined function of the dilaton and complex structure moduli, \tilde{K}_{pert} represents perturbative corrections which do not depend on the axionic fields because of their shift symmetry and the last term is a non-perturbative correction which can in principle depend on either the large or the poly-instanton cycle. This term induces a kinetic mixing between the open string axion θ and either of the two ultra-light closed string axions c_b and c_p . As we shall see in Sec. 4.2.1, the open string axion ψ gets eaten up by the anomalous $U(1)$ on the D7-stack, and so light closed string axions cannot decay to this heavy mode. This is the reason why we did not include any non-perturbative effect in the Kähler metric for ϕ .

- The tree-level superpotential $W_{\text{tree}} = \int_X G_3 \wedge \Omega$, with Ω the Calabi-Yau $(3, 0)$ -form, is generated by turning on background three-form fluxes $G_3 = F_3 - iSH_3$ and depends just on the dilaton and the U -moduli but not on the T -moduli [35].
- The non-perturbative superpotential receives a single contribution from the ED3-instanton wrapped around D_s together with poly-instanton effects from the ED3-instanton wrapped around the Wilson surface D_p and takes the same form as (4.16):

$$W_{\text{np}} = A_s e^{-2\pi T_s} - 2\pi A_s A_p e^{-2\pi T_s} e^{-2\pi T_p}. \quad (4.41)$$

The prefactors A_s and A_p depend on S and U -moduli. Given that T_p is charged under the anomalous diagonal $U(1)$ on the D7-stack, A_p has to depend also on the charged matter field ϕ in order to make W_{np} gauge invariant. If we make the dependence of A_p on ϕ explicit by replacing $A_p \rightarrow A_p \phi^n$ with arbitrary n ,

and we use the fact that ϕ and T_p behave under a $U(1)$ transformation as:

$$\delta\phi = i q_\phi \phi \quad \text{and} \quad \delta T_p = i \frac{q_p}{2\pi}, \quad (4.42)$$

the variation of W_{np} under a $U(1)$ transformation becomes:

$$\delta W_{\text{np}} = W_{\text{np}} \left(n \frac{\delta\phi}{\phi} - 2\pi\delta T_p \right) = i W_{\text{np}} (n q_\phi - q_p). \quad (4.43)$$

Hence W is gauge invariant only if $n = q_p/q_\phi$. Notice that $n > 0$ since, as we shall see in Sec. 4.2.1, a consistent D-term stabilisation can yield a non-zero VEV for ϕ only if q_ϕ and q_p have the same sign.

4.2 Moduli stabilisation

In this section we shall show how to stabilise all closed string moduli together with the two charged open string modes ϕ and C . The total $N = 1$ supergravity scalar potential descending from the K and W described in Sec. 4.1.5, includes both F- and D-term contributions of the form:

$$V = V_F + V_D = e^K \left(K^{I\bar{J}} D_I W D_{\bar{J}} \bar{W} - 3|W|^2 \right) + \frac{g_{D7}^2}{2} D_{D7}^2 + \frac{g_{D3}^2}{2} D_{D3}^2, \quad (4.44)$$

where the Kähler covariant derivative is $D_I W = \partial_I W + W \partial_I K$, the gauge coupling of the field theory living on the D7-stack is given by (4.30) while $g_{D3}^{-2} = \text{Re}(S)$ for the quiver gauge theory on the D3-stack. The two D-term contributions look like:

$$D_{D7} = q_\phi \phi \frac{\partial K}{\partial \phi} - \xi_{D7}, \quad \text{and} \quad D_{D3} = q_C C \frac{\partial K}{\partial C} - \xi_{D3}, \quad (4.45)$$

where the FI-term for the D7-stack is given by (4.35) whereas the FI-term for the D3-brane stack is:

$$\xi_{D3} = q_i \frac{\partial K}{\partial T_{q_i}} = q_i \frac{\tau_{q_i}}{\mathcal{V}} \quad \text{for either } i = 1 \text{ or } i = 2. \quad (4.46)$$

In LVS models the Calabi-Yau volume is exponentially large in string units, and so $1/\mathcal{V} \ll 1$ is a small parameter which can be used to control the relative strength of different contributions to the total scalar potential (4.44). Let us analyse each of these contributions separately.

4.2.1 Stabilisation at $\mathcal{O}(1/\mathcal{V}^2)$

As can be seen from the volume scaling of the two FI-terms (4.35) and (4.46), the total D-term potential scales as $V_D \sim M_p^4/\mathcal{V}^2 \sim M_s^4$. Therefore its leading order contribution has to be vanishing since otherwise the effective field theory would not be under control since the scalar potential would be of order the string scale. As we shall see in more detail below, this leading order supersymmetric stabilisation fixes $|\phi|$ in terms of $\tilde{\tau}_p \equiv \tau_p + x\tau_s$ and τ_{q_i} in terms of $|C|$. The open string axion ψ and the closed string axion c_{q_i} are eaten up by the two anomalous $U(1)$'s living respectively on the D7 and D3-stack. Additional $\mathcal{O}(1/\mathcal{V}^2)$ tree-level contributions to the scalar potential arise from background fluxes which stabilise the dilaton and the complex structure moduli in a supersymmetric manner at $D_S W_{\text{tree}} = D_{U_a} W_{\text{tree}} = 0$ [35]. At this level of approximation the Kähler moduli are still flat due to the no-scale cancellation. They can be lifted by subdominant corrections to the effective action which can be studied by assuming a constant tree-level superpotential $W_0 = \langle W_{\text{tree}} \rangle$ that is naturally of $\mathcal{O}(1)$. Summarising the total $\mathcal{O}(1/\mathcal{V}^2)$ contribution to the scalar potential looks schematically like (we show the dependence just on the scalar fields which get frozen):

$$V_{\mathcal{O}(1/\mathcal{V}^2)} = V_D(|\phi|, \tau_{q_i}) + V_F^{\text{tree}}(S, U). \quad (4.47)$$

Let us focus in particular on the dynamics of the total D-term potential which from (4.35), (4.44) and (4.46) reads:

$$V_D = \frac{g_{D7}^2}{2} \left(q_\phi \frac{|\phi|^2}{\text{Re}(S)} - \frac{f_p \sqrt{2\mu}}{4\pi} \frac{\sqrt{\tilde{\tau}_p}}{\mathcal{V}} \right)^2 + \frac{g_{D3}^2}{2} \left(q_C \tilde{K}(T_i, \bar{T}_i) |C|^2 - q_i \frac{\tau_{q_i}}{\mathcal{V}} \right)^2. \quad (4.48)$$

Supersymmetry is preserved if:

$$q_\phi \frac{|\phi|^2}{\text{Re}(S)} = \frac{f_p \sqrt{2\mu}}{4\pi} \frac{\sqrt{\tilde{\tau}_p}}{\mathcal{V}} \quad \text{and} \quad q_C \tilde{K}(T_i, \bar{T}_i) |C|^2 = q_i \frac{\tau_{q_i}}{\mathcal{V}}. \quad (4.49)$$

These two relations fix one direction in the $(|\phi|, \tilde{\tau}_p)$ -plane and one direction in the $(|C|, \tau_{q_i})$ -plane. Each of these two directions corresponds to the supersymmetric partner of the axion which is eaten up by the relative anomalous $U(1)$ gauge boson in the process of anomaly cancellation. The axions which become the longitudinal components of the massive gauge bosons are combinations of open string axions with decay constant f_{op} and closed string axions with decay constant f_{cl} . The Stückelberg mass of the anomalous $U(1)$'s scales as [220]:

$$M_{U(1)}^2 \simeq g^2 (f_{\text{op}}^2 + f_{\text{cl}}^2), \quad (4.50)$$

where:

$$\begin{aligned}
\text{D7 case: } f_{\text{op}}^2 &= \frac{|\phi|^2}{\text{Re}(S)} = \frac{f_p \sqrt{2\mu}}{4\pi q_\phi} \frac{\sqrt{\tilde{\tau}_p}}{\mathcal{V}} \gg f_{\text{cl}}^2 = \frac{1}{4} \frac{\partial^2 K}{\partial \tau_p^2} = \frac{1}{4\sqrt{2\mu}} \frac{1}{\mathcal{V} \sqrt{\tilde{\tau}_p}}, \\
\text{D3 case: } f_{\text{op}}^2 &= \tilde{K}(T_i, \bar{T}_i) |C|^2 = \frac{q_i}{q_c} \frac{\tau_{q_i}}{\mathcal{V}} \ll f_{\text{cl}}^2 = \frac{1}{4} \frac{\partial^2 K}{\partial \tau_{q_i}^2} = \frac{1}{2\mathcal{V}}, \tag{4.51}
\end{aligned}$$

for:

$$\tilde{\tau}_p \gg z_p \equiv \frac{\pi q_\phi}{2\mu f_p} \quad \text{and} \quad \tau_{q_i} \ll z_{q_i} \equiv \frac{q_c}{2q_i}. \tag{4.52}$$

In Sec. 4.2.2 and 4.2.3 we shall explain how to fix the remaining flat directions, showing that the conditions in (4.52) can be satisfied dynamically. These conditions imply that for the D7 case the combination of axions eaten up is mostly given by the open string axion ψ , and so (4.49) should be read off as fixing $|\phi|$ in terms of $\tilde{\tau}_p$, while for the D3 brane case the combination of axions eaten up is mostly given by the closed string axion c_{q_i} which means that (4.49) fixes τ_{q_i} in terms of $|C|$. Notice that from (4.52) the $U(1)$ gauge bosons acquire a mass of order the string scale: $M_{U(1)} \sim M_p/\sqrt{\mathcal{V}} \sim M_s$.

4.2.2 Stabilisation at $\mathcal{O}(1/\mathcal{V}^3)$

As we shall explain more in detail below, $\mathcal{O}(1/\mathcal{V}^3)$ effects arise from both the leading α' and $\tilde{\tau}_p$ -dependent g_s corrections to K in (4.38) together with the single instanton contribution in (4.41). They give rise to a scalar potential which depends on τ_s, c_s, τ_p and τ_b but not on the associated axions c_p and c_b since both T_p - and T_b -dependent non-perturbative corrections to W are much more suppressed due to the double exponential suppression of poly-instanton effects and the exponentially large value of $\tau_b \sim \mathcal{V}^{2/3}$. These $\mathcal{O}(1/\mathcal{V}^3)$ contributions alone would yield an AdS minimum which breaks supersymmetry spontaneously [43, 44, 42]. Additional contributions of the same order of magnitude can arise rather naturally from a hidden D7 T-brane stack [92] or from anti-D3 branes at the tip of a warped throat [88, 90, 91] and can be tuned to obtain a dS vacuum. The Kähler moduli develop non-zero F-terms and mediate supersymmetry breaking to each open string sector via gravitational interactions. Matter fields on the D7-stack are unsequestered, and so acquire soft masses of order $m_{3/2}$. After using the vanishing D-term condition to write $|\phi|$ in terms of $\tilde{\tau}_p$, the resulting F-term potential for the matter fields also scales as $\mathcal{O}(1/\mathcal{V}^3)$. Thus the full $\mathcal{O}(1/\mathcal{V}^3)$ scalar potential behaves as:

$$V_{\mathcal{O}(1/\mathcal{V}^3)} = V_F^{\alpha'}(\mathcal{V}) + V_F^{g_s}(\mathcal{V}, \tilde{\tau}_p) + V_F^{E3}(\tau_s, c_s, \mathcal{V}) + V_F^{\text{matter}}(\mathcal{V}, \tilde{\tau}_p) + V_{\text{up}}(\mathcal{V}). \tag{4.53}$$

All these $\mathcal{O}(1/\mathcal{V}^3)$ contributions take the following precise form:

$$\begin{aligned}
V_F^{\alpha'}(\mathcal{V}) &= \frac{3\zeta}{32\pi\sqrt{g_s}} \frac{W_0^2}{\mathcal{V}^3}, & V_F^{g_s}(\mathcal{V}, \tilde{\tau}_p) &= \frac{3g_s\lambda_p}{64\pi} (g_s C_p^{\text{KKK}})^2 \frac{W_0^2}{\mathcal{V}^3\sqrt{\tilde{\tau}_p}}, \\
V_F^{E3}(\tau_s, c_s, \mathcal{V}) &= \frac{4g_s\pi A_s^2}{3\lambda_s} \frac{\sqrt{\tau_s} e^{-4\pi\tau_s}}{\mathcal{V}} + g_s A_s \cos(2\pi c_s) \frac{W_0\tau_s e^{-2\pi\tau_s}}{\mathcal{V}^2}, \\
V_F^{\text{matter}}(\mathcal{V}, \tilde{\tau}_p) &= m_{3/2}^2 \frac{|\phi|^2}{\text{Re}(S)} = \frac{3g_s\lambda_p}{64\pi z_p} \frac{W_0^2\sqrt{\tilde{\tau}_p}}{\mathcal{V}^3},
\end{aligned} \tag{4.54}$$

where the string loop potential includes only the leading Kaluza-Klein contribution from K_{g_s} in (4.38) which is given by [41]:

$$V_F^{g_s}(\mathcal{V}, \tilde{\tau}_p) = \left(\frac{g_s}{8\pi}\right) (g_s C_p^{\text{KKK}})^2 \frac{W_0^2}{\mathcal{V}^2} \frac{\partial^2 K}{\partial \tau_p^2},$$

and in V_F^{matter} we substituted the relation (4.49) which expresses $|\phi|$ in terms of $\tilde{\tau}_p$. Summing up the four contributions in (4.54), the total scalar potential at $\mathcal{O}(1/\mathcal{V}^3)$ has a minimum at (for $2\pi\tau_s \gg 1$):

$$\begin{aligned}
c_s &= k + \frac{1}{2} \quad \text{with } k \in \mathbb{Z}, & \mathcal{V} &= \frac{3\lambda_s}{8\pi A_s} W_0 \sqrt{\tau_s} e^{2\pi\tau_s}, \\
\tau_s &= \left(\frac{\zeta}{2\lambda_s}\right)^{2/3} \frac{1}{g_s} (1 + \epsilon) \sim \frac{1}{g_s}, & \tilde{\tau}_p &= z_p (g_s C_p^{\text{KKK}})^2 \sim \frac{1}{g_s},
\end{aligned} \tag{4.55}$$

for $C_p^{\text{KKK}} \sim g_s^{-3/2} \gg 1$ and:

$$\epsilon = \left(\frac{2\lambda_p}{3\zeta z_p}\right) g_s^{3/2} \sqrt{\tilde{\tau}_p} \sim g_s^{5/2} C_p^{\text{KKK}} \sim g_s \ll 1. \tag{4.56}$$

Notice that the condition $\tilde{\tau}_p \gg z_p$ in (4.52), which ensures that the closed string axion c_p is not eaten up by the anomalous $U(1)$ on the D7-stack and so can play the rôle of DM, can be easily satisfied if $C_p^{\text{KKK}} \sim g_s^{-3/2} \gg 1$. We point out that the coefficients of the string loop corrections are complex structure moduli dependent, and so their values can be tuned by appropriate choices of background fluxes. Therefore for $z_p \sim \mathcal{O}(1)$, $\tilde{\tau}_p \sim \tau_s \sim \tau_p \sim g_s^{-1} \gg 1$. This behaviour justifies also the scaling of the small parameter ϵ in (4.56).

As stressed above, this minimum is AdS but can be uplifted to dS via several different positive definite contributions. Two examples which emerge rather naturally in type IIB flux compactifications are T-branes [92] or anti-D3 branes [88, 90, 91].

4.2.3 Stabilisation at $\mathcal{O}(1/\mathcal{V}^{3+p})$

Taking into account all contributions to the scalar potential up to $\mathcal{O}(1/\mathcal{V}^3)$, there are still four flat directions: the charged matter field $|C|$, the open string axion θ and the two closed string axions c_p and c_b . We shall now show how to stabilise the DM axion c_p and $|C|$ which sets the decay constant of the ALP θ and fixes τ_{q_i} from (4.49). The bulk closed string axion c_b receives scalar potential contributions only from T_b -dependent non-perturbative corrections, and so it is almost massless: $m_{c_b} \sim m_{\tau_b} e^{-\pi \mathcal{V}^{2/3}} \sim 0$.

The closed string axion c_p and the open string matter field $|C|$ receive a potential respectively via poly-instanton corrections to the effective action and soft supersymmetry breaking terms. As we shall see below, these terms scale as $\mathcal{O}(1/\mathcal{V}^{3+p})$ with $p > 0$. The only exception which leads to $p = 0$ is the case where flavour D7-branes desquester the open string sector on the D3-brane at a singularity. However, as shown in Sec. 4.1.2, these effects would not modify the VEV of $|C|$ which sets the open string axion decay constant, and so, without loss of generality, we shall consider just the sequestered case. The resulting $\mathcal{O}(1/\mathcal{V}^{3+p})$ scalar potential looks schematically as (showing again just the dependence on the fields which get stabilised at this order in the inverse volume expansion of V):

$$V_{\mathcal{O}(1/\mathcal{V}^{3+p})} = V_F^{\text{poly}}(c_s) + V_F^{\text{matter}}(|C|). \quad (4.57)$$

The leading order expression of the C -dependent soft supersymmetry breaking terms is given by (4.8). A more complete expression in terms of the canonically normalised field $\hat{C} = |\hat{C}| e^{i\theta} = \sqrt{\tilde{K}} C$ (see Sec. 4.3.1 for more details) is (the c_i 's are $\mathcal{O}(1)$ coefficients) [192]:

$$V_F(|\hat{C}|) = c_2 m_0^2 |\hat{C}|^2 + c_3 A |\hat{C}|^3 + c_4 \lambda |\hat{C}|^4 + \mathcal{O}(|\hat{C}|^5) + c_5 \frac{\tau_{q_i}^2}{\mathcal{V}^3} \left[1 + \mathcal{O}\left(\frac{1}{\mathcal{V}}\right) \right], \quad (4.58)$$

where the first three terms originate from expanding the F-term potential in powers of $|\hat{C}|$ up to fourth order, whereas the last term comes from the fact that the τ_{q_i} -dependent term in (4.38) breaks the no-scale structure. Using (4.49) we can rewrite the last term in (4.58) in terms of $|\hat{C}|$ and parameterising the soft terms in Planck units as $m_0 \sim \mathcal{V}^{-\alpha_2}$, $A \sim \mathcal{V}^{-\alpha_3}$ and $\lambda \sim \mathcal{V}^{-\alpha_4}$, we obtain (up to fourth order in $|\hat{C}|$):

$$V_F(|\hat{C}|) = \frac{c_2}{\mathcal{V}^{\alpha_2}} |\hat{C}|^2 + \frac{c_3}{\mathcal{V}^{\alpha_3}} |\hat{C}|^3 + \frac{k_4}{\mathcal{V}^{\alpha_4}} |\hat{C}|^4 \quad \text{with} \quad k_4 = c_4 \lambda + \frac{4c_5 z_{q_i}^2}{\mathcal{V}^{1-\alpha_4}}. \quad (4.59)$$

If the soft masses are non-tachyonic, the VEV of the matter field $|\hat{C}|$ is zero, and so the open string axion θ cannot play the rôle of the ALP a_{ALP} which gives the 3.5 keV line by converting into photons in astrophysical magnetic fields. On the other hand, as explained in Sec. 4.1.2, if $c_2 < 0$ $|\hat{C}|$ can develop a non-vanishing VEV. Open string modes living on D3-branes localised at singularities are geometrically sequestered from the sources of supersymmetry breaking in the bulk, resulting in $\alpha_3 = 2$, $\alpha_4 = 1$ and $\alpha_2 = 3/2$ or $\alpha_2 = 2$ depending on the exact moduli dependence of \tilde{K}_{pert} in (4.40) and the details of the uplifting mechanism to a dS vacuum [209, 210]. The VEVs of $|\hat{C}|$ and τ_{q_i} from (4.49) are therefore:

$$\alpha_2 = \frac{3}{2} \text{ case: } \quad |\hat{C}| = f_{a_{ALP}} = \frac{M_p}{\mathcal{V}} \quad \Leftrightarrow \quad \tau_{q_i} = \frac{2z_{q_i}}{\mathcal{V}} \ll z_{q_i}, \quad (4.60)$$

$$\alpha_2 = 2 \text{ case: } \quad |\hat{C}| = f_{a_{ALP}} = \frac{M_p}{\mathcal{V}^2} \quad \Leftrightarrow \quad \tau_{q_i} = \frac{2z_{q_i}}{\mathcal{V}^3} \ll z_{q_i}, \quad (4.61)$$

where we have identified the open string axion θ with the ALP $a_{ALP} = f_{a_{ALP}} \theta$. Notice that the ALP decay constant in (4.60) reproduces exactly the ALP coupling to gauge bosons in (4.10) while the $f_{a_{ALP}}$ in (4.61) gives the coupling in (4.11). We stress that (4.60) and (4.61) show also how the condition $\tau_{q_i} \ll z_{q_i}$ in (4.52) is easily satisfied for $1/\mathcal{V} \ll 1$. This ensures that the blow-up mode τ_{q_i} is indeed collapsed to a singularity. Let us remind the reader that i can be either $i = 2$ or $i = 3$. When τ_{q_1} and τ_{q_2} are identified by the orientifold involution, an open string axion is the standard QCD axion a_{QCD} while the other is a_{ALP} with $|\hat{C}|$ a Standard Model gauge singlet with a large VEV. On the other hand, when the two blow-up modes τ_{q_1} and τ_{q_2} are separately invariant under the involution, \hat{C} belongs to a hidden sector and, as described in Sec. 4.1.2, its axion θ has a coupling to ordinary photons of the form (4.15) which is induced by $U(1)$ kinetic mixing.

The axionic partner c_p of the Kähler modulus τ_p which controls the volume of the Wilson divisor supporting poly-instanton effects, receives the following scalar potential contributions from the second term in (4.41) with $A_p \rightarrow A_p \phi^n$ and $n = q_p/q_\phi$:

$$\begin{aligned} V_F^{\text{poly}}(c_p) &= -2g_s \pi A_s A_p \phi^n \left[\frac{8(1-x)\pi A_s}{3\lambda_s} \cos(2\pi c_p) \sqrt{\tau_s} e^{-2\pi\tau_s} \right. \\ &\quad \left. + W_0 \cos[2\pi(c_s + c_p)] \frac{((1-x)\tau_s + \tilde{\tau}_p)}{\mathcal{V}} \right] \frac{e^{-2\pi\tau_s} e^{-2\pi\tau_p}}{\mathcal{V}}, \end{aligned}$$

which, after using the first D-term relation in (4.49) and substituting the VEVs in

(4.55), reduces to (setting without loss of generality $\phi = |\phi|$ with $\psi = 0$):

$$V_F^{\text{poly}}(c_p) = \frac{A}{\mathcal{V}^{3+p}} \cos(2\pi c_p), \quad (4.62)$$

where:

$$A = \frac{3g_s \lambda_s A_p}{4} \left(\frac{3\lambda_p C_p^{\text{KK}}}{8\sqrt{z_p}} \right)^{n/2} \left(\frac{3\lambda_s \sqrt{\tau_s}}{8\pi A_s} \right)^\kappa \tilde{\tau}_p \sqrt{\tau_s} W_0^{2+\kappa},$$

with:

$$\kappa \equiv \frac{\tau_p}{\tau_s} > 0 \quad \text{and} \quad p = \frac{n}{2} + \kappa > 0. \quad (4.63)$$

Therefore the DM axion c_p is stabilised at $\mathcal{O}(1/\mathcal{V}^{3+p})$ at $c_p = 1/2 + k$ with $k \in \mathbb{Z}$ and $A > 0$.

4.3 Mass spectrum and couplings

In this section we shall first determine the expressions for all canonically normalised fields and their mass spectrum, and then we will compute the strength of the coupling of the light DM axion c_p to the open string ALP θ which is induced by non-perturbative corrections to the matter Kähler metric in (4.40).

4.3.1 Canonical normalisation

Similarly to the scalar potential, also the kinetic Lagrangian derived from the Kähler potential for the moduli given by the three terms in (4.38) and for the matter fields given by (4.39), can be organised in an expansion in $1/\mathcal{V} \ll 1$. Hence the kinetic terms can be canonically normalised order by order in this inverse volume expansion. The detailed calculation is presented in App. C.0.2 and here we just quote the main results which are useful to work out the strength of the DM-ALP coupling. The expressions for the canonically normalised fields at leading order look like (the moduli and the matter fields are dimensionless while canonically normalised scalar fields have standard mass dimensions):

$$\begin{aligned} \frac{|\hat{C}|}{M_p} &= \sqrt{2\tilde{K}}|C|, & a_{ALP} &= |\hat{C}|\theta = f_{a_{ALP}}\theta, & \frac{|\hat{\phi}|}{M_p} &= \sqrt{\frac{2}{\text{Re}(S)}}|\phi|, & \frac{\phi_{q_i}}{M_p} &= \frac{\tau_{q_i}}{\sqrt{\mathcal{V}}}, \\ \frac{\phi_b}{M_p} &= \sqrt{\frac{3}{2}} \ln \tau_b, & \frac{a_b}{M_p} &= \sqrt{\frac{3}{2}} \frac{c_b}{\tau_b}, & \frac{\phi_s}{M_p} &= \sqrt{\frac{4\lambda_s}{3\mathcal{V}}} \tau_s^{3/4}, & & \\ \frac{a_s}{M_p} &= \sqrt{\frac{3\lambda_s}{4\mathcal{V}\sqrt{\tau_s}}} c_s, & \frac{\tilde{\phi}_p}{M_p} &= \sqrt{\frac{4\lambda_p}{3\mathcal{V}}} \tilde{\tau}_p^{3/4}, & \frac{\tilde{a}_p}{M_p} &= \sqrt{\frac{3\lambda_p}{4\mathcal{V}\sqrt{\tilde{\tau}_p}}} \tilde{c}_p, & & \end{aligned} \quad (4.64)$$

where we did not include the axions ψ and c_{q_i} which are eaten up by two anomalous $U(1)$'s on the D7- and D3-brane stack respectively. Notice that the Kähler modulus $T_p = \tau_p + i c_p$ is given by the following combinations of the canonically normalised fields $\Phi_s = \phi_s + i a_s$ and $\tilde{\Phi}_p = \tilde{\phi}_p + i \tilde{a}_p$:

$$\tau_p = \tilde{\tau}_p - x\tau_s = \left(\frac{3\mathcal{V}}{4}\right)^{2/3} \left[\frac{1}{\lambda_p^{2/3}} \left(\frac{\tilde{\phi}_p}{M_p}\right)^{4/3} - \frac{x}{\lambda_s^{2/3}} \left(\frac{\phi_s}{M_p}\right)^{4/3} \right], \quad (4.65)$$

and:

$$c_p = \tilde{c}_p - x c_s = \sqrt{\frac{4\mathcal{V}}{3}} \left(\frac{\tilde{\tau}_p^{1/4}}{\sqrt{\lambda_p}} \frac{\tilde{a}_p}{M_p} - \frac{x\tau_s^{1/4}}{\sqrt{\lambda_s}} \frac{a_s}{M_p} \right). \quad (4.66)$$

4.3.2 Mass spectrum

The mass matrix around the global minimum and its eigenvalues are derived in detail in App. C.0.3. Here we just show the leading order volume scaling of the mass of all moduli and charged matter fields for $g_s \sim 0.1$ (in order to trust our approach based on perturbation theory) and $\mathcal{V} \sim 10^7$. As explained in Sec. 4.1.2, this choice of the internal volume leads naturally to TeV-scale soft terms for sequestered scenarios with D3-branes at singularities, while it guarantees the absence of any cosmological moduli problem for unsequestered cases with flavour D7-branes. The resulting mass spectrum looks like:

$$\begin{aligned}
m_{c_{q_i}} &\sim m_{\tau_{q_i}} \sim m_\psi \sim m_{|\phi|} \sim M_s \sim g_s^{1/4} \sqrt{\pi} \frac{M_p}{\sqrt{\mathcal{V}}} \sim 10^{15} \text{ GeV}, \\
m_{\tau_s} &\sim m_{c_s} \sim \sqrt{\frac{g_s}{8\pi}} \frac{M_p}{\mathcal{V}} \ln \mathcal{V} \sim 10^{11} \text{ GeV}, \\
m_{3/2} &\sim \sqrt{\frac{g_s}{8\pi}} \frac{M_p}{\mathcal{V}} \sim 10^{10} \text{ GeV}, \\
m_{\tilde{\tau}_p} &\sim \sqrt{\frac{g_s}{8\pi}} \frac{M_p}{\mathcal{V} \sqrt{\ln \mathcal{V}}} \sim 10^9 \text{ GeV}, \\
m_{\tau_b} &\sim \sqrt{\frac{g_s}{8\pi}} \frac{M_p}{\mathcal{V}^{3/2} \sqrt{\ln \mathcal{V}}} \sim 10^6 \text{ GeV}, \\
m_{|C|} &\sim \sqrt{\frac{g_s}{8\pi}} \frac{M_p}{\mathcal{V}^2} \sim 1 \text{ TeV}, \\
m_{c_p} &\sim \sqrt{\frac{g_s}{8\pi}} \frac{M_p}{\mathcal{V}^{1+p/2}} \sqrt{\ln \mathcal{V}} \sim 10 \text{ keV} \quad \text{for } p = \frac{9}{2}, \\
m_\theta &\sim \frac{\Lambda_{\text{hid}}^2}{f_{a_{ALP}}} \lesssim 10^{-12} \text{ eV}, \\
m_{c_b} &\sim \sqrt{\frac{g_s}{8\pi}} \frac{M_p}{\mathcal{V}^{2/3}} e^{-\pi \mathcal{V}^{2/3}} \sim 0,
\end{aligned} \tag{4.67}$$

where we focused on the sequestered case with $\alpha_2 = 2$ illustrated in Sec. 4.2.3 and Λ_{hid} represents the scale of strong dynamics in the hidden sector which gives mass to the open string axion $\theta = a_{ALP}/f_{a_{ALP}}$ whose decay constant is $f_{a_{ALP}} = |\hat{C}| \simeq M_p/\mathcal{V}^2$. As explained in Sec. 4.1.2, this decay constant leads to a coupling to hidden photons controlled by the scale $M_{\text{hid}} \sim 10^6 \text{ GeV}$ that can yield a coupling to ordinary photons via $U(1)$ kinetic mixing given by (4.15) which can be naturally suppressed by an effective scale of order $M \sim 10^{12} \text{ GeV}$. Notice that the DM axion c_p can acquire a mass from poly-instanton effects of order $m_{c_p} \sim 10 \text{ keV}$ if $p = \frac{n}{2} + \kappa = \frac{9}{2}$, which can be obtained for any $\mathcal{O}(1)$ value of n by appropriately choosing the flux dependent underlying parameters so that $\kappa \equiv \frac{\tau_p}{\tau_s} = \frac{1}{2}(9 - n)$.

4.3.3 DM-ALP coupling

As shown by the mass spectrum in (4.67) and by the coupling to ordinary photons in (4.15), the open string axion θ is a natural candidate for the ALP mode a_{ALP} which converts into photons in the magnetic field of galaxy clusters and generates the 3.5 keV line. However a monochromatic line requires the decay into a pair of ALP particles of a DM particle a_{DM} with mass $m_{\text{DM}} \sim 7 \text{ keV}$. According to the mass spectrum in (4.67) a_{DM} could be either the local closed string axion c_p or the bulk

closed string mode c_b (if T_b -dependent non-perturbative effects do not suppress its mass too much). We shall now show that non-perturbative corrections to the matter Kähler metric in (4.39) can induce a coupling of the form $\frac{a_{\text{DM}}}{\Lambda} \partial_\mu a_{\text{ALP}} \partial^\mu a_{\text{ALP}}$ due to kinetic mixing between the closed string axion a_{DM} and the open string axion a_{ALP} . We shall also work out the value of the coupling Λ , finding that it can lie around the Planck/GUT scale only if the DM particle is the local axion c_p (c_b would give a trans-Planckian Λ). Finally we will explain how in our model a direct DM decay to photons induced by potential couplings of the form $\frac{a_{\text{DM}}}{4M_{\text{DM}}} F^{\mu\nu} \tilde{F}_{\mu\nu}$ is naturally suppressed by construction.

In order to compute the DM-ALP coupling, let us focus on contributions to the kinetic Lagrangian of the form:

$$\mathcal{L}_{\text{kin}} \supset \frac{\partial^2 K}{\partial C \partial \bar{C}} \partial_\mu C \partial^\mu \bar{C} = \tilde{K}(T_i, \bar{T}_i) (\partial_\mu |C| \partial^\mu |C| + |C|^2 \partial_\mu \theta \partial^\mu \theta). \quad (4.68)$$

If we now expand the closed string axions c_i and the charged open string mode $C = |C| e^{i\theta}$ around the minimum as:

$$c_i(x) \rightarrow \langle c_i \rangle + c_i(x), \quad |C|(x) \rightarrow \langle |C| \rangle + |C(x)|, \quad \theta(x) \rightarrow \langle \theta \rangle + \theta(x), \quad (4.69)$$

the kinetic terms (4.68) become:

$$\left[\langle \tilde{K} \rangle - B_i e^{-b_i \tau_i} \left(\cos(b_i \langle c_i \rangle) \frac{b_i}{2} \hat{c}_i^2 + \sin(b_i \langle c_i \rangle) b_i \hat{c}_i \right) \right] (\partial_\mu |C| \partial^\mu |C| + |C|^2 \partial_\mu \theta \partial^\mu \theta). \quad (4.70)$$

If we now express the open string mode C in terms of the canonically normalised fields \hat{C} and a_{ALP} using (4.64), (4.70) contains DM-ALP interaction terms of the form:

$$\frac{B_i}{2 \langle \tilde{K} \rangle} e^{-b_i \tau_i} \left(\cos(b_i \langle c_i \rangle) \frac{b_i}{2} \hat{c}_i^2 + \sin(b_i \langle c_i \rangle) b_i \hat{c}_i \right) \partial_\mu a_{\text{ALP}} \partial^\mu a_{\text{ALP}}, \quad (4.71)$$

showing that, in order to obtain a three-leg vertex which can induce a two-body DM decay into a pair of ultra-light ALPs, the VEV of c_i has to be such that $b_i \langle c_i \rangle = (2k+1)\frac{\pi}{2}$ with $k \in \mathbb{Z}$. Let us therefore focus on this case and consider separately the two options with either $i = b$ or $i = p$:

- **$i = b$ case:** Plugging in (4.71) the canonical normalisation for c_b from (4.64),

we find a DM-ALP coupling of the form:

$$\frac{a_b}{\Lambda} \partial_\mu a_{ALP} \partial^\mu a_{ALP} \quad \text{with} \quad \Lambda = \frac{\sqrt{6} \langle \tilde{K} \rangle}{B_b b_b} \frac{e^{b_b \langle \tau_b \rangle}}{\langle \tau_b \rangle} M_p \sim \frac{e^{b_b \mathcal{V}^{2/3}}}{B_b \mathcal{V}^{4/3}} M_p \gg M_p, \quad (4.72)$$

which reproduces the value of Λ in (4.19) for $a_{\text{DM}} = c_b$. According to the phenomenological constraints discussed in Sec. 4.1.1, c_b cannot play the rôle of the DM particle since the scale of its ALP coupling is trans-Planckian.

- **$i = p$ case:** Writing $b_p = \frac{2\pi}{N}$ and using the fact that the minimum for c_p lies at $\langle c_p \rangle = \frac{1}{2} + k_1$ with $k_1 \in \mathbb{Z}$, the condition $b_p \langle c_p \rangle = (2k_2 + 1) \frac{\pi}{2}$ with $k_2 \in \mathbb{Z}$ can be satisfied if $\frac{N}{2} = \frac{(2k_1+1)}{(2k_2+1)}$. Hence in the simplest case with $k_1 = k_2 = 0$ we just need $N = 2$. Plugging in (4.71) the canonical normalisation for c_p from (4.66), the DM-ALP coupling turns out to be:

$$\frac{\tilde{a}_p}{\Lambda} \partial_\mu a_{ALP} \partial^\mu a_{ALP} \quad \text{with} \quad \Lambda = \frac{\sqrt{3\lambda_p}}{\tilde{\tau}_p^{1/4}} \frac{\langle \tilde{K} \rangle}{B_p b_p} \frac{e^{b_p \langle \tau_p \rangle}}{\sqrt{\mathcal{V}}} M_p \sim \frac{M_p}{B_p \mathcal{V}^{7/6 - \kappa/N}}, \quad (4.73)$$

which reproduces the value of Λ in (4.19) for $a_{\text{DM}} = c_p$. This scale of the DM-ALP coupling can easily be around the Planck/GUT scale. For example if $N = 2$ and the underlying parameters are chosen such that $\kappa \equiv \tau_p/\tau_s = 2$, $\Lambda \sim M_p/\mathcal{V}^{1/6} \sim 10^{17}$ GeV for $\mathcal{V} \sim 10^7$ and $B_p \sim \mathcal{O}(1)$. Due to the poly-instanton nature of the non-perturbative effects supported by the Wilson divisor D_p , the prefactor B_p can however be exponentially small. Comparing T_p -dependent poly-instanton corrections to the superpotential in (4.41) with T_p -dependent non-perturbative corrections to the matter Kähler metric in (4.40), B_p at the minimum could scale as $B_p \sim \mathcal{O}(\mathcal{V}^{-1})$. In this case Λ can be below the Planck scale only if $\kappa \ll N$.

Let us conclude this section by showing that the branching ratio for direct DM decay into ordinary photons is negligible. Using the fact that the gauge kinetic function for the D7-stack is given by $f_{D7} = T_s + T_p$ (we neglect the flux dependent shift) and the canonical normalisation (4.66), the closed string axion $c_p = \langle c_p \rangle + \hat{c}_p$ couples to Abelian gauge bosons living on the hidden D7-stack via an interaction term of the form:

$$\frac{\hat{c}_p}{4(\langle \tau_s \rangle + \langle \tau_p \rangle)} F_{\text{hid}}^{\mu\nu} \tilde{F}_{\mu\nu}^{\text{hid}} \sim \frac{\tilde{a}_p}{4M_s} F_{\text{hid}}^{\mu\nu} \tilde{F}_{\mu\nu}^{\text{hid}}. \quad (4.74)$$

One-loop effects generate a kinetic mixing between hidden photons on the D7-stack and ordinary photons on the D3-stack which is controlled by the mixing parameter

$\chi \sim 10^{-3}$ given in (4.14). Thus the DM axion c_p develops an effective coupling to visible sector photons which from (4.15) looks like:

$$\frac{\tilde{a}_p}{4 M_{\text{DM}}} F_{\mu\nu} \tilde{F}^{\mu\nu} \sim \frac{\chi^2 \tilde{a}_p}{4 M_s} F_{\mu\nu} \tilde{F}^{\mu\nu} \quad \Leftrightarrow \quad M_{\text{DM}} \sim \frac{M_s}{\chi^2} \sim 10^5 \frac{M_p}{\sqrt{\mathcal{V}}} \sim 10^{20} \text{ GeV}, \quad (4.75)$$

which is naturally much larger than the scale Λ controlling the DM coupling to ALPs.

4.4 Summary

In this chapter we described how to perform a successful global embedding in type IIB string compactifications of the model of [180] for the recently observed 3.5 keV line from galaxy clusters. The main feature of this model is the fact that the monochromatic 3.5 keV line is not generated by the direct decay of a 7 keV dark matter particle into a pair of photons but it originates from DM decay into ultra-light ALPs which subsequently convert into photons in the cluster magnetic field. Therefore the final signal strength does not depend just on the DM distribution but also on the magnitude of the astrophysical magnetic field and its coherence length which, together with the ALP to photon coupling, determine the probability for ALPs to convert into photons. These additional features make the model of [180] particularly interesting since it manages to explain not just the observation of a 3.5 keV line from galaxy clusters but also the morphology of the signal (e.g. the intensity of the line from Perseus seems to be peaked at the centre where the magnetic field is in fact more intense) and its non-observation in dwarf spheroidal galaxies (due to the fact that their magnetic field is not very intense and has a relatively small spatial extension). These phenomenological features seem to make this model more promising than standard explanations where DM directly decays into a pair of photons.

Despite this observational success, the model of [180] for the 3.5 keV line did not have a concrete microscopic realisation. In this work we filled this gap by describing how to construct an explicit type IIB Calabi-Yau compactification which can reproduce all the main phenomenological features of the DM to ALP to photon model. We focused in particular on LVS models since they generically lead to very light axions because some of the moduli are stabilised by perturbative corrections to the effective action. The DM particle is realised as a local closed string axion which develops a tiny mass due to poly-instanton corrections to the superpotential. By an appropriate choice of background and gauge fluxes, the DM mass can be around 7

keV. The ultra-light ALP is instead given by the phase of an open string mode living on D3-branes at singularities. The ALP decay constant is set by the radial part of this open string mode which is charged under an anomalous $U(1)$. Thus the radial part gets fixed in terms of a moduli-dependent FI-term. In sequestered models with low-energy supersymmetry, the resulting decay constant is naturally in the right ballpark to reproduce a coupling to ordinary photons via $U(1)$ kinetic mixing which is around the intermediate scale, in full agreement with current observations. Notice that future helioscope experiments like IAXO might be able to detect ultra-light ALPs with intermediate scale couplings to photons [204]. Moreover the DM-ALP coupling is generated by kinetic mixing induced by non-perturbative corrections to the Kähler potential. For suitable choices of the underlying flux dependent parameters, the scale which controls the associated coupling can be around the GUT/Planck scale, again in good agreement with present observational constraints.

Part IV

Conclusions

Chapter 5

Summary and final remarks

Let us give a brief summary with possible extensions of the models in this thesis:

- In the chapter 2, we extended previous work by constructing the first explicit realisations of fibre inflation models in concrete type IIB Calabi-Yau orientifolds with consistent brane setups, full closed string moduli fixing and chiral matter on D7-branes. The underlying compactification manifold features $h^{1,1} = 4$ Kähler moduli which after D-term stabilisation gets effectively reduced to the standard 3 moduli of fibre inflation models.

Due to the fact that in the single-field case not all our approximations are fully under control, in Sec. 2.3.2 we performed a complete numerical analysis of the 3-field cosmological evolution. For $W_0 \sim 100$ and $|\lambda| = 10^{-6}$, the multi-field analysis of Sec. 2.3.2 revealed that the accuracy of our approximations improves. In particular, the allowed number of efoldings of inflation increases due to the extra motion along the volume and blow-up directions. Hence inflation can successfully work also for smaller values of \mathcal{V} which cause a smaller Kähler cone for the fibre modulus. This, in turn, requires smaller values of W_0 to match the COBE normalisation of the density perturbations, which enlarges the hierarchy between $m_{3/2}$ and the KK scales in the model.

We point out however that some of the underlying parameters are not flux-dependent, and so are not tunable in the string landscape. Two examples of this kind of parameters are the effective Euler number χ_{eff} which controls the strength of $\mathcal{O}(\alpha'^3)$ corrections due to O7-planes [37] and the combinatorial factor λ which is the coefficient of $\mathcal{O}(\alpha'^3)$ higher derivatives [75]. Both of these microscopic parameters have not been computed in full detail yet, even if λ has been estimated to be of order 10^{-3} [76]. Hence in Sec. 2.3.2 we also presented a case with $|\lambda| = 0.001$ where it is hard to obtain enough efoldings

inside the Kähler cone and generate, at the same time, the correct amplitude of the density perturbations in a framework where all the approximations are fully under control. Hence we chose the flux superpotential so that the contribution of the inflaton quantum fluctuations to the scalar power spectrum is negligible. In this case a viable inflationary phenomenology can therefore be achieved only in the presence of a non-standard mechanism for the generation of the density perturbations. A promising case could be the curvaton scenario where the initial isocurvature fluctuations could be produced by the quantum oscillations of the two light bulk closed string axions [111].

Besides a complete computation of the exact value of both χ_{eff} and λ , and the detailed derivation of a curvaton-like mechanism, there are several other important open issues for future work. A crucial one is a better determination of the actual Calabi-Yau Kähler cone since the one that we used is just an approximation inherited from the Mori cone of the ambient toric variety. It would also be interesting to develop a more systematic study of the constraints that the Kähler cone sets on the inflationary dynamics by performing a complete scan over all $h^{1,1} = 3$ and $h^{1,1} = 4$ K3 fibred CY threefolds with at least a del Pezzo divisor [112]. Moreover, our chiral global models still lack an explicit implementation of a mechanism responsible for the realisation of a dS vacuum. Finally, the study of the post-inflationary cosmological evolution of our universe is of primary importance in order to discriminate among different models that feature the same inflationary predictions of fibre inflation models. A first step forward towards understanding (p-)reheating has been taken in [113, 114]. A full understanding of this mechanism requires further investigation of the underlying microscopic dynamics.

- In chapter 3, we investigated the possibility to generate PBHs from string inflation by taking the most conservative point of view since we focused on models which are effectively single-field and, above all, we considered PBH formation with horizon re-entry in a radiation dominated era. However, two generic features of string compactifications are the presence of several scalar fields which might play an important rôle during inflation [154, 155, 156, 157, 110, 111, 158, 159], and light moduli with only gravitational couplings to ordinary matter which are long-lived and tend to give rise to early periods of matter domination [62, 65, 58, 59, 63, 55, 56, 66]. Hence in the future it would be very interesting to study the impact on PBH formation in string models of additional light fields, like for example the axionic partner of the inflaton of fibre inflation models.

We finally mention the fact that PBHs can be generated with the required efficiency only if $\delta\rho \sim 0.1\rho$ at small distance scales. It would therefore be important to perform a more careful analysis of stochastic effects since the perturbative expansion might not be fully justified [160]. Finally, we stress that non-gaussianities in large momentum fluctuations might alter significantly the PBH production mechanism and, in turn, their present abundance [142]. We leave a deeper study of both stochastic and non-gaussianity effects for future investigation.

- In the chapter 4, we have discussed in full depth moduli stabilisation, the mass spectrum and the resulting strength of all relevant couplings but we just described the geometrical and topological conditions on the underlying Calabi-Yau manifold without presenting an explicit example built via toric geometry. Let us however stress that the construction of a concrete Calabi-Yau example with all the desired features for a successful microscopic realisation of our model for the 3.5 keV line is crucial to have a fully trustworthy scenario. Moreover, it would be very interesting to have a more concrete computation of non-perturbative corrections to the 4D $N = 1$ Kähler potential.

Another aspect which would deserve further investigation is the cosmological history of our setup from inflation to the present epoch. Here we just point out that the rôle of the inflaton could be played by a small blow-up mode like τ_s [72, 71]. On the other hand, reheating might be due to the volume mode τ_b which gets displaced from its minimum during inflation [56] and later on decays giving rise to a reheating temperature of order $T_{\text{rh}} \sim 1 - 10$ GeV [63]. Such a low reheating temperature would dilute standard thermal WIMP dark matter and reproduce it non-thermally [63]. Given that in sequestered models with unified gaugino masses the WIMP is generically a Higgsino-like neutralino with an under-abundant non-thermal production in vast regions of the underlying parameter space [64, 221], an additional DM component in the form of a very light axion like c_p would be needed. Finally, one should make sure that tight dark radiation bounds are satisfied since τ_b could decay both to a pair of ultra-light closed string axions c_b and to a pair of DM axions c_p which could behave as extra neutrino-like species [58, 61]. It is important to notice, however that the decay of τ_b to open string axions θ living on D3-branes at singularities is negligible since it is highly suppressed by sequestering effects [58]. The DM axions c_p are produced non-thermally at the QCD phase transition via the standard misalignment mechanism. Given that the decay constant of the local closed string axion c_p is of order the string scale which

from (4.67) is rather high, i.e. $M_s \sim 10^{15}$ GeV, axion DM overproduction can be avoided only if the initial misalignment angle is very small. This might be due to a selection effect from the inflationary dynamics [222]. We finally stress that if inflation is driven by a blow-up mode like τ_s , the Hubble scale during inflation is rather low, $H \sim m_{\tau_b} \sim 10^6$ GeV, and so axion isocurvature perturbations would not be in tension with CMB data [223].

The models within this thesis are just one prove of how to reconcile phenomenological cosmology and string theory. One of the main characters in this work was fibre inflation. In fact, fibre inflation has been shown one of the most useful models within string theory to reproduce cosmological data. The ‘simplicity’ of the model makes it more appealing and easier to work. One further step in the advancement of these works could be a full unification with the standard model of particle physics. We could try to construct a working model with fibre inflation where we could have the chiral matter and the gauge group present in the standard model. There is still a lot of work that needs to be done but this thesis tells us the beginnings of the wonderful adventures of the fibre inflationary model and its use into cosmology. We hope that this thesis in fact inspire to construct more adventures of this wonderful theory.

Appendix A

Warped Type IIB SUGRA: equations of motion

In this appendix, we compute the equations of motion for the fields in the action (1.85). Precisely,

$$\begin{aligned}
S_{\text{IIB}} &= \frac{1}{2\kappa_{10}^2} \int d^{10}x \sqrt{-g} \left(R - \frac{\partial_M \tau \partial^M \bar{\tau}}{2(\text{Im}\tau)^2} - \frac{1}{2}|F_1|^2 - \frac{|G_3|^2}{2\text{Im}\tau} - \frac{1}{4}|\tilde{F}_5|^2 \right) \\
&\quad + \frac{1}{2\kappa_{10}^2} \int C_4 \wedge \frac{G_3 \wedge \bar{G}_3}{4i \text{Im}\tau} + S_{\text{local}}.
\end{aligned} \tag{A.1}$$

We consider the ansatz $F_1 = 0$, (1.88), (1.89), and (1.91), that is,

$$ds_{10}^2 = g_{\mu\nu}(y) dx^\mu dx^\nu + g_{mn}(y) dy^m dy^n, \tag{A.2}$$

$$\mathcal{L}_G = -\frac{1}{4\kappa_{10}^2} \int d^{10}x \sqrt{-g} \frac{|G_3|^2}{\text{Im}\tau} = -\frac{1}{8\kappa_{10}^2} \int_{X_6} d^6y \frac{G_3 \wedge *_6 \bar{G}_3}{\text{Im}\tau}, \tag{A.3}$$

$$\tilde{F}_5 = (1 + *_{10}) [d\alpha \wedge dx^0 \wedge dx^1 \wedge dx^2 \wedge dx^3]. \tag{A.4}$$

Here, $g_{\mu\nu} = e^{2A(y)} \eta_{\mu\nu}$ and $g_{mn} = e^{-2A(y)} \tilde{g}_{mn}$. Now, the equations of motion to be computed are:

1. equation for g_{MN} with $M, N = 0, \dots, 9$;
2. equation for the 5-form \tilde{F}_5 .

Now, we will compute these equation one by one.

A.0.1 Equation of motion for the metric g_{MN}

To find the equation of motion for g_{MN} , we perform

$$-\frac{2}{\sqrt{-g}} \frac{\delta S_{\text{IIB}}}{\delta g^{MN}} = 0 \quad \Rightarrow \quad R_{MN} - \frac{1}{2} g_{MN} R = \kappa_{10}^2 T_{MN}, \quad (\text{A.5})$$

where R_{MN} is the 10-dimensional Ricci tensor, R is the Ricci scalar, and $T_{MN} = T_{MN}^{\text{sugra}} + T_{MN}^{\text{local}}$. The term T_{MN} is the total stress tensor of the supergravity fields and the localized objects. We can rewrite the equation (A.5) as the trace reversed Einstein equation, given by

$$R_{MN} = \kappa_{10}^2 \left(T_{MN} - \frac{1}{8} g_{MN} T \right), \quad (\text{A.6})$$

where $T = g^{MN} T_{MN}$. From equation (A.2), we can see that only the compact and non-compact components of g_{MN} are different from zero. In this work, the compact components are not necessary. For that reason, we only compute the non-compact ones. Setting $M, N \rightarrow \mu, \nu$ in (A.6), we obtain

$$R_{\mu\nu} = \kappa_{10}^2 \left(T_{\mu\nu} - \frac{1}{8} g_{\mu\nu} T \right). \quad (\text{A.7})$$

The stress tensor $T_{\mu\nu}^{\text{sugra}}$ is given by

$$\begin{aligned} T_{\mu\nu}^{\text{sugra}} &= -\frac{2}{\sqrt{-g}} \frac{\delta}{\delta g^{\mu\nu}} \left[\frac{e^{-8A}}{2\kappa_{10}^2} \sqrt{-g} \partial_m \alpha \partial^m \alpha - \sqrt{-g} \frac{G_{mnp} \bar{G}^{mnp}}{24\kappa_{10}^2 \text{Im}\tau} \right] \\ &= -\frac{g_{\mu\nu}}{\kappa_{10}^2} \left(\frac{G_{mnp} \bar{G}^{mnp}}{24 \text{Im}\tau} + \frac{e^{-8A}}{2} \partial_m \alpha \partial^m \alpha \right). \end{aligned} \quad (\text{A.8})$$

Here, the compact indices m, n , and p are contracted using the metric \tilde{g}_{mn} . Therefore, replacing (A.8) in (A.7), we find

$$R_{\mu\nu} = -g_{\mu\nu} \left(\frac{G_{mnp} \bar{G}^{mnp}}{48 \text{Im}\tau} + \frac{e^{-8A}}{4} \partial_m \alpha \partial^m \alpha \right) + \kappa_{10}^2 \left(T_{\mu\nu}^{\text{loc}} - \frac{1}{8} g_{\mu\nu} T^{\text{loc}} \right). \quad (\text{A.9})$$

From the ansatz for the metric (A.2), we can compute the components of the Ricci tensor. To do that, we compute the Christoffel symbols, given by

$$\Gamma_{MN}^L = \frac{1}{2} g^{LP} (\partial_M g_{NP} + \partial_N g_{MP} - \partial_P g_{MN}). \quad (\text{A.10})$$

The only non-zero components of the Cristoffel symbols are

$$\begin{cases} \Gamma_{\mu\nu}^m = -\frac{1}{2}\eta_{\mu\nu}e^{2A}\tilde{g}^{mn}\partial_n(e^{2A}) & , & \Gamma_{m\nu}^\mu = \frac{1}{2}\delta_\nu^\mu e^{-2A}\partial_m(e^{2A}), \\ \Gamma_{n\ell}^m = \tilde{\Gamma}_{n\ell}^m + \frac{1}{2}[\delta_\ell^m\partial_n(e^{-2A}) + \delta_n^m\partial_\ell(e^{-2A}) - \tilde{g}_{n\ell}\partial^m(e^{-2A})]. \end{cases} \quad (\text{A.11})$$

Therefore, the Ricci tensor is given by

$$\begin{aligned} R_{\mu\nu} &= \partial_m \Gamma_{\mu\nu}^m + \Gamma_{mn}^m \Gamma_{\mu\nu}^n + \Gamma_{\rho n}^\rho \Gamma_{\mu\nu}^n - \Gamma_{\mu\rho}^m \Gamma_{m\nu}^\rho - \Gamma_{\mu m}^\rho \Gamma_{\rho\nu}^m \\ &= -\frac{1}{2}\eta_{\mu\nu} \left[e^{2A}\partial^m(e^{2A}) \left(\tilde{\Gamma}_{nm}^n + 3e^{2A}\partial_m(e^{-2A}) \right) + 2\partial_m(e^{2A})\partial^m A + \partial_m(e^{2A})\partial^m(e^{2A}) \right]. \end{aligned} \quad (\text{A.12})$$

Then, using (A.11) in (A.12), we obtain

$$\begin{aligned} R_{\mu\nu} &= -\eta_{\mu\nu}e^{4A} \left(\partial_n\partial^n A + \tilde{\Gamma}_{mn}^m \partial^n A \right) \\ &= -\eta_{\mu\nu}e^{4A}\tilde{\nabla}^2 A \\ &= -\frac{1}{4} \left(\tilde{\nabla}^2 e^{4A} - e^{-4A}\partial_m e^{4A}\partial^m e^{4A} \right). \end{aligned} \quad (\text{A.13})$$

Finally, replacing (A.13) in (A.9) and tracing, we find

$$\tilde{\nabla}^2 e^{4A} = e^{2A} \frac{G_{mnp}\tilde{G}^{mnp}}{12\text{Im}\tau} + e^{-6A} [\partial_m\alpha\partial^m\alpha + \partial_m e^{4A}\partial^m e^{4A}] + \frac{\kappa_{10}^2}{2} e^{2A} (T_m^m - T_\mu^\mu)^{\text{loc}} \quad (\text{A.14})$$

A.0.2 Equation of motion for the 5-form \tilde{F}_5

The equation of motion for \tilde{F}_5 is given by

$$d *_{10} \tilde{F}_5 = J, \quad (\text{A.15})$$

where J is a 6-form source for \tilde{F}_5 . The source J is given by the form of the action (A.1), which is given by

$$J = H_3 \wedge F_3 + 2\kappa_{10}^2 \mu_3 \rho_3^{\text{loc}}. \quad (\text{A.16})$$

Here, we use as an action of localized source given by

$$S_{\text{local}} = -\mu_3 \int_{\mathbb{M}_4 \times \Sigma} \sqrt{-g} d^4 \chi + \mu_3 \int_{\mathbb{M}_4 \times \Sigma} C_4, \quad (\text{A.17})$$

where Σ is a 3-cycle on X_6 . The condition $d *_{10} \tilde{F}_5 = dF_5$ comes from the self duality of the \tilde{F}_5 .

Appendix B

Another chiral global example

B.0.1 Toric data

Let us consider the following toric data for a CY threefold with $h^{1,1} = 4$ which is a K3-fibration over a \mathbb{P}^1 base along with a so-called ‘small’ divisor:

	x_1	x_2	x_3	x_4	x_5	x_6	x_7	x_8
8	0	0	0	1	1	1	1	4
6	0	0	1	0	1	0	1	3
6	0	1	0	0	0	1	1	3
4	1	0	0	0	0	0	1	2
	dP ₅	NdP ₁₁	NdP ₁₁	dP ₇	K3	K3	SD1	SD2

with Hodge numbers $(h^{2,1}, h^{1,1}) = (106, 4)$ and Euler number $\chi = -204$. The Stanley-Reisner ideal is:

$$\text{SR} = \{x_1x_4, x_1x_7, x_3x_5, x_4x_5, x_2x_3x_7, x_2x_6x_8, x_4x_6x_8\}.$$

This corresponds to the CY threefold used in [115] to build global models with chiral matter on D7-branes and Kähler moduli stabilisation but without any inflationary dynamics. A detailed divisor analysis using `cohomCalc` [102, 103] shows that the divisor D_4 is a del Pezzo dP₇ which we find to be shrinkable after investigating the CY volume form. Further, each of the divisors $\{D_2, D_3\}$ are non-diagonal del Pezzo surfaces and $\{D_5, D_6\}$ are two K3 surfaces while the divisors $\{D_7, D_8\}$ are

two ‘special deformation’ divisors with Hodge diamond:

$$\begin{array}{ccccc}
 & & 1 & & 1 \\
 & 0 & & 0 & \\
 \text{SD1} \equiv & 3 & 38 & 3 & \\
 & 0 & & 0 & \\
 & & 1 & & 1
 \end{array}
 \quad \text{and} \quad
 \begin{array}{ccccc}
 & & 1 & & \\
 & 0 & & 0 & \\
 \text{SD2} \equiv & 25 & 172 & 25 & \\
 & 0 & & 0 & \\
 & & 1 & &
 \end{array}$$

The intersection form in the basis of smooth divisors $\{D_1, D_4, D_5, D_6\}$ can be written as:

$$I_3 = 2 D_1 D_5 D_6 - 2 D_1^2 D_5 - 2 D_1^2 D_6 + 2 D_4^3 + 4 D_1^3. \quad (\text{B.1})$$

Writing the Kähler form in the above basis of divisors as $J = t_1 D_1 + t_4 D_4 + t_5 D_5 + t_6 D_6$ and using the intersection polynomial (B.1), the CY overall volume takes the form:

$$\mathcal{V} = 2 t_1 t_5 t_6 - t_1^2 t_5 - t_1^2 t_6 + \frac{t_4^3}{3} + \frac{2}{3} t_1^3. \quad (\text{B.2})$$

In order to express \mathcal{V} in terms of four-cycle moduli, we need to know the Kähler cone conditions which can be determined from the following Kähler cone generators:

$$K_1 = D_1 + D_5 + D_6, \quad K_2 = D_1 - D_4 + D_5 + D_6, \quad K_3 = D_5, \quad K_4 = D_6. \quad (\text{B.3})$$

Expanding the Kähler form J in these Kähler cone generators as $J = \sum_{i=1}^4 r_i K_i$ results in the following conditions for the two-cycle moduli:

$$r_1 = t_1 + t_4 > 0, \quad r_2 = -t_4 > 0, \quad r_3 = t_5 - t_1 > 0, \quad r_4 = t_6 - t_1 > 0. \quad (\text{B.4})$$

Using the four-cycle moduli, $\tau_i = \partial_{t_i} \mathcal{V}$, given by:

$$\tau_1 = 2(t_5 - t_1)(t_6 - t_1), \quad \tau_4 = t_4^2, \quad \tau_5 = t_1(2t_6 - t_1), \quad \tau_6 = t_1(2t_5 - t_1), \quad (\text{B.5})$$

the overall volume can be rewritten as:

$$\mathcal{V} = \frac{1}{3} \left(t_1 \tau_1 + t_5 \tau_5 + t_6 \tau_6 - \tau_4^{3/2} \right). \quad (\text{B.6})$$

The second Chern class of the CY threefold X is instead given by:

$$c_2(X) = 2 D_6 D_8 + 8 D_7 D_8 - 2 D_6^2 - 4 D_6 D_7 - 12 D_7^2, \quad (\text{B.7})$$

which results in the following values of the topological quantities Π_i 's:

$$\Pi_1 = 4, \quad \Pi_2 = \Pi_3 = 16, \quad \Pi_4 = 8, \quad \Pi_5 = \Pi_6 = 24, \quad \Pi_7 = 44, \quad \Pi_8 = 136.$$

The intersection curves between two coordinate divisors are given in Tab. B.1 while their volumes are listed in Tab. B.2.

	D_1	D_2	D_3	D_4	D_5	D_6	D_7	D_8
D_1	\mathcal{C}_5	\mathbb{P}^1	\mathbb{P}^1	\emptyset	\mathbb{P}^1	\mathbb{P}^1	\emptyset	\mathbb{T}^2
D_2	\mathbb{P}^1	$\mathbb{P}^1 \sqcup \mathbb{P}^1$	$\mathbb{P}^1 \sqcup \mathbb{P}^1$	\mathbb{T}^2	\mathbb{T}^2	\emptyset	\mathbb{P}^1	\mathcal{C}_3
D_3	\mathbb{P}^1	$\mathbb{P}^1 \sqcup \mathbb{P}^1$	$\mathbb{P}^1 \sqcup \mathbb{P}^1$	\mathbb{T}^2	\emptyset	\mathbb{T}^2	\mathbb{P}^1	\mathcal{C}_3
D_4	\emptyset	\mathbb{T}^2	\mathbb{T}^2	\mathcal{C}_3	\emptyset	\emptyset	\mathbb{T}^2	\mathcal{C}_3
D_5	\mathbb{P}^1	\mathbb{T}^2	\emptyset	\emptyset	\emptyset	\mathbb{T}^2	\mathcal{C}_2	\mathcal{C}_9
D_6	\mathbb{P}^1	\emptyset	\mathbb{T}^2	\emptyset	\mathbb{T}^2	\emptyset	\mathcal{C}_2	\mathcal{C}_9
D_7	\emptyset	\mathbb{P}^1	\mathbb{P}^1	\mathbb{T}^2	\mathcal{C}_2	\mathcal{C}_2	\mathcal{C}_3	\mathcal{C}_{19}
D_8	\mathbb{T}^2	\mathcal{C}_3	\mathcal{C}_3	\mathcal{C}_3	\mathcal{C}_9	\mathcal{C}_9	\mathcal{C}_{19}	\mathcal{C}_{89}

Table B.1: Intersection curves of two coordinate divisors. Here \mathcal{C}_g denotes a curve with Hodge numbers $h^{0,0} = 1$ and $h^{1,0} = g$.

	D_1	D_2	D_3	D_4	D_5	D_6	D_7	D_8
D_1	$4t_1 - 2(t_5 + t_6)$	$2(t_5 - t_1)$	$2(t_6 - t_1)$	0	$2(t_6 - t_1)$	$2(t_5 - t_1)$	0	$2(t_5 + t_6) - 4t_1$
D_2	$2(t_5 - t_1)$	$2t_4$	$2(t_1 + t_4)$	$-2t_4$	$2t_1$	0	$2(t_5 + t_4)$	$2(t_1 + 2t_4 + 2t_5)$
D_3	$2(t_6 - t_1)$	$2(t_1 + t_4)$	$2t_4$	$-2t_4$	0	$2t_1$	$2(t_6 + t_4)$	$2(t_1 + 2t_4 + 2t_6)$
D_4	0	$-2t_4$	$-2t_4$	$2t_4$	0	0	$-2t_4$	$-4t_4$
D_5	$2(t_6 - t_1)$	$2t_1$	0	0	0	$2t_1$	$2t_6$	$2(2t_6 + t_1)$
D_6	$2(t_5 - t_1)$	0	$2t_1$	0	$2t_1$	0	$2t_5$	$2(2t_5 + t_1)$
D_7	0	$2(t_5 + t_4)$	$2(t_6 + t_4)$	$-2t_4$	$2t_6$	$2t_5$	$2(t_4 + t_5 + t_6)$	$4t_4 + 6(t_5 + t_6)$
D_8	$2(t_5 + t_6) - 4t_1$	$2(t_1 + 2t_4 + 2t_5)$	$2(t_1 + 2t_4 + 2t_6)$	$-4t_4$	$2(2t_6 + t_1)$	$2(2t_5 + t_1)$	$4t_4 + 6(t_5 + t_6)$	$4[t_1 + 2t_4 + 4(t_5 + t_6)]$

Table B.2: Volumes of intersection curves between two coordinate divisors.

B.0.2 Orientifold involution

We focus on orientifold involutions of the form $\sigma : x_i \rightarrow -x_i$ with $i = 1, \dots, 8$ which feature an O7-plane on D_i and O3-planes at the fixed points listed in Tab. B.3. The effective non-trivial fixed point set in Tab. B.3 has been obtained after taking care of the SR ideal symmetry. Moreover, the total number of O3-planes N_{O3} is obtained from the triple intersections restricted to the CY hypersurface, while the effective Euler number χ_{eff} has been computed as:

$$\chi_{\text{eff}} = \chi(X) + 2 \int_X [\text{O7}] \wedge [\text{O7}] \wedge [\text{O7}]. \quad (\text{B.8})$$

In what follows we shall focus on the orientifold involution $\sigma : x_7 \rightarrow -x_7$ which features two non-intersecting O7-planes located in D_1 and D_7 and two O3-planes at $\{D_2D_3D_4\}$.

σ	O7	O3	N_{O3}	$\chi(\text{O7})$	χ_{eff}
$x_1 \rightarrow -x_1$	$D_1 \sqcup D_7$	$\{D_2D_3D_4\}$	2	54	-192
$x_2 \rightarrow -x_2$	D_2	$\{D_1D_6D_8, D_3D_4D_7, D_6D_7D_8\}$	$\{2, 2, 6\}$	14	-208
$x_3 \rightarrow -x_3$	D_3	$\{D_1D_5D_8, D_2D_4D_7, D_5D_7D_8\}$	$\{2, 2, 6\}$	14	-208
$x_4 \rightarrow -x_4$	D_4	$\{D_1D_2D_3, D_1D_5D_6, D_2D_5D_8, D_3D_6D_8, D_5D_6D_7\}$	$\{2, 2, 4, 4, 2\}$	10	-200
$x_5 \rightarrow -x_5$	D_5	$\{D_1D_3D_8, D_3D_7D_8, D_2D_4D_8\}$	$\{2, 2, 4\}$	24	-204
$x_6 \rightarrow -x_6$	D_6	$\{D_1D_2D_8, D_2D_7D_8, D_3D_4D_8\}$	$\{2, 2, 4\}$	24	-204
$x_7 \rightarrow -x_7$	$D_1 \sqcup D_7$	$\{D_2D_3D_4\}$	2	54	-192
$x_8 \rightarrow -x_8$	D_8	\emptyset	0	224	-28

Table B.3: Fixed point set for the involutions which are reflections of the eight coordinates x_i with $i = 1, \dots, 8$.

B.0.3 Brane setup

If the D7-tadpole cancellation condition is satisfied by placing four D7-branes on top of the O7-plane, the string loop corrections to the scalar potential involve only KK effects since winding contributions are absent due to the absence of any intersection between D7-branes and/or O7-planes. Thus loop effects are too simple to generate a viable inflationary plateau. We shall therefore focus on a slightly more complicated D7-brane setup which gives rise also to winding loop effects. This can be achieved by placing D7-branes not entirely on top of the O7-plane as follows:

$$8[\text{O7}] \equiv 8([D_1] + [D_7]) = 8(2[D_1] + [D_2] + [D_5]) . \quad (\text{B.9})$$

This brane setup involves three stacks of D7-branes wrapped around the divisors D_1 , D_2 and D_5 . Moreover, the condition for D3-tadpole cancellation becomes:

$$N_{\text{D3}} + \frac{N_{\text{flux}}}{2} + N_{\text{gauge}} = \frac{N_{\text{O3}}}{4} + \frac{\chi(\text{O7})}{12} + \sum_a \frac{N_a (\chi(D_a) + \chi(D'_a))}{48} = 14 ,$$

showing that there is space for turning on both gauge and background three-form fluxes for complex structure and dilaton stabilisation.

B.0.4 Gauge fluxes

In order to obtain a chiral visible sector on the D7-brane stacks wrapping D_1 , D_2 and D_5 we need to turn on worldvolume gauge fluxes of the form:

$$\mathcal{F}_i = \sum_{j=1}^{h^{1,1}} f_{ij} \hat{D}_j + \frac{1}{2} \hat{D}_i - \iota_{D_i}^* B \quad \text{with} \quad f_{ij} \in \mathbb{Z} \quad \text{and} \quad i = 1, 2, 5, \quad (\text{B.10})$$

where the half-integer contribution is due to Freed-Witten anomaly cancellation [97, 98].

However we want to generate just one moduli-dependent Fayet-Iliopoulos term in order to fix only one Kähler modulus via D-term stabilisation. In fact, if the number of FI-terms is larger than one, there is no light Kähler modulus which can play the rôle of the inflaton. Moreover we wrap a D3-brane instanton on the rigid divisor D_4 in order to generate a non-perturbative contribution to the superpotential which is crucial for LVS moduli stabilisation. In order to cancel the Freed-Witten anomaly, the D3-instanton has to support a half-integer flux, and so the general expression of the total gauge flux on D_4 becomes:

$$\mathcal{F}_4 = \sum_{j=1}^{h^{1,1}} f_{4j} \hat{D}_j + \frac{1}{2} \hat{D}_4 - \iota_{D_4}^* B \quad \text{with} \quad f_{4j} \in \mathbb{Z}. \quad (\text{B.11})$$

However a non-vanishing \mathcal{F}_4 would not be gauge invariant, and so would prevent a non-perturbative contribution to the superpotential. We need therefore to check if it is possible to perform an appropriate choice of B -field which can simultaneously set $\mathcal{F}_1 = \mathcal{F}_2 = 0$ (we choose to have a non-vanishing gauge flux only on D_5 to have just one moduli-dependent FI-term) and $\mathcal{F}_4 = 0$. If we set:

$$B = \frac{1}{2} \hat{D}_1 + \frac{1}{2} \hat{D}_2 + \frac{1}{2} \hat{D}_4, \quad (\text{B.12})$$

the condition $\mathcal{F}_1 = \mathcal{F}_2 = \mathcal{F}_4 = 0$ reduces to the requirement that the following forms are integer:

$$\iota_{D_1}^* \left(\frac{1}{2} \hat{D}_2 + \frac{1}{2} \hat{D}_4 \right) \quad \iota_{D_2}^* \left(\frac{1}{2} \hat{D}_1 + \frac{1}{2} \hat{D}_4 \right) \quad \iota_{D_4}^* \left(\frac{1}{2} \hat{D}_1 + \frac{1}{2} \hat{D}_2 \right), \quad (\text{B.13})$$

since in this case the integer flux quanta f_{ij} can always be adjusted to yield vanishing gauge fluxes. Taking an arbitrary integer form $A \in H^2(\mathbb{Z}, X)$ which can be expanded

as $A = a_j \hat{D}_j$ with $a_j \in \mathbb{Z}$, the pullbacks in (B.13) give rise to integer forms if:

$$\begin{aligned} b_1 &\equiv \int_X \left(\frac{1}{2} \hat{D}_2 + \frac{1}{2} \hat{D}_4 \right) \wedge \hat{D}_1 \wedge A \in \mathbb{Z} \\ b_2 &\equiv \int_X \left(\frac{1}{2} \hat{D}_1 + \frac{1}{2} \hat{D}_4 \right) \wedge \hat{D}_2 \wedge A \in \mathbb{Z} \\ b_4 &\equiv \int_X \left(\frac{1}{2} \hat{D}_1 + \frac{1}{2} \hat{D}_2 \right) \wedge \hat{D}_4 \wedge A \in \mathbb{Z} \end{aligned}$$

Using the intersection polynomial (B.1) we find $b_1 = a_5 - a_1 \in \mathbb{Z}$, $b_2 = b_1 - a_4 \in \mathbb{Z}$ and $b_4 = -a_4 \in \mathbb{Z}$, showing how the choice of B -field in (B.12) can indeed allow for $\mathcal{F}_1 = \mathcal{F}_2 = \mathcal{F}_4 = 0$. The only non-zero gauge flux is \mathcal{F}_5 which does not feature any half-integer contribution since $c_1(D_5) = 0$ given that D_5 is a K3 surface. Given that all the intersection numbers are even, the pullback of the B -field on D_5 does also not generate an half-integer flux. We shall therefore consider a non-vanishing gauge flux on the worldvolume of D_5 of the form:

$$\mathcal{F}_5 = \sum_{j=1}^{h^{1,1}} f_{5j} \hat{D}_j \quad \text{with} \quad f_{5j} \in \mathbb{Z}. \quad (\text{B.14})$$

B.0.5 FI-term and chirality

Given that the divisor D_5 is transversely invariant under the orientifold involution and it is wrapped by four D7-branes, it supports an $Sp(8)$ gauge group which is broken down to $U(4) = SU(4) \times U(1)$ by a non-zero flux \mathcal{F}_5 along the diagonal $U(1)$. This non-trivial gauge flux \mathcal{F}_5 induces also a $U(1)$ -charge q_{i5} for the i -th Kähler modulus of the form:

$$q_{i5} = \int_X \hat{D}_i \wedge \hat{D}_5 \wedge \mathcal{F}_5. \quad (\text{B.15})$$

Thus $\mathcal{F}_5 \neq 0$ yields:

$$q_{15} = 2(f_{56} - f_{51}) \quad q_{45} = q_{55} = 0 \quad q_{65} = 2f_{51}, \quad (\text{B.16})$$

together with a flux-dependent correction to the gauge kinetic function which looks like:

$$\text{Re}(f_5) = \alpha_5^{-1} = \frac{4\pi}{g_5^2} = \tau_5 - h(\mathcal{F}_5) \text{Re}(S), \quad (\text{B.17})$$

where:

$$h(\mathcal{F}_5) = \frac{1}{2} \int_X \hat{D}_5 \wedge \mathcal{F}_5 \wedge \mathcal{F}_5 = \frac{1}{2} (f_{51} q_{15} + f_{56} q_{65}). \quad (\text{B.18})$$

Moreover a non-vanishing gauge flux \mathcal{F}_5 induces a moduli-dependent FI-term of the form:

$$\xi = \frac{1}{4\pi\mathcal{V}} \int_X \hat{D}_5 \wedge J \wedge \mathcal{F}_5 = \frac{1}{4\pi\mathcal{V}} \sum_{j=1}^{h^{1,1}} q_{j5} t_j = \frac{1}{4\pi\mathcal{V}} (q_{15} t_1 + q_{65} t_6). \quad (\text{B.19})$$

For vanishing open string VEVs (induced for example by non-tachyonic scalar masses), a leading-order supersymmetric stabilisation requires $\xi = 0$ which implies:

$$t_6 = -\frac{q_{15}}{q_{65}} t_1 = \left(1 - \frac{f_{56}}{f_{51}}\right) t_1 \equiv \alpha t_1. \quad (\text{B.20})$$

This $U(1)$ factor becomes massive via the Stückelberg mechanism and develops an $\mathcal{O}(M_s)$ mass by eating up a linear combination of an open and a closed string axion which is mostly given by the open string mode.

Besides breaking the worldvolume gauge group and inducing moduli-dependent FI-terms, non-trivial gauge fluxes on D7-branes generate also 4D chiral modes. In fact, open strings stretching between the D7-branes on D_5 and the O7-planes or the image branes give rise to the following zero-modes in the symmetric and antisymmetric representations of $U(4)$:

$$I_5^{(S)} = -\frac{1}{2} \int_X \hat{D}_5 \wedge [\text{O7}] \wedge \mathcal{F}_5 - \int_X \hat{D}_5 \wedge \hat{D}_5 \wedge \mathcal{F}_5 = -\left(q_{15} + \frac{q_{65}}{2}\right), \quad (\text{B.21})$$

$$I_5^{(A)} = \frac{1}{2} \int_X \hat{D}_5 \wedge [\text{O7}] \wedge \mathcal{F}_5 - \int_X \hat{D}_5 \wedge \hat{D}_5 \wedge \mathcal{F}_5 = -I_5^{(S)}. \quad (\text{B.22})$$

Due to the absence of worldvolume fluxes on the D7-branes wrapped around D_1 and D_2 , the gauge groups supported by these two D7-stacks are respectively $SO(16)$ (since D_1 is an O7-locus) and $Sp(8)$ (since D_2 is transversely invariant) which are both unbroken. Thus open strings stretched between the D7-branes on D_5 and D_1 (or its image brane) give rise to chiral zero-modes in the bi-fundamental representation (4,16) of $U(4)$ and $SO(16)$ whose number is:

$$I_{51} = \int_X \hat{D}_5 \wedge \hat{D}_1 \wedge \mathcal{F}_5 = q_{15}. \quad (\text{B.23})$$

On the other hand, the number of 4D chiral zero-modes in the bi-fundamental representation (4,8) of $U(4)$ and $Sp(8)$ (corresponding to open strings stretching between the D7s on D_5 and D_2) is:

$$I_{52} = \int_X \hat{D}_5 \wedge \hat{D}_2 \wedge \mathcal{F}_5 = q_{65}. \quad (\text{B.24})$$

We need finally to check that there are no chiral intersections between the D7s on D_5 and the instanton on D_4 to make sure that the prefactor of the non-perturbative contribution to the superpotential is indeed non-zero. This is ensured by the fact that:

$$I_{54} = \int_X \hat{D}_5 \wedge \hat{D}_4 \wedge \mathcal{F}_5 = 0. \quad (\text{B.25})$$

B.0.6 Inflationary potential

Using the D-term fixing relation (B.20), the Kähler cone conditions (B.4) simplify to $t_5 > t_1 > -t_4 > 0$ and $\alpha > 1$. Moreover the CY volume (B.6) reduces to:

$$\mathcal{V} = (2\alpha - 1) t_5 t_1^2 - \left(\alpha - \frac{2}{3} \right) t_1^3 + \frac{t_4^3}{3} = t_b \tau_f - \frac{1}{3} \tau_4^{3/2}. \quad (\text{B.26})$$

Given that this form is linear in t_5 , the effective CY volume after D-term stabilisation looks like a K3 fibre τ_f over a \mathbb{P}^1 base t_b whose volumes are given by:

$$\tau_f = \tau_5 = (2\alpha - 1) t_1^2 \quad \text{and} \quad t_b = t_5 - \frac{\left(\alpha - \frac{2}{3} \right)}{(2\alpha - 1)} t_1. \quad (\text{B.27})$$

Notice that the Kähler cone condition $t_5 > t_1$ can be rewritten as:

$$\tau_f < \sigma(\alpha) \mathcal{V}^{2/3}, \quad (\text{B.28})$$

where:

$$\sigma(\alpha) \equiv (2\alpha - 1) \left(\frac{3}{3\alpha - 1} \right)^{2/3} \quad \text{with} \quad \alpha > 1. \quad (\text{B.29})$$

In terms of the canonically normalised inflaton shifted from its minimum, the condition (B.28) reads:

$$\tau_f = \langle \tau_f \rangle e^{2\hat{\phi}/\sqrt{3}} < \sigma \mathcal{V}^{2/3} \quad \Leftrightarrow \quad \hat{\phi} < \frac{\sqrt{3}}{2} \ln \left(\frac{\sigma}{\langle \tau_f \rangle} \mathcal{V}^{2/3} \right). \quad (\text{B.30})$$

Let us now focus on the inflationary potential. The winding loop corrections look like (with $\kappa = g_s/(8\pi)$ for $e^{K_{cs}} = 1$):

$$V_{g_s}^w = -\kappa \frac{W_0^2}{\mathcal{V}^3} \frac{C_w}{\sqrt{\tau_f}}, \quad (\text{B.31})$$

where:

$$C_w = \sqrt{2\alpha - 1} \left(C_1^w + \frac{C_2^w}{\alpha} \right). \quad (\text{B.32})$$

On the other hand, the KK loop corrections read (neglecting τ_4 -dependent terms which yield subdominant contributions):

$$V_{g_s}^{\text{KK}} = \kappa g_s^2 \frac{W_0^2}{\mathcal{V}^2} \sum_{i,j=1,5,6} C_i^{\text{KK}} C_j^{\text{KK}} K_{ij}. \quad (\text{B.33})$$

After substituting $t_6 = \alpha t_1$, we obtain:

$$Z \mathcal{V}^2 \sum_{i,j} C_i^{\text{KK}} C_j^{\text{KK}} K_{ij} = a t_1^2 + C_5^2 t_5 (t_5 - t_1) - (1 - Z) \left(b t_1^2 + c t_1 t_5 + \frac{C_5^2}{2} t_5^2 \right),$$

where:

$$\begin{aligned} a &= C_1 (C_1 + C_5 + C_6) + C_5 \left(C_6 + \frac{C_5}{2} \right) + C_6^2 \left(\alpha^2 - \alpha + \frac{1}{2} \right) \\ b &= \alpha C_1 C_6 + \frac{\alpha^2}{2} C_6^2 + \frac{C_1^2}{2} \quad c = C_5 (C_1 + \alpha C_6), \end{aligned}$$

and:

$$Z = 1 - \frac{2}{3\alpha - 1} \left(\frac{\tau_f}{\sigma \mathcal{V}^{2/3}} \right)^{3/2}.$$

Notice that the Kähler cone conditions $\tau_f < \sigma \mathcal{V}^{2/3}$ and $\alpha > 1$ imply $0 < Z < 1$. This guarantees the absence of any singularity in the Kähler metric. Expressing the scalar potential in terms of the 4-cycle moduli, we end up with:

$$V_{g_s}^{\text{KK}} = \kappa g_s^2 \frac{W_0^2}{Z \mathcal{V}^2} \left[\frac{C_5^2}{\tau_f^2} - \frac{2}{3(2\alpha - 1)^{3/2}} \frac{C_5^2}{\mathcal{V} \sqrt{\tau_f}} + d \frac{\tau_f}{\mathcal{V}^2} \left(1 - h \frac{\tau_f^{3/2}}{\mathcal{V}} \right) \right], \quad (\text{B.34})$$

where $h = u/d$ with:

$$\begin{aligned} d &= \frac{a}{(2\alpha - 1)} - \frac{2}{3} \frac{c}{(2\alpha - 1)^2} - \frac{C_5^2}{(2\alpha - 1)^3} \left(\alpha^2 - \frac{\alpha}{3} - \frac{2}{9} \right) \\ u &= \frac{2b}{3(2\alpha - 1)^{5/2}} + \frac{2c}{3} \frac{(\alpha - \frac{2}{3})}{(2\alpha - 1)^{7/2}} + \frac{C_5^2}{3} \frac{(\alpha - \frac{2}{3})^2}{(2\alpha - 1)^{9/2}}. \end{aligned}$$

If all the coefficients of the KK corrections take natural $\mathcal{O}(1)$ values, the term in (B.34) proportional to h is suppressed by $h \ll 1$, and so it can be safely neglected.

On the other hand, higher derivative $\alpha^3 F^4$ corrections take the form (neglecting the t_4 -dependent term and setting $t_6 = \alpha t_1$):

$$V_{F^4} = -4\kappa^2 \frac{\lambda W_0^4}{g_s^{3/2} \mathcal{V}^4} [(6\alpha + 1)t_1 + 6t_5], \quad (\text{B.35})$$

which in terms of four-cycle moduli looks like:

$$V_{F^4} = -4\kappa^2 \frac{\lambda W_0^4}{g_s^{3/2} \mathcal{V}^4} \left[\frac{12\alpha^2 + 2\alpha - 5}{(2\alpha - 1)^{3/2}} \sqrt{\tau_f} + 6 \frac{\mathcal{V}}{\tau_f} \right]. \quad (\text{B.36})$$

Therefore the total inflationary potential becomes:

$$V = V_{g_s^w} + V_{g_s^{\text{KK}}} + V_{F^4} = \kappa \frac{W_0^2}{\mathcal{V}^2} \left(\frac{A_1}{\tau_f^2} + \frac{A_2}{\mathcal{V} \tau_f} - \frac{A_3}{\mathcal{V} \sqrt{\tau_f}} + \frac{B_1 \sqrt{\tau_f}}{\mathcal{V}^2} + \frac{B_2 \tau_f}{\mathcal{V}^2} \right), \quad (\text{B.37})$$

where (with $\lambda = -|\lambda| < 0$):

$$A_1 = \frac{g_s^2}{Z} C_5^2 \quad A_2 = \frac{3}{\pi} \frac{|\lambda| W_0^2}{\sqrt{g_s}} \quad A_3 = C_w + \frac{g_s^2}{Z} \frac{2 C_5^2}{3(2\alpha - 1)^{3/2}} \simeq C_w \quad (\text{B.38})$$

and:

$$B_1 = \frac{12\alpha^2 + 2\alpha - 5}{6(2\alpha - 1)^{3/2}} A_2 \quad B_2 = \frac{g_s^2 d}{Z}. \quad (\text{B.39})$$

The potential (B.37) could support single-field slow-roll inflation driven by τ_f [14, 78]. In order to get enough efoldings before hitting the walls of the Kähler cone given in (B.30), we need to focus on the region in field space where the inflaton minimum is of order $\langle \tau_f \rangle \ll \mathcal{V}^{2/3}$. Numerical estimates show that we need values of order $\langle \tau_f \rangle \sim \mathcal{O}(1)$ and $\mathcal{V} \sim \mathcal{O}(10^4)$ which, in turn, imply $W_0 \sim \mathcal{O}(100)$ in order to match the observed amplitude of the density perturbations. For $g_s \lesssim \mathcal{O}(0.1)$, $|\lambda| \sim \mathcal{O}(10^{-3})$ and natural $\mathcal{O}(1)$ values of the coefficients of the string loop effects, the terms in (B.37) proportional to B_1 and B_2 are both negligible with respect to the first three terms in the vicinity of the minimum where $\tau_f \sim \mathcal{O}(1) \ll \mathcal{V}^{2/3}$.

The scalar potential (B.37) written in terms of the canonically normalised inflaton $\phi = \langle \phi \rangle + \hat{\phi}$ looks like (with $k = 2/\sqrt{3}$):

$$V = \kappa \frac{A_1 W_0^2}{\langle \tau_f \rangle^2 \mathcal{V}^2} \left(C_{\text{ds}} + e^{-2k\hat{\phi}} + \lambda_1 Z e^{-k\hat{\phi}} - \lambda_2 Z e^{-\frac{k\hat{\phi}}{2}} + \mathcal{R}_1 Z e^{\frac{k\hat{\phi}}{2}} + \mathcal{R}_2 e^{k\hat{\phi}} \right), \quad (\text{B.40})$$

where we added a constant $C_{\text{ds}} = \lambda_2 Z - \lambda_1 Z - 1 - \mathcal{R}_1 Z - \mathcal{R}_2$ to obtain a Minkowski (or slightly dS) vacuum and:

$$\lambda_1 = \frac{3\langle \tau_f \rangle}{\pi C_5^2} \frac{|\lambda| W_0^2}{g_s^{5/2} \mathcal{V}} \sim \mathcal{O}(1 - 10) \quad \lambda_2 \simeq \frac{\langle \tau_f \rangle^{3/2}}{C_5^2} \frac{C_w}{g_s^2 \mathcal{V}} \sim \mathcal{O}(1 - 10),$$

while:

$$\mathcal{R}_1 = \frac{12\alpha^2 + 2\alpha - 5}{6(2\alpha - 1)^{3/2}} \frac{\lambda_1 \langle \tau_f \rangle^{3/2}}{\mathcal{V}} \ll 1 \quad \mathcal{R}_2 = \frac{\langle \tau_f \rangle^3}{C_5^2} \frac{d}{\mathcal{V}^2} \ll 1.$$

The three negative exponentials in (B.40) compete to give a minimum at $\langle \tau_f \rangle \sim \mathcal{O}(1)$ while the two positive exponentials cause a steepening behaviour at large $\hat{\phi}$.

In this appendix we shall not present a detailed quantitative analysis of inflation. We however point out that, if the approximated expression (B.30) is correct, in this case the Kähler cone bounds seem to be more constraining than in the case discussed in the main text since the inflaton direction τ_f is bounded by $\mathcal{V}^{2/3}$ instead of $\mathcal{V}/\sqrt{\tau_s}$. Thus a viable inflationary dynamics in this case would require a more severe tuning of the underlying parameters and a better understanding of the validity of our effective field theory approach.

Appendix C

Computational details

C.0.1 Closed string axion decay constants

In type IIB string compactifications on Calabi-Yau orientifolds axion-like particles emerge in the low-energy $N = 1$ effective field theory from the dimensional reduction of the Ramond-Ramond forms C_p with $p = 2, 4$. The Kaluza-Klein decomposition under the orientifold projection of these forms is given by [224]:

$$C_2 = c^{i-}(x) \hat{D}_{i-} \quad \text{and} \quad C_4 = c_{i+}(x) \tilde{D}^{i+} + Q_2^{i+}(x) \wedge \hat{D}_{i+} + V^{a+}(x) \wedge \alpha_{a+} - \tilde{V}_{a+}(x) \wedge \beta^{a+},$$

where $i_{\pm} = 1, \dots, h_{\pm}^{1,1}$, $a_+ = 1, \dots, h_+^{1,2}$, \tilde{D}^{i+} is a basis of $H_+^{2,2}$ dual to the $(1, 1)$ -forms \hat{D}_{i+} and $(\alpha_{a+}, \beta^{a+})$ is a real, symplectic basis of $H_+^3 = H_+^{1,2} \oplus H_+^{2,1}$.

As explained in Sec. 4.2.1, in our model the orientifold-odd axions c_{i-} , if present, are eaten up by anomalous $U(1)$'s in the process of anomaly cancellation. We shall therefore focus on the case with $h_-^{1,1} = 0$ where the Kähler moduli take the simple expression $T_i = \tau_i + i c_i$ with $i = 1, \dots, h_+^{1,1} = h^{1,1}$.

The coupling of orientifold-even closed string axions to $F \wedge F$ can be derived from the Kaluza-Klein reduction of the Chern-Simons term of the D-brane action. Moreover, the periods of the canonically unnormalised axions c_i are integer multiples of M_p and their kinetic terms read [187]:

$$\mathcal{L}_{\text{kin}} = K_{ij} \partial_{\mu} c_i \partial^{\mu} c_j = \frac{1}{8} \eta_i \partial_{\mu} c'_i \partial^{\mu} c'_i, \quad (\text{C.1})$$

where the c'_i 's are the axions which diagonalise the Kähler metric K_{ij} and η_i are its eigenvalues. A proper canonical normalisation of the kinetic terms can then be easily obtained by defining:

$$\frac{1}{8} \eta_i \partial_{\mu} c'_i \partial^{\mu} c'_i \equiv \frac{1}{2} \partial_{\mu} a_i \partial^{\mu} a_i \quad \text{with} \quad a_i = \frac{1}{2} \sqrt{\eta_i} c'_i, \quad (\text{C.2})$$

which shows that the canonically normalised axions a_i acquire periods of the form:

$$\frac{2}{\sqrt{\eta_i}} a_i = \frac{2}{\sqrt{\eta_i}} a_i + M_p \quad \Rightarrow \quad a_i = a_i + \frac{\sqrt{\eta_i}}{2} M_p. \quad (\text{C.3})$$

We can then set the conventional axionic period as:

$$a_i = a_i + 2\pi f_{a_i} \quad \text{with} \quad f_{a_i} = \frac{\sqrt{\eta_i} M_p}{4\pi}, \quad (\text{C.4})$$

where f_{a_i} is the standard axion decay constant. Closed string axions which propagate in the bulk of the extra dimensions have a decay constant of order the Kaluza-Klein scale $M_{\text{KK}} \sim M_p/\mathcal{V}^{2/3}$, whereas the decay constant of closed string axions whose corresponding saxion parameterises the volume of localised blow-up modes is controlled by the string scale $M_s \sim M_p/\sqrt{\mathcal{V}}$:

$$f_{a_i} \simeq \begin{cases} M_p/\tau_i \sim M_{\text{KK}} & \text{bulk axion} \\ M_p/\sqrt{\mathcal{V}} \sim M_s & \text{local axion} \end{cases} \quad (\text{C.5})$$

Notice however that the axion coupling to the Abelian gauge bosons living on the D-brane wrapping the four-cycle whose volume is controlled by the associated saxion τ_i , is given by:

$$\frac{g_i^2}{32\pi^2} \frac{a_i}{f_{a_i}} F_{\mu\nu}^{(i)} \tilde{F}^{\mu\nu} = \frac{1}{32\pi^2} \frac{a_i}{\tau_i f_{a_i}} F_{\mu\nu}^{(i)} \tilde{F}^{\mu\nu}, \quad (\text{C.6})$$

since the gauge coupling is set by the saxion as $g_i^2 = \tau_i$. Hence combining (C.5) with (C.6) we realise that that the coupling of bulk closed string axions to gauge bosons is controlled by $M \sim \tau_i f_{a_i} \sim M_p$, in agreement with the fact that moduli couple to ordinary matter with gravitational strength. On the other hand the coupling of local closed string axions to gauge bosons is set by the string scale M_s which in LVS models with exponentially large volume can be considerably smaller than the Planck scale.

C.0.2 Canonical normalisation

The kinetic terms for all Kähler moduli and the charged open string modes ϕ and C can be derived from the total Kähler potential $K = K_{\text{mod}} + K_{\text{matter}}$, where K_{mod} is given by the three contributions in (4.38) and K_{matter} is shown in (4.39) and (4.40), as follows:

$$\mathcal{L}_{\text{kin}} = \frac{\partial^2 K}{\partial \chi_i \partial \bar{\chi}_{\bar{j}}} \partial_\mu \chi_i \partial^\mu \bar{\chi}_{\bar{j}}, \quad (\text{C.7})$$

where χ_i denotes an arbitrary scalar field of our model. As can be seen from (4.39), the D7 open string mode ϕ mixes only with the dilaton S , and so can be easily written in terms of the corresponding canonically normalised field $\hat{\phi}$ as:

$$\frac{\hat{\phi}}{M_p} = \sqrt{\frac{2}{\text{Re}(S)}} \phi. \quad (\text{C.8})$$

From the first term in (4.38) we also realise that cross-terms between the blow-up mode τ_{q_i} and any of the other Kähler moduli are highly suppressed when evaluated at the minimum for $\tau_{q_i} \simeq 0$ (more precisely, as discussed in Sec. 4.2.3, depending on the level of sequestering of soft masses, we can have either $\tau_{q_i} \sim \mathcal{V}^{-1} \ll 1$ or $\tau_{q_i} \sim \mathcal{V}^{-3} \ll 1$). Hence it is straightforward to write also τ_{q_i} in terms of the corresponding canonically normalised field ϕ_{q_i} as:

$$\frac{\phi_{q_i}}{M_p} = \frac{\tau_{q_i}}{\sqrt{\mathcal{V}}} \quad \text{for } i = 1, 2. \quad (\text{C.9})$$

The remaining fields T_b, T_s, T_p and C mix with each other, leading to a non-trivial Kähler metric whose components take the following leading order expressions for $\mathcal{V} \simeq \lambda_b \tau_b^{3/2} \gg 1$:

$$\begin{aligned} K_{T_i \bar{T}_j} &\simeq \frac{3}{8\mathcal{V}} \begin{pmatrix} \frac{2\lambda_b}{\sqrt{\tau_b}} & -\frac{3}{\tau_b} (\lambda_s \sqrt{\tau_s} + x \lambda_p \sqrt{\tilde{\tau}_p}) & -\frac{3}{\tau_b} \lambda_p \sqrt{\tilde{\tau}_p} \\ -\frac{3}{\tau_b} (\lambda_s \sqrt{\tau_s} + x \lambda_p \sqrt{\tilde{\tau}_p}) & \frac{\lambda_s}{\sqrt{\tau_s}} + \frac{x^2 \lambda_p}{\sqrt{\tilde{\tau}_p}} & \frac{x \lambda_p}{\sqrt{\tilde{\tau}_p}} \\ -\frac{3}{\tau_b} \lambda_p \sqrt{\tilde{\tau}_p} & \frac{x \lambda_p}{\sqrt{\tilde{\tau}_p}} & \frac{\lambda_p}{\sqrt{\tilde{\tau}_p}} \end{pmatrix} \\ K_{T_b \bar{C}} &\simeq -\frac{\tilde{K}}{2\tau_b} C, \quad K_{T_s \bar{C}} \simeq \frac{\tilde{K}}{2\mathcal{V}} (\lambda_s \sqrt{\tau_s} + x \lambda_p \sqrt{\tilde{\tau}_p}) C, \\ K_{T_p \bar{C}} &\simeq \frac{\tilde{K}}{2\mathcal{V}} \lambda_p \sqrt{\tilde{\tau}_p} C, \quad K_{C \bar{C}} = \tilde{K}. \end{aligned}$$

In the large volume limit, different contributions to the kinetic Lagrangian can be organised in an expansion in $1/\mathcal{V} \ll 1$ as follows:

$$\mathcal{L}_{\text{kin}} = \mathcal{L}_{\text{kin}}^{\mathcal{O}(1)} + \mathcal{L}_{\text{kin}}^{\mathcal{O}(\mathcal{V}^{-1})} + \mathcal{L}_{\text{kin}}^{\mathcal{O}(\mathcal{V}^{-4/3})},$$

where, trading T_p for $\tilde{T}_p = T_p + xT_s$, we have:

$$\begin{aligned}
\mathcal{L}_{\text{kin}}^{\mathcal{O}(1)} &= \frac{3}{4\tau_b^2} \partial_\mu \tau_b \partial^\mu \tau_b, \\
\mathcal{L}_{\text{kin}}^{\mathcal{O}(\mathcal{V}^{-1})} &= \frac{3}{8\mathcal{V}} \left[\frac{\lambda_s}{\sqrt{\tau_s}} (\partial_\mu \tau_s \partial^\mu \tau_s + \partial_\mu c_s \partial^\mu c_s) + \frac{\lambda_p}{\sqrt{\tilde{\tau}_p}} (\partial_\mu \tilde{\tau}_p \partial^\mu \tilde{\tau}_p + \partial_\mu \tilde{c}_p \partial^\mu \tilde{c}_p) \right] \\
&\quad - \frac{9}{4\mathcal{V}} \frac{\partial_\mu \tau_b}{\tau_b} \left(\lambda_s \sqrt{\tau_s} \partial^\mu \tau_s + \lambda_p \sqrt{\tilde{\tau}_p} \partial^\mu \tilde{\tau}_p \right), \\
\mathcal{L}_{\text{kin}}^{\mathcal{O}(\mathcal{V}^{-4/3})} &= \frac{3}{4\tau_b^2} \partial_\mu c_b \partial^\mu c_b.
\end{aligned}$$

At leading order the kinetic terms become canonical if τ_b is replaced by ϕ_b defined as:

$$\frac{\phi_b}{M_p} = \sqrt{\frac{3}{2}} \ln \tau_b, \quad (\text{C.10})$$

whereas $\mathcal{L}_{\text{kin}}^{\mathcal{O}(\mathcal{V}^{-1})}$ becomes diagonal if the small modulus T_s and the Wilson modulus \tilde{T}_p are substituted by:

$$\begin{aligned}
\frac{\phi_s}{M_p} &= \sqrt{\frac{4\lambda_s}{3\mathcal{V}}} \tau_s^{3/4}, & \frac{a_s}{M_p} &= \sqrt{\frac{3\lambda_s}{4\mathcal{V}\sqrt{\tau_s}}} c_s, \\
\frac{\tilde{\phi}_p}{M_p} &= \sqrt{\frac{4\lambda_p}{3\mathcal{V}}} \tilde{\tau}_p^{3/4}, & \frac{\tilde{a}_p}{M_p} &= \sqrt{\frac{3\lambda_p}{4\mathcal{V}\sqrt{\tilde{\tau}_p}}} \tilde{c}_p,
\end{aligned} \quad (\text{C.11})$$

and the canonical normalisation (C.10) for τ_b gets modified by the inclusion of a subleading mixing with τ_s and $\tilde{\tau}_p$ of the form:

$$\frac{\phi_b}{M_p} = \sqrt{\frac{3}{2}} \ln \tau_b - \sqrt{\frac{2}{3}} \frac{1}{\mathcal{V}} (\lambda_s \tau_s^{3/2} + \lambda_p \tilde{\tau}_p^{3/2}). \quad (\text{C.12})$$

Finally the kinetic term in $\mathcal{L}_{\text{kin}}^{\mathcal{O}(\mathcal{V}^{-4/3})}$ are canonically normalised if the bulk axion c_b gets redefined as:

$$\frac{a_b}{M_p} = \sqrt{\frac{3}{2}} \frac{c_b}{\tau_b}. \quad (\text{C.13})$$

The $U(1)$ -charged open string mode C appears in the kinetic Lagrangian only at $\mathcal{O}(|C|^2 \mathcal{V}^{-2/3})$ which according to (4.60) and (4.61) can scale as either $\mathcal{V}^{-8/3}$ or $\mathcal{V}^{-14/3}$. This part of the kinetic Lagrangian looks like:

$$\mathcal{L}_{\text{kin}} \supset \tilde{K} |C|^2 \left(\frac{\partial_\mu |C|}{|C|} \frac{\partial^\mu |C|}{|C|} + \partial_\mu \theta \partial^\mu \theta - \frac{\partial_\mu \tau_b}{\tau_b} \frac{\partial^\mu |C|}{|C|} \right), \quad (\text{C.14})$$

and becomes diagonal by redefining:

$$\frac{|\hat{C}|}{M_p} = \sqrt{2\tilde{K}}|C| \quad \text{and} \quad a_{ALP} = |\hat{C}|\theta = f_{a_{ALP}}\theta.$$

C.0.3 Mass matrix

As described in Sec. 4.2.1, the moduli stabilised at tree-level are τ_{q_i} and $|\phi|$ while the corresponding axions are eaten up by two anomalous $U(1)$'s. Given that they fixed at $\mathcal{O}(1/\mathcal{V}^2)$, all these modes develop a mass of order the string scale:

$$m_{\tau_{q_i}} \sim m_{c_{q_i}} \sim m_{|\phi|} \sim m_\psi \sim M_s = g_s^{1/4} \sqrt{\pi} \frac{M_p}{\sqrt{\mathcal{V}}}. \quad (\text{C.15})$$

On the other hand, τ_b , τ_s , $\tilde{\tau}_p$ and the closed string axion c_s are stabilised at $\mathcal{O}(1/\mathcal{V}^3)$. The masses of the corresponding canonically normalised fields derived in App. C.0.2 are given by the eigenvalues of the mass matrix evaluated at the minimum of the $\mathcal{O}(1/\mathcal{V}^3)$ scalar potential. The leading order contributions of all the elements of this 4×4 matrix read:

$$\begin{aligned} \frac{\partial^2 V}{\partial \phi_b \partial \phi_b} &= \left(\frac{g_s}{8\pi}\right) \frac{9\lambda_s \tau_s^{3/2} W_0^2}{2\mathcal{V}^3}, \\ \frac{\partial^2 V}{\partial \phi_b \partial \phi_s} &= \left(\frac{g_s}{8\pi}\right) \frac{3\sqrt{2\lambda_s} \tau_s^{3/4}}{\sqrt{\mathcal{V}}} \left(\frac{W_0}{\mathcal{V}}\right)^2 (2\pi\tau_s), \\ \frac{\partial^2 V}{\partial \phi_s \partial \phi_s} &= \frac{\partial^2 V}{\partial a_s \partial a_s} = 4 \left(\frac{g_s}{8\pi}\right) \left(\frac{W_0}{\mathcal{V}}\right)^2 (2\pi\tau_s)^2, \\ \frac{\partial^2 V}{\partial \tilde{\phi}_p \partial \tilde{\phi}_p} &= \left(\frac{g_s}{8\pi}\right) \frac{1}{4z_p \tilde{\tau}_p} \left(\frac{W_0}{\mathcal{V}}\right)^2, \\ \frac{\partial^2 V}{\partial \phi_b \partial \tilde{\phi}_p} &= \frac{\partial^2 V}{\partial \phi_b \partial a_s} = \frac{\partial^2 V}{\partial \phi_s \partial \tilde{\phi}_p} = \frac{\partial^2 V}{\partial \phi_s \partial a_s} = \frac{\partial^2 V}{\partial \tilde{\phi}_p \partial a_s} = 0, \end{aligned}$$

The eigenvalues of this mass matrix turn out to be:

$$\begin{aligned} m_{\phi_s}^2 &= m_{a_s}^2 = 4 \left(\frac{g_s}{8\pi}\right) \left(\frac{W_0}{\mathcal{V}}\right)^2 (2\pi\tau_s)^2 \simeq m_{3/2}^2 (\ln \mathcal{V})^2, \\ m_{\tilde{\phi}_p}^2 &= \left(\frac{g_s}{8\pi}\right) \frac{\pi}{2z_p} \left(\frac{W_0}{\mathcal{V}}\right)^2 \frac{1}{2\pi\tilde{\tau}_p} \simeq \frac{m_{3/2}^2}{\ln \mathcal{V}} \quad \text{and} \quad m_{\phi_b}^2 = 0, \end{aligned} \quad (\text{C.16})$$

where the gravitino mass is given by:

$$m_{3/2}^2 = e^K |W|^2 \simeq \left(\frac{g_s}{8\pi}\right) \left(\frac{W_0}{\mathcal{V}}\right)^2. \quad (\text{C.17})$$

The mass of the canonically normalised large modulus ϕ_b becomes non-zero once we include subleading $1/(2\pi\tau_s) \sim 1/\ln \mathcal{V} \ll 1$ corrections to the elements of the mass matrix, and scales as (with c an $\mathcal{O}(1)$ numerical coefficient):

$$m_{\phi_b}^2 = c \lambda_s \tau_s^{3/2} \left(\frac{g_s}{8\pi} \right) \frac{W_0^2}{\mathcal{V}^3} \frac{1}{2\pi\tau_s} \simeq \frac{m_{3/2}^2}{\mathcal{V} \ln \mathcal{V}}. \quad (\text{C.18})$$

As explained in Sec. 4.2.3, the charged matter field $|C|$ is fixed by soft supersymmetry breaking contributions to the scalar potential and can acquire a mass of order $m_{3/2}/\sqrt{\mathcal{V}}$ or $m_{3/2}/\mathcal{V}$ depending on the level of sequestering. The corresponding phase $\theta = a_{ALP}/f_{a_{ALP}}$ behaves as an open string ALP which develops a mass of order:

$$m_{a_{ALP}} \sim \frac{\Lambda_{\text{hid}}^2}{f_{a_{ALP}}} \sim \frac{\Lambda_{\text{hid}}^2}{|\hat{C}|}, \quad (\text{C.19})$$

where Λ_{hid} is the scale of strong dynamics effects in the hidden sector. In order to obtain a phenomenologically viable value $m_{a_{ALP}} \lesssim 10^{-12}$ eV, we need to have $\Lambda_{\text{hid}} \lesssim 10^4$ eV if $f_{a_{ALP}} \sim m_{3/2} \sim 10^{10}$ GeV or $\Lambda_{\text{hid}} \lesssim 1$ eV if $f_{a_{ALP}} \sim m_{3/2}/\mathcal{V} \sim 1$ TeV.

The DM axion c_p is stabilised by tiny poly-instanton corrections at $\mathcal{O}(1/\mathcal{V}^{3+p})$. Using the fact that $K_{T_p \bar{T}_p}^{-1} \sim \mathcal{V} \sqrt{\tilde{\tau}_p}$ and the expression (4.62) for the scalar potential for c_p , its mass can be easily estimated as:

$$m_{\tilde{a}_p}^2 \sim K_{T_p \bar{T}_p}^{-1} \frac{\partial^2 V_F^{\text{poly}}(c_p)}{\partial c_p^2} \sim \left(\frac{g_s}{8\pi} \right) \frac{W_0^2}{\mathcal{V}^{2+p}} 2\pi \tilde{\tau}_p \sim \frac{m_{3/2}^2}{\mathcal{V}^p} \ln \mathcal{V}. \quad (\text{C.20})$$

If the volume is of order $\mathcal{V} \sim 10^7$, this mass can be around 10 keV if $p = 9/2$. As explained in Sec. 4.3.2 this value of p can be accommodated by an appropriate choice of underlying flux parameters. Finally the axion c_b of the large modulus $T_b = \tau_b + i c_b$ can receive a potential only from highly suppressed non-perturbative contributions to the superpotential of the form $W_{\text{np}} \supset A_b e^{-2\pi T_b}$ which can be shown to lead to a mass for the axion c_b that scales as:

$$m_{a_b}^2 \sim \left(\frac{g_s}{8\pi} \right) \frac{M_p^2}{\mathcal{V}^{4/3}} e^{-\frac{2\pi}{\lambda_b^{2/3}} \mathcal{V}^{2/3}} \sim 0. \quad (\text{C.21})$$

Bibliography

- [1] M. Cicoli, V. A. Diaz, V. Guidetti and M. Rummel, JHEP **1710**, 192 (2017)
- [2] M. Cicoli, D. Ciupke, V. A. Diaz, V. Guidetti, F. Muia and P. Shukla, JHEP **1711**, 207 (2017).
- [3] M. Cicoli, V. A. Diaz and F. G. Pedro, JCAP **1806**, no. 06, 034 (2018).
- [4] D. N. Spergel *et al.* [WMAP Collaboration], Astrophys. J. Suppl. **148**, 175 (2003).
- [5] D. N. Spergel *et al.* [WMAP Collaboration], Astrophys. J. Suppl. **170**, 377 (2007).
- [6] E. Komatsu *et al.* [WMAP Collaboration], Astrophys. J. Suppl. **180**, 330 (2009).
- [7] N. Aghanim *et al.* [Planck Collaboration], “Planck 2018 results. VI. Cosmological parameters,” arXiv:1807.06209 [astro-ph.CO].
- [8] A. H. Guth, Phys. Rev. D **23**, 347 (1981).
- [9] A. D. Linde, Phys. Lett. **108B**, 389 (1982).
- [10] V. F. Mukhanov and G. V. Chibisov, JETP Lett. **33**, 532 (1981) [Pisma Zh. Eksp. Teor. Fiz. **33**, 549 (1981)].
- [11] A. H. Guth and S. Y. Pi, Phys. Rev. Lett. **49**, 1110 (1982).
- [12] A. D. Linde, Phys. Lett. **129B**, 177 (1983).
- [13] M. Cicoli and F. Quevedo, Class. Quant. Grav. **28**, 204001 (2011).
- [14] M. Cicoli, C. P. Burgess and F. Quevedo, JCAP **0903**, 013 (2009).
- [15] L. McAllister, E. Silverstein and A. Westphal, Phys. Rev. D **82**, 046003 (2010).

- [16] V. Mukhanov, “Physical Foundations of Cosmology,” Cambridge University Press, (2008).
- [17] D. Baumann and L. McAllister, “Inflation and String Theory,” Cambridge University Press, (2015).
- [18] C. P. Burgess, “Intro to Effective Field Theories and Inflation,” arXiv:1711.10592 [hep-th].
- [19] O. Y. Gnedin and J. P. Ostriker, “Limits on collisional dark matter from elliptical galaxies in clusters,” *Astrophys. J.* **561**, 61 (2001).
- [20] E. Aprile *et al.* [XENON100 Collaboration], “Dark Matter Results from 225 Live Days of XENON100 Data,” *Phys. Rev. Lett.* **109**, 181301 (2012).
- [21] D. S. Akerib *et al.* [LUX Collaboration], “Results from a search for dark matter in the complete LUX exposure,” *Phys. Rev. Lett.* **118**, no. 2, 021303 (2017).
- [22] W. B. Atwood *et al.* [Fermi-LAT Collaboration], “The Large Area Telescope on the Fermi Gamma-ray Space Telescope Mission,” *Astrophys. J.* **697**, 1071 (2009).
- [23] G. Steigman and M. S. Turner, “Cosmological Constraints on the Properties of Weakly Interacting Massive Particles,” *Nucl. Phys. B* **253**, 375 (1985).
- [24] R. D. Peccei and H. R. Quinn, “CP Conservation in the Presence of Instantons,” *Phys. Rev. Lett.* **38**, 1440 (1977).
- [25] G. Ballesteros and M. Taoso, *Phys. Rev. D* **97**, no. 2, 023501 (2018) doi:10.1103/PhysRevD.97.023501 [arXiv:1709.05565 [hep-ph]].
- [26] B. P. Abbott *et al.* [LIGO Scientific and Virgo Collaborations], *Phys. Rev. Lett.* **116**, no. 6, 061102 (2016) doi:10.1103/PhysRevLett.116.061102 [arXiv:1602.03837 [gr-qc]].
- [27] B. P. Abbott *et al.* [LIGO Scientific and VIRGO Collaborations], *Phys. Rev. Lett.* **118**, no. 22, 221101 (2017) doi:10.1103/PhysRevLett.118.221101 [arXiv:1706.01812 [gr-qc]].
- [28] R. Blumenhagen, D. Lüst, and S. Theisen, “Basic Concepts of String Theory”, Cambridge University Press, (2013).
- [29] L. E. Ibáñez and A. M. Uranga, “String Theory and Particle Physics: An Introduction to String Phenomenology”, Cambridge University Press, (2012).

- [30] K. Becker, M. Becker, and J. H. Schwarz, "String Theory and M-Theory: A Modern Introduction", Cambridge University Press, (2007).
- [31] J. Polchinski, "String Theory, Vols. 1 y 2", Cambridge University Press, (2005).
- [32] M. Duff, B.E.W. Nilsson, and C. Pope, "Kaluza-Klein Supergravity", Phys. Rept. 130 (1986) 1-142.
- [33] J. Wess and J. Bagger, "Supersymmetry And Supergravity", Princeton University Press, Princeton, (1992).
- [34] T. W. Grimm and J. Louis, Nucl. Phys. B699 (2004) 387-426
- [35] S. B. Giddings, S. Kachru and J. Polchinski, "Hierarchies from fluxes in string compactifications," Phys. Rev. D **66** (2002) 106006.
- [36] K. Becker, M. Becker, M. Haack and J. Louis, "Supersymmetry breaking and alpha-prime corrections to flux induced potentials," JHEP **0206** (2002) 060.
- [37] R. Minasian, T. G. Pugh and R. Savelli, "F-theory at order α^3 ," JHEP **1510** (2015) 050.
- [38] G. von Gersdorff and A. Hebecker, Phys. Lett. B **624**, 270 (2005).
- [39] M. Berg, M. Haack and B. Kors, "String loop corrections to Kahler potentials in orientifolds," JHEP **0511** (2005) 030.
- [40] M. Berg, M. Haack and E. Pajer, "Jumping Through Loops: On Soft Terms from Large Volume Compactifications," JHEP **0709** (2007) 031.
- [41] M. Cicoli, J. P. Conlon and F. Quevedo, "Systematics of String Loop Corrections in Type IIB Calabi-Yau Flux Compactifications," JHEP **0801** (2008) 052.
- [42] M. Cicoli, J. P. Conlon and F. Quevedo, "General Analysis of LARGE Volume Scenarios with String Loop Moduli Stabilisation," JHEP **0810** (2008) 105.
- [43] V. Balasubramanian, P. Berglund, J. P. Conlon and F. Quevedo, "Systematics of moduli stabilisation in Calabi-Yau flux compactifications," JHEP **0503** (2005) 007
- [44] J. P. Conlon, F. Quevedo and K. Suruliz, "Large-volume flux compactifications: Moduli spectrum and D3/D7 soft supersymmetry breaking," JHEP **0508** (2005) 007

- [45] D. H. Lyth, “What would we learn by detecting a gravitational wave signal in the cosmic microwave background anisotropy?,” *Phys. Rev. Lett.* **78** (1997) 1861 doi:10.1103/PhysRevLett.78.1861 [hep-ph/9606387].
- [46] L. McAllister and E. Silverstein, “String Cosmology: A Review,” *Gen. Rel. Grav.* **40** (2008) 565 doi:10.1007/s10714-007-0556-6 [arXiv:0710.2951 [hep-th]].
- [47] D. Baumann and L. McAllister, “Advances in Inflation in String Theory,” *Ann. Rev. Nucl. Part. Sci.* **59** (2009) 67 doi:10.1146/annurev.nucl.010909.083524 [arXiv:0901.0265 [hep-th]].
- [48] C. P. Burgess, M. Cicoli and F. Quevedo, “String Inflation After Planck 2013,” *JCAP* **1311** (2013) 003 doi:10.1088/1475-7516/2013/11/003 [arXiv:1306.3512 [hep-th]].
- [49] C. P. Burgess, M. Cicoli, F. Quevedo and M. Williams, “Inflating with Large Effective Fields,” *JCAP* **1411** (2014) 045 doi:10.1088/1475-7516/2014/11/045 [arXiv:1404.6236 [hep-th]].
- [50] R. Blumenhagen, S. Moster and E. Plauschinn, “Moduli Stabilisation versus Chirality for MSSM like Type IIB Orientifolds,” *JHEP* **0801** (2008) 058 doi:10.1088/1126-6708/2008/01/058 [arXiv:0711.3389 [hep-th]].
- [51] D. R. Green, “Reheating Closed String Inflation,” *Phys. Rev. D* **76** (2007) 103504 doi:10.1103/PhysRevD.76.103504 [arXiv:0707.3832 [hep-th]].
- [52] R. H. Brandenberger, A. Knauf and L. C. Lorenz, “Reheating in a Brane Monodromy Inflation Model,” *JHEP* **0810** (2008) 110 doi:10.1088/1126-6708/2008/10/110 [arXiv:0808.3936 [hep-th]].
- [53] N. Barnaby, J. R. Bond, Z. Huang and L. Kofman, “Preheating After Modular Inflation,” *JCAP* **0912** (2009) 021 doi:10.1088/1475-7516/2009/12/021 [arXiv:0909.0503 [hep-th]].
- [54] M. Cicoli and A. Mazumdar, “Reheating for Closed String Inflation,” *JCAP* **1009** (2010) no.09, 025 doi:10.1088/1475-7516/2010/09/025 [arXiv:1005.5076 [hep-th]]; M. Cicoli and A. Mazumdar, “Inflation in string theory: A Graceful exit to the real world,” *Phys. Rev. D* **83** (2011) 063527 doi:10.1103/PhysRevD.83.063527 [arXiv:1010.0941 [hep-th]].
- [55] K. Dutta and A. Maharana, “Inflationary constraints on modulus dominated cosmology,” *Phys. Rev. D* **91** (2015) no.4, 043503 doi:10.1103/PhysRevD.91.043503 [arXiv:1409.7037 [hep-ph]].

- [56] M. Cicoli, K. Dutta, A. Maharana and F. Quevedo, “Moduli Vacuum Misalignment and Precise Predictions in String Inflation,” *JCAP* **1608** (2016) no.08, 006 doi:10.1088/1475-7516/2016/08/006 [arXiv:1604.08512 [hep-th]].
- [57] S. Bhattacharya, K. Dutta and A. Maharana, “Constraints on Kähler Moduli Inflation from Reheating,” arXiv:1707.07924 [hep-ph].
- [58] M. Cicoli, J. P. Conlon and F. Quevedo, “Dark radiation in LARGE volume models,” *Phys. Rev. D* **87** (2013) no.4, 043520 doi:10.1103/PhysRevD.87.043520 [arXiv:1208.3562 [hep-ph]].
- [59] T. Higaki and F. Takahashi, “Dark Radiation and Dark Matter in Large Volume Compactifications,” *JHEP* **1211** (2012) 125 doi:10.1007/JHEP11(2012)125 [arXiv:1208.3563 [hep-ph]].
- [60] A. Hebecker, P. Mangat, F. Rompineve and L. T. Witkowski, “Dark Radiation predictions from general Large Volume Scenarios,” *JHEP* **1409** (2014) 140 doi:10.1007/JHEP09(2014)140 [arXiv:1403.6810 [hep-ph]].
- [61] M. Cicoli and F. Muia, “General Analysis of Dark Radiation in Sequestered String Models,” *JHEP* **1512** (2015) 152 doi:10.1007/JHEP12(2015)152 [arXiv:1511.05447 [hep-th]].
- [62] B. S. Acharya, P. Kumar, K. Bobkov, G. Kane, J. Shao and S. Watson, “Non-thermal Dark Matter and the Moduli Problem in String Frameworks,” *JHEP* **0806** (2008) 064 doi:10.1088/1126-6708/2008/06/064 [arXiv:0804.0863 [hep-ph]].
- [63] R. Allahverdi, M. Cicoli, B. Dutta and K. Sinha, “Nonthermal dark matter in string compactifications,” *Phys. Rev. D* **88** (2013) no.9, 095015 doi:10.1103/PhysRevD.88.095015 [arXiv:1307.5086 [hep-ph]]; R. Allahverdi, M. Cicoli, B. Dutta and K. Sinha, “Correlation between Dark Matter and Dark Radiation in String Compactifications,” *JCAP* **1410** (2014) 002 doi:10.1088/1475-7516/2014/10/002 [arXiv:1401.4364 [hep-ph]].
- [64] L. Aparicio, M. Cicoli, B. Dutta, S. Krippendorff, A. Maharana, F. Muia and F. Quevedo, “Non-thermal CMSSM with a 125 GeV Higgs,” *JHEP* **1505** (2015) 098 doi:10.1007/JHEP05(2015)098 [arXiv:1502.05672 [hep-ph]]; L. Aparicio, B. Dutta, M. Cicoli, F. Muia and F. Quevedo, “Light Higgsino Dark Matter from Non-thermal Cosmology,” *JHEP* **1611** (2016) 038 [arXiv:1607.00004 [hep-ph]].

- [65] G. Kane, J. Shao, S. Watson and H. B. Yu, “The Baryon-Dark Matter Ratio Via Moduli Decay After Affleck-Dine Baryogenesis,” *JCAP* **1111** (2011) 012 doi:10.1088/1475-7516/2011/11/012 [arXiv:1108.5178 [hep-ph]].
- [66] R. Allahverdi, M. Cicoli and F. Muia, “Affleck-Dine Baryogenesis in Type IIB String Models,” *JHEP* **1606** (2016) 153 doi:10.1007/JHEP06(2016)153 [arXiv:1604.03120 [hep-th]].
- [67] J. P. Conlon, R. Kallosh, A. D. Linde and F. Quevedo, “Volume Modulus Inflation and the Gravitino Mass Problem,” *JCAP* **0809** (2008) 011 doi:10.1088/1475-7516/2008/09/011 [arXiv:0806.0809 [hep-th]]; M. Cicoli, F. Muia and F. G. Pedro, “Microscopic Origin of Volume Modulus Inflation,” *JCAP* **1512** (2015) no.12, 040 doi:10.1088/1475-7516/2015/12/040 [arXiv:1509.07748 [hep-th]].
- [68] T. He, S. Kachru and A. Westphal, “Gravity waves and the LHC: Towards high-scale inflation with low-energy SUSY,” *JHEP* **1006** (2010) 065 doi:10.1007/JHEP06(2010)065 [arXiv:1003.4265 [hep-th]].
- [69] S. Antusch, K. Dutta and S. Halter, “Combining High-scale Inflation with Low-energy SUSY,” *JHEP* **1203** (2012) 105 doi:10.1007/JHEP03(2012)105 [arXiv:1112.4488 [hep-th]].
- [70] W. Buchmuller, E. Dudas, L. Heurtier and C. Wieck, “Large-Field Inflation and Supersymmetry Breaking,” *JHEP* **1409** (2014) 053 doi:10.1007/JHEP09(2014)053 [arXiv:1407.0253 [hep-th]].
- [71] J. P. Conlon and F. Quevedo, “Kahler moduli inflation,” *JHEP* **0601** (2006) 146 doi:10.1088/1126-6708/2006/01/146 [hep-th/0509012].
- [72] M. Cicoli, I. García-Etxebarria, C. Mayrhofer, F. Quevedo, P. Shukla and R. Valandro, “Global Orientifolded Quivers with Inflation,” arXiv:1706.06128 [hep-th].
- [73] M. Berg, M. Haack, J. U. Kang and S. Sjors, “Towards the one-loop Kähler metric of Calabi-Yau orientifolds,” *JHEP* **1412** (2014) 077 doi:10.1007/JHEP12(2014)077 [arXiv:1407.0027 [hep-th], arXiv:1407.0027].
- [74] M. Haack and J. U. Kang, “One-loop Einstein-Hilbert term in minimally supersymmetric type IIB orientifolds,” *JHEP* **1602** (2016) 160 doi:10.1007/JHEP02(2016)160 [arXiv:1511.03957 [hep-th]].

- [75] D. Ciupke, J. Louis and A. Westphal, “Higher-Derivative Supergravity and Moduli Stabilization,” *JHEP* **1510** (2015) 094 doi:10.1007/JHEP10(2015)094 [arXiv:1505.03092 [hep-th]].
- [76] T. W. Grimm, K. Mayer and M. Weissenbacher, “Higher derivatives in Type II and M-theory on Calabi-Yau threefolds,” arXiv:1702.08404 [hep-th].
- [77] B. J. Broy, D. Ciupke, F. G. Pedro and A. Westphal, “Starobinsky-Type Inflation from α' -Corrections,” *JCAP* **1601** (2016) 001 doi:10.1088/1475-7516/2016/01/001 [arXiv:1509.00024 [hep-th]].
- [78] M. Cicoli, D. Ciupke, S. de Alwis and F. Muia, “ α' Inflation: moduli stabilisation and observable tensors from higher derivatives,” *JHEP* **1609** (2016) 026 doi:10.1007/JHEP09(2016)026 [arXiv:1607.01395 [hep-th]].
- [79] C. P. Burgess, M. Cicoli, S. de Alwis and F. Quevedo, “Robust Inflation from Fibrous Strings,” *JCAP* **1605** (2016) no.05, 032 doi:10.1088/1475-7516/2016/05/032 [arXiv:1603.06789 [hep-th]].
- [80] Y. Akrami *et al.* [Planck Collaboration], “Planck 2018 results. X. Constraints on inflation,” arXiv:1807.06211 [astro-ph.CO].
- [81] R. Kallosh, A. Linde, D. Roest, A. Westphal and Y. Yamada, “Fibre Inflation and α -attractors,” arXiv:1707.05830 [hep-th].
- [82] M. Cicoli, F. Muia and P. Shukla, “Global Embedding of Fibre Inflation Models,” *JHEP* **1611** (2016) 182 doi:10.1007/JHEP11(2016)182 [arXiv:1611.04612 [hep-th]].
- [83] M. Cicoli, M. Kreuzer and C. Mayrhofer, “Toric K3-Fibred Calabi-Yau Manifolds with del Pezzo Divisors for String Compactifications,” *JHEP* **1202** (2012) 002 doi:10.1007/JHEP02(2012)002 [arXiv:1107.0383 [hep-th]].
- [84] M. Kreuzer and H. Skarke, “Complete classification of reflexive polyhedra in four-dimensions,” *Adv. Theor. Math. Phys.* **4** (2002) 1209 [hep-th/0002240].
- [85] S. Angus, “Dark Radiation in Anisotropic LARGE Volume Compactifications,” *JHEP* **1410** (2014) 184 doi:10.1007/JHEP10(2014)184 [arXiv:1403.6473 [hep-ph]].
- [86] M. Cicoli, J. P. Conlon, A. Maharana and F. Quevedo, “A Note on the Magnitude of the Flux Superpotential,” *JHEP* **1401** (2014) 027 doi:10.1007/JHEP01(2014)027 [arXiv:1310.6694 [hep-th]].

- [87] F. Bonetti and M. Weissenbacher, “The Euler characteristic correction to the Kähler potential $\tilde{\chi}$ revisited,” JHEP **1701** (2017) 003 doi:10.1007/JHEP01(2017)003 [arXiv:1608.01300 [hep-th]].
- [88] S. Kachru, R. Kallosh, A. D. Linde and S. P. Trivedi, “De Sitter vacua in string theory,” Phys. Rev. D **68** (2003) 046005 doi:10.1103/PhysRevD.68.046005 [hep-th/0301240].
- [89] R. Kallosh and T. Wrase, “Emergence of Spontaneously Broken Supersymmetry on an Anti-D3-Brane in KKLT dS Vacua,” JHEP **1412** (2014) 117 doi:10.1007/JHEP12(2014)117 [arXiv:1411.1121 [hep-th]];
R. Kallosh, F. Quevedo and A. M. Uranga, “String Theory Realizations of the Nilpotent Goldstino,” JHEP **1512** (2015) 039 doi:10.1007/JHEP12(2015)039 [arXiv:1507.07556 [hep-th]]; L. Aparicio, F. Quevedo and R. Valandro, “Moduli Stabilisation with Nilpotent Goldstino: Vacuum Structure and SUSY Breaking,” JHEP **1603** (2016) 036 doi:10.1007/JHEP03(2016)036 [arXiv:1511.08105 [hep-th]]; M. P. Garcia del Moral, S. Parameswaran, N. Quiroz and I. Zavala, “Anti-D3 branes and moduli in non-linear supergravity,” arXiv:1707.07059 [hep-th]; J. Moritz, A. Retolaza and A. Westphal, “Towards de Sitter from 10D,” arXiv:1707.08678 [hep-th].
- [90] E. A. Bergshoeff, K. Dasgupta, R. Kallosh, A. Van Proeyen and T. Wrase, “ $\overline{D3}$ and dS,” JHEP **1505** (2015) 058 doi:10.1007/JHEP05(2015)058 [arXiv:1502.07627 [hep-th]].
- [91] I. Garca-Etxebarria, F. Quevedo and R. Valandro, “Global String Embeddings for the Nilpotent Goldstino,” JHEP **1602** (2016) 148 doi:10.1007/JHEP02(2016)148 [arXiv:1512.06926 [hep-th]].
- [92] M. Cicoli, F. Quevedo and R. Valandro, “De Sitter from T-branes,” JHEP **1603** (2016) 141 doi:10.1007/JHEP03(2016)141 [arXiv:1512.04558 [hep-th]].
- [93] M. Cicoli, A. Maharana, F. Quevedo and C. P. Burgess, “De Sitter String Vacua from Dilaton-dependent Non-perturbative Effects,” JHEP **1206** (2012) 011 doi:10.1007/JHEP06(2012)011 [arXiv:1203.1750 [hep-th]].
- [94] A. Westphal, “String Cosmology $\tilde{\chi}$ Large-Field Inflation in String Theory,” Adv. Ser. Direct. High Energy Phys. **22** (2015) 351.
- [95] M. Remazeilles, C. Dickinson, H. K. K. Eriksen and I. K. Wehus, “Sensitivity and foreground modelling for large-scale cosmic microwave background B-mode

- polarization satellite missions,” *Mon. Not. Roy. Astron. Soc.* **458** (2016) no.2, 2032 doi:10.1093/mnras/stw441 [arXiv:1509.04714 [astro-ph.CO]].
- [96] M. Remazeilles, C. Dickinson, H. K. Eriksen and I. K. Wehus, “Joint Bayesian estimation of tensor and lensing B-modes in the power spectrum of CMB polarization data,” arXiv:1707.02981 [astro-ph.CO].
- [97] R. Minasian and G. W. Moore, “K theory and Ramond-Ramond charge,” *JHEP* **9711** (1997) 002 doi:10.1088/1126-6708/1997/11/002 [hep-th/9710230].
- [98] D. S. Freed and E. Witten, “Anomalies in string theory with D-branes,” *Asian J. Math.* **3** (1999) 819 [hep-th/9907189].
- [99] M. Dine, N. Seiberg and E. Witten, “Fayet-Iliopoulos Terms in String Theory,” *Nucl. Phys. B* **289** (1987) 589. doi:10.1016/0550-3213(87)90395-6
- [100] M. Dine, I. Ichinose and N. Seiberg, “F Terms and d Terms in String Theory,” *Nucl. Phys. B* **293** (1987) 253. doi:10.1016/0550-3213(87)90072-1
- [101] R. Altman, J. Gray, Y. H. He, V. Jejjala and B. D. Nelson, “A Calabi-Yau Database: Threefolds Constructed from the Kreuzer-Skarke List,” *JHEP* **1502** (2015) 158 doi:10.1007/JHEP02(2015)158 [arXiv:1411.1418 [hep-th]].
- [102] R. Blumenhagen, B. Jurke, T. Rahn and H. Roschy, “Cohomology of Line Bundles: A Computational Algorithm,” *J. Math. Phys.* **51** (2010) 103525 doi:10.1063/1.3501132, 10.1063/1.3523343 [arXiv:1003.5217 [hep-th]].
- [103] R. Blumenhagen, B. Jurke and T. Rahn, “Computational Tools for Cohomology of Toric Varieties,” *Adv. High Energy Phys.* **2011** (2011) 152749 doi:10.1155/2011/152749 [arXiv:1104.1187 [hep-th]].
- [104] M. Cicoli, S. Krippendorff, C. Mayrhofer, F. Quevedo and R. Valandro, “D-Branes at del Pezzo Singularities: Global Embedding and Moduli Stabilisation,” *JHEP* **1209**, 019 (2012) doi:10.1007/JHEP09(2012)019 [arXiv:1206.5237 [hep-th]].
- [105] P. G. Camara, L. E. Ibanez and A. M. Uranga, “Flux-induced SUSY-breaking soft terms on D7-D3 brane systems,” *Nucl. Phys. B* **708** (2005) 268 doi:10.1016/j.nuclphysb.2004.11.035 [hep-th/0408036].
- [106] D. Ciupke, “Scalar Potential from Higher Derivative $\mathcal{N} = 1$ Superspace,” arXiv:1605.00651 [hep-th].

- [107] M. Cicoli, S. Downes and B. Dutta, “Power Suppression at Large Scales in String Inflation,” *JCAP* **1312** (2013) 007 doi:10.1088/1475-7516/2013/12/007 [arXiv:1309.3412 [hep-th]]; M. Cicoli, S. Downes, B. Dutta, F. G. Pedro and A. Westphal, “Just enough inflation: power spectrum modifications at large scales,” *JCAP* **1412** (2014) no.12, 030 doi:10.1088/1475-7516/2014/12/030 [arXiv:1407.1048 [hep-th]].
- [108] D. Klaeuer and E. Palti, “Super-Planckian Spatial Field Variations and Quantum Gravity,” *JHEP* **1701** (2017) 088 doi:10.1007/JHEP01(2017)088 [arXiv:1610.00010 [hep-th]].
- [109] R. Blumenhagen, I. Valenzuela and F. Wolf, “The Swampland Conjecture and F-term Axion Monodromy Inflation,” arXiv:1703.05776 [hep-th].
- [110] J. J. Blanco-Pillado, D. Buck, E. J. Copeland, M. Gomez-Reino and N. J. Nunes, “Kahler Moduli Inflation Revisited,” *JHEP* **1001** (2010) 081 doi:10.1007/JHEP01(2010)081 [arXiv:0906.3711 [hep-th]].
- [111] D. H. Lyth and D. Wands, “Generating the curvature perturbation without an inflaton,” *Phys. Lett. B* **524** (2002) 5 doi:10.1016/S0370-2693(01)01366-1 [hep-ph/0110002]; T. Moroi and T. Takahashi, “Effects of cosmological moduli fields on cosmic microwave background,” *Phys. Lett. B* **522** (2001) 215 Erratum: [*Phys. Lett. B* **539** (2002) 303] doi:10.1016/S0370-2693(02)02070-1, 10.1016/S0370-2693(01)01295-3 [hep-ph/0110096]; C. P. Burgess, M. Cicoli, M. Gomez-Reino, F. Quevedo, G. Tasinato and I. Zavala, “Non-standard primordial fluctuations and nongaussianity in string inflation,” *JHEP* **1008** (2010) 045 doi:10.1007/JHEP08(2010)045 [arXiv:1005.4840 [hep-th]].
- [112] M. Cicoli, D. Ciupke, C. Mayrhofer and P. Shukla, “A Geometrical Upper Bound on the Inflaton Range,” arXiv:1801.05434 [hep-th].
- [113] P. Cabella, A. Di Marco and G. Pradisi, “Fiber inflation and reheating,” *Phys. Rev. D* **95** (2017) no.12, 123528 doi:10.1103/PhysRevD.95.123528 [arXiv:1704.03209 [astro-ph.CO]].
- [114] S. Antusch, F. Cefala, S. Krippendorff, F. Muia, S. Orani and F. Quevedo, “Oscillons from String Moduli,” arXiv:1708.08922 [hep-th].
- [115] M. Cicoli, C. Mayrhofer and R. Valandro, “Moduli Stabilisation for Chiral Global Models,” *JHEP* **1202** (2012) 062 [arXiv:1110.3333 [hep-th]].

- [116] M. Sasaki, T. Suyama, T. Tanaka and S. Yokoyama, *Class. Quant. Grav.* **35**, no. 6, 063001 (2018).
- [117] S. W. Hawking, “Black hole explosions,” *Nature* **248**, 30 (1974).
- [118] Y. Ali-Haïmoud and M. Kamionkowski, “Cosmic microwave background limits on accreting primordial black holes,” *Phys. Rev. D* **95**, no. 4, 043534 (2017).
- [119] V. Poulin, P. D. Serpico, F. Calore, S. Clesse and K. Kohri, “CMB bounds on disk-accreting massive primordial black holes,” *Phys. Rev. D* **96**, no. 8, 083524 (2017).
- [120] D. Gaggero, G. Bertone, F. Calore, R. M. T. Connors, M. Lovell, S. Markoff and E. Storm, *Phys. Rev. Lett.* **118**, no. 24, 241101 (2017).
- [121] S. Hawking, ‘Gravitationally collapsed objects of very low mass,’ *Mon. Not. Roy. Astron. Soc.* **152**, 75 (1971).
- [122] B. J. Carr and S. W. Hawking, *Mon. Not. Roy. Astron. Soc.* **168**, 399 (1974).
- [123] M. Kawasaki, N. Kitajima and T. T. Yanagida, *Phys. Rev. D* **87**, no. 6, 063519 (2013).
- [124] B. Carr, F. Kuhnel and M. Sandstad, *Phys. Rev. D* **94**, no. 8, 083504 (2016) doi:10.1103/PhysRevD.94.083504 [arXiv:1607.06077 [astro-ph.CO]].
- [125] J. Garcia-Bellido, M. Peloso and C. Unal, *JCAP* **1612**, no. 12, 031 (2016) doi:10.1088/1475-7516/2016/12/031 [arXiv:1610.03763 [astro-ph.CO]].
- [126] P. Ivanov, P. Naselsky and I. Novikov, *Phys. Rev. D* **50**, 7173 (1994).
- [127] J. Garcia-Bellido and E. Ruiz Morales, *Phys. Dark Univ.* **18**, 47 (2017) doi:10.1016/j.dark.2017.09.007 [arXiv:1702.03901 [astro-ph.CO]].
- [128] J. M. Ezquiaga, J. Garcia-Bellido and E. Ruiz Morales, *Phys. Lett. B* **776**, 345 (2018) doi:10.1016/j.physletb.2017.11.039 [arXiv:1705.04861 [astro-ph.CO]].
- [129] C. Germani and T. Prokopec, *Phys. Dark Univ.* **18**, 6 (2017) doi:10.1016/j.dark.2017.09.001 [arXiv:1706.04226 [astro-ph.CO]].
- [130] M. P. Hertzberg and M. Yamada, *Phys. Rev. D* **97**, no. 8, 083509 (2018) doi:10.1103/PhysRevD.97.083509 [arXiv:1712.09750 [astro-ph.CO]].
- [131] E. Pajer and M. Peloso, *Class. Quant. Grav.* **30**, 214002 (2013) doi:10.1088/0264-9381/30/21/214002 [arXiv:1305.3557 [hep-th]].

- [132] C. P. Burgess, R. Kallosh and F. Quevedo, JHEP **0310**, 056 (2003) doi:10.1088/1126-6708/2003/10/056 [hep-th/0309187].
- [133] A. A. Starobinsky, Phys. Lett. B **91**, 99 (1980) [Phys. Lett. **91B**, 99 (1980)] [Adv. Ser. Astrophys. Cosmol. **3**, 130 (1987)]. doi:10.1016/0370-2693(80)90670-X
- [134] R. Kallosh and A. Linde, JCAP **1310**, 033 (2013) doi:10.1088/1475-7516/2013/10/033 [arXiv:1307.7938 [hep-th]].
- [135] R. Kallosh and A. Linde, Comptes Rendus Physique **16**, 914 (2015) doi:10.1016/j.crhy.2015.07.004 [arXiv:1503.06785 [hep-th]].
- [136] J. J. M. Carrasco, R. Kallosh and A. Linde, JHEP **1510**, 147 (2015) doi:10.1007/JHEP10(2015)147 [arXiv:1506.01708 [hep-th]].
- [137] K. Kannike, L. Marzola, M. Raidal and H. Veerm de, JCAP **1709**, no. 09, 020 (2017) doi:10.1088/1475-7516/2017/09/020 [arXiv:1705.06225 [astro-ph.CO]].
- [138] H. Motohashi and W. Hu, Phys. Rev. D **96**, no. 6, 063503 (2017) doi:10.1103/PhysRevD.96.063503 [arXiv:1706.06784 [astro-ph.CO]].
- [139] M. Sasaki, Prog. Theor. Phys. **76**, 1036 (1986).
- [140] V. F. Mukhanov, Sov. Phys. JETP **67**, 1297 (1988) [Zh. Eksp. Teor. Fiz. **94N7**, 1 (1988)].
- [141] F. G. Pedro and A. Westphal, JHEP **1404**, 034 (2014) doi:10.1007/JHEP04(2014)034 [arXiv:1309.3413 [hep-th]].
- [142] G. Franciolini, A. Kehagias, S. Matarrese and A. Riotto, JCAP **1803**, no. 03, 016 (2018) doi:10.1088/1475-7516/2018/03/016 [arXiv:1801.09415 [astro-ph.CO]].
- [143] B. J. Carr, K. Kohri, Y. Sendouda and J. Yokoyama, Phys. Rev. D **81**, 104019 (2010) doi:10.1103/PhysRevD.81.104019 [arXiv:0912.5297 [astro-ph.CO]].
- [144] K. Inomata, M. Kawasaki, K. Mukaida, Y. Tada and T. T. Yanagida, Phys. Rev. D **96**, no. 4, 043504 (2017) doi:10.1103/PhysRevD.96.043504 [arXiv:1701.02544 [astro-ph.CO]].
- [145] B. Carr, M. Raidal, T. Tenkanen, V. Vaskonen and H. Veerm de, Phys. Rev. D **96**, no. 2, 023514 (2017) doi:10.1103/PhysRevD.96.023514 [arXiv:1705.05567 [astro-ph.CO]].

- [146] T. S. Bunch and P. C. W. Davies, Proc. Roy. Soc. Lond. A **360**, 117 (1978).
- [147] J. Martin, H. Motohashi and T. Suyama, Phys. Rev. D **87**, no. 2, 023514 (2013) doi:10.1103/PhysRevD.87.023514 [arXiv:1211.0083 [astro-ph.CO]].
- [148] H. Motohashi, A. A. Starobinsky and J. Yokoyama, JCAP **1509**, 018 (2015) doi:10.1088/1475-7516/2015/09/018 [arXiv:1411.5021 [astro-ph.CO]].
- [149] W. H. Kinney, Phys. Rev. D **72**, 023515 (2005) doi:10.1103/PhysRevD.72.023515 [gr-qc/0503017].
- [150] N. C. Tsamis and R. P. Woodard, Phys. Rev. D **69**, 084005 (2004) doi:10.1103/PhysRevD.69.084005 [astro-ph/0307463].
- [151] M. H. Namjoo, H. Firouzjahi and M. Sasaki, EPL **101**, no. 3, 39001 (2013) doi:10.1209/0295-5075/101/39001 [arXiv:1210.3692 [astro-ph.CO]].
- [152] S. M. Leach and A. R. Liddle, Phys. Rev. D **63**, 043508 (2001) doi:10.1103/PhysRevD.63.043508 [astro-ph/0010082].
- [153] M. Gerbino, K. Freese, S. Vagnozzi, M. Lattanzi, O. Mena, E. Giusarma and S. Ho, Phys. Rev. D **95**, no. 4, 043512 (2017) doi:10.1103/PhysRevD.95.043512 [arXiv:1610.08830 [astro-ph.CO]].
- [154] S. Dimopoulos, S. Kachru, J. McGreevy and J. G. Wacker, JCAP **0808**, 003 (2008) doi:10.1088/1475-7516/2008/08/003 [hep-th/0507205].
- [155] R. Easther and L. McAllister, JCAP **0605**, 018 (2006) doi:10.1088/1475-7516/2006/05/018 [hep-th/0512102].
- [156] J. R. Bond, L. Kofman, S. Prokushkin and P. M. Vaudrevange, Phys. Rev. D **75**, 123511 (2007) doi:10.1103/PhysRevD.75.123511 [hep-th/0612197].
- [157] P. Berglund and G. Ren, arXiv:0912.1397 [hep-th].
- [158] M. Cicoli, G. Tasinato, I. Zavala, C. P. Burgess and F. Quevedo, JCAP **1205**, 039 (2012) doi:10.1088/1475-7516/2012/05/039 [arXiv:1202.4580 [hep-th]].
- [159] M. Cicoli, K. Dutta and A. Maharana, JCAP **1408**, 012 (2014) doi:10.1088/1475-7516/2014/08/012 [arXiv:1401.2579 [hep-th]].
- [160] C. Pattison, V. Vennin, H. Assadullahi and D. Wands, JCAP **1710**, no. 10, 046 (2017) doi:10.1088/1475-7516/2017/10/046 [arXiv:1707.00537 [hep-th]].

- [161] E. Bulbul, M. Markevitch, A. Foster, R. K. Smith, M. Loewenstein and S. W. Randall, “Detection of An Unidentified Emission Line in the Stacked X-ray spectrum of Galaxy Clusters,” *Astrophys. J.* **789** (2014) 13 doi:10.1088/0004-637X/789/1/13 [arXiv:1402.2301 [astro-ph.CO]].
- [162] A. Boyarsky, O. Ruchayskiy, D. Iakubovskiy and J. Franse, “Unidentified Line in X-Ray Spectra of the Andromeda Galaxy and Perseus Galaxy Cluster,” *Phys. Rev. Lett.* **113** (2014) 251301 doi:10.1103/PhysRevLett.113.251301 [arXiv:1402.4119 [astro-ph.CO]].
- [163] O. Urban, N. Werner, S. W. Allen, A. Simionescu, J. S. Kaastra and L. E. Strigari, “A Suzaku Search for Dark Matter Emission Lines in the X-ray Brightest Galaxy Clusters,” *Mon. Not. Roy. Astron. Soc.* **451** (2015) no.3, 2447 doi:10.1093/mnras/stv1142 [arXiv:1411.0050 [astro-ph.CO]].
- [164] J. Franse *et al.*, “Radial Profile of the 3.55 keV line out to R_{200} in the Perseus Cluster,” *Astrophys. J.* **829** (2016) no.2, 124 doi:10.3847/0004-637X/829/2/124 [arXiv:1604.01759 [astro-ph.CO]].
- [165] F. A. Aharonian *et al.* [Hitomi Collaboration], “Hitomi constraints on the 3.5 keV line in the Perseus galaxy cluster,” arXiv:1607.07420 [astro-ph.HE].
- [166] S. Riemer-Sørensen, “Constraints on the presence of a 3.5 keV dark matter emission line from Chandra observations of the Galactic centre,” *Astron. Astrophys.* **590** (2016) A71 doi:10.1051/0004-6361/201527278 [arXiv:1405.7943 [astro-ph.CO]].
- [167] T. E. Jeltema and S. Profumo, “Discovery of a 3.5 keV line in the Galactic Centre and a critical look at the origin of the line across astronomical targets,” *Mon. Not. Roy. Astron. Soc.* **450** (2015) no.2, 2143 doi:10.1093/mnras/stv768 [arXiv:1408.1699 [astro-ph.HE]].
- [168] A. Boyarsky, J. Franse, D. Iakubovskiy and O. Ruchayskiy, “Checking the Dark Matter Origin of a 3.53 keV Line with the Milky Way Center,” *Phys. Rev. Lett.* **115** (2015) 161301 doi:10.1103/PhysRevLett.115.161301 [arXiv:1408.2503 [astro-ph.CO]].
- [169] E. Carlson, T. Jeltema and S. Profumo, “Where do the 3.5 keV photons come from? A morphological study of the Galactic Center and of Perseus,” *JCAP* **1502** (2015) no.02, 009 doi:10.1088/1475-7516/2015/02/009 [arXiv:1411.1758 [astro-ph.HE]].

- [170] M. E. Anderson, E. Churazov and J. N. Bregman, “Non-Detection of X-Ray Emission From Sterile Neutrinos in Stacked Galaxy Spectra,” *Mon. Not. Roy. Astron. Soc.* **452** (2015) no.4, 3905 doi:10.1093/mnras/stv1559 [arXiv:1408.4115 [astro-ph.HE]].
- [171] D. Malyshev, A. Neronov and D. Eckert, “Constraints on 3.55 keV line emission from stacked observations of dwarf spheroidal galaxies,” *Phys. Rev. D* **90** (2014) 103506 doi:10.1103/PhysRevD.90.103506 [arXiv:1408.3531 [astro-ph.HE]].
- [172] T. E. Jeltema and S. Profumo, “Deep XMM Observations of Draco rule out at the 99% Confidence Level a Dark Matter Decay Origin for the 3.5 keV Line,” *Mon. Not. Roy. Astron. Soc.* **458** (2016) no.4, 3592 doi:10.1093/mnras/stw578 [arXiv:1512.01239 [astro-ph.HE]].
- [173] O. Ruchayskiy *et al.*, “Searching for decaying dark matter in deep XMM-Newton observation of the Draco dwarf spheroidal,” *Mon. Not. Roy. Astron. Soc.* **460** (2016) no.2, 1390 doi:10.1093/mnras/stw1026 [arXiv:1512.07217 [astro-ph.HE]].
- [174] D. Iakubovskiy, E. Bulbul, A. R. Foster, D. Savchenko and V. Sadova, “Testing the origin of 3.55 keV line in individual galaxy clusters observed with XMM-Newton,” arXiv:1508.05186 [astro-ph.HE].
- [175] F. Hofmann, J. S. Sanders, K. Nandra, N. Clerc and M. Gaspari, “7.1 keV sterile neutrino constraints from X-ray observations of 33 clusters of galaxies with Chandra ACIS,” *Astron. Astrophys.* **592** (2016) A112 doi:10.1051/0004-6361/201527977 [arXiv:1606.04091 [astro-ph.CO]].
- [176] D. Iakubovskiy, “Observation of the new emission line at 3.5 keV in X-ray spectra of galaxies and galaxy clusters,” *Advances in Astronomy and Space Physics* 2016, Vol. 6, No. 1, p. 3-15 doi:10.17721/2227-1481.6.3-15 [arXiv:1510.00358 [astro-ph.HE]].
- [177] L. Gu, J. Kaastra, A. J. J. Raassen, P. D. Mullen, R. S. Cumbee, D. Lyons and P. C. Stancil, “A novel scenario for the possible X-ray line feature at 3.5 keV: Charge exchange with bare sulfur ions,” *Astron. Astrophys.* **584** (2015) L11 doi:10.1051/0004-6361/201527634 [arXiv:1511.06557 [astro-ph.HE]].
- [178] S. Dodelson and L. M. Widrow, “Sterile-neutrinos as dark matter,” *Phys. Rev. Lett.* **72** (1994) 17 doi:10.1103/PhysRevLett.72.17 [hep-ph/9303287].

- [179] T. Asaka and M. Shaposhnikov, “The nuMSM, dark matter and baryon asymmetry of the universe,” *Phys. Lett. B* **620** (2005) 17 doi:10.1016/j.physletb.2005.06.020 [hep-ph/0505013].
- [180] M. Cicoli, J. P. Conlon, M. C. D. Marsh and M. Rummel, “3.55 keV photon line and its morphology from a 3.55 keV axionlike particle line,” *Phys. Rev. D* **90** (2014) 023540 doi:10.1103/PhysRevD.90.023540 [arXiv:1403.2370 [hep-ph]].
- [181] P. D. Alvarez, J. P. Conlon, F. V. Day, M. C. D. Marsh and M. Rummel, “Observational consistency and future predictions for a 3.5 keV ALP to photon line,” *JCAP* **1504** (2015) no.04, 013 doi:10.1088/1475-7516/2015/04/013 [arXiv:1410.1867 [hep-ph]].
- [182] J. P. Conlon, F. Day, N. Jennings, S. Krippendorf and M. Rummel, “Consistency of Hitomi, XMM-Newton and Chandra 3.5 keV data from Perseus,” arXiv:1608.01684 [astro-ph.HE].
- [183] P. Svrcek and E. Witten, “Axions In String Theory,” *JHEP* **0606** (2006) 051 doi:10.1088/1126-6708/2006/06/051 [hep-th/0605206].
- [184] J. P. Conlon, “The QCD axion and moduli stabilisation,” *JHEP* **0605** (2006) 078 doi:10.1088/1126-6708/2006/05/078 [hep-th/0602233].
- [185] A. Arvanitaki, S. Dimopoulos, S. Dubovsky, N. Kaloper and J. March-Russell, “String Axiverse,” *Phys. Rev. D* **81** (2010) 123530 doi:10.1103/PhysRevD.81.123530 [arXiv:0905.4720 [hep-th]].
- [186] B. S. Acharya, K. Bobkov and P. Kumar, “An M Theory Solution to the Strong CP Problem and Constraints on the Axiverse,” *JHEP* **1011** (2010) 105 doi:10.1007/JHEP11(2010)105 [arXiv:1004.5138 [hep-th]].
- [187] M. Cicoli, M. Goodsell and A. Ringwald, “The type IIB string axiverse and its low-energy phenomenology,” *JHEP* **1210** (2012) 146 doi:10.1007/JHEP10(2012)146 [arXiv:1206.0819 [hep-th]].
- [188] R. Blumenhagen, M. Cvetič, S. Kachru and T. Weigand, “D-Brane Instantons in Type II Orientifolds,” *Ann. Rev. Nucl. Part. Sci.* **59** (2009) 269 doi:10.1146/annurev.nucl.010909.083113 [arXiv:0902.3251 [hep-th]].
- [189] G. Aldazabal, L. E. Ibanez, F. Quevedo and A. M. Uranga, “D-branes at singularities: A Bottom up approach to the string embedding of the standard model,” *JHEP* **0008** (2000) 002 doi:10.1088/1126-6708/2000/08/002 [hep-th/0005067].

- [190] J. P. Conlon, A. Maharana and F. Quevedo, “Towards Realistic String Vacua,” *JHEP* **0905** (2009) 109 doi:10.1088/1126-6708/2009/05/109 [arXiv:0810.5660 [hep-th]].
- [191] M. Cicoli, S. Krippendorf, C. Mayrhofer, F. Quevedo and R. Valandro, “D3/D7 Branes at Singularities: Constraints from Global Embedding and Moduli Stabilisation,” *JHEP* **1307** (2013) 150 doi:10.1007/JHEP07(2013)150 [arXiv:1304.0022 [hep-th]].
- [192] M. Cicoli, D. Klevers, S. Krippendorf, C. Mayrhofer, F. Quevedo and R. Valandro, “Explicit de Sitter Flux Vacua for Global String Models with Chiral Matter,” *JHEP* **1405** (2014) 001 doi:10.1007/JHEP05(2014)001 [arXiv:1312.0014 [hep-th]].
- [193] M. Wijnholt, “Geometry of Particle Physics,” *Adv. Theor. Math. Phys.* **13** (2009) no.4, 947 [hep-th/0703047].
- [194] R. Blumenhagen and M. Schmidt-Sommerfeld, “Power Towers of String Instantons for N=1 Vacua,” *JHEP* **0807** (2008) 027 doi:10.1088/1126-6708/2008/07/027 [arXiv:0803.1562 [hep-th]].
- [195] R. Blumenhagen, X. Gao, T. Rahn and P. Shukla, “A Note on Poly-Instanton Effects in Type IIB Orientifolds on Calabi-Yau Threefolds,” *JHEP* **1206** (2012) 162 doi:10.1007/JHEP06(2012)162 [arXiv:1205.2485 [hep-th]].
- [196] S. A. Abel, M. D. Goodsell, J. Jaeckel, V. V. Khoze and A. Ringwald, “Kinetic Mixing of the Photon with Hidden U(1)s in String Phenomenology,” *JHEP* **0807** (2008) 124 doi:10.1088/1126-6708/2008/07/124 [arXiv:0803.1449 [hep-ph]].
- [197] J. W. Brockway, E. D. Carlson and G. G. Raffelt, “SN1987A gamma-ray limits on the conversion of pseudoscalars,” *Phys. Lett. B* **383** (1996) 439 doi:10.1016/0370-2693(96)00778-2 [astro-ph/9605197].
- [198] J. A. Grifols, E. Masso and R. Toldra, “Gamma-rays from SN1987A due to pseudoscalar conversion,” *Phys. Rev. Lett.* **77** (1996) 2372 doi:10.1103/PhysRevLett.77.2372 [astro-ph/9606028].
- [199] A. Payez, C. Evoli, T. Fischer, M. Giannotti, A. Mirizzi and A. Ringwald, “Revisiting the SN1987A gamma-ray limit on ultralight axion-like particles,” *JCAP* **1502** (2015) no.02, 006 doi:10.1088/1475-7516/2015/02/006 [arXiv:1410.3747 [astro-ph.HE]].

- [200] J. P. Conlon, M. C. D. Marsh and A. J. Powell, “Galaxy cluster thermal x-ray spectra constrain axionlike particles,” *Phys. Rev. D* **93** (2016) no.12, 123526 doi:10.1103/PhysRevD.93.123526 [arXiv:1509.06748 [hep-ph]].
- [201] M. Berg, J. P. Conlon, F. Day, N. Jennings, S. Krippendorf, A. J. Powell and M. Rummel, “Searches for Axion-Like Particles with NGC1275: Observation of Spectral Modulations,” arXiv:1605.01043 [astro-ph.HE].
- [202] M. C. D. Marsh, H. R. Russell, A. C. Fabian, B. P. McNamara, P. Nulsen and C. S. Reynolds, “A New Bound on Axion-Like Particles,” arXiv:1703.07354 [hep-ph].
- [203] J. P. Conlon, F. Day, N. Jennings, S. Krippendorf and M. Rummel, “Constraints on Axion-Like Particles from Non-Observation of Spectral Modulations for X-ray Point Sources,” *JCAP* **1707** (2017) no.07, 005 doi:10.1088/1475-7516/2017/07/005 [arXiv:1704.05256 [astro-ph.HE]].
- [204] I. Irastorza *et al.* [IAXO Collaboration], “The International Axion Observatory IAXO. Letter of Intent to the CERN SPS committee,” CERN-SPSC-2013-022.
- [205] A. Spector, “ALPS II technical overview and status report,” arXiv:1611.05863 [physics.ins-det].
- [206] J. P. Conlon and M. C. D. Marsh, “Excess Astrophysical Photons from a 0.1 keV Cosmic Axion Background,” *Phys. Rev. Lett.* **111** (2013) no.15, 151301 doi:10.1103/PhysRevLett.111.151301 [arXiv:1305.3603 [astro-ph.CO]].
- [207] M. B. Green and J. H. Schwarz, “Anomaly Cancellation in Supersymmetric D=10 Gauge Theory and Superstring Theory,” *Phys. Lett.* **149B** (1984) 117. doi:10.1016/0370-2693(84)91565-X
- [208] J. P. Conlon and F. G. Pedro, “Moduli Redefinitions and Moduli Stabilisation,” *JHEP* **1006** (2010) 082 doi:10.1007/JHEP06(2010)082 [arXiv:1003.0388 [hep-th]].
- [209] R. Blumenhagen, J. P. Conlon, S. Krippendorf, S. Moster and F. Quevedo, “SUSY Breaking in Local String/F-Theory Models,” *JHEP* **0909** (2009) 007 doi:10.1088/1126-6708/2009/09/007 [arXiv:0906.3297 [hep-th]].
- [210] L. Aparicio, M. Cicoli, S. Krippendorf, A. Maharana, F. Muia and F. Quevedo, “Sequestered de Sitter String Scenarios: Soft-terms,” *JHEP* **1411**, 071 (2014) doi:10.1007/JHEP11(2014)071 [arXiv:1409.1931 [hep-th]].

- [211] M. Berg, D. Marsh, L. McAllister and E. Pajer, “Sequestering in String Compactifications,” *JHEP* **1106** (2011) 134 doi:10.1007/JHEP06(2011)134 [arXiv:1012.1858 [hep-th]].
- [212] M. Goodsell, J. Jaeckel, J. Redondo and A. Ringwald, “Naturally Light Hidden Photons in LARGE Volume String Compactifications,” *JHEP* **0911** (2009) 027 doi:10.1088/1126-6708/2009/11/027 [arXiv:0909.0515 [hep-ph]].
- [213] M. Cicoli, M. Goodsell, J. Jaeckel and A. Ringwald, “Testing String Vacua in the Lab: From a Hidden CMB to Dark Forces in Flux Compactifications,” *JHEP* **1107** (2011) 114 doi:10.1007/JHEP07(2011)114 [arXiv:1103.3705 [hep-th]].
- [214] P. G. Camara and E. Dudas, “Multi-instanton and string loop corrections in toroidal orbifold models,” *JHEP* **0808** (2008) 069 doi:10.1088/1126-6708/2008/08/069 [arXiv:0806.3102 [hep-th]].
- [215] D. Robles-Llana, M. Rocek, F. Saueressig, U. Theis and S. Vandoren, “Nonperturbative corrections to 4D string theory effective actions from $SL(2, \mathbb{Z})$ duality and supersymmetry,” *Phys. Rev. Lett.* **98** (2007) 211602 doi:10.1103/PhysRevLett.98.211602 [hep-th/0612027].
- [216] P. Berglund and P. Mayr, “Non-perturbative superpotentials in F-theory and string duality,” *JHEP* **1301** (2013) 114 doi:10.1007/JHEP01(2013)114 [hep-th/0504058].
- [217] P. Candelas and X. de la Ossa, “Moduli Space of Calabi-Yau Manifolds,” *Nucl. Phys. B* **355** (1991) 455. doi:10.1016/0550-3213(91)90122-E
- [218] L. Aparicio, D. G. Cerdeno and L. E. Ibanez, “Modulus-dominated SUSY-breaking soft terms in F-theory and their test at LHC,” *JHEP* **0807** (2008) 099 doi:10.1088/1126-6708/2008/07/099 [arXiv:0805.2943 [hep-ph]].
- [219] J. P. Conlon, D. Cremades and F. Quevedo, “Kahler potentials of chiral matter fields for Calabi-Yau string compactifications,” *JHEP* **0701** (2007) 022 doi:10.1088/1126-6708/2007/01/022 [hep-th/0609180].
- [220] N. Arkani-Hamed, M. Dine and S. P. Martin, “Dynamical supersymmetry breaking in models with a Green-Schwarz mechanism,” *Phys. Lett. B* **431** (1998) 329 doi:10.1016/S0370-2693(98)00494-8 [hep-ph/9803432].

- [221] L. Aparicio, M. Cicoli, B. Dutta, F. Muia and F. Quevedo, “Light Higgsino Dark Matter from Non-thermal Cosmology,” *JHEP* **1611** (2016) 038 doi:10.1007/JHEP11(2016)038 [arXiv:1607.00004 [hep-ph]].
- [222] A. D. Linde, “Axions in inflationary cosmology,” *Phys. Lett. B* **259** (1991) 38. doi:10.1016/0370-2693(91)90130-I
- [223] P. Fox, A. Pierce and S. D. Thomas, “Probing a QCD string axion with precision cosmological measurements,” hep-th/0409059.
- [224] T. W. Grimm and J. Louis, “The Effective action of $N = 1$ Calabi-Yau orientifolds,” *Nucl. Phys. B* **699** (2004) 387 doi:10.1016/j.nuclphysb.2004.08.005 [hep-th/0403067].